Fundamentals of Molecular Spectroscopy

THIRD EDITION

C. N. BANWELL
Lecturer in Chemistry
University of Sussex

McGRAW-HILL BOOK COMPANY

London · New York · St Louis · San Francisco · Auckland · Bogotá
Caracas · Lisbon · Madrid · Mexico · Milan · Montreal
New Delhi · Panama · Paris · San Juan · São Paulo · Singapore
Sydney · Tokyo · Toronto

Published by
McGRAW-HILL Book Company Europe
SHOPPENHANGERS ROAD · MAIDENHEAD · BERKSHIRE · SL6 2QL · ENGLAND
TELEPHONE 0628 23432 · FAX 0628 770224

British Library Cataloguing in Publication Data

Banwell, C. N.
Fundamentals of molecular spectroscopy.—3rd ed.
1. Molecular Spectra
I. Title
535.8'4 QC454.M6
ISBN 0–07–084139–X

Library of Congress Cataloging in Publication Data

Banwell, C. N.
Fundamentals of molecular spectroscopy.
Bibliography: p.
Includes index.
1. Molecular spectra. I. Title.
QD96.M65B36 1983 535.8'4 82–23949
ISBN 0–07–084139–X

10 PB 94

Typeset by Santype International Ltd., Salisbury, Wilts.
Printed and bound in Great Britain by
Page Bros, Norwich

CONTENTS

LIST OF TABLES

PREFACE

During the writing of this, the third edition of *Fundamentals of Molecular Spectroscopy*, I have borne very firmly in mind the aims of the original book—to emphasize the overall unity of the subject, and to offer a pictorial rather than a mathematical description of the principles of spectroscopy. The latter aim has received some criticism (although, it must be said, from teachers of the subject rather than from those trying to learn it); but, while it is true that universities and polytechnics now offer excellent courses in subjects such as quantum mechanics, a grasp of which can illuminate many areas of spectroscopy, experience shows that most students approaching spectroscopy for the first time prefer the simpler treatment offered here.

The general organization of the book remains unchanged, each chapter after the first presenting the fundamentals of a particular spectroscopic technique. Although each chapter is thus essentially self-contained, the intention is that the book shall be read as a whole, since concepts introduced in early chapters are often used later without further discussion.

In fact, although it is an almost unbelievable ten years since the second edition was published, there has been relatively little change in the basic ideas of spectroscopy, and much of the book is essentially unaltered. What changes have occurred have been mainly in the extension of existing techniques, and their increasing availability due to improvements in instrumentation. In this respect the two main areas of interest are the use of lasers as radiation sources, and the very rapid expansion in the use of Fourier transform techniques. Accordingly I have added a section on lasers to Chapter 1 and expanded the references to them in later chapters, particularly in Chapter 3. Equally, a general description of the Fourier transform method has been included in Chapter 1, and Chapter 7 has been extensively rewritten to take account of the wealth of additional information accessible from the application of this technique to nuclear magnetic resonance spectroscopy.

When a book has been in use for 15 years it becomes impossible to acknowledge the help received from the very many people, students and teachers, who have commented on it. My greatest debt is, of course, to Professor Sheppard of the University of East Anglia, who first introduced me to the beauty and fascination of spectroscopy, but I hope that all those who see their comments and suggestions incorporated into this edition will accept this general acknowledgement of my indebtedness, and will not think me churlish for leaving them unnamed.

C. N. BANWELL
University of Sussex

CHAPTER
ONE
INTRODUCTION

1.1 CHARACTERIZATION OF ELECTROMAGNETIC RADIATION

Molecular spectroscopy may be defined as the study of the interaction of electromagnetic waves and matter. Throughout this book we shall be concerned with what spectroscopy can tell us of the structure of matter, so it is essential in this first chapter to discuss briefly the nature of electromagnetic radiation and the sort of interactions which may occur; we shall also consider, in outline, the experimental methods of spectroscopy.

Electromagnetic radiation, of which visible light forms an obvious but very small part, may be considered as a simple harmonic wave propagated from a source and travelling in straight lines except when refracted or reflected. The properties which undulate—corresponding to the physical displacement of a stretched string vibrating, or the alternate compressions and rarefactions of the atmosphere during the passage of a sound wave—are interconnected electric and magnetic fields. We shall see later that it is these undulatory fields which interact with matter giving rise to a spectrum.

It is trivial to show that any simple harmonic wave has properties of the sine wave, defined by $y = A \sin \theta$, which is plotted in Fig. 1.1. Here y is the displacement with a maximum value A, and θ is an angle varying between 0 and 360° (or 0 and 2π radians). The relevance of this representation to a travelling wave is best seen by considering the left-hand side of

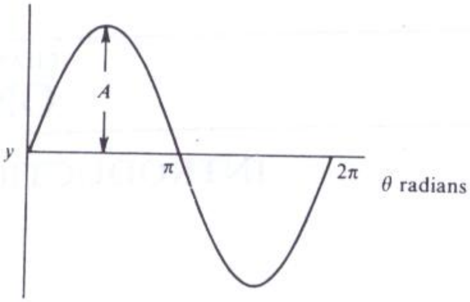

Figure 1.1 The curve of $y = A \sin \theta$.

Fig. 1.2. A point P travels with uniform angular velocity ω rad s^{-1} in a circular path of radius A; we measure the time from the instant when P passes O' and then, after a time t seconds, we imagine P to have described an angle $\theta = \omega t$ radians. Its vertical displacement is then $y = A \sin \theta = A \sin \omega t$, and we can plot this displacement against time as on the right-hand side of Fig. 1.2. After a time of $2\pi/\omega$ seconds, P will return to O', completing a 'cycle'. Further cycles of P will repeat the pattern and we can describe the displacement as a continuous function of time by the graph of Fig. 1.2.

In one second the pattern will repeat itself $\omega/2\pi$ times, and this is referred to as the *frequency* (ν) of the wave. The SI unit of frequency is called the hertz (abbreviated to Hz) and has the dimensions of reciprocal seconds (abbreviated s^{-1}). We may then write:

$$y = A \sin \omega t = A \sin 2\pi\nu t \tag{1.1}$$

as a basic equation of wave motion.

So far we have discussed the variation of displacement with time, but in order to consider the nature of a *travelling* wave, we are more interested in

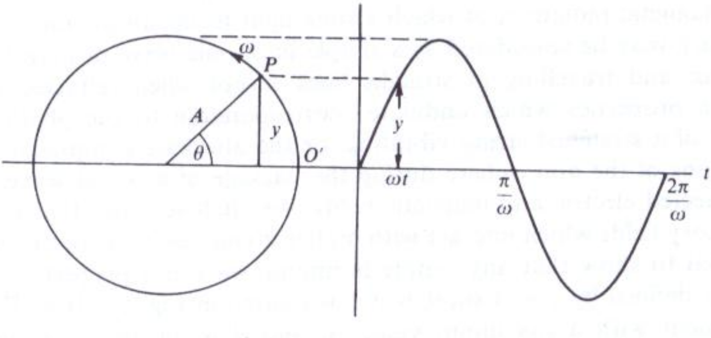

Figure 1.2 The description of a sine curve in terms of the circular motion of a point P at a uniform angular velocity of ω rad s^{-1}.

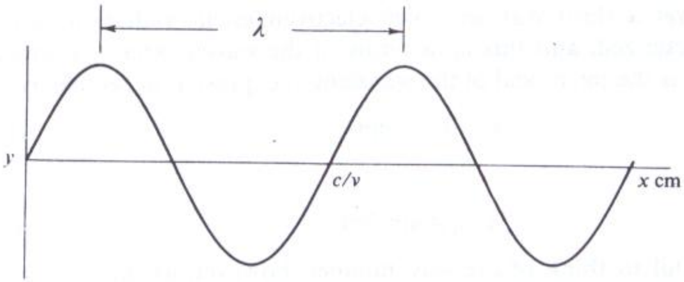

Figure 1.3 The concept of a travelling wave with a wavelength λ.

the distance variation of the displacement. For this we need the fundamental distance–time relationship:

$$x = ct \tag{1.2}$$

where x is the distance covered in time t at a speed c. Combining (1.1) and (1.2) we have:

$$y = A \sin 2\pi\nu t = A \sin \frac{2\pi\nu x}{c}$$

and the wave is shown in Fig. 1.3. Besides the frequency ν, we now have another property by which we can characterize the wave—its *wavelength* λ, which is the distance travelled during a complete cycle. When the velocity is c metres per second and there are ν cycles per second, there are evidently ν waves in c metres, or

$$\nu\lambda = c \qquad \lambda = c/\nu \quad \text{metres} \tag{1.3}$$

so we have:

$$y = A \sin \frac{2\pi x}{\lambda} \tag{1.4}$$

In spectroscopy wavelengths are expressed in a variety of units, chosen so that in any particular range (see Fig. 1.4) the wavelength does not involve large powers of ten. Thus, in the microwave region, λ is measured in centimetres or millimetres, while in the infra-red it is usually given in micrometres (μm)—formerly called the *micron*—where

$$1\ \mu\text{m} = 10^{-6}\ \text{m} \tag{1.5}$$

In the visible and ultra-violet region, λ is still often expressed in Ångstrom units (Å) where $1\ \text{Å} = 10^{-10}$ m, although the proper SI unit for this region is the nanometre:

$$1\ \text{nm} = 10^{-9}\ \text{m} = 10\ \text{Å} \tag{1.6}$$

There is yet a third way in which electromagnetic radiation can be usefully characterized, and this is in terms of the *wavenumber* $\bar{\nu}$. Formally this is defined as the reciprocal of the wavelength expressed in *centimetres*:

$$\bar{\nu} = 1/\lambda \quad \mathrm{cm}^{-1} \tag{1.7}$$

and hence

$$y = A \sin 2\pi\bar{\nu}x \tag{1.8}$$

It is more useful to think of the wavenumber, however, as the number of compete waves or cycles contained in each centimetre length of radiation. Since the formal definition is based on the centimetre rather than the metre, the wavenumber is, of course, a non-SI unit; it is, however, so convenient a unit for the discussion of infra-red spectra that—like the Ångstrom—it will be many years before it falls into disuse.

It is unfortunate that the conventional symbols of wavenumber ($\bar{\nu}$) and frequency (ν) are similar; confusion should not arise, however, if the units of any expression are kept in mind, since wavenumber is invariably expressed in reciprocal centimetres (cm^{-1}) and frequency in cycles per second (s^{-1} or Hz). The two are, in fact, proportional: $\nu = c\bar{\nu}$, where the proportionality constant is the velocity of radiation expressed in *centimetres* per second (that is, 3×10^{10} cm s^{-1}); the velocity in SI units is, of course, 3×10^{8} m s^{-1}.

1.2 THE QUANTIZATION OF ENERGY

Towards the end of the last century experimental data were observed which were quite incompatible with the previously accepted view that matter could take up energy continuously. In 1900 Max Planck published the revolutionary idea that the energy of an oscillator is discontinuous and that any change in its energy content can occur only by means of a jump between two distinct energy states. The idea was later extended to cover many other forms of the energy of matter.

A molecule in space can have many sorts of energy; e.g., it may possess rotational energy by virtue of bodily rotation about its centre of gravity; it will have vibrational energy due to the periodic displacement of its atoms from their equilibrium positions; it will have electronic energy since the electrons associated with each atom or bond are in unceasing motion, etc. The chemist or physicist is early familiar with the electronic energy states of an atom or molecule and accepts the idea that an electron can exist in one of several discrete energy levels: he learns to speak of the energy as being *quantized*. In much the same way the rotational, vibrational, and other energies of a molecule are also quantized—a particular molecule can exist in a variety of rotational, vibrational, etc., energy levels and can move from one level to another only by a sudden jump involving a finite amount of energy.

Consider two possible energy states of a system—two rotational energy levels of a molecule, for example—labelled E_1 and E_2 in the following diagram. The suffixes 1 and 2 used to distinguish these levels are, in fact, *quantum numbers*. The actual significance of quantum numbers goes far deeper than their use as a convenient label—in particular, we shall later see that analytical expressions for energy levels usually involve an algebraic function of one or more quantum numbers. Transitions can take place between the levels E_1 and E_2 provided the appropriate amount of energy, $\Delta E = E_2 - E_1$, can be either absorbed or emitted by the system. Planck suggested that such absorbed or emitted energy can take the form of electromagnetic radiation and that the frequency of the radiation has the simple form:

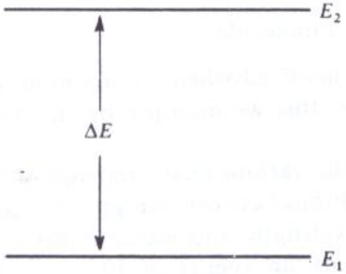

$$\nu = \Delta E/h \quad \text{Hz}$$

i.e.,

$$\Delta E = h\nu \quad \text{joules} \tag{1.9}$$

where we express our energies E in terms of the joule, and h is a universal constant—Planck's constant. This suggestion has been more than amply confirmed by experiment.

The significance of this is that if we take a molecule in state 1 and direct on to it a beam of radiation of a single frequency ν (monochromatic radiation), where $\nu = \Delta E/h$, energy will be absorbed from the beam and the molecule will jump to state 2. A detector placed to collect the radiation after its interaction with the molecule will show that its intensity has decreased. Also if we use a beam containing a wide range of frequencies ('white' radiation), the detector will show that energy has been absorbed *only* from that frequency $\nu = \Delta E/h$, all other frequencies being undiminished in intensity. In this way we have produced a spectrum—an *absorption* spectrum.

Alternatively the molecule may already be in state 2 and may revert to state 1 with the consequent emission of radiation. A detector would show this radiation to have frequency $\nu = \Delta E/h$ only, and the *emission* spectrum so found is plainly complementary to the absorption spectrum of the previous paragraph.

The actual energy differences between the rotational, vibrational, and electronic energy levels are very small and may be measured in joules per molecule (or atom). In these units Planck's constant has the value:

$$h = 6{\cdot}63 \times 10^{-34} \text{ joules s molecule}^{-1}$$

Often we are interested in the total energy involved when a gram-molecule of a substance changes its energy state: for this we multiply by the Avogadro number $N = 6{\cdot}02 \times 10^{23}$.

However, the spectroscopist measures the various characteristics of the absorbed or emitted radiation during transitions between energy states and he often, rather loosely, uses frequency, wavelength, and wavenumber as if they were energy units. Thus in referring to 'an energy of 10 cm^{-1}' he means 'a separation between two energy states such that the associated radiation has a wavenumber value of 10 cm^{-1}'. The first expression is so simple and convenient that it is essential to become familiar with wavenumber and frequency energy units if one is to understand the spectroscopist's language. Throughout this book we shall use the symbol ε to represent energy in cm^{-1}.

It cannot be too firmly stressed at this point that the frequency of radiation associated with an energy change does *not* imply that the transition between energy levels occurs a certain number of times each second. Thus an electronic transition in an atom or molecule may absorb or emit radiation of frequency some 10^{15} Hz, but the electronic transition does not itself *occur* 10^{15} times per second. It may occur once or many times and on each occurrence it will absorb or emit an energy quantum of the appropriate frequency.

1.3 REGIONS OF THE SPECTRUM

Figure 1.4 illustrates in pictorial fashion the various, rather arbitrary, regions into which electromagnetic radiation has been divided. The boundaries between the regions are by no means precise, although the molecular processes associated with each region are quite different. Each succeeding chapter in this book deals essentially with one of these processes.

In increasing frequency the regions are:

1. Radiofrequency region: 3×10^{6}–3×10^{10} Hz; 10 m–1 cm wavelength. Nuclear magnetic resonance (n.m.r.) and electron spin resonance (e.s.r.) spectroscopy. The energy change involved is that arising from the reversal of spin of a nucleus or electron, and is of the order 0·001–10 joules/mole (Chapter 7).

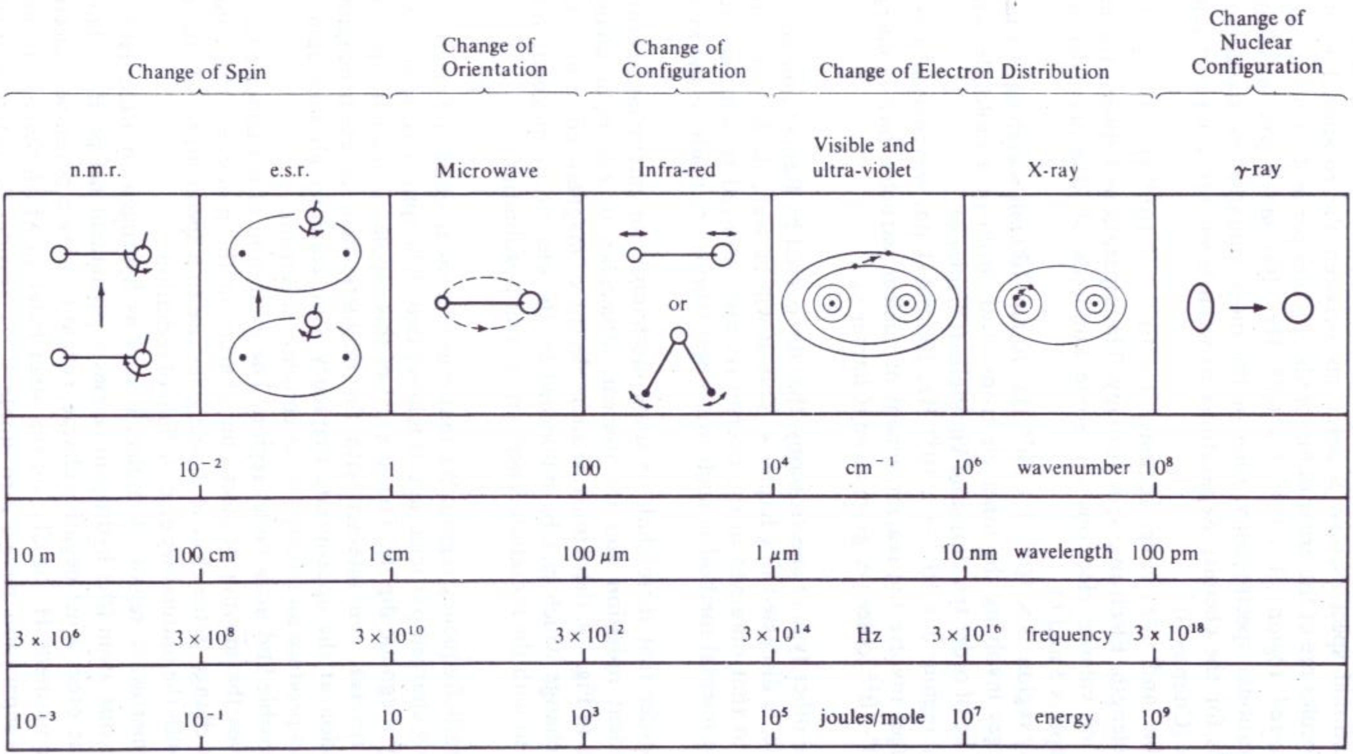

Figure 1.4 The regions of the electromagnetic spectrum.

2. Microwave region: 3×10^{10}–3×10^{12} Hz; 1 cm–100 μm wavelength. Rotational spectroscopy. Separations between the rotational levels of molecules are of the order of hundreds of joules per mole (Chapter 2).
3. Infra-red region: 3×10^{12}–3×10^{14} Hz; 100 μm–1 μm wavelength. Vibrational spectroscopy. One of the most valuable spectroscopic regions for the chemist. Separations between levels are some 10^4 joules/mole (Chapter 3).
4. Visible and ultra-violet regions: 3×10^{14}–3×10^{16} Hz; 1 μm–10 nm wavelength. Electronic spectroscopy. The separations between the energies of valence electrons are some hundreds of kilojoules per mole (Chapters 5 and 6).
5. X-ray region: 3×10^{16}–3×10^{18} Hz; 10 nm–100 pm wavelength. Energy changes involving the inner electrons of an atom or a molecule, which may be of order ten thousand kilojoules (Chapter 5).
6. γ-ray region: 3×10^{18}–3×10^{20} Hz; 100 pm–1 pm wavelength. Energy changes involve the rearrangement of nuclear particles, having energies of 10^9–10^{11} joules per gram atom (Chapter 8).

One other type of spectroscopy, that discovered by Raman and bearing his name, is discussed in Chapter 4. This, it will be seen, yields information similar to that obtained in the microwave and infra-red regions, although the experimental method is such that observations are made in the visible region.

In order that there shall be some mechanism for interaction between the incident radiation and the nuclear, molecular, or electronic changes depicted in Fig. 1.4, there must be some electric or magnetic effect produced by the change which can be influenced by the electric or magnetic fields associated with the radiation. There are several possibilities:

1. The radiofrequency region. We may consider the nucleus and electron to be tiny charged particles, and it follows that their spin is associated with a tiny magnetic dipole. The reversal of this dipole consequent upon the spin reversal can interact with the magnetic field of electromagnetic radiation at the appropriate frequency. Consequently all such spin reversals produce an absorption or emission spectrum.
2. The visible and ultra-violet region. The excitation of a valence electron involves the moving of electronic charges in the molecule. The consequent change in the electric dipole gives rise to a spectrum by its interaction with the undulatory electric field of radiation.
3. The microwave region. A molecule such as hydrogen chloride, HCl, in which one atom (the hydrogen) carries a permanent net positive charge and the other a net negative charge, is said to have a permanent electric dipole moment. H_2 or Cl_2, on the other hand, in which there is no such charge separation, have a zero dipole. If we consider the rotation of HCl

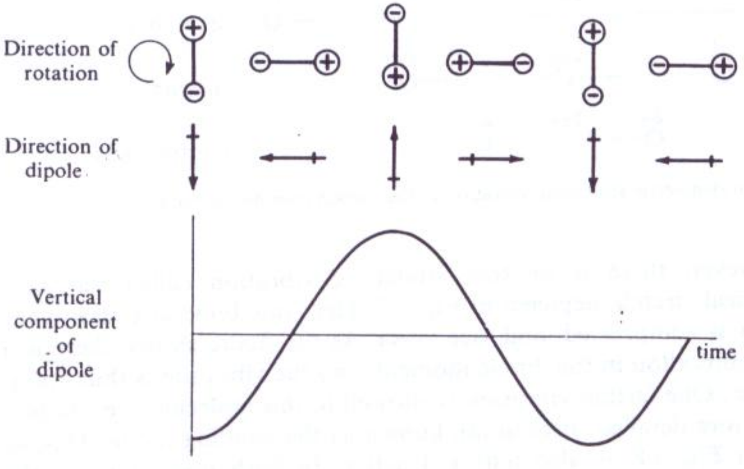

Figure 1.5 The rotation of a diatomic molecule, HCl, showing the fluctuation in the dipole moment measured in a particular direction.

(Fig. 1.5, where we notice that if only a pure rotation takes place, the centre of gravity of the molecule must not move), we see that the plus and minus charges change places periodically, and the component dipole moment in a given direction (say upwards in the plane of the paper) fluctuates regularly. This fluctuation is plotted in the lower half of Fig. 1.5, and it is seen to be exactly similar in form to the fluctuating electric field of radiation (cf. Fig. 1.2). Thus interaction can occur, energy can be absorbed or emitted, and the rotation gives rise to a spectrum. All molecules having a permanent moment are said to be 'microwave active'. If there is no dipole, as in H_2 or Cl_2, no interaction can take place and the molecule is 'microwave inactive'. This imposes a limitation on the applicability of microwave spectroscopy.

4. The infra-red region. Here it is a vibration, rather than a rotation, which must give rise to a dipole change. Consider the carbon dioxide molecule as an example, in which the three atoms are arranged linearly with a small net positive charge on the carbon and small negative charges on the oxygens:

$$\overset{\delta-}{\mathrm{O}}\text{———}\overset{2\delta+}{\mathrm{C}}\text{———}\overset{\delta-}{\mathrm{O}}$$

During the mode of vibration known as the 'symmetric stretch', the molecule is alternately stretched and compressed, both C—O bonds changing simultaneously, as in Fig. 1.6. Plainly the dipole moment remains zero throughout the whole of this motion, and this particular vibration is thus 'infra-red inactive'.

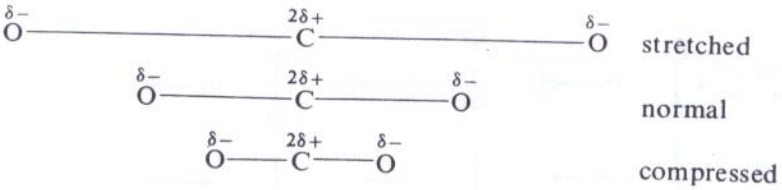

Figure 1.6 The symmetric stretching vibration of the carbon dioxide molecule.

However, there is another stretching vibration called the antisymmetrical stretch, depicted in Fig. 1.7. Here one bond stretches while the other is compressed, and vice versa. As the figure shows, there is a periodic alteration in the dipole moment, and the vibration is thus 'infra-red active'. One further vibration is allowed to this molecule (see Chapter 3 for a more detailed discussion), known as the bending mode. This, as shown in Fig. 1.8, is also infra-red active. In both these motions the centre of gravity does not move.

Although dipole change requirements do impose some limitation on the application of infra-red spectroscopy, the appearance or non-appearance of certain vibration frequencies can give valuable information about the structure of a particular molecule (see Chapter 3).

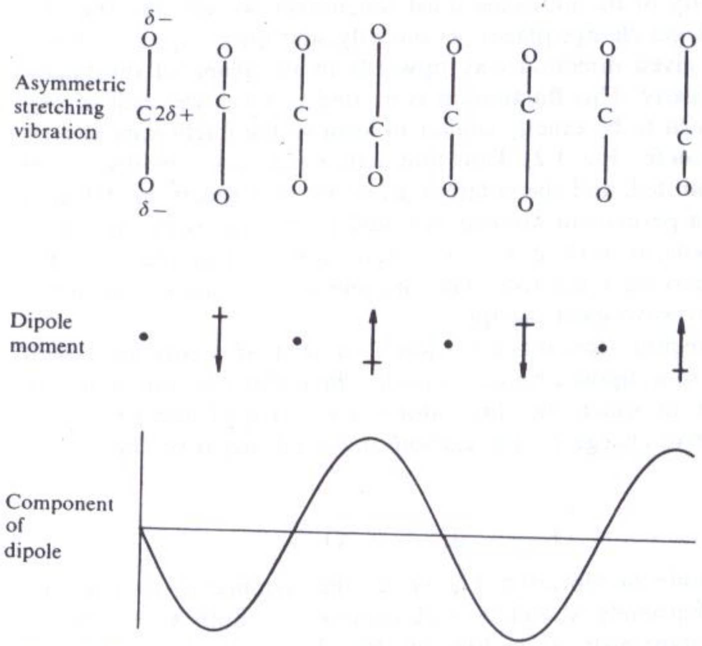

Figure 1.7 The asymmetric stretching vibration of the carbon dioxide molecule showing the fluctuation in the dipole moment.

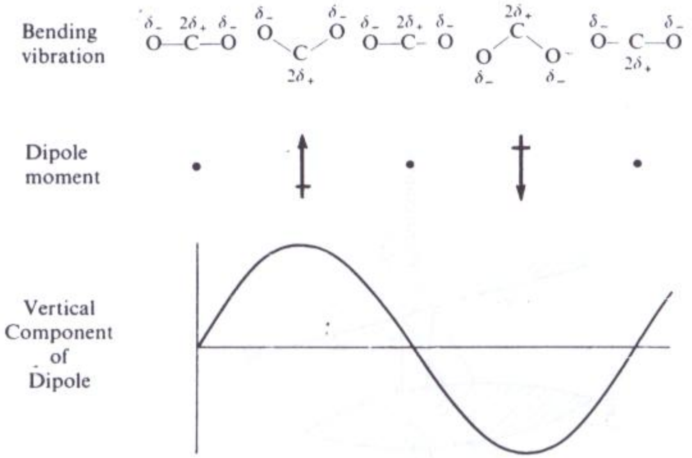

Figure 1.8 The bending motion of the carbon dioxide molecule and its associated dipole fluctuation.

5. There is a rather special requirement for a molecular motion to be 'Raman active'; this is that the electrical *polarizability* of the molecule must change during the motion. This will be discussed fully in Chapter 4.

1.4 REPRESENTATION OF SPECTRA

We show in Fig. 1.9 a highly schematic diagram of a spectrometer suitable for use in the visible and ultra-violet regions of the spectrum. A 'white' source is focused by lens 1 on to a narrow slit (arranged perpendicularly to the plane of the paper) and is then made into a parallel beam by lens 2. After passing through the sample it is separated into its constituent frequencies by a prism and is then focused on to a photographic plate by lens 3; the vertical image of the slit will thus appear on the plate. Rays have been drawn to show the points at which two frequencies, ν_1 and ν_2, are focused.

If the sample container is empty, the photographic plate, after development, should ideally show an even blackening over the whole range of frequencies covered (i.e., from A to B). The ideal situation is seldom realized, if only because the source does not usually radiate all frequencies with the same intensity, but in any case the blackening of the plate serves to indicate the relative intensities of the frequencies emitted by the source.

If we now imagine the sample space to be filled with a substance having only two possible energy levels, E_1 and E_2, the photographic plate, after development, will show a blackening at all points except at the frequency $\nu = (E_2 - E_1)/h$, since energy at this frequency will have been absorbed by

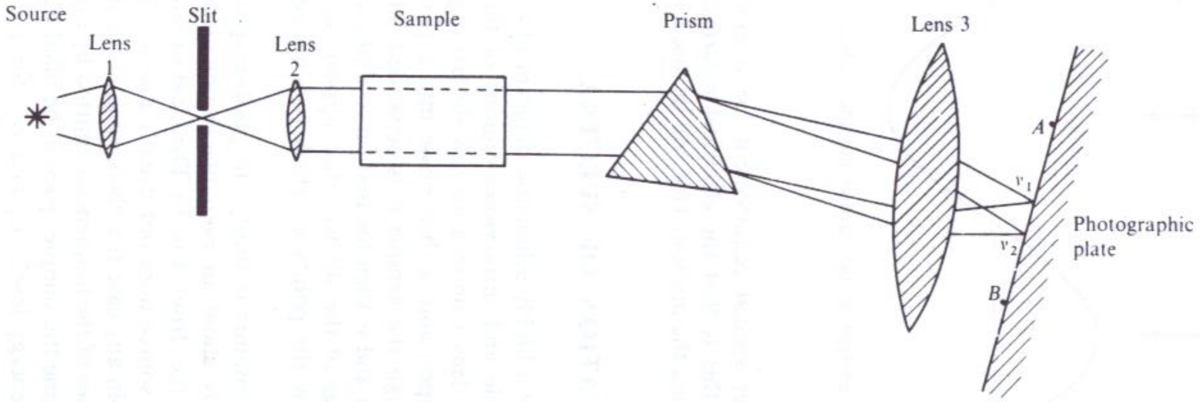

Figure 1.9 Schematic diagram of a spectrometer suitable for operation in the visible region.

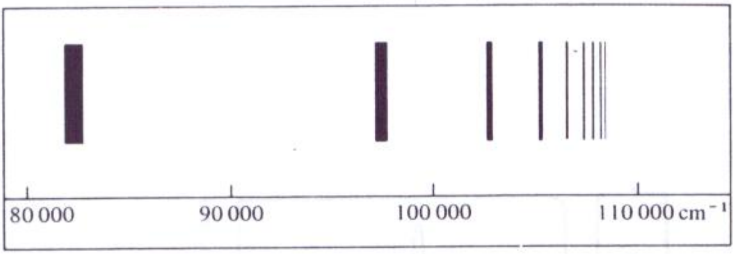

Figure 1.10 Schematic diagram of the absorption spectrum of atomic hydrogen recorded on a photographic plate.

the sample in raising each molecule from state 1 to state 2. Further if, as is almost always the case, there are many possible energy levels, E_1, E_2, ..., E_j, E_k, ... available to the sample, a series of absorption lines will appear on the photographic plate at frequencies given by $\nu = (E_j - E_k)/h$. A typical spectrum may then appear as in Fig. 1.10.

At this point it may be helpful to consider what happens to the energy absorbed in the sort of process described above. In the ultra-violet, visible, and infra-red regions it is an experimental fact that a given sample continues to show an absorption spectrum for as long as we care to irradiate it—in other words, a finite number of sample molecules appear to be capable of absorbing an infinite amount of energy. Plainly the molecules must be able to rid themselves of the absorbed energy.

A possible mechanism for this is by thermal collisions. An energized molecule collides with its neighbours and gradually loses its excess energy to them as kinetic energy—the sample as a whole becomes warm.

Another mechanism is that energy gained from radiation is lost as radiation once more. A molecule in the ground state absorbs energy at frequency ν and its energy is raised an amount $\Delta E = h\nu$ above the ground state. It is thus in an excited, unstable condition, but by emitting radiation of frequency ν again, it can revert to the ground state and is able to reabsorb from the radiation beam once more. In this case, it is often asked how an absorption spectrum can arise at all, since the absorbed energy is re-emitted by the sample. The answer is simply that the radiation is re-emitted in a random direction and the proportion of such radiation reaching the detector is minute—in fact re-emitted radiation has as much chance of reaching the source as the detector. The net effect, then, is an absorption from the directed beam and, when re-emission occurs, a scattering into the surroundings. The scattered radiation can, of course, be collected and observed as an emission spectrum which will be—with important reservations to be discussed in Chapter 4—the complement of the absorption spectrum. Under the right conditions much of the radiation emitted from a sample can be in a very coherent beam—so-called laser radiation. We discuss this in Sec. 1.10.

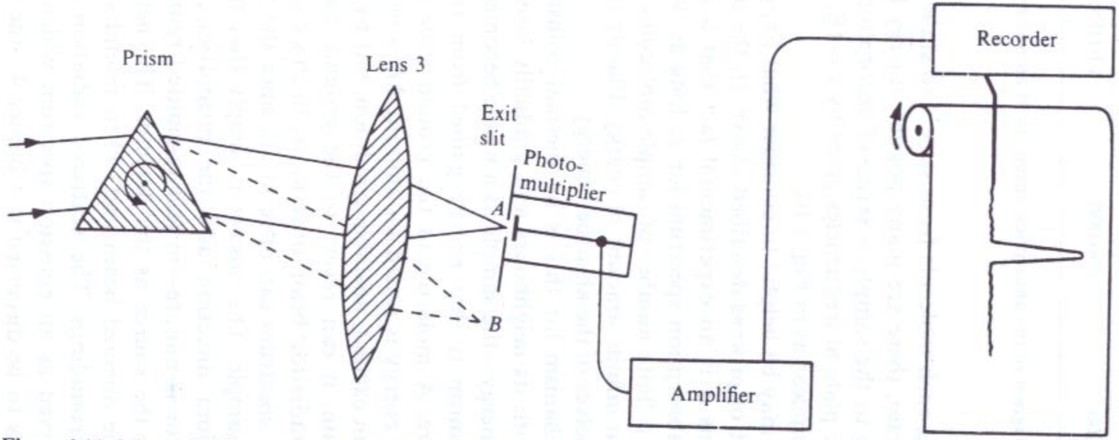

Figure 1.11 Schematic diagram of a spectrometer employing a photomultiplier or other sensitive element as detector and recording the spectrum graphically on chart paper.

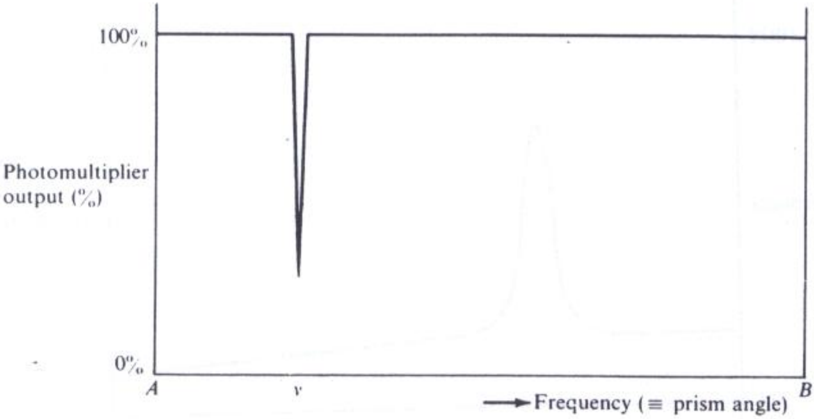

Figure 1.12 The idealized spectrum of a molecule undergoing a single transition.

In modern spectrometers the detector is rarely the simple photographic plate of Fig. 1.9. One of the most sensitive and useful devices in the visible and ultra-violet region is the photomultiplier tube, consisting of a light-sensitive surface which emits electrons when light falls upon it. The tiny electron current may be amplified and applied to an ammeter or pen recorder. The spectrometer would then appear somewhat as in Fig. 1.11, where the sensitive element of the photomultiplier is situated at the point *A* of Fig. 1.9. The physical width of the beam falling on the detector can be limited by the provision of an 'exit slit' just in front of the detector entrance.

The frequency of the light falling on the photomultiplier may be altered either by physically moving the latter from *A* to *B* or, more usually, by steady rotation of the prism. If, as before, we imagine the sample to contain a substance having just two energy levels, the photomultiplier output will, ideally, vary with the prism orientation as in Fig. 1.12. We say that the spectrum has been *scanned* between the frequencies represented by *A* and *B*, and such a picture is referred to, rather grandly, as a spectrum in the 'frequency domain', to indicate that it records the detector output against frequency. In Sec. 1.8 we shall discuss 'time domain' spectroscopy, where the detector output is recorded as a function of time.

Again, the ideal situation of Fig. 1.12 is seldom attained. Not only does the source emissivity vary with frequency, but often the sensitivity of the photomultiplier is also frequency-dependent. Thus the baseline—the 'sample-empty' condition—is never horizontal, although matters can usually be arranged so that it is approximately linear. Further, since it is impossible to make either of the slits infinitely narrow, a *range* of frequencies, rather than just a single frequency, falls on the photomultiplier at any given setting of the prism. This results in a broadening of the absorbance peak, and the final spectrum may appear rather as in Fig. 1.13. In this

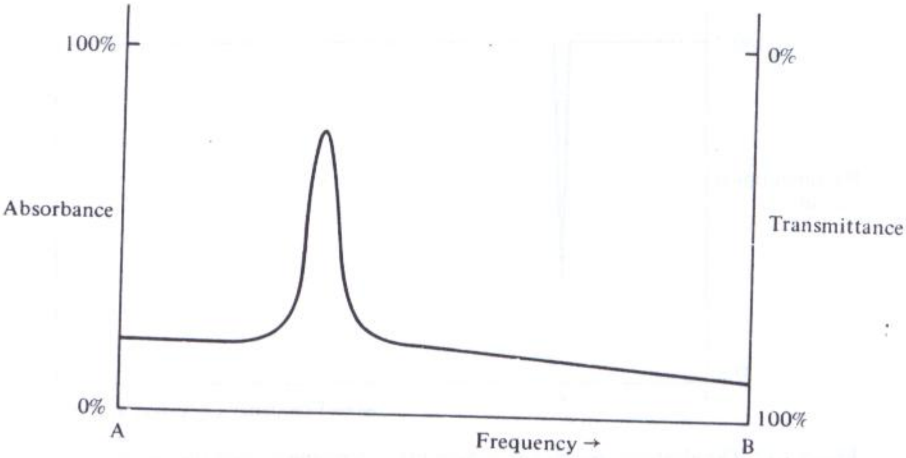

Figure 1.13 The usual appearance of the spectrum of a molecule undergoing a single transition (cf. Fig. 1.12); here the background is no longer constant and the absorption region is of finite width.

figure, too, we have plotted absorbance upwards from 0 to 100% and transmittance—its complement—downwards. This is the usual way in which such spectra are represented.

If there are again several energy levels available to the sample, it is very unlikely that there is the same probability of transition between the various levels. The question of transition probability will be discussed more fully in Sec. 1.7 but here we may note that differences in transition probability will mean that the absorbance (or transmittance) at each absorbing frequency will differ. This is shown by the varying intensities of the lines on the photographic plate of Fig. 1.10 and, more precisely, by the recorder trace of Fig. 1.14(*a*).

Figure 1.14(*a*) shows the sort of record which is produced by most modern spectrometers, whatever the region in which they operate. One other form of presentation is often adopted, however, particularly in the microwave and radiofrequency regions, and this is to record the *derivative* of the spectral trace instead of the trace itself. The derivative of a curve is simply its slope at a given point. In calculus notation, the derivative of the spectral trace is $\mathrm{d}A/\mathrm{d}\nu$, where A is the absorbance. The derivative record is thus a plot of the slope $\mathrm{d}A/\mathrm{d}\nu$ against ν; this is shown in Fig. 1.14(*b*) corresponding to the plot of Fig. 1.14(*a*).

Although at first sight more complex, the derivative trace has advantages over the direct record in some circumstances. Firstly, it indicates rather more precisely the centre of each absorbance peak: at the centre of a peak, the A curve is horizontal, hence $\mathrm{d}A/\mathrm{d}\nu$ is zero, and the centres are marked by the intersection of the derivative curve with the axis. Further, for

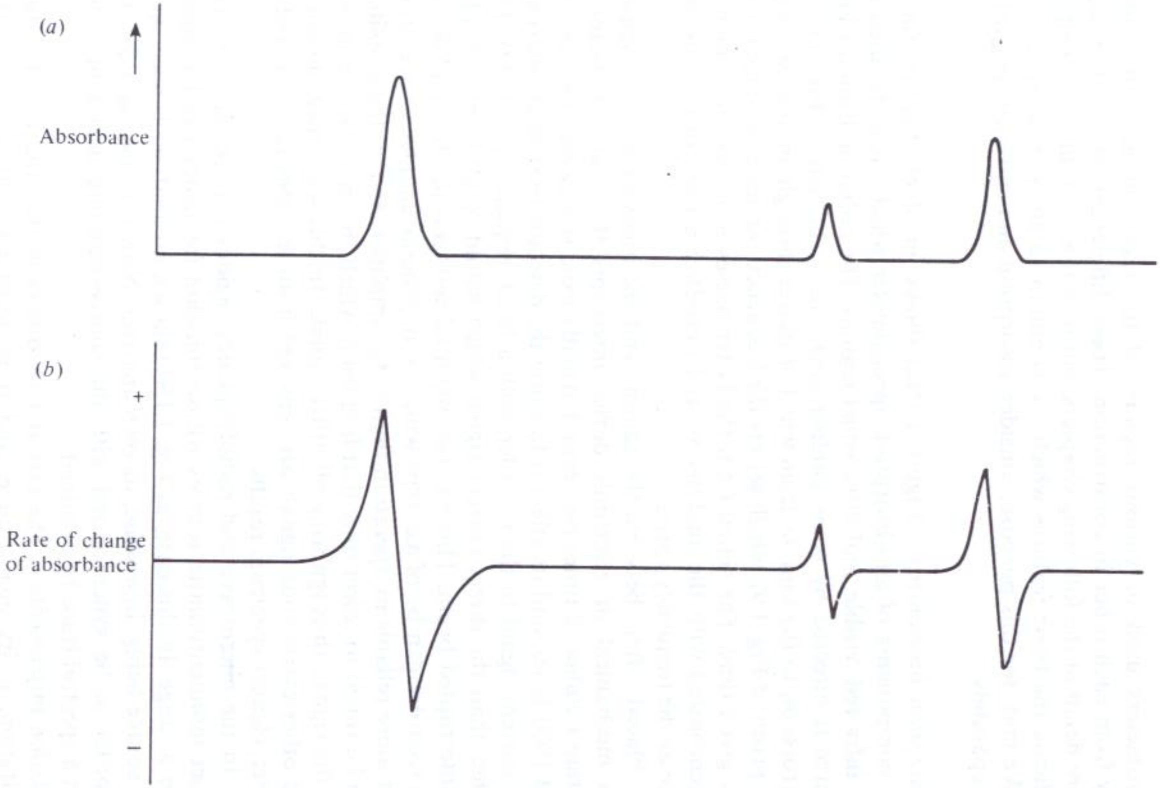

Figure 1.14 To illustrate the relation between absorption and derivative spectra: in (*a*) the absorption nuclear magnetic resonance spectrum of benzyl alcohol, $C_6H_5CH_2OH$, is shown, and in (*b*) the derivative (or dispersion) spectrum of the same molecule.

instrumental reasons, it is often better to measure the relative intensities of absorbance peaks from the derivative curve than from the direct trace.

1.5 BASIC ELEMENTS OF PRACTICAL SPECTROSCOPY

Spectrometers used in various regions of the spectrum naturally differ widely from each other in construction. These differences will be discussed in more detail in the following chapters, but here it will probably be helpful to indicate the basic features which are common to all types of spectrometer. We may, for this purpose, consider absorption and emission spectrometers separately.

1. *Absorption instruments.* Figure 1.15(*a*) shows, in block diagram form, the components of an absorption spectrometer which might be used in the infra-red, visible, and ultra-violet regions. The radiation from a white source is directed by some guiding device (e.g., the lens of Fig. 1.9, or mirrors) on to the sample, from which it passes through an analyser (e.g., the prism of Fig. 1.9), which selects the frequency reaching the detector at any given time. The signal from the latter passes to a recorder which is synchronized with the analyser so as to produce a trace of the absorbance as the frequency varies.

   Placed, often, between the sample and the analyser is a *modulator*; this mechanical or electronic device interrupts the radiation beam a certain number of times per second, usually fixed somewhere between 10 and 1000 times, and its effect is to cause the detector to send an alternating current signal to the recorder, with a fixed frequency of 10–1000 Hz, rather than the direct current signal which would result from a steady, uninterrupted beam. This has two main advantages: (*a*) the amplifier in the recorder can be of a.c. type which is, in general, simpler to construct and more reliable in operation than a d.c. amplifier, and (*b*) the amplifier can be tuned to select only that frequency which the modulator imposes on the signal, thus ignoring all other signals. In this way stray radiation and other extraneous signals are removed from the spectral trace and a better, cleaner spectrum results.

   In the microwave and radiofrequency regions it is possible to construct monochromatic sources whose emission frequency can be varied over a range. In this case, as Fig. 1.15(*b*) shows, no analyser is necessary, the source being, in a sense, its own analyser. Now it is necessary for the recorder to be synchronized with the source-scanning device in order that a spectral trace be obtained.
2. *Emission instruments.* The layout now differs in that the sample, after excitation, is its own source, and it is necessary only to collect the emitted radiation, analyse, and record it in the usual way. Figure 1.16

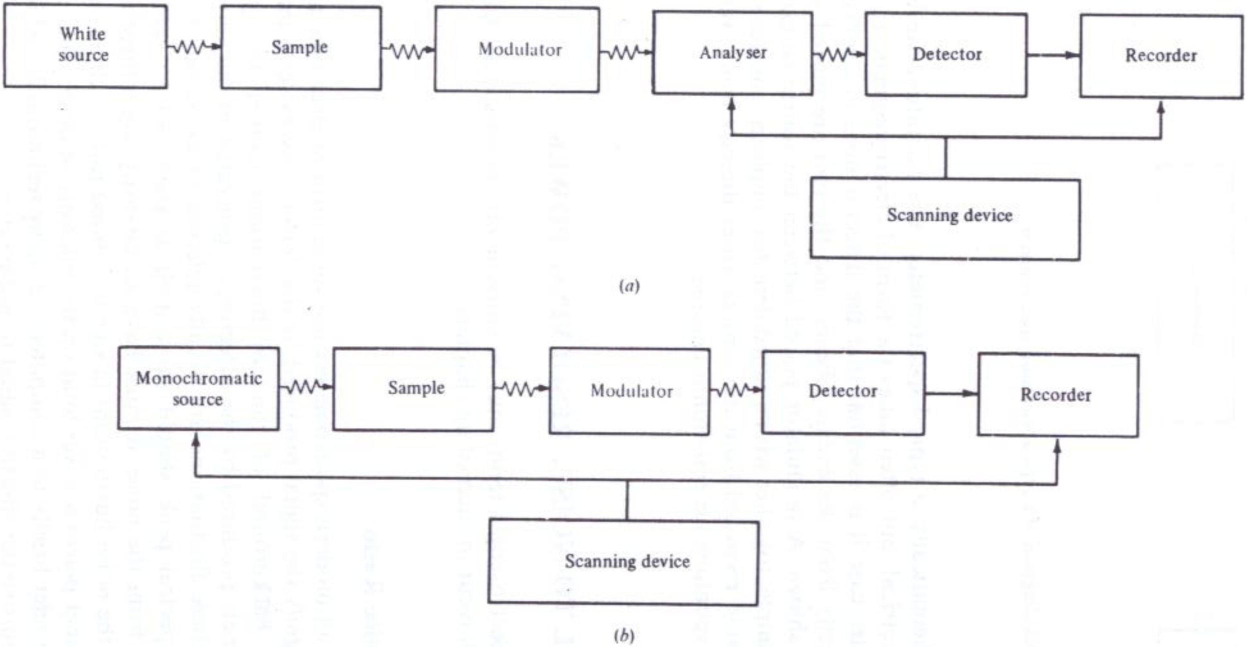

Figure 1.15 Block diagram of a typical absorption spectrometer for use in (*a*) the infra-red, visible, and ultra-violet regions where a 'white' source is available, and (*b*) the microwave and radiofrequency regions where the source can be tuned over a considerable range of frequencies.

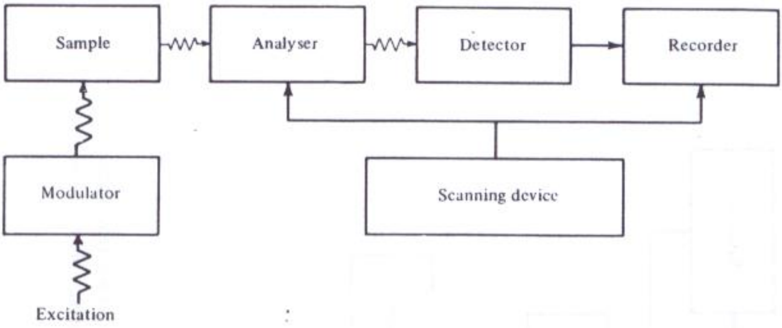

Figure 1.16 Block diagram of a typical emission spectrometer.

shows, schematically, a typical spectrometer. The excitation can be thermal or electrical, but often takes the form of electromagnetic radiation. In the latter case it is essential that the detector does not collect radiation directly from the exciting beam, and the two are placed at right angles as shown. A modulator placed between the source of excitation and the sample, together with a tuned detector-amplifier, ensures that the only emission recorded from the sample arises directly from excitation; any other spontaneous emission is ignored.

1.6 SIGNAL-TO-NOISE: RESOLVING POWER

Two other spectroscopic terms may be conveniently discussed at this point since they will recur in succeeding chapters.

Signal-to-Noise Ratio

Since almost all modern spectrometers use some form of electronic amplification to magnify the signal produced by the detector, every recorded spectrum has a background of random fluctuations caused by spurious electronic signals produced by the detector, or generated in the amplifying equipment. These fluctuations are usually referred to as 'noise'. In order that a real spectral peak should show itself as such and be sufficiently distinguished from the noise, it must have an intensity some three or four times that of the noise fluctuations (a signal-to-noise ratio of three or four). This requirement places a lower limit on the intensity of observable signals. In Sec. 1.9 we refer briefly to a computer-averaging technique by which it is possible to improve the effective signal-to-noise ratio.

Resolving Power

This is a somewhat imprecise concept which can, however, be defined rather arbitrarily and is often used as a measure of the performance of a spectrometer. We shall here consider it in general terms only.

No molecular absorption takes place at a single frequency only, but always over a spread of frequencies, usually very narrow but sometimes quite large (see Sec. 1.7); it is for this reason that we have up to now drawn spectra with broadened line shapes (cf. Fig. 1.14(*a*)).

Let us consider two such lines close together, as on the right of Fig. 1.17(*a*): the dotted curve represents the absorption due to each line separately, the full line their combined absorption. We shall first take the exit slit width to be larger than the separation between the lines. Scanning the

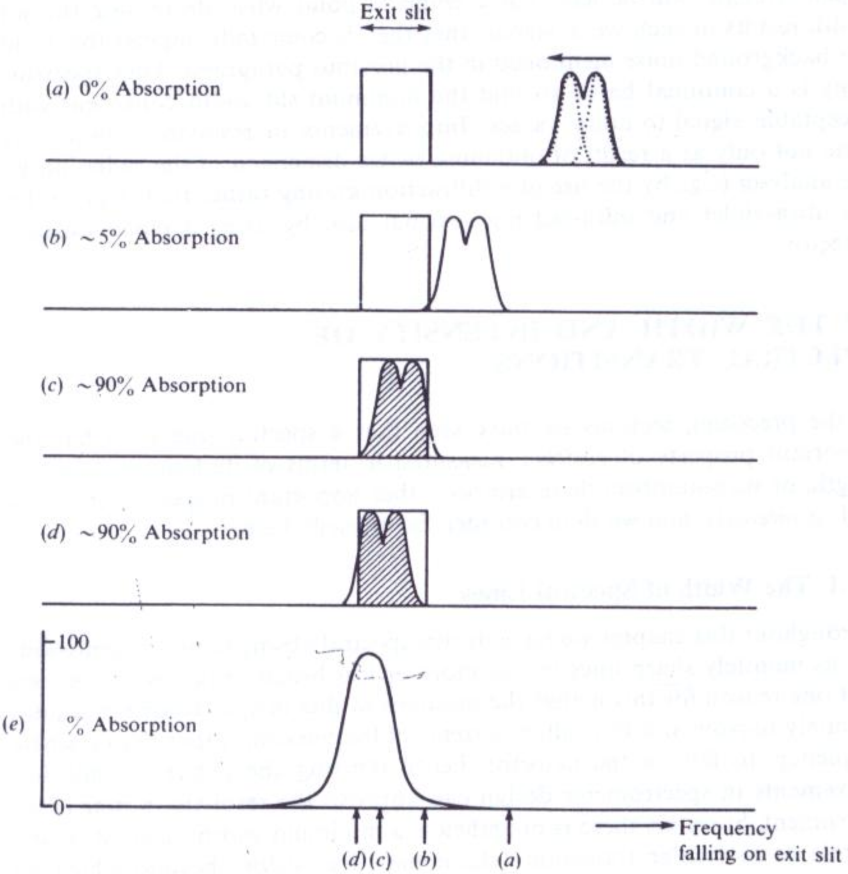

Figure 1.17 Illustrating the relation between slit width and resolving power: see text for discussion.

spectrum plainly involves moving the twin absorbance peaks steadily to the left so that they pass across the exit slit and into the detector; the situation at successive stages is shown in (*b*), (*c*), and (*d*) of Fig. 1.17, the shaded area showing the amount of absorbance which the detector would register. At (*e*) of this figure, the absorbance is plotted against frequency, together with the approximate positions of stages (*a*), (*b*), (*c*), and (*d*).

It is quite evident that the separation between the lines has disappeared under these conditions—the lines are not *resolved*. It is equally evident that the use of a much narrower slit would result in their resolution—the *resolving power* would be increased. In fact, provided the slit width is less than the separation between the lines, the detector output will show a minimum between them.

However, it must be remembered that a narrower slit allows less total energy from the beam to reach the detector and consequently the intrinsic signal strength will be less. There comes a point when decreasing the slit width results in such weak signals that they become indistinguishable from the background noise mentioned in the previous paragraph. Thus spectroscopy is a continual battle to find the minimum slit width consistent with acceptable signal-to-noise values. Improvements in resolving power may arise not only as a result of obtaining better dispersion of the radiation by the analyser (e.g., by the use of a diffraction grating rather than a prism for the ultra-violet and infra-red regions) but also by using a more sensitive detector.

1.7 THE WIDTH AND INTENSITY OF SPECTRAL TRANSITIONS

In the preceding sections we have seen that a spectral transition has the important property of *position*, measured in terms of its frequency, wavelength, or wavenumber; there are two other important properties, its *width* and its *intensity*, and we shall consider these briefly here.

1.7.1 The Width of Spectral Lines

Throughout this chapter we have drawn spectral absorptions and emissions not as infinitely sharp lines but as more or less broad peaks; we have seen that one reason for this is that the mechanical slits in spectrometers are not infinitely narrow and thus allow a *range* of frequencies, rather than a single frequency, to fall on the detector, hence blurring the pattern. While improvements in spectrometer design can improve the resolving power of an instrument, however, there is nonetheless a minimum width inherent in any atomic or molecular transition—the *natural line width*—beyond which no instrument, however superior, will show a sharpening. This width arises essentially because the energy levels of atomic and molecular systems are not precisely determined, but have a certain fuzziness or imprecision. Several factors contribute to this.

1. *Collision broadening.* Atoms or molecules in liquid and gaseous phases are in continual motion and collide frequently with each other. These collisions inevitably cause some deformation of the particles and hence perturb, to some extent, the energies of at least the outer electrons in each. This immediately gives a possible explanation for the width of visible and ultra-violet spectral lines, since these deal largely with transitions between outer electronic shells. Equally vibrational and rotational spectra are broadened since collisions interfere with these motions too. In general, molecular interactions are more severe in liquids than in gases, and gas-phase spectra usually exhibit sharper lines than those of the corresponding liquid.

   In the case of solids, the motions of the particles are more limited in extent and less random in direction, so that solid-phase spectra are often sharp but show evidence of interactions by the splitting of lines into two or more components.
2. *Doppler broadening.* Again in liquids and gases the motion of the particles causes their absorption and emission frequencies to show a Doppler shift; since the motion is random in a given sample, shifts to both high and low frequencies occur and hence the spectral line is broadened. In general, for liquids collision broadening is the most important factor, whereas for gases, where collision broadening is less pronounced, the Doppler effect often determines the natural line width.
3. *Heisenberg uncertainty principle.* Even in an isolated, stationary molecule or atom the energy levels are not infinitely sharp, due to the operation of a fundamental and very important principle, the Uncertainty Principle of Heisenberg. In effect this says that, if a system exists in an energy state for a limited time δt seconds, then the energy of that state will be uncertain (fuzzy) to an extent δE where

   $$\delta E \times \delta t \approx h/2\pi \approx 10^{-34} \text{ J s} \tag{1.10}$$

   where h is again Planck's constant. Thus we see that the lowest energy state of a system *is* sharply defined since, left to itself, the system will remain in that state for an infinite time; thus $\delta t = \infty$, and $\delta E = 0$. But, for example, the lifetime of an excited electronic state is usually only about 10^{-8} s, which gives a value for δE of about $10^{-34}/10^{-8} = 10^{-26}$ J. A transition between this state and the ground state will thus have an energy uncertainty of δE, and a corresponding uncertainty in the associated radiation frequency of $\delta E/h$, which we can write as:

   $$\delta \nu = \frac{\delta E}{h} \approx \frac{h}{2\pi h \delta t} \approx \frac{1}{2\pi \delta t} \tag{1.11}$$

Thus for our example of an excited electronic state lifetime of 10^{-8} s, $\delta\nu \approx 10^8$ Hz. This apparently large uncertainty is, in fact, small compared with the usual radiation frequency of such transitions, 10^{14}–10^{16} Hz, and so the natural line width is said to be small; in fact, the apparent widths of electronic transitions are far more dependent on collision and Doppler broadening than on energy uncertainties.

On the other hand an excited electron *spin* state may exist for some 10^{-7} s which, from Eq. (1.11), leads to a frequency uncertainty of some 10^7 Hz for a transition. This, compared with the usual frequency of such transitions, 10^8–10^9 Hz, represents a very broad transition indeed, and here the Heisenberg uncertainty relation is by far the most important effect.

Further examples of the application of Heisenberg's principle will be given in later chapters.

1.7.2 The Intensity of Spectral Lines

When discussing spectral intensities there are three main factors to be considered: the likelihood of a system in one state changing to another state—the *transition probability*; the number of atoms or molecules initially in the state from which the transition occurs—the *population*; and the amount of material present giving rise to the spectrum—the *concentration* or *path length* of the sample.

1. *Transition probability*. The detailed calculation of absolute transition probabilities is basically a straightforward matter, but as it involves a knowledge of the precise quantum mechanical wave functions of the two states between which the transition occurs, it can seldom be done with accuracy and is, in any case, beyond the scope of this book. We shall generally content ourselves with qualitative statements about relative transition probabilities without attempting any detailed calculations.

   At a much lower level of sophistication, however, it is often possible to decide whether a particular transition is forbidden or allowed (i.e., whether the transition probability is zero or non-zero). This process is essentially the deduction of *selection rules*, which allow us to decide between which levels transitions will give rise to spectral lines, and it can often be carried out through pictorial arguments very like those we have already used in discussing the activity or otherwise of processes in Sec. 1.3.
2. *Population of states*. If we have two levels from which transitions to a third are equally probable, then obviously the most intense spectral line will arise from the level which initially has the greater population. There

is a simple statistical rule governing the population of a set of energy levels.

For example, if we have a total of N molecules distributed between two different energy states, a lower and an upper with energies E_{lower} and E_{upper}, respectively, we would intuitively expect most of the molecules to occupy the lower state. Proper statistical analysis bears this out and shows that, *at equilibrium*

$$\frac{N_{\text{upper}}}{N_{\text{lower}}} = \exp(-\Delta E/kT) \tag{1.12}$$

where $\Delta E = E_{\text{upper}} - E_{\text{lower}}$, T is the temperature in K, and k is a universal constant. The expression is known as the Boltzmann distribution, after its originator, and k, which has a value of $1{\cdot}38 \times 10^{-23}$ J K^{-1}, as Boltzmann's constant. Examples showing the use of this very important expression will recur throughout the remaining chapters.

3. *Path length of sample*. Clearly if a sample is absorbing energy from a beam of radiation, the more sample the beam traverses the more energy will be absorbed from it. We might expect that twice as much sample would give twice the absorption, but a very simple argument shows that this is not so. Consider two identical samples of the same material, S_1 and S_2, and assume that S_1 or S_2 alone absorb 50 per cent of the energy falling on them, allowing the remaining 50 per cent to pass through. If we pass a beam of initial intensity I_0 through S_1, 50 per cent of I_0 will be absorbed and the intensity of the beam leaving S_1 will be $\frac{1}{2}I_0$; if we then pass this beam through S_2 a further 50 per cent will be absorbed, and $\frac{1}{2} \times \frac{1}{2}I_0 = \frac{1}{4}I_0$ will leave S_2. Thus two 50 per cent absorptions in succession do not add up to 100 per cent but only to 75 per cent absorption. An exactly similar relationship exists between the *concentration* of a sample and the amount of energy absorption—a doubling of the concentration produces something less than a doubling of the absorption.

   These relationships are best expressed in terms of the Beer–Lambert law, which is:

$$\frac{I}{I_0} = \exp(-\varepsilon cl) \tag{1.13}$$

where I_0 is the intensity of radiation falling on the sample, and I that part transmitted, c and l are the sample concentration and length, and ε is the extinction coefficient or absorption coefficient, which is a constant for a given type of transition (e.g., electronic, vibrational, etc.) occurring within a particular sample. Clearly ε is closely connected with the transition probability discussed above, a large probability being associated with a large ε, and vice versa.

1.8 FOURIER TRANSFORM SPECTROSCOPY

One of the major disadvantages of the conventional method of producing a spectrum, such as that of Fig. 1.13, is its inherent slowness. Essentially each point of the spectrum has to be recorded separately—the spectrometer is set to start reading at one end, the frequency is swept smoothly across the whole span of the spectrum, and the detector signal is monitored and recorded. The inefficiency of such a method is clear when one considers taking a spectrum with only one or two 'lines' in it—we have to sweep from one end to the other in order to find the lines, but most of the time is spent recording nothing but background noise. Until recently it was only in the visible and ultra-violet regions that the whole of a spectrum could be recorded simultaneously—on a photographic plate—but a new development, Fourier transform spectroscopy, is providing simultaneous and almost instantaneous recording of the whole spectrum in the magnetic resonance, microwave, and infra-red regions. In this section we shall briefly discuss the basic ideas of the technique, leaving to later chapters more detailed consideration of its methods and applications.

Although equally applicable to both emission and absorption spectroscopy, it is probably easier to visualize Fourier transform (FT) spectroscopy in terms of emission, so let us take the spectrum of Fig. 1.13 to represent the emission of radiation by a sample. Further we shall, for the moment, ignore the line-broadening discussed in the previous section, and think of this radiation as a pure sine wave at some quite precise frequency, ν. If a detector capable of responding sufficiently rapidly receives this emitted radiation, its output will be an oscillating signal, again of frequency ν. Note that we here consider the detector output as a function of *time* ('time domain' spectroscopy) rather than as the function of frequency ('frequency domain') plotted in Fig. 1.13.

Now consider a sample-emitting radiation at two different frequencies; a detector receiving the total radiation will 'see' the *sum* of the two sine waves. We illustrate, diagrammatically, the two separate but superimposed waves in Fig. 1.18(*a*), and their sum in (*b*), and we note that the detector output shows an oscillation due to the frequency of the two waves, but also a slow increase and decrease in overall amplitude. This latter is often called the 'beat' frequency, by analogy with a similar phenomenon for musical tones, and it arises because the two component waves are sometimes 'in step' (as at points *A* and *B* in Fig. 1.18 where their amplitudes reinforce each other), and sometimes out of step (as at *C* where they cancel). In fact the beat frequency is always equal to the *difference* in frequency of the component waves—if they differ in frequency by 10 cycles per second (Hz) then the beat oscillation is also at 10 Hz. This is illustrated by Fig. 1.18(*c*) and (*d*) where we show sine waves with half the frequency separation of those in Fig. 1.18(*a*) and (*b*), and we see that the beat frequency has also halved.

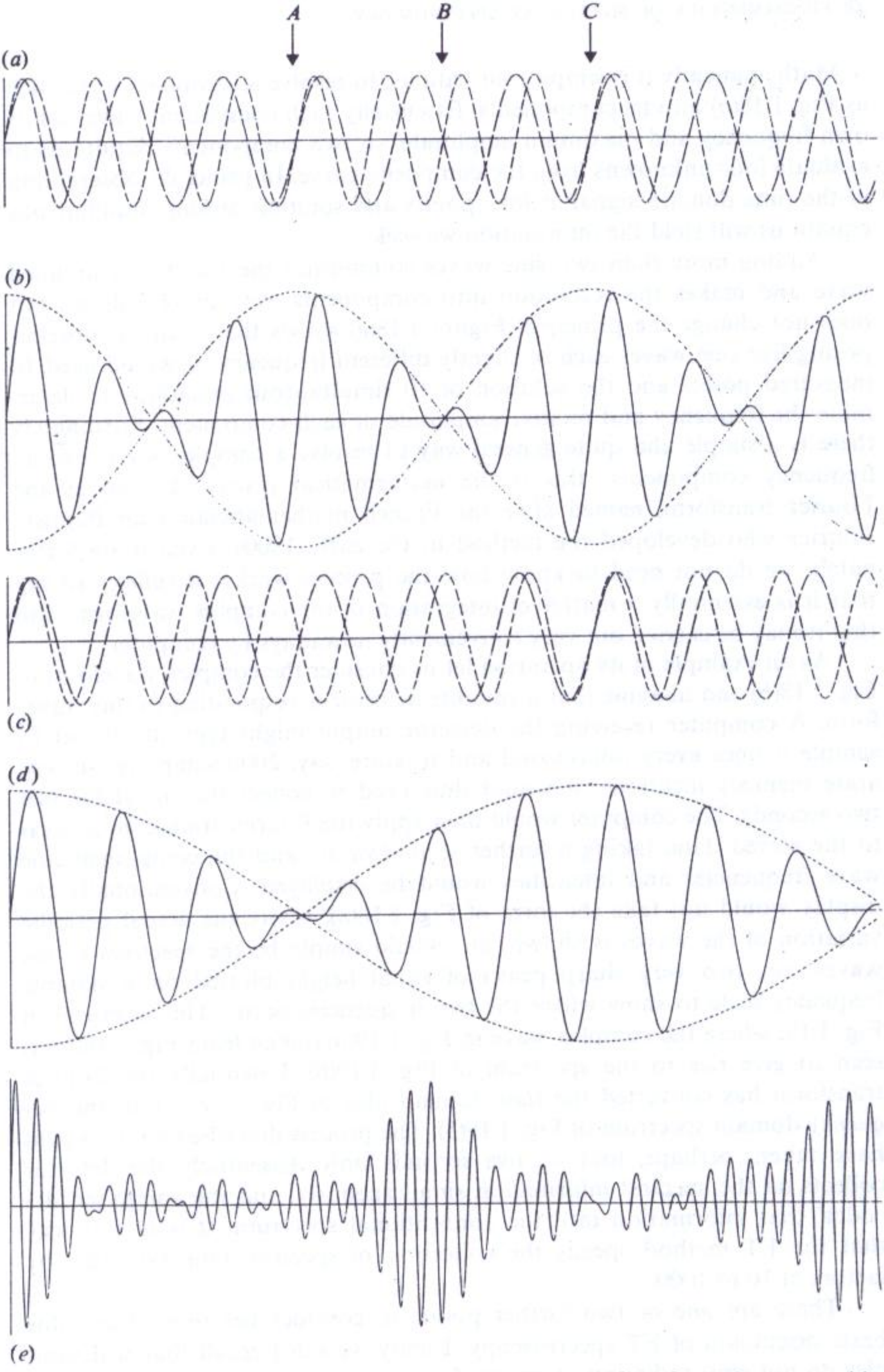

Figure 1.18 Adding of sine waves. (*a*) and (*c*) show the superposition of two sine waves with slightly different frequency, with (*b*) and (*d*) their sums; (*e*) shows the summation of five sine waves with different frequencies.

Mathematically it is simple, but tedious, to resolve a combined wave such as Fig. 1.18(*b*) into its components. Essentially each component wave has its own frequency and maximum amplitude, so two components require us to evaluate four unknowns from the composite curve. In principle, observation of the time domain signal at four points and solution of four simultaneous equations will yield the information we seek.

Adding more than two sine waves complicates the resultant combined wave and makes the resolution into components even more tedious, but does not change the principle. Figure 1.18(*e*) shows the result of superimposing five sine waves each of slightly different frequency. It would need 10 measured points and the solution of 10 simultaneous equations to determine the frequency and relative amplitude of each component. Fortunately there is a simple and quite general way to resolve a complex wave into its frequency components; this is the mathematical process known as the Fourier transform, named after the French mathematician Jean Baptiste Fourier who developed the method in the early 1800s. Even more fortunately we do not need to know how the process works: it suffices to say that it is essentially a matter of integration of the complex waveform, and that it may be carried out very conveniently nowadays by computer.

As an example of its operation let us consider the complex waveform of Fig. 1.18(*b*) and imagine that a suitable detector is responding to this waveform. A computer receiving the detector output might typically be set to sample it once every millisecond and to store, say, 2000 samplings in separate memory locations; it would thus need to collect the signal for just two seconds. The computer would then apply the Fourier transform process to the stored data, taking a further second or so, and the component sine wave frequencies and intensities would be displayed. Conventionally the display would not take the form of Fig. 1.18(*a*), where the actual periodic variation of the waves is shown, but would simply be the *spectrum* of the waves, i.e., two very sharp peaks of equal height plotted on a suitable frequency scale to show where the two frequencies occur. This is shown in Fig. 1.19, where the complex wave in Fig. 1.19(*a*) (taken from Fig. 1.18(*b*)) is seen to give rise to the spectrum of Fig. 1.19(*b*). Essentially the Fourier transform has converted the *time* domain plot of Fig. 1.19(*a*) into the *frequency* domain spectrum of Fig. 1.19(*b*). The process described above would have taken, perhaps, four or five seconds only. Essentially the detector collects *all* the spectral information simultaneously, and the computer 'decodes' that information into the conventional spectrum. It is in this way that the FT method speeds the collection of spectral data, typically, by factors of 10 to 1000.

There are one or two further points to consider before we leave this basic discussion of FT spectroscopy. Firstly we must recall that real samples do not emit radiation at precise frequencies; as we saw in the previous section, each emission is more or less broadened by various processes, and

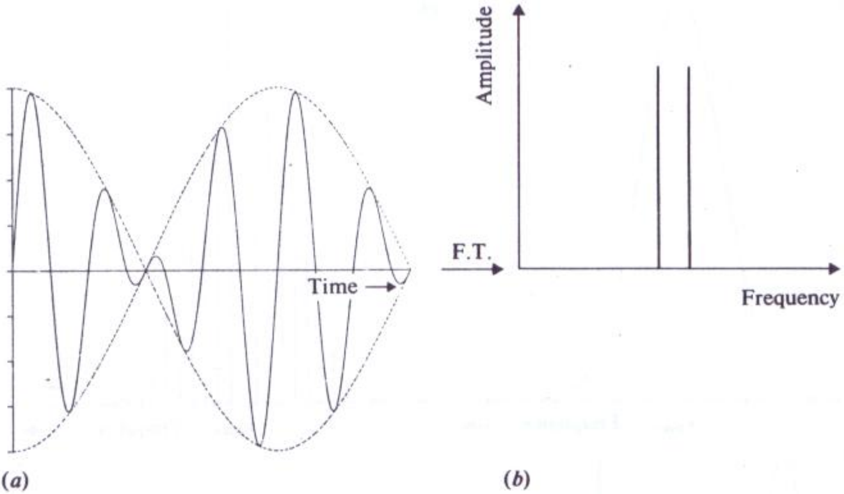

Figure 1.19 The use of the Fourier transform to convert the summed sine waves of (*a*) into their frequency spectrum, (*b*).

so each 'line' is really a small package of slightly different frequencies. We show a typical package in Fig. 1.20(*a*). In Fig. 1.20(*b*) we see that the package can be considered as arising from a large number of sample molecules radiating at exactly ν_{max}, the frequency maximum of the package, with a smaller number of molecules radiating at frequencies away from that maximum, the number decreasing as the separation increases. Now, if we want to discover the total signal emitted by such a package we could, if we had the time, plot out a sine wave for each frequency using an intensity proportional to the number of molecules radiating at that frequency, and then add all the sine waves together. We are fortunately spared this task because it turns out that the Fourier transform is a reciprocal process; just as FT converts a time domain signal to a frequency domain spectrum, so it will carry out the reverse conversion. Thus if we supply the frequency curve of Fig. 1.20(*a*) to a computer and carry out the FT, the resultant display will be exactly the same as adding the component sine waves. The result is shown in Fig. 1.20(*c*).

We see that a detector receiving the total radiation from a single broad-line emission will show an oscillating signal whose overall amplitude decays smoothly to zero. The oscillation is the beat pattern set up by all the superimposed, but slightly different, sine waves emitted by the samples; and the signal decays because, if we imagine all the waves in the package to be 'in step' initially, after some time has elapsed the many different frequencies concerned will be very much out of step, and on average half will have their amplitudes in the positive sense and half in the negative, thus giving a

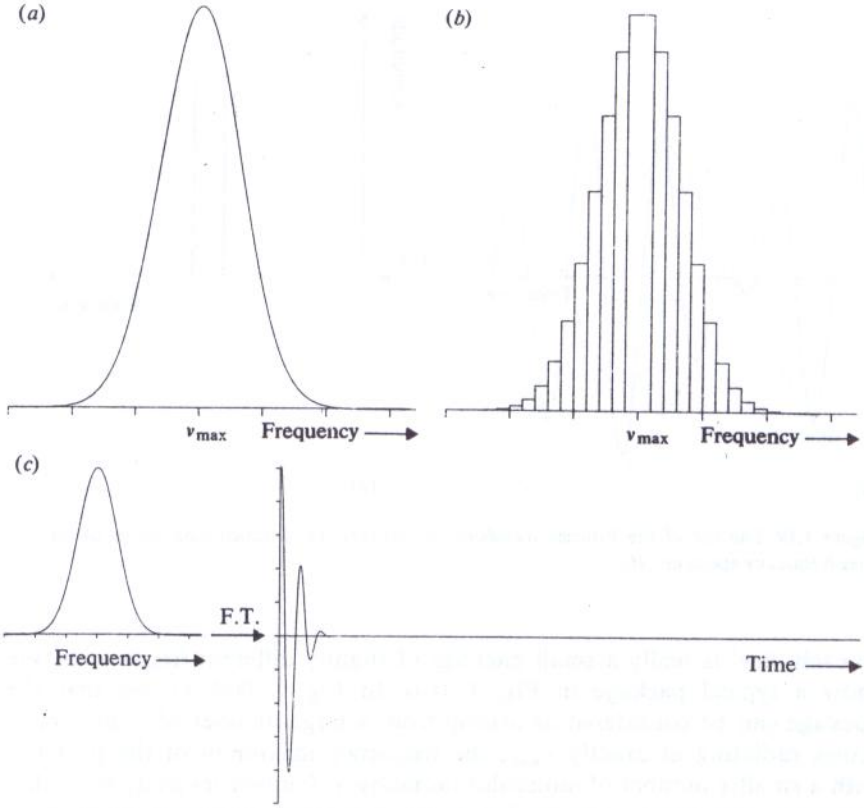

Figure 1.20 (*a*) shows the frequency distribution of a broad spectral line and (*b*) an approximate histogram of the frequencies; (*c*) is the Fourier transform of (*a*).

resultant sum of zero. Another way to think of this is to remember that two waves setting out in step with an infinitesimally small difference in frequency will take an infinite time to get back in step again, i.e., they will never do so. The distribution of Fig. 1.20(*a*) has many infinitely close frequencies within it and so, after a few cycles, none of the individual waves ever get back into step again. If the band had been *infinitely* broad, i.e., containing an infinite number of infinitesimally close neighbours, none would have ever been in step after the first instant, and the FT of such a 'white' source is a single decaying signal with no beats. We shall return to this in a moment.

The corollary of these arguments is that the *rate of decay* of the overall signal is dependent on the *width* of the original spectral peak. This is illustrated in Figs. 1.21(*a*) and (*b*) where (*a*) shows the FT of a relatively narrow signal and (*b*) that of a broader signal at the same central frequency.

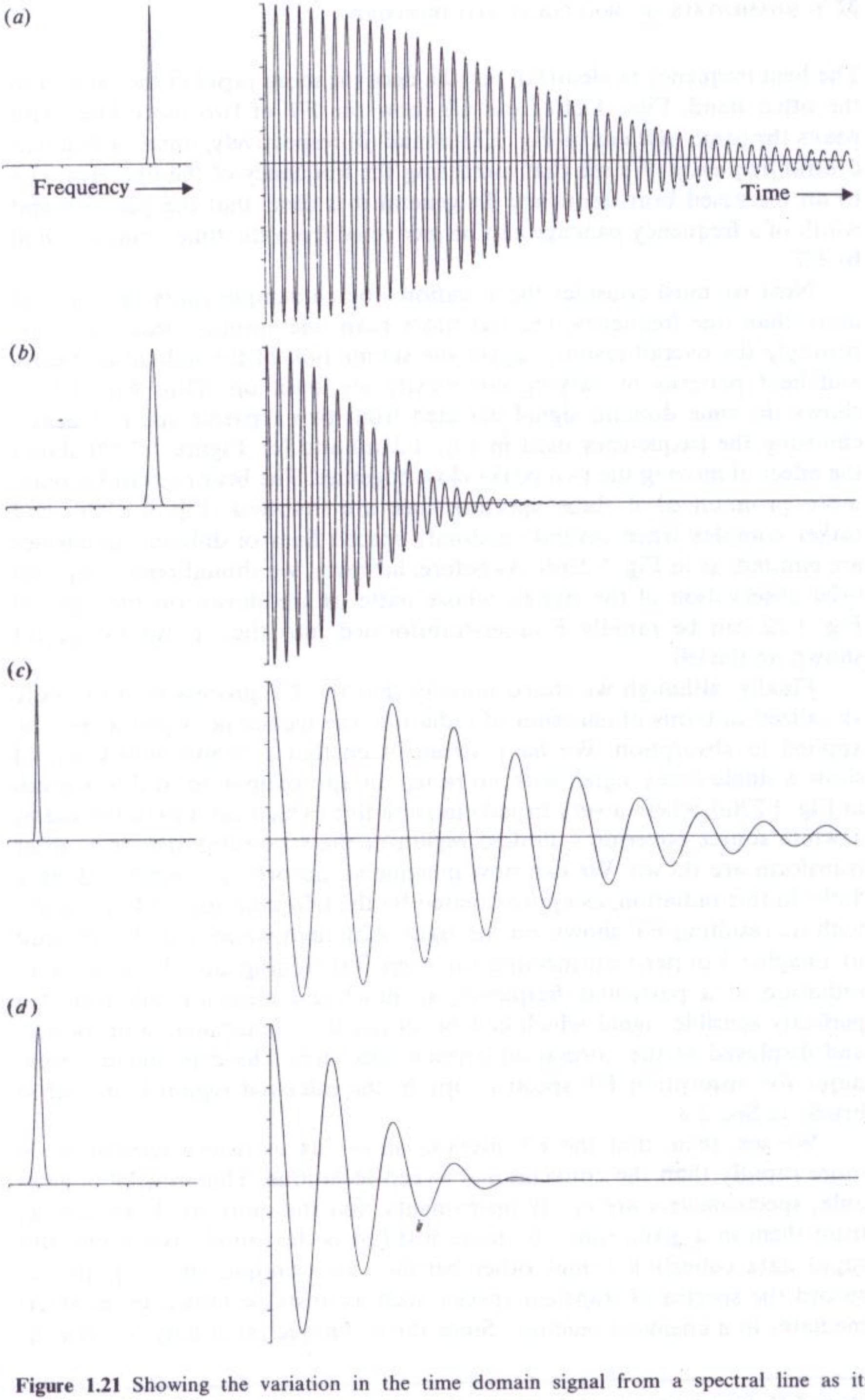

Figure 1.21 Showing the variation in the time domain signal from a spectral line as its position and breadth vary.

The beat frequency is identical, but the decay is more rapid in the latter. On the other hand, Figs. 1.21(*c*) and (*d*) show the FT of two more lines with peaks the same *width* as in Fig. 1.21(*a*) and (*b*) respectively, but at a different central *frequency*. We see that increasing the frequency of the line gives rise to an increased beat frequency. In general it is clear that the position and width of a frequency package can be recovered from the time domain signal by FT.

Next we must consider the situation when a sample emits radiation at more than one frequency, i.e., has more than one spectral peak. Not surprisingly the overall result is again the summation of the individual peaks, and beat patterns of varying complexity are built up. Thus Fig. 1.22(*a*) shows the time domain signal detected from two separate spectral peaks, choosing the frequencies used in Fig. 1.21(*a*) and (*c*). Figure 1.22(*b*) shows the effect of moving the two peaks close together. The beat pattern becomes more pronounced if three spectral lines are involved (Fig. 1.22(*c*)), and rather complex when several randomly spaced lines of different intensities are emitted, as in Fig. 1.22(*d*). As before, however, we should remember that brief observation of the signals whose patterns are shown on the right of Fig. 1.22 can be rapidly Fourier-transformed into their resultant spectra shown on the left.

Finally, although we stated initially that the FT process is most easily visualized in terms of emission of radiation, the technique is just as readily applied to absorption. We have already seen that a 'white' source would show a single decay signal with no beats; an approximation to this is given in Fig. 1.23(*a*), where a very broad emission line (which can be considered as a white source covering a limited region of the spectrum) and its Fourier transform are shown. We can now imagine an absorbing sample making a 'hole' in this radiation, as approximated by the left-hand side of Fig. 1.23(*b*), with its resulting FT shown on the right. Although we may find it difficult to imagine Fourier-transforming (or even just adding up) the *absence* of radiation at a particular frequency, in practice a detector will collect a perfectly sensible signal which can be stored by a computer, transformed, and displayed as the normal adsorption spectrum. The experimental technique for absorption FT spectroscopy in the infra-red region is described briefly in Sec. 3.8.

We see, then, that the FT method allows us to record spectra much more rapidly than the conventional sweep technique. This in itself is valuable; spectrometers are costly instruments, and the more work we can get from them in a given time, the more justified is the initial investment. But rapid data collection brings other benefits, for example, in being able to record the spectra of transient species such as unstable molecules or intermediates in a chemical reaction. Since the technique essentially reduces the

Figure 1.22 Time domain signals from several spectral lines.

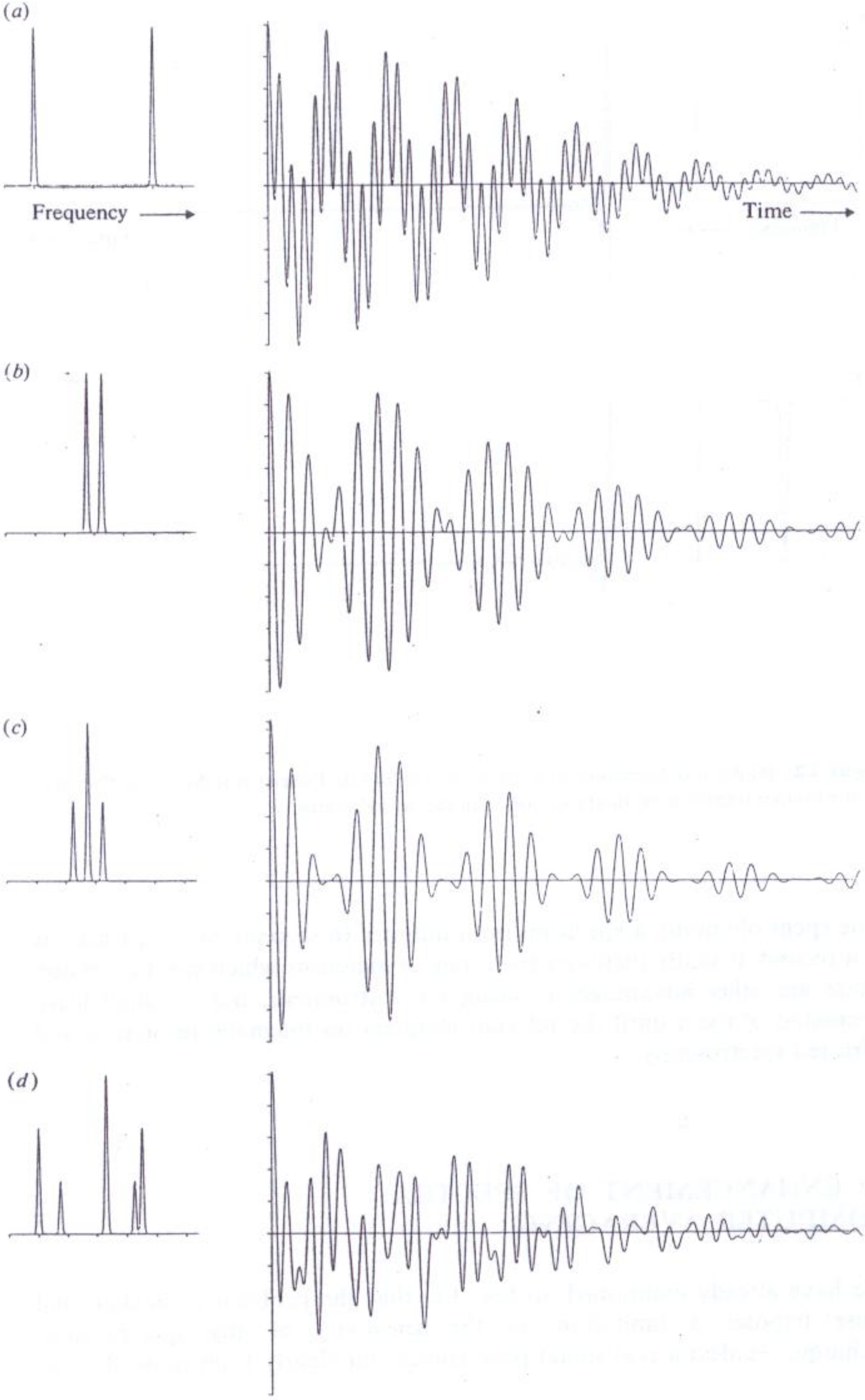
(a)
Frequency →
Time →
(b)
(c)
(d)

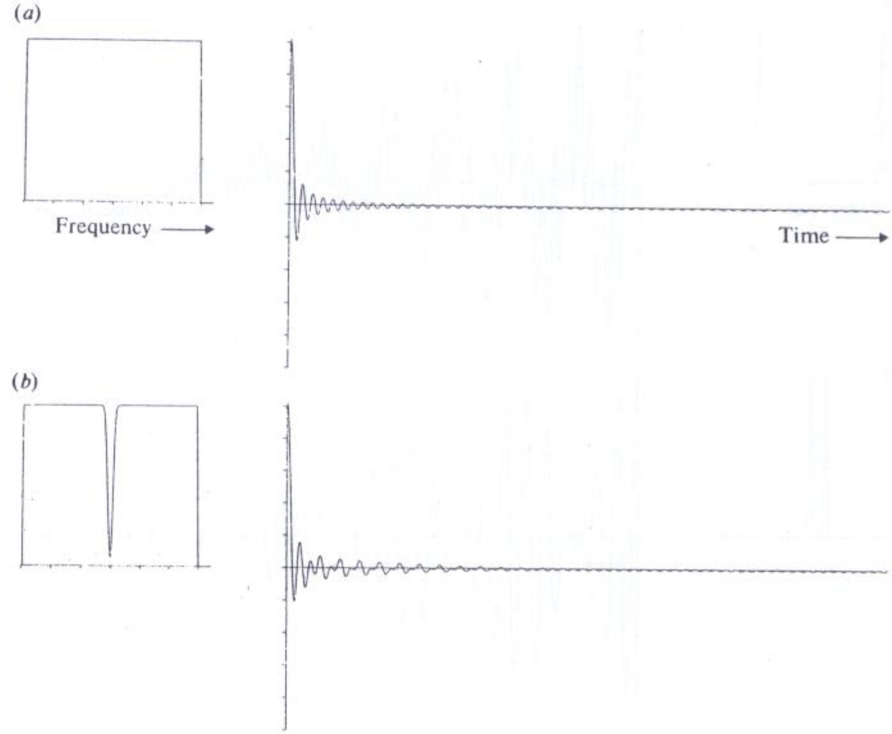

Figure 1.23 (*a*) An approximation to a 'white' source and its Fourier transform. (*b*) The effect on the Fourier transform of an absorption from the 'white' source.

time spent obtaining a spectrum from minutes to seconds or even fractions of a second, it vastly increases the range of materials which can be studied. There are other advantages in using FT instruments, but we shall leave discussion of them until the relevant chapters on magnetic resonance and infra-red spectroscopy.

1.9 ENHANCEMENT OF SPECTRA: COMPUTER AVERAGING

We have already mentioned, in Sec. 1.6, that the problem of background noise imposes a limitation on the sensitivity of any spectroscopic technique—unless a real signal peak stands out clearly from noise fluctuations it is impossible to be sure that it *is* a signal. A signal-to-noise (S/N) ratio of 3 or 4 is usually reckoned necessary for unambiguous recognition of a signal. There are several ways in which S/N can be improved for a given sample, but all require the expenditure of time. Thus it is possible electronically to damp out oscillations of the recorder pen so that it is less susceptible to high-frequency noise. The baseline of the spectrum will then be smoother, but, because the pen responds more slowly to any change (including changes in signal), one must sweep more slowly across the spectrum. Nor is FT spectroscopy immune from noise—detector and amplifier noises occur during the collection of data, and are transformed into spurious frequencies in the spectrum.

The advent of cheaper and more powerful computers offers another method of signal enhancement, known as 'computer averaging of transients' or the CAT technique, which involves recording the spectrum stepwise into a computer. Of course, this is already done if FT is intended, but it is just as easy to sample a frequency domain spectrum at, say, 2000 closely spaced points, and to store the intensity at each point in 2000 separate computer memory locations. This process may then be repeated as many times as we wish, but each time *adding* the new data into that already existing. Although in any one scan a weak signal may not be visible above the noise level, after n summed scans the signal will be n times larger in the store, whereas the noise, being random, will sometimes contribute to the store in a positive sense and sometimes negatively, so it will accumulate less rapidly. In fact it may be shown that n scans increase the noise level in the store by $n^{1/2}$, so the net gain in S/N is $n/n^{1/2} = n^{1/2}$.

If a single scan takes several minutes, as is usually the case in conventional frequency-sweep spectroscopy, the necessity to store 100 scans in order to give an improvement in S/N by a factor of 10 is rather costly in instrument time, so CAT techniques are not often applied to such measurements. However, the combination of CAT with FT is very powerful indeed. Here one time-domain scan can be completed in a second or two, and 100 scans will only occupy a couple of minutes; thus a tenfold gain in S/N can be achieved in a total time often less than that required for a non-enhanced spectrum by ordinary sweep methods. So useful is the combination of CAT with FT that virtually all FT spectrometers are routinely equipped with CAT facilities.

Other benefits follow from the addition of a computer to a spectrometer. The spectrum of a solvent or other background can be stored in the computer and subtracted from the observed spectrum in order to isolate the spectrum of the substance, or peak intensities can be automatically measured and converted to sample concentrations. Even the operation of the spectrometer itself can usefully be entrusted to the computer—samples can be changed automatically, and the optimum operating conditions can be determined and set for each new sample.

1.10 STIMULATED EMISSION: LASERS

We have already mentioned that, once radiation has been absorbed by a sample, the sample can lose its excess energy either by thermal collisions or by re-emission of radiation. In this section we shall consider the latter process in more detail, because it leads to the very important topic of laser radiation.

Radiation may be emitted by an excited molecule or atom either *spontaneously* or as the result of some stimulus acting on the molecule, called *stimulated emission*. Which of these two processes is most likely to occur in any given case depends on the energy jump involved, i.e., on the frequency of the radiation being emitted. For high-frequency transitions (infra-red, visible, and ultra-violet upwards) spontaneous emission is by far the most likely; conversely, for low-frequency changes (microwave and magnetic resonance) spontaneous emission is unlikely and, if the right conditions obtain, stimulated emission will occur.

Stimulated emission is a resonance phenomenon—an excited state drops to the ground state (emitting radiation of frequency $\nu = \Delta E/h$, where ΔE is the energy gap), only when a photon (i.e., radiation) of the same frequency ν interacts with the system. We illustrate the situation in Fig. 1.24. On the left, in both (*a*) and (*b*), we show the excitation of a molecule by absorption of radiation of frequency $\nu_{\text{ex.}}$. At the right in (*a*) we show spon-

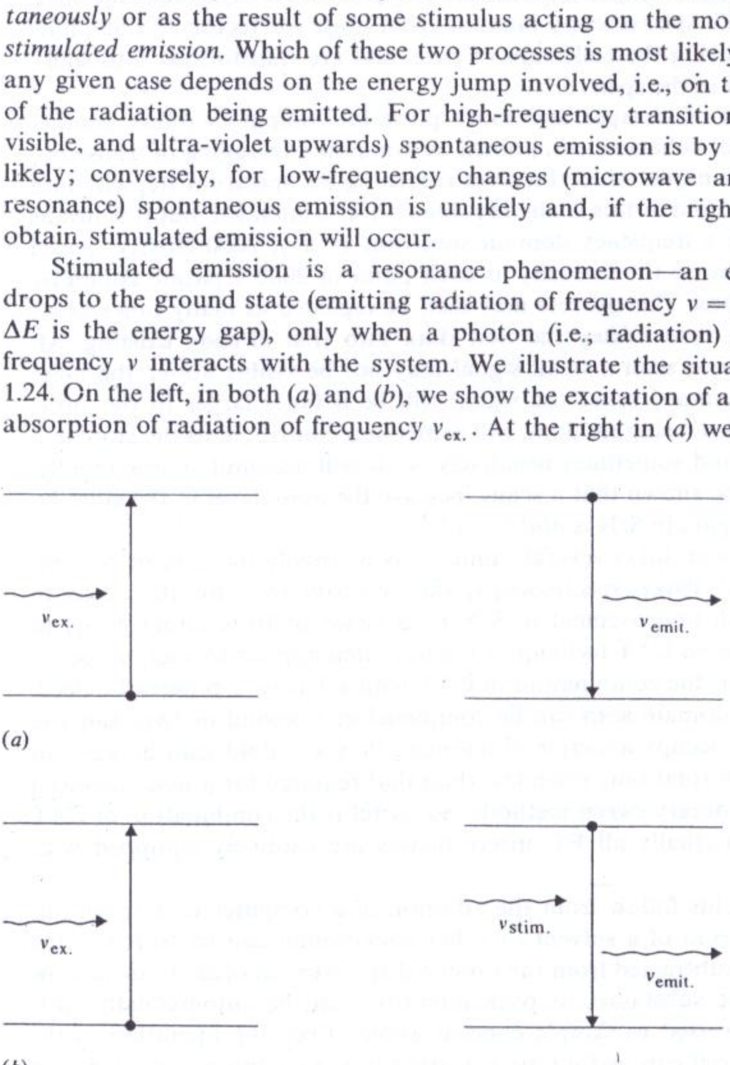

Figure 1.24 Showing (*a*) spontaneous and (*b*) stimulated emission from an excited energy state.

taneous emission, when radiation $\nu_{\text{emit.}}$ is spontaneously given out, and, in (*b*) stimulated emission where a photon of frequency $\nu_{\text{stim.}}$ interacts with the excited state and causes radiation of frequency $\nu_{\text{emit.}}$ to be released. Note particularly that, although we have given different subscripts to $\nu_{\text{ex.}}$, $\nu_{\text{emit.}}$, and $\nu_{\text{stim.}}$ in order to indicate their origins, they all represent *exactly the same frequency*, the frequency $\Delta E/h$.

Radiation emitted under stimulation of this sort has three very important qualities. Firstly it is of a very *precisely defined* frequency: the excited state does not spontaneously decay, so it is inherently long-lived, which implies (see the discussion of Heisenberg uncertainty in Sec. 1.7.1) a narrow energy level. Secondly the emitted radiation is *in phase* with the stimulating radiation: the excited state is stimulated to emit by interaction with the oscillating electromagnetic field of $\nu_{\text{stim.}}$, so it is not surprising that the maximum amplitude of the emitted wave coincides with that of $\nu_{\text{stim.}}$. And, since the waves are exactly the same frequency, they remain in phase as they leave the sample. Finally, the stimulating and emitted radiation are *coherent*, which means that they travel in precisely the same direction. In contrast *spontaneous* emission can occur at any time (so each emitted photon is not necessarily in phase with any other), in any direction, and within a more or less broad range of frequencies.

Of course the stimulating radiation of Fig. 1.24 is still present in the system after emission has occurred—it is in no way absorbed—so it can go on to interact with another excited molecule to induce more emission. Equally the emitted radiation has the right frequency to stimulate emission from yet another excited molecule. Clearly, all the time a supply of excited molecules exists, this process is likely to cascade and a great deal of radiation may be emitted coherently. This *amplification* of the original stimulating photon is reflected in the name of the process—*l*ight *a*mplification by *s*timulated *e*mission of *r*adiation, or *laser*.

In fact, as we have said, light (or, more properly, visible radiation) is far more likely to be emitted *spontaneously*, and so not to have the coherent properties of laser radiation. It was in the microwave region that the first successful amplification by stimulated emission was performed (and the process was therefore christened *maser*, standing for *m*icrowave *a*mplification by *s*timulated *e*mission of *r*adiation). For the process to be possible in higher-frequency regions it is necessary to find systems with long-lived excited states so that stimulated, rather than spontaneous, emission may predominate, and this may only be achieved if more than two energy levels are involved.

Consider the three energy levels of Fig. 1.25(*a*). Excitation from the ground state, level 1, to the normal excited state, level 2, can occur by absorption of radiation, as usual. Provided that, as well as emitting spontaneously, level 2 can transfer some molecules into a metastable state (level 3) which cannot easily revert spontaneously to the ground state, then the

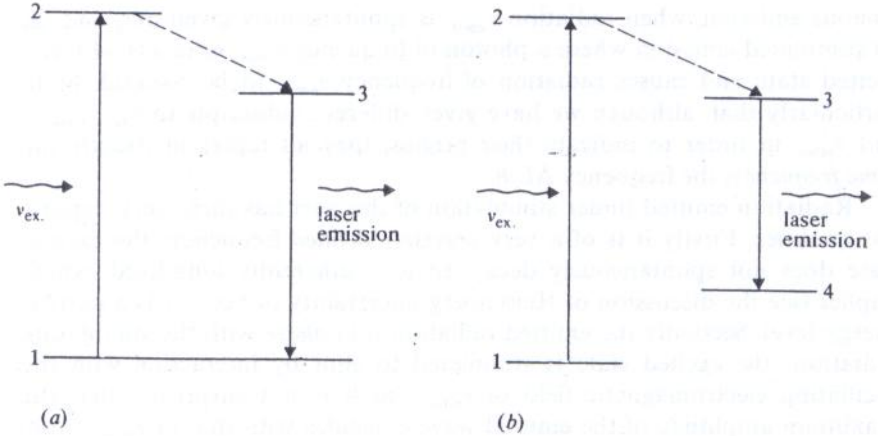

Figure 1.25 Showing the energy levels of (*a*) a three-level and (*b*) a four-level system operating as a laser.

population of level 3 builds up, and laser action becomes feasible. The ruby laser is an example of this type of three-level system. Ruby is basically aluminium oxide containing a trace (about 0·05 per cent) of chromium ions, which gives it its characteristic colour. A discharge tube wound round a rod of ruby is flashed very briefly to raise the chromium ions into an excited electronic state; they drop rapidly by thermal, non-radiative processes, into a metastable state some 14000 cm^{-1} above the ground state, and they then revert to the ground state, by laser action, emitting radiation at about 690 nm wavelength. The decay from excited to metastable state releases quite large amounts of heat, so the ruby must be allowed to cool before another excitation cycle is commenced; it is thus operated as a pulsed laser.

In some cases the laser emission arises by reversion of level 3 to a lower state other than the original level 1, as shown in the four-level system of Fig. 1.25(*b*). This situation occurs particularly when, as is quite possible, levels 3 and 4 belong to an entirely *different* molecular species from levels 1 and 2. For example in the helium–neon laser it is the helium atoms which are initially excited (level 1 to 2), and which then transfer their excitation energy to neon atoms by collisions; this can happen only because neon has an excited state with almost exactly the same energy as the excited state of helium, so a resonance transfer of energy is possible. It also happens that the excited state of neon does not readily undergo an ordinary spectroscopic transition back to its ground state, so the conditions are ideal for laser action. Provided the exciting radiation for helium is maintained, so replenishing the population of excited helium atoms, this type of laser can operate continuously. We shall discuss the precise electronic energy levels involved in more detail in Chapter 5.

The extreme coherence of laser radiation makes it ideal in applications like communications, distance measurement, etc., but from the spectroscopic point of view its very narrow frequency spread makes it directly useful in only one area. This is Raman spectroscopy where, as we shall see in Chapter 4, the requirement is for an intense monochromatic source. For this the laser—almost *any* laser—is ideal.

For virtually all other spectroscopic measurements, however, either a wide-band or a tunable source is desirable. Lasers cannot be wide-band (although the CO_2 laser, to be described in Sec. 3.8.4, comes close to this), but recent developments have led to their becoming tunable. In order to change the emission frequency of a laser system it is necessary to be able to modify the energy levels between which transitions take place. Solids emitting laser radiation can be subjected to varying temperatures or pressures in order smoothly to change the relevant energies, but the extent of such changes is relatively small. More usefully, lasers made from coloured organic substances in solution—the so-called dye lasers—are widely tunable. In these the active material is usually a rare-earth ion held in the centre of an organic 'ligand' which complexes firmly to the ion. The tuning is brought about by changes in temperature, solvent, or concentration, and it is now possible to produce laser emission anywhere from the near infra-red to the ultra-violet. The possibilities for using such intense, sharply defined but variable-frequency sources routinely in spectroscopy are tremendous, and this technique will certainly become increasingly important in the near future.

PROBLEMS

(Useful constants: $N = 6{\cdot}023 \times 10^{23}$ mol^{-1}; $k = 1{\cdot}381 \times 10^{-23}$ J K^{-1}; $h = 6{\cdot}626 \times 10^{-34}$ J s; $c = 2{\cdot}998 \times 10^{8}$ m s^{-1}.)

1.1 The wavelength of the radiation absorbed during a particular spectroscopic transition is observed to be 10 μm. Express this in frequency (Hz) and in wavenumber (cm^{-1}), and calculate the energy change during the transition in both joules per molecule and joules per mole. If the energy change were twice as large, what would be the wavelength of the corresponding radiation?

1.2 Which of the following molecules would show (*a*) a microwave (rotational) spectrum, (*b*) an infra-red (vibrational) spectrum: Br_2, HBr, CS_2?

1.3 A particular molecule is known to undergo spectroscopic transitions between the ground state and two excited states, (*a*) and (*b*), its lifetime in (*a*) being about 10 s, and in (*b*) about 0·1 s. Calculate the approximate uncertainty in the excited state energy levels and the widths of the associated spectral 'lines' in hertz.

1.4 A certain transition involves an energy change of $4{\cdot}005 \times 10^{-22}$ J molecule^{-1}. If there are 1000 molecules in the ground state, what is the approximate equilibrium population of the excited state at temperatures of (*a*) 29 K, (*b*) 145 K, (*c*) 290 K and (*d*) 2900 K? What would your answer have been if the energy change were 10 times greater?

CHAPTER

TWO

MICROWAVE SPECTROSCOPY

2.1 THE ROTATION OF MOLECULES

We saw in the previous chapter that spectroscopy in the microwave region is concerned with the study of rotating molecules. The rotation of a three-dimensional body may be quite complex and it is convenient to resolve it into rotational components about three mutually perpendicular directions through the centre of gravity—the principal axes of rotation. Thus a body has three principal *moments of inertia*, one about each axis, usually designated I_A, I_B, and I_C.

Molecules may be classified into groups according to the relative values of their three principal moments of inertia—which, it will be seen, is tantamount to classifying them according to their shapes. We shall describe this classification here before discussing the details of the rotational spectra arising from each group.

1. *Linear molecules.* These, as the name implies, are molecules in which all the atoms are arranged in a straight line, such as hydrogen chloride HCl, or carbon oxysulphide OCS, illustrated below. The three directions of rotation may be taken as (*a*) about the bond axis, (*b*) end-over-end

H——Cl

O——C——S

rotation in the plane of the paper, and (*c*) end-over-end rotation at right angles to the plane. It is self-evident that the moments of (*b*) and (*c*) are the same (i.e., $I_B = I_C$) while that of (*a*) is very small. As an approximation we may say that $I_A = 0$, although it should be noted that this *is* only an approximation (see p. 46).

Thus for linear molecules we have:

$$I_B = I_C \qquad I_A = 0 \tag{2.1}$$

2. *Symmetric tops.* Consider a molecule such as methyl fluoride, where the three hydrogen atoms are bonded tetrahedrally to the carbon, as shown below. As in the case of linear molecules, the end-over-end rotation in,

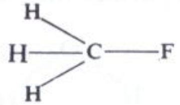

and out of, the plane of the paper are still identical and we have $I_B = I_C$. The moment of inertia about the C—F bond axis (chosen as the main rotational axis since the centre of gravity lies along it) is now not negligible, however, because it involves the rotation of three comparatively massive hydrogen atoms off this axis. Such a molecule spinning about this axis can be imagined as a top, and hence the name of the class. We have then:

$$\text{Symmetric tops:} \quad I_B = I_C \neq I_A \qquad I_A \neq 0 \tag{2.2}$$

There are two subdivisions of this class which we may mention: if, as in methyl fluoride above, $I_B = I_C > I_A$, then the molecule is called a *prolate* symmetric top; whereas if $I_B = I_C < I_A$, it is referred to as *oblate.* An example of the latter type is boron trichloride, which, as shown, is planar and symmetrical. In this case $I_A = 2I_B = 2I_C$

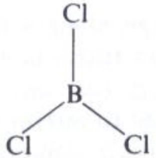

3. *Spherical tops.* When a molecule has all three moments of inertia identical, it is called a spherical top. A simple example is the tetrahedral molecule methane CH_4. We have then:

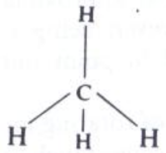

$$\text{Spherical tops:} \quad I_A = I_B = I_C \tag{2.3}$$

In fact these molecules are only of academic interest in this chapter. Since they can have no dipole moment owing to their symmetry, rotation alone can produce no dipole change and hence no rotational spectrum is observable.

4. *Asymmetric tops.* These molecules, to which the majority of substances belong, have all three moments of inertia different:

$$I_A \neq I_B \neq I_C \tag{2.4}$$

Simple examples are water H_2O, and vinyl chloride $CH_2{=}CHCl$.

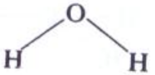

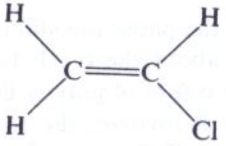

Perhaps it should be pointed out that one can (and often does) describe the classification of molecules into the four rotational classes in far more rigorous terms than have been used above (see, for example, Herzberg, *Molecular Spectra and Molecular Structure*, vol. II). However, for the purposes of this book the above description is adequate.

2.2 ROTATIONAL SPECTRA

We have seen that rotational energy, along with all other forms of molecular energy, is quantized: this means that a molecule cannot have any arbitrary amount of rotational energy (i.e., any arbitrary value of angular momentum) but its energy is limited to certain definite values depending on the shape and size of the molecule concerned. The permitted energy values—the so-called rotational energy *levels*—may in principle be calculated for any molecule by solving the Schrödinger equation for the system represented by that molecule. For simple molecules the mathematics involved is straightforward but tedious, while for complicated systems it is probably impossible without gross approximations. We shall not concern ourselves unduly with this, however, being content merely to accept the results of existing solutions and to point out where reasonable approximations may lead.

We shall consider each class of rotating molecule in turn, discussing the linear molecule in most detail, because much of its treatment can be directly extended to symmetrical and unsymmetrical molecules.

2.3 DIATOMIC MOLECULES

2.3.1 The Rigid Diatomic Molecule

We start with this, the simplest of all linear molecules, shown in Fig. 2.1. Masses m_1 and m_2 are joined by a rigid bar (the bond) whose length is

$$r_0 = r_1 + r_2 \tag{2.5}$$

The molecule rotates end-over-end about a point C, the centre of gravity: this is defined by the moment, or balancing, equation:

$$m_1 r_1 = m_2 r_2 \tag{2.6}$$

The moment of inertia about C is defined by:

$$\begin{aligned} I &= m_1 r_1^2 + m_2 r_2^2 \\ &= m_2 r_2 r_1 + m_1 r_1 r_2 \qquad \text{(from (2.6))} \\ &= r_1 r_2(m_1 + m_2) \end{aligned} \tag{2.7}$$

But, from (2.5) and (2.6):

$$m_1 r_1 = m_2 r_2 = m_2(r_0 - r_1)$$

therefore,

$$r_1 = \frac{m_2 r_0}{m_1 + m_2} \quad \text{and} \quad r_2 = \frac{m_1 r_0}{m_1 + m_2} \tag{2.8}$$

Replacing (2.8) into (2.7):

$$I = \frac{m_1 m_2}{m_1 + m_2} r_0^2 = \mu r_0^2 \tag{2.9}$$

where we have written $\mu = m_1 m_2/(m_1 + m_2)$, and μ is called the *reduced mass* of the system. Equation (2.9) defines the moment of inertia conveniently in terms of the atomic masses and the bond length.

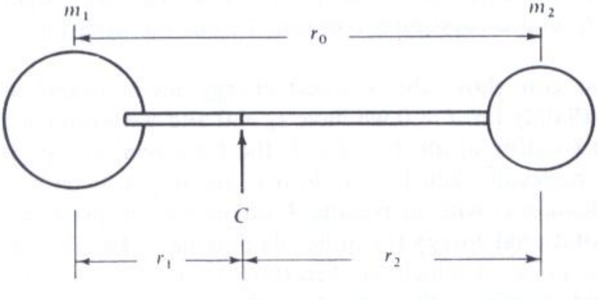

Figure 2.1 A rigid diatomic molecule treated as two masses, m_1 and m_2, joined by a rigid bar of length $r_0 = r_1 + r_2$.

By the use of the Schrödinger equation it may be shown that the rotational energy levels allowed to the rigid diatomic molecule are given by the expression:

$$E_J = \frac{h^2}{8\pi^2 I} J(J+1) \text{ joules} \qquad \text{where } J = 0, 1, 2, \ldots \tag{2.10}$$

In this expression h is Planck's constant, and I is the moment of inertia, either I_B or I_C, since both are equal. The quantity J, which can take integral values from zero upwards, is called the *rotational quantum number*: its restriction to integral values arises directly out of the solution to the Schrödinger equation and is by no means arbitrary, and it is this restriction which effectively allows only certain discrete rotational energy levels to the molecule.

Equation (2.10) expresses the allowed energies in joules; we, however, are interested in differences between these energies, or, more particularly, in the corresponding frequency, $\nu = \Delta E/h$ Hz, or wavenumber, $\bar{\nu} = \Delta E/hc$ cm^{-1}, of the radiation emitted or absorbed as a consequence of changes between energy levels. In the rotational region spectra are usually discussed in terms of wavenumber, so it is useful to consider energies expressed in these units. We write:

$$\varepsilon_J = \frac{E_J}{hc} = \frac{h}{8\pi^2 Ic} J(J+1) \text{ cm}^{-1} \qquad (J = 0, 1, 2, \ldots) \tag{2.11}$$

where c, the velocity of light, is here expressed in cm s^{-1}, since the unit of wavenumber is reciprocal *centimetres*.

Equation (2.11) is usually abbreviated to:

$$\varepsilon_J = BJ(J+1) \text{ cm}^{-1} \qquad (J = 0, 1, 2, \ldots) \tag{2.12}$$

where B, the *rotational constant*, is given by

$$B = \frac{h}{8\pi^2 I_B c} \quad \text{cm}^{-1} \tag{2.13}$$

in which we have used explicitly the moment of inertia I_B. We might equally well have used I_C and a rotational constant C, but the notation of (2.13) is conventional.

From Eq. (2.12) we can show the allowed energy levels diagrammatically as in Fig. 2.2. Plainly for $J = 0$ we have $\varepsilon_J = 0$ and we would say that the molecule is not rotating at all. For $J = 1$, the rotational energy is $\varepsilon_1 = 2B$ and a rotating molecule then has its lowest angular momentum. We may continue to calculate ε_J with increasing J values and, in principle, there is no limit to the rotational energy the molecule may have. In practice, of course, there comes a point at which the centrifugal force of a rapidly rotating diatomic molecule is greater than the strength of the bond, and the molecule is disrupted, but this point is not reached at normal temperatures.

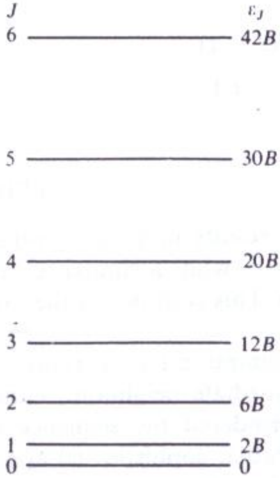

Fig. 2.2

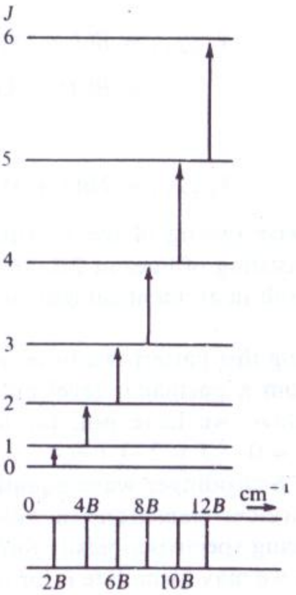

Fig. 2.3

Figure 2.2 The allowed rotational energy levels of a rigid diatomic molecule.

Figure 2.3 Allowed transitions between the energy levels of a rigid diatomic molecule and the spectrum which arises from them.

We now need to consider *differences* between the levels in order to discuss the spectrum. If we imagine the molecule to be in the $J = 0$ state (the *ground rotational state*, in which no rotation occurs), we can let incident radiation be absorbed to raise it to the $J = 1$ state. Plainly the energy absorbed will be:

$$\varepsilon_{J=1} - \varepsilon_{J=0} = 2B - 0 = 2B \quad \text{cm}^{-1}$$

and, therefore,

$$\bar{\nu}_{J=0 \to J=1} = 2B \quad \text{cm}^{-1} \tag{2.14}$$

In other words, an absorption line will appear at $2B$ cm^{-1}. If now the molecule is raised from the $J = 1$ to the $J = 2$ level by the absorption of more energy, we see immediately:

$$\begin{aligned} \bar{\nu}_{J=1 \to J=2} &= \varepsilon_{J=2} - \varepsilon_{J=1} \\ &= 6B - 2B = 4B \quad \text{cm}^{-1} \end{aligned} \tag{2.15}$$

In general, to raise the molecule from the state J to state $J + 1$, we would have:

$$\begin{aligned}\bar{\nu}_{J\to J+1} &= B(J+1)(J+2) - BJ(J+1)\\ &= B[J^2 + 3J + 2 - (J^2 + J)]\end{aligned}$$

or

$$\bar{\nu}_{J\to J+1} = 2B(J+1)\ \text{cm}^{-1} \tag{2.16}$$

Thus a stepwise raising of the rotational energy results in an absorption spectrum consisting of lines at $2B$, $4B$, $6B$, ..., cm^{-1}, while a similar lowering would result in an identical emission spectrum. This is shown at the foot of Fig. 2.3.

In deriving this pattern we have made the assumption that a transition can occur from a particular level only to its immediate neighbour, either above or below: we have not, for instance, considered the sequence of transitions $J = 0 \to J = 2 \to J = 4$ .... In fact, a rather sophisticated application of the Schrödinger wave equation shows that, for this molecule, we need only consider transitions in which J changes by one unit—all other transitions being spectroscopically *forbidden*. Such a result is called a *selection rule*, and we may formulate it for the rigid diatomic rotator as:

$$\text{Selection rule:}\quad \Delta J = \pm 1 \tag{2.17}$$

Thus Eq. (2.16) gives the *whole* spectrum to be expected from such a molecule.

Of course, only if the molecule is asymmetric (heteronuclear) will this spectrum be observed, since if it is homonuclear there will be no dipole component change during the rotation, and hence no interaction with radiation. Thus molecules such as HCl and CO will show a rotational spectrum, while N_2 and O_2 will not. Remember also, that rotation about the bond axis was rejected in Sec. 2.1: we can now see that there are two reasons for this. Firstly, the moment of inertia is very small about the bond so, applying Eqs (2.10) or (2.11) we see that the energy levels would be extremely widely spaced: this means that a molecule requires a great deal of energy to be raised from the $J = 0$ to the $J = 1$ state, and such transitions do not occur under normal spectroscopic conditions. Thus diatomic (and all linear) molecules are in the $J = 0$ state for rotation about the bond axis, and they may be said to be not rotating. Secondly, even if such a transition should occur, there will be no dipole change and hence no spectrum.

To conclude this section we shall apply Eq. (2.16) to an observed spectrum in order to determine the moment of inertia and hence the bond length. Gilliam et al.† have measured the first line ($J = 0$) in the rotation

---

† Gilliam, Johnson, and Gordy, *Physical Review*, **78**, 140 (1950).

spectrum of carbon monoxide as 3·842 35 cm^{-1}. Hence from Eq. (2.16):

$$\bar{\nu}_{0\rightarrow 1} = 3{\cdot}842\,35 = 2B \quad \text{cm}^{-1}$$

or,

$$B = 1{\cdot}921\,18\ \text{cm}^{-1}$$

Rewriting Eq. (2.13) as: $I = h/8\pi^2 Bc$, we have

$$I_{\text{CO}} = \frac{6{\cdot}626 \times 10^{-34}}{8\pi^2 \times 2{\cdot}997\,93 \times 10^{10} \times B} = \frac{27{\cdot}9907 \times 10^{-47}}{B}\ \text{kg m}^2$$

$$= 14{\cdot}5695_4 \times 10^{-47}\ \text{kg m}^2$$

where we express the velocity of light in cm s^{-1}, since B is in cm^{-1}. But the moment of inertia is μr^2 (cf. Eq. (2.9)) and, knowing the relative atomic weights (H = 1·0080) to be C = 12·0000, O = 15·9994, and the absolute mass of the hydrogen atom to be $1{\cdot}673\,43 \times 10^{-27}$ kg, we can calculate the masses of carbon and oxygen, respectively, as 19·921 68 and $26{\cdot}561\,36 \times 10^{-27}$ kg. The reduced mass is then:

$$\mu = \frac{19{\cdot}921\,68 \times 26{\cdot}561\,36 \times 10^{-54}}{46{\cdot}483\,03 \times 10^{-27}} = 11{\cdot}383\,65 \times 10^{-27}\ \text{kg}$$

Hence:

$$r^2 = \frac{I}{\mu} = 1{\cdot}2799 \times 10^{-20}\ \text{m}^2$$

and

$$r_{\text{CO}} = 0{\cdot}1131\ \text{nm (or } 1{\cdot}131\ \text{Å)}$$

2.3.2 The Intensities of Spectral Lines

We want now to consider briefly the relative intensities of the spectral lines of Eq. (2.16); for this a prime requirement is plainly a knowledge of the relative probabilities of transition between the various energy levels. Does, for instance, a molecule have more or less chance of making the transition $J = 0 \rightarrow J = 1$ than the transition $J = 1 \rightarrow J = 2$? We mentioned above calculations which show that a change of $\Delta J = \pm 2, \pm 3$, etc., was forbidden—in other words, the transition probability for all these changes is zero. Precisely similar calculations show that the probability of all changes with $\Delta J = \pm 1$ is almost the same—all, to a good approximation, are equally likely to occur.

This does not mean, however, that all spectral lines will be equally intense. Although the intrinsic probability that a single molecule in the $J = 0$ state, say, will move to $J = 1$ is the same as that of a single molecule moving from $J = 1$ to $J = 2$, in an assemblage of molecules, such as in a normal gas sample, there will be different numbers of molecules in each level to begin with, and therefore different total numbers of molecules will carry out transitions between the various levels. In fact, since the intrinsic probabilities are identical, the line intensities will be directly proportional to the initial numbers of molecules in each level.

The first factor governing the population of the levels is the Boltzmann distribution (cf. Sec. 1.7.2). Here we know that the rotational energy in the lowest level is zero, since $J = 0$, so, if we have N_0 molecules in this state, the number in any higher state is given by:

$$N_J/N_0 = \exp(-E_J/kT) = \exp\{-BhcJ(J+1)/kT\} \tag{2.18}$$

where, we must remember, c is the velocity of light in cm s^{-1} when B is in cm^{-1}. A very simple calculation shows how N_J varies with J; for example, taking a typical value of $B = 2$ cm^{-1}, and room temperature (say $T = 300$ K), the relative population in the $J = 1$ state is:

$$\frac{N_1}{N_0} = \exp\left\{-\frac{2 \times 6{\cdot}63 \times 10^{-34} \times 3 \times 10^{10} \times 1 \times 2}{1{\cdot}38 \times 10^{-23} \times 300}\right\}$$
$$= \exp(-0{\cdot}019) \approx 0{\cdot}98$$

and we see that there are almost as many molecules in the $J = 1$ state, at equilibrium, as in the $J = 0$. In a similar way the two graphs of Fig. 2.4 have been calculated, showing the more rapid decrease of N_J/N_0 with increasing J and with larger B.

A second factor is also required—the possibility of *degeneracy* in the energy states. Degeneracy is the existence of two or more energy states which have exactly the *same* energy. In the case of the diatomic rotator we may approach the problem in terms of its angular momentum.

The defining equations for the energy and angular momentum of a rotator are:

$$E = \tfrac{1}{2}I\omega^2 \qquad \mathbf{P} = I\omega$$

where I is the moment of inertia, ω the rotational frequency (in radians per second), and $\mathbf{P}$ the angular momentum. Rearrangement of these gives

$$\mathbf{P} = \sqrt{2EI}$$

The energy level expression of Eq. (2.10) can be rewritten:

$$2EI = J(J+1)\frac{h^2}{4\pi^2}$$

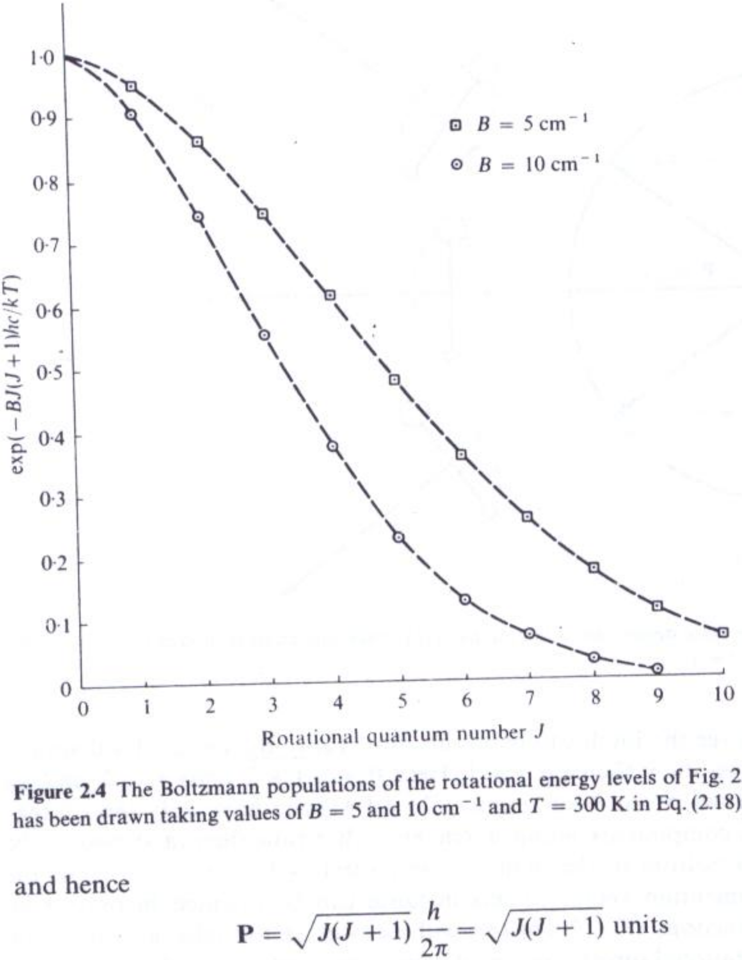

Figure 2.4 The Boltzmann populations of the rotational energy levels of Fig. 2.2. The diagram has been drawn taking values of $B = 5$ and $10\ \text{cm}^{-1}$ and $T = 300$ K in Eq. (2.18).

and hence

$$\mathbf{P} = \sqrt{J(J+1)}\,\frac{h}{2\pi} = \sqrt{J(J+1)}\ \text{units} \tag{2.19}$$

where, following convention, we take $h/2\pi$ as the fundamental unit of angular momentum. Thus we see that **P**, like E, is quantized.

Throughout the above derivation **P** has been printed in bold face type to show that it is a *vector*—i.e., it has *direction* as well as *magnitude*. The direction of the angular momentum vector is conventionally taken to be along the axis about which rotation occurs and it is usually drawn as an arrow of length proportional to the magnitude of the momentum. The number of different directions which an angular momentum vector may take up is limited by a quantum mechanical law which may be stated:

'For integral values of the rotational quantum number (in this case J), the angular momentum vector may only take up directions such that its component along a given reference direction is zero or an integral multiple of angular momentum units.'

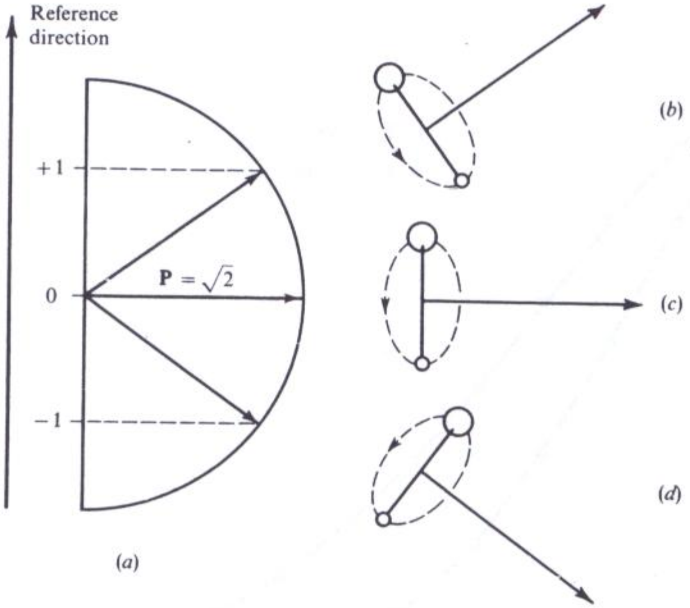

Figure 2.5 The three degenerate orientations of the rotational angular momentum vector for a molecule with $J = 1$.

We can see the implications of this most easily by means of a diagram. In Fig. 2.5 we show the case $J = 1$. Here $\mathbf{P} = \sqrt{1 \times 2}$ units $= \sqrt{2}$, and, as Fig. 2.5(*a*) shows, a vector of length $\sqrt{2}\,(= 1{\cdot}41)$ can have only *three* integral or zero components along a reference direction (here assumed to be from top to bottom in the plane of the paper): +1, 0, and −1. Thus the angular momentum vector in this instance can be oriented in only three different directions (Fig. 2.5(*b*)–(*d*)) with respect to the reference direction. All three rotational directions are, of course, associated with the same angular momentum and hence the same rotational energy: the $J = 1$ level is thus threefold degenerate.

Figure 2.6(*a*) and (*b*) shows the situation for $J = 2$ ($\mathbf{P} = \sqrt{6}$) and $J = 3$ ($\mathbf{P} = 2\sqrt{3}$) with fivefold and sevenfold degeneracy respectively. In general it may readily be seen that *each energy level is $2J + 1$-fold degenerate.*

Thus we see that, although the molecular population in each level decreases exponentially (Eq. (2.18)), the number of degenerate levels available increases rapidly with J. The total relative population at an energy E_J will plainly be:

$$\text{Population} \propto (2J + 1) \exp(-E_J/kT) \tag{2.20}$$

When this is plotted against J the points fall on a curve of the type shown in Fig. 2.7, indicating that the population rises to a maximum and then

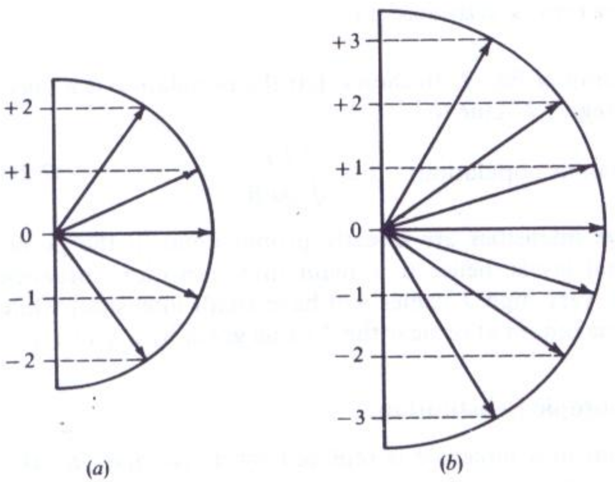

(*a*) (*b*)

Figure 2.6 The five and seven degenerate rotational orientations for a molecule with $J = 2$ and $J = 3$ respectively.

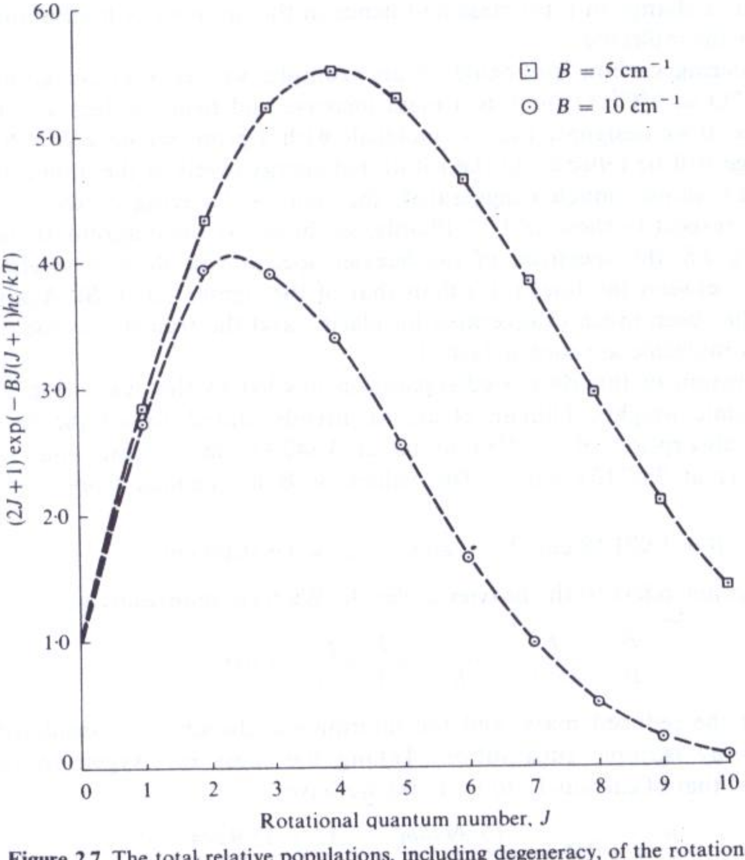

Figure 2.7 The total relative populations, including degeneracy, of the rotational energy levels of a diatomic molecule. The diagram has been drawn for the same conditions as Fig. 2.4.

diminishes. Differentiation of Eq. (2.20) shows that the population is a maximum at the nearest integral J value to:

$$\text{Maximum population:}\quad J = \sqrt{\frac{kT}{2hcB}} - \frac{1}{2} \qquad (2.21)$$

We have seen that line intensities are directly proportional to the populations of the rotational levels, hence it is plain that transitions between levels with very low or very high J values will have small intensities while the intensity will be a maximum at or near the J value given by Eq. (2.21).

2.3.3 The Effect of Isotopic Substitution

When a particular atom in a molecule is replaced by its isotope—an element identical in every way except for its atomic mass—the resulting substance is identical chemically with the original. In particular there is no appreciable change in internuclear distance on isotopic substitution. There is, however, a change in total mass and hence in the moment of inertia and B value for the molecule.

Considering carbon monoxide as an example, we see that on going from $^{12}C^{16}O$ to $^{13}C^{16}O$ there is a mass increase and hence a decrease in the B value. If we designate the ^{13}C molecule with a prime we have $B > B'$. This change will be reflected in the rotational energy levels of the molecule and Fig. 2.8 shows, much exaggerated, the relative lowering of the ^{13}C levels with respect to those of ^{12}C. Plainly, as shown by the diagram at the foot of Fig. 2.8, the spectrum of the heavier species will show a smaller separation between the lines ($2B'$) than that of the lighter one ($2B$). Again the effect has been much exaggerated for clarity, and the transitions due to the heavier molecule are shown dashed.

Observation of this decreased separation has led to the evaluation of precise atomic weights. Gilliam et al., as already stated, found the first rotational absorption of $^{12}C^{16}O$ to be at $3{\cdot}842\,35\ \text{cm}^{-1}$, while that of $^{13}C^{16}O$ was at $3{\cdot}673\,37\ \text{cm}^{-1}$. The values of B determined from these figures are:

$$B = 1{\cdot}921\,18\ \text{cm}^{-1} \qquad \text{and} \qquad B' = 1{\cdot}836\,69\ \text{cm}^{-1}$$

where the prime refers to the heavier molecule. We have immediately:

$$\frac{B}{B'} = \frac{h}{8\pi^2 Ic} \cdot \frac{8\pi^2 I'c}{h} = \frac{I'}{I} = \frac{\mu'}{\mu} = 1{\cdot}046$$

where μ is the reduced mass, and the internuclear distance is considered unchanged by isotopic substitution. Taking the mass of oxygen to be 15·9994 and that of carbon-12 to be 12·00, we have:

$$\frac{\mu'}{\mu} = 1{\cdot}046 = \frac{15{\cdot}9994m'}{15{\cdot}9994 + m'} \times \frac{12 + 15{\cdot}9994}{12 \times 15{\cdot}9994}$$

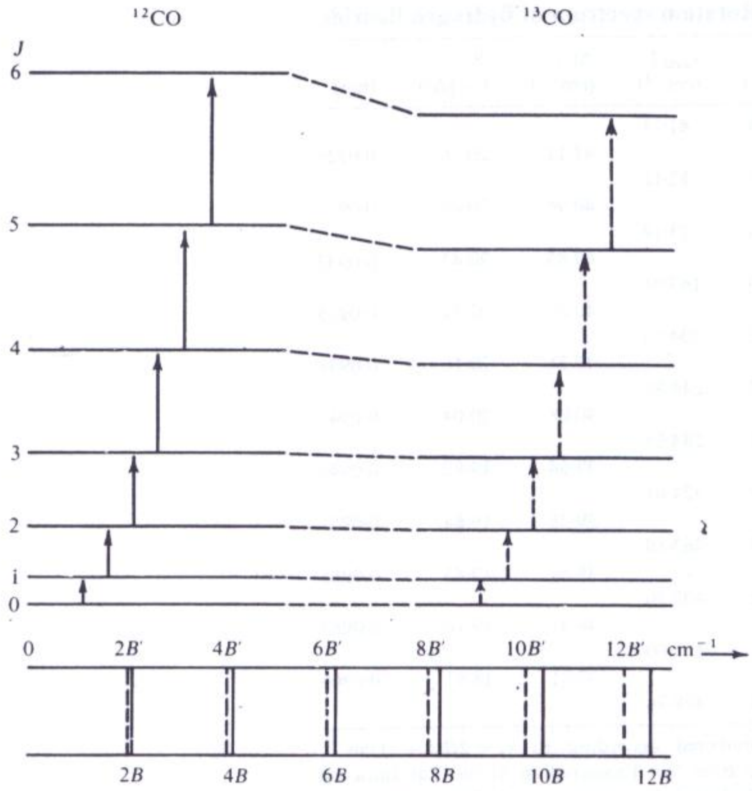

Figure 2.8 The effect of isotopic substitution on the energy levels and hence rotational spectrum of a diatomic molecule such as carbon monoxide.

from which m', the atomic weight of carbon-13, is found to be 13·0007. This is within 0·02 per cent of the best value obtained in other ways.

It is noteworthy that the data quoted above were obtained by Gilliam et al. from $^{13}C^{16}O$ molecules in natural abundance (i.e., about 1 per cent of ordinary carbon monoxide). Thus, besides allowing an extremely precise determination of atomic weights, microwave studies can give directly an estimate of the abundance of isotopes by comparison of absorption intensities.

2.3.4 The Non-Rigid Rotator

At the end of Sec. 2.3.1 we indicated how internuclear distances could be calculated from microwave spectra. It must be admitted that we selected our data carefully at this point—spectral lines for carbon monoxide, other than the first, would not have shown the constant 2*B* separation predicted

Table 2.1 Rotation spectrum of hydrogen fluoride

J	$\bar{\nu}_{\text{obs.}}$† (cm^{-1})	$\bar{\nu}_{\text{calc.}}$‡ (cm^{-1})	$\Delta\bar{\nu}_{\text{obs.}}$ (cm^{-1})	B $(=\frac{1}{2}\Delta\bar{\nu})$	r (nm)
0	41·08	41·11			
			41·11	20·56	0·0929
1	82·19	82·18			
			40·96	20·48	0·0931
2	123·15	123·14			
			40·85	20·43	0·0932
3	164·00	163·94			
			40·62	20·31	0·0935
4	204·62	204·55			
			40·31	20·16	0·0938
5	244·93	244·89			
			40·08	20·04	0·0941
6	285·01	284·93			
			39·64	19·82	0·0946
7	324·65	324·61			
			39·28	19·64	0·0951
8	363·93	363·89			
			38·89	19·45	0·0955
9	402·82	402·70			
			38·31	19·16	0·0963
10	441·13	441·00			
			37·81	18·91	0·0969
11	478·94	478·74			

† Lines numbered according to $\bar{\nu}_J = 2B(J+1)$ cm^{-1}. Observed data from 'An Examination of the Far Infra-red Spectrum of Hydrogen Fluoride' by A. A. Mason and A. H. Nielsen, published as Scientific Report No. 5, August 1963, Contract No. AF 19(604)-7981, by kind permission of the authors.

‡ See Sec. 2.3.5 for details of the calculation.

by Eq. (2.16). This is shown by the spectrum of hydrogen fluoride given in Table 2.1; it is evident that the separation between successive lines (and hence the apparent B value) decreases steadily with increasing J.

The reason for this decrease may be seen if we calculate internuclear distances from the B values. The calculations are exactly similar to those of Sec. 2.3.1 and the results are shown in column 6 of Table 2.1. Plainly the bond length increases with J and we can see that our assumption of a *rigid* bond is only an approximation; in fact, of course, all bonds are elastic to some extent, and the increase in length with J merely reflects the fact that the more quickly a diatomic molecule rotates the greater is the centrifugal force tending to move the atoms apart.

Before showing how this elasticity may be quantitatively allowed for in rotational spectra, we shall consider briefly two of its consequences. First, when the bond is elastic, a molecule may have vibrational energy—i.e., the bond will stretch and compress periodically with a certain fundamental frequency dependent upon the masses of the atoms and the elasticity (or force constant) of the bond. If the motion is simple harmonic (which, we shall see in Chapter 3, is usually a very good approximation to the truth) the force constant is given by:

$$k = 4\pi^2\bar{\omega}^2c^2\mu \tag{2.22}$$

where $\bar{\omega}$ is the vibration frequency (expressed in cm^{-1}), and c and μ have their previous definitions. Plainly the variation of B with J is determined by the force constant—the weaker the bond, the more readily will it distort under centrifugal forces.

The second consequence of elasticity is that the quantities r and B vary during a vibration. When these quantities are measured by microwave techniques many hundreds of vibrations occur during a rotation, and hence the measured value is an average. However, from the defining equation of B we have:

$$B = \frac{h}{8\pi^2 Ic} = \frac{h}{8\pi^2 c\mu r^2}$$

or

$$B \propto 1/r^2 \tag{2.23}$$

since all other quantities are independent of vibration. Now, although in simple harmonic motion a molecular bond is compressed and extended an equal amount on each side of the equilibrium distance and the average value of the distance is therefore unchanged, the average value of $1/r^2$ is *not* equal to $1/r_e^2$, where r_e is the equilibrium distance. We can see this most easily by an example. Consider a bond of equilibrium length 0·1 nm vibrating between the limits 0·09 and 0·11 nm. We have:

$$\langle r\rangle_{\text{av.}} = \frac{0{\cdot}09 + 0{\cdot}11}{2} = 0{\cdot}1 = r_e$$

but

$$\left\langle \frac{1}{r^2} \right\rangle_{\text{av.}} = \frac{(1/0{\cdot}09)^2 + (1/0{\cdot}11)^2}{2} = 103{\cdot}05\ \text{nm}^2$$

and therefore $\langle r\rangle_{\text{av.}} = \sqrt{1/103{\cdot}5} = 0{\cdot}0985$ nm. The difference, though small, is not negligible compared with the precision with which B can be measured spectroscopically. And in fact the real situation is rather worse. We shall see in Chapter 3 that real vibrations are not simple harmonic, since a real bond may be stretched more easily than it may be compressed, and this usually results in $r_{\text{av.}}$ being greater than $r_{\text{eq.}}$.

It is usual, then, to define three different sets of values for B and r. At the equilibrium separation, r_e, between the nuclei, the rotational constant is B_e; in the vibrational ground state the average internuclear separation is r_0 associated with a rotational constant B_0; while if the molecule has excess vibrational energy the quantities are r_v and B_v, where v is the vibrational quantum number.

During the remainder of this chapter we shall ignore the small differences between B_0, B_e, and B_v—the discrepancy is most important in the consideration of vibrational spectra in Chapter 3.

We should note, in passing that the rotational spectrum of hydrogen fluoride given in Table 2.1 extends from the microwave well into the infra-red region (cf. Fig. 1.4). This underlines the comment made in Chapter 1 that there is no fundamental distinction between spectral regions, only differences in technique. Since hydrogen fluoride, together with other diatomic hydrides, has a small moment of inertia and hence a large B value, the spacings between rotational energy levels become large and fall into the infra-red region after only a few transitions. Historically, indeed, the moments of inertia and bond lengths of these molecules were first determined from spectral studies using infra-red techniques.

2.3.5 The Spectrum of a Non-Rigid Rotator

The Schrödinger wave equation may be set up for a non-rigid molecule, and the rotational energy levels are found to be:

$$E_J = \frac{h^2}{8\pi^2 I} J(J+1) - \frac{h^4}{32\pi^4 I^2 r^2 k} J^2(J+1)^2 \text{ J}$$

or

$$\varepsilon_J = E_J/hc = BJ(J+1) - DJ^2(J+1)^2 \text{ cm}^{-1} \tag{2.24}$$

where the rotational constant, B, is as defined previously, and the *centrifugal distortion constant* D, is given by:

$$D = \frac{h^3}{32\pi^4 I^2 r^2 kc} \quad \text{cm}^{-1} \tag{2.25}$$

which is a positive quantity. Equation (2.24) applies for a simple harmonic force field only; if the force field is anharmonic, the expression becomes:

$$\varepsilon_J = BJ(J+1) - DJ^2(J+1)^2 + HJ^3(J+1)^3 + KJ^4(J+1)^4 \cdots \text{cm}^{-1} \tag{2.26}$$

where H, K, etc., are small constants dependent upon the geometry of the molecule. They are, however, negligible compared with D and most modern spectroscopic data are adequately fitted by Eq. (2.24).

From the defining equations of B and D it may be shown directly that

$$D = \frac{16B^3\pi^2\mu c^2}{k} = \frac{4B^3}{\bar{\omega}^2} \tag{2.27}$$

where $\bar{\omega}$ is the vibrational frequency of the bond, and k has been expressed according to Eq. (2.22). We shall see in Chapter 3 that vibrational frequencies are usually of the order of 10^3 cm^{-1}, while B we have found to be of the order of 10 cm^{-1}. Thus we see that D, being of the order 10^{-3} cm^{-1}, is very small compared with B. For small J, therefore, the correction term $DJ^2(J+1)^2$ is almost negligible, while for J values of 10 or more it may become appreciable.

Figure 2.9 shows, much exaggerated, the lowering of rotational levels when passing from the rigid to the non-rigid diatomic molecule. The spectra are also compared, the dashed lines connecting corresponding energy levels and transitions of the rigid and the non-rigid molecules. It should be noted that the selection rule for the latter is still $\Delta J = \pm 1$.

We may easily write an analytical expression for the transitions:

$$\begin{aligned} \varepsilon_{J+1} - \varepsilon_J = \bar{\nu}_J &= B[(J+1)(J+2) - J(J+1)] \\ &\quad - D[(J+1)^2(J+2)^2 - J^2(J+1)^2] \\ &= 2B(J+1) - 4D(J+1)^3 \text{ cm}^{-1} \end{aligned} \tag{2.28}$$

where $\bar{\nu}_J$ represents equally the upward transition from J to $J+1$, or the downward from $J+1$ to J. Thus we see analytically, and from Fig. 2.9, that the spectrum of the elastic rotor is similar to that of the rigid molecule except that each line is displaced slightly to low frequency, the displacement increasing with $(J+1)^3$.

A knowledge of D gives rise to two useful items of information. Firstly, it allows us to determine the J value of lines in an observed spectrum. If we have measured a few isolated transitions it is not always easy to determine from which J value they arise; however, fitting Eq. (2.28) to them—provided three consecutive lines have been measured—gives unique values for B, D, and J. The precision of such fitting is shown by Table 2.1 where the wavenumbers are calculated from the equation:

$$\bar{\nu}_J = 41{\cdot}122(J+1) - 8{\cdot}52 \times 10^{-3}(J+1)^3 \text{ cm}^{-1} \tag{2.29}$$

Secondly, a knowledge of D enables us to determine—although rather inaccurately—the vibrational frequency of a diatomic molecule. From the above data for hydrogen fluoride and Eq. (2.27) we have:

$$\bar{\omega}^2 = \frac{4B^3}{D} = 16{\cdot}33 \times 10^6 \text{ (cm}^{-1})^2$$

i.e.,

$$\bar{\omega} \approx 4050 \text{ cm}^{-1}$$

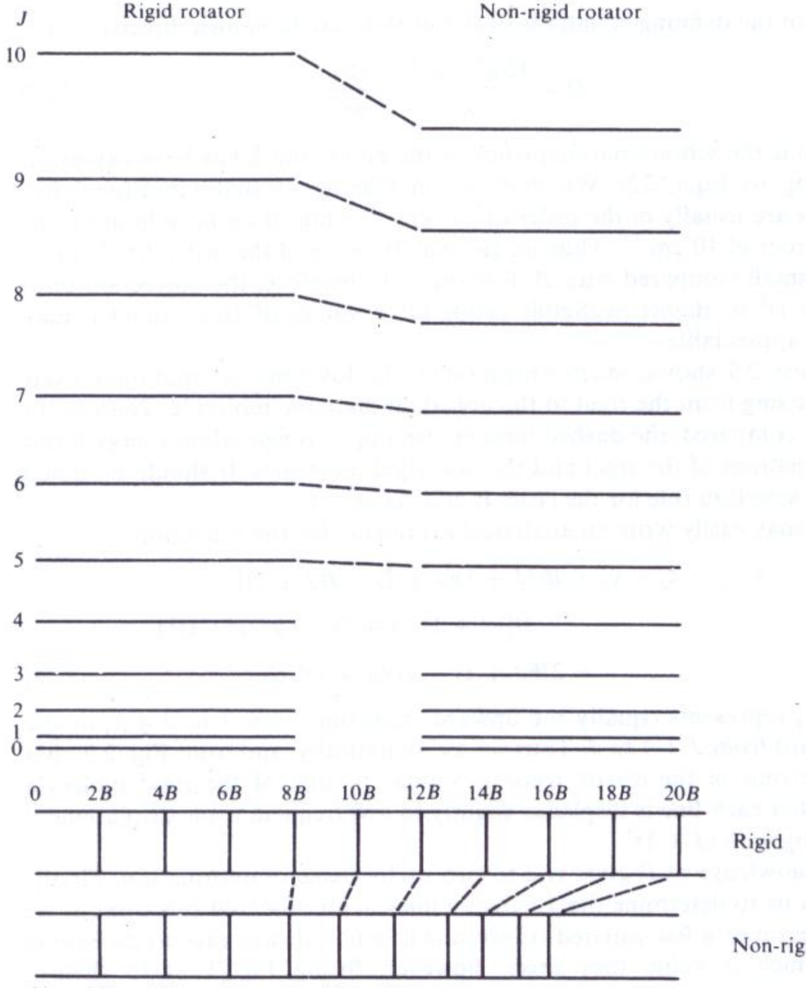

Figure 2.9 The change in rotational energy levels and rotational spectrum when passing from a rigid to a non-rigid diatomic molecule. Levels on the right calculated using $D = 10^{-3}B$.

In the next chapter we shall see that a more precise determination leads to the value $4138{\cdot}3\ \mathrm{cm}^{-1}$; the two per cent inaccuracy in the present calculation is due partly to the assumption of simple harmonic motion, and partly to the very small, and hence relatively inaccurate, value of D.

The force constant follows directly:

$$k = 4\pi^2 c^2 \bar{\omega}^2 \mu = 960\ \mathrm{N\ m^{-1}}$$

which indicates, as expected, that H—F is a relatively strong bond.

2.4 POLYATOMIC MOLECULES

2.4.1 Linear Molecules

We consider first molecules such as carbon oxysulphide OCS, or chloroacetylene HC≡CCl, where all the atoms lie on a straight line, since this type gives rise to a particularly simple spectra in the microwave region. Since $I_B = I_C$; $I_A = 0$, as for diatomic molecules, the energy levels are given by a formula identical with Eq. (2.26), i.e.,

$$\varepsilon_J = BJ(J+1) - DJ^2(J+1)^2 + \cdots \text{ cm}^{-1} \tag{2.30}$$

and the spectrum will show the same $2B$ separation modified by the distortion constant. In fact, the whole of the discussion on diatomic molecules applies equally to all linear molecules; three points, however, should be underlined:

1. Since the moment of inertia for the end-over-end rotation of a polyatomic linear molecule is considerably greater than that of a diatomic molecule, the B value will be much smaller, and the spectral lines more closely spaced. Thus B values for diatomic molecules are about 10 cm^{-1}, while for triatomic molecules they can be 1 cm^{-1} or less, and for larger molecules smaller still.
2. The molecule must, as usual, possess a dipole moment if it is to exhibit a rotational spectrum. Thus OCS will be microwave active, while OCO (more usually written CO_2) will not. In particular, it should be noted that isotopic substitution does not lead to a dipole moment since the bond lengths and atomic charges are unaltered by the substitution. Thus $^{16}OC^{18}O$ is microwave inactive.
3. A non-cyclic polyatomic molecule containing N atoms has altogether $N - 1$ individual bond lengths to be determined. Thus in the triatomic molecule OCS there is the CO distance, r_{CO}, and the CS distance, r_{CS}. On the other hand, there is only *one* moment of inertia for the end-over-end rotation of OCS, and only this one value can be determined from the spectrum. Table 2.2 shows the data for this molecule. Over the four lines observed there is seen to be no appreciable centrifugal distortion, and, taking the value of B as 0·2027 cm^{-1}, we calculate:

$$I_B = \frac{h}{8\pi^2 Bc} = 137{\cdot}95 \times 10^{-47} \text{ kg m}^2$$

From this one observation it is plainly impossible to deduce the two unknowns, r_{CO} and r_{CS}. The difficulty can be overcome, however, if we study a molecule with different atomic masses but the *same* bond lengths—i.e., an isotopically substituted molecule—since this will have a different moment of inertia.

Table 2.2 Microwave spectrum of carbon oxysulphide

$J \to J+1$	$\bar{\nu}_{\text{obs.}}$ (cm^{-1})	$\Delta\bar{\nu}$	B (cm^{-1})
$0 \to 1$	…		
		$2 \times 0{\cdot}4055$	0·2027
$1 \to 2$	0·8109		
		0·4054	0·2027
$2 \to 3$	1·2163		
		0·4054	0·2027
$3 \to 4$	1·6217		
		0·4054	0·2027
$4 \to 5$	2·0271		

Let us consider the rotation of OCS in some detail. Figure 2.10 shows the molecule, where r_O, r_C, and r_S represent the distances of the atoms from the centre of gravity. Consideration of moments gives:

$$m_O r_O + m_C r_C = m_S r_S \tag{2.31}$$

where m_i is the mass of atom i. The moment of inertia is:

$$I = m_O r_O^2 + m_C r_C^2 + m_S r_S^2 \tag{2.32}$$

and we have the further equations:

$$r_O = r_{CO} + r_C \qquad r_S = r_{CS} - r_C \tag{2.33}$$

where r_{CO} and r_{CS} are the bond lengths of the molecule. It is these we wish to determine. Substituting (2.33) in (2.31) and collecting terms:

$$(m_C + m_O + m_S)r_C = m_S r_{CS} - m_O r_{CO}$$

or

$$M r_C = m_S r_{CS} - m_O r_{CO} \tag{2.34}$$

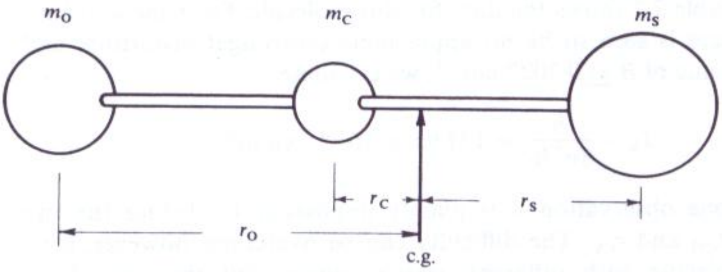

Figure 2.10 The molecule of carbon oxysulphide, OCS, showing the distances of each atom from the centre of gravity.

where we write M for the total mass of the molecule. Substituting (2.33) in (2.32):

$$\begin{aligned} I &= m_O(r_{CO} + r_C)^2 + m_C r_C^2 + m_S(r_{CS} - r_C)^2 \\ &= Mr_C^2 + 2r_C(m_O r_{CO} - m_S r_{CS}) + m_O r_{CO}^2 + m_S r_{CS}^2 \end{aligned}$$

and finally substituting for r_C from Eq. (2.34):

$$I = m_O r_{CO}^2 + m_S r_{CS}^2 - \frac{(m_O r_{CO} - m_S r_{CS})^2}{M} \tag{2.35}$$

Considering now the isotopic molecule, ^{18}OCS, we may write m'_O for m_O throughout Eq. (2.35):

$$I' = m'_O r_{CO}^2 + m_S r_{CS}^2 - \frac{(m'_O r_{CO} - m_S r_{CS})^2}{M'} \tag{2.36}$$

and we can now solve for r_{CO} and r_{CS}, provided we have extracted a value for I' from the microwave spectrum of the isotopic molecule. Note that we do *not* need to write r'_{CO}, since we assume that the bond length is unaltered by isotopic substitution. This assumption may be checked by studying the molecules ^{16}OC^{34}S and ^{18}OC^{34}S, since we would then have four moments of inertia. The bond distances found are quite consistent, and hence justify the assumption.

The extension of the above discussion to molecules with more than three atoms is straightforward; it suffices to say here that microwave studies have led to very precise determinations of many bond lengths in such molecules.

2.4.2 Symmetric Top Molecule

Although the rotational energy levels of this type of molecule are more complicated than those of linear molecules, we shall see that, because of their symmetry, their pure rotational spectra are still relatively simple. Choosing methyl fluoride again as our example we remember that

$$I_B = I_C \neq I_A \qquad I_A \neq 0$$

There are now two directions of rotation in which the molecule might absorb or emit energy—that about the main symmetry axis (the C—F bond in this case) and that perpendicular to this axis.

We thus need two quantum numbers to describe the degree of rotation, one for I_A and one for I_B or I_C. However, it turns out to be very convenient mathematically to have a quantum number to represent the *total* angular momentum of the molecule, which is the sum of the separate angular momenta about the two different axes. This is usually chosen to be the quantum number J. Reverting for a moment to *linear* molecules, remember that we there used J to represent the end-over-end rotation of a molecule:

however, this was the *only* sort of rotation allowed, so it is quite consistent to use J, in general, to represent the *total angular momentum*. It is then conventional to use K to represent the angular momentum about the top axis—i.e., about the C—F bond in this case.

Let us briefly consider what values are allowed to K and J. Both must, by the conditions of quantum mechanics, be integral or zero. The total angular momentum can be as large as we like, that is, J can be 0, 1, 2, ..., ∞ (except, of course, for the theoretical possibility that a real molecule will be disrupted at very high rotational speeds). Once we have chosen J, however, K is rather more limited. Let us consider the case when $J = 3$. Plainly the rotational energy can be divided in several ways between motion about the main symmetry axis and motion perpendicular to this. If *all* the rotation is about the axis, $K = 3$; but note that K cannot be greater than J since J is the *total* angular momentum. Equally we could have $K = 2$, 1, or 0, in which case the motion perpendicular to the axis increases accordingly. Additionally, however, K can be negative—we can imagine positive and negative values of K to correspond with clockwise and anticlockwise rotation about the symmetry axis—and so can have values -1, -2, or -3.

In general, then, for a total angular momentum J, we see that K can take values:

$$K = J, J-1, J-2, \ldots, 0, \ldots, -(J-1), -J \qquad (2.37)$$

which is a total of $2J + 1$ values altogether. This figure of $2J + 1$ is important and will recur.

If we take first the case of a *rigid* symmetric top—i.e., one in which the bonds are supposed not to stretch under centrifugal forces—the Schrödinger equation may be solved to give the allowed energy levels for rotation as:

$$\varepsilon_{J,K} = E_{J,K}/hc = BJ(J+1) + (A-B)K^2 \quad \text{cm}^{-1} \qquad (2.38)$$

where, as before,

$$B = \frac{h}{8\pi^2 I_B c} \qquad \text{and} \qquad A = \frac{h}{8\pi^2 I_A c}$$

Note that the energy depends on K^2, so that it is immaterial whether the top spins clockwise or anticlockwise: the energy is the same for a given angular momentum. For all $K > 0$, therefore, the rotational energy levels are *doubly degenerate*.

The selection rules for this molecule may be shown to be:

$$\Delta J = \pm 1 \text{ (as before)} \qquad \text{and} \qquad \Delta K = 0 \qquad (2.39)$$

and, when these are applied to Eq. (2.38), the spectrum is given by:

$$\begin{aligned}\varepsilon_{J+1,K} - \varepsilon_{J,K} = \bar{\nu}_{J,K} &= B(J+1)(J+2) + (A-B)K^2 \\ &\quad -[BJ(J+1) + (A-B)K^2] \\ &= 2B(J+1) \text{ cm}^{-1} \qquad (2.40)\end{aligned}$$

Thus the spectrum is independent of K, and hence rotational changes about the symmetry axis do not give rise to a rotational spectrum. The reason for this is quite evident—rotation about the symmetry axis does not change the dipole moment perpendicular to the axis (which always remains zero), and hence the rotation cannot interact with radiation. Equation (2.40) shows that the spectrum is just the same as for a linear molecule and that only one moment of inertia—that for end-over-end rotation—can be measured.

Both Eqs (2.38) and (2.40) are for a rigid molecule, however, and we have already seen that microwave spectroscopy is well able to detect the departure of real molecules from this idealized state. When centrifugal stretching is taken into account, the energy levels become:

$$\begin{aligned}\varepsilon_{J,K} = BJ(J+1) + (A-B)K^2 - D_J J^2(J+1)^2 \\ - D_{JK} J(J+1)K^2 - D_K K^4 \quad \text{cm}^{-1} \qquad (2.41)\end{aligned}$$

where, in an obvious notation, D_J, D_{JK}, and D_K are small correction terms for non-rigidity. The selection rules are unchanged (Eq. (2.39)), and so the spectrum is:

$$\begin{aligned}\bar{\nu}_{J,K} &= \varepsilon_{J+1,K} - \varepsilon_{J,K} \\ &= 2B(J+1) - 4D_J(J+1)^3 - 2D_{JK}(J+1)K^2 \quad \text{cm}^{-1} \qquad (2.42)\end{aligned}$$

We see that the spectrum will be basically that of a linear molecule (including centrifugal stretching) with an additional term depending on K^2.

It is easy to see why this spectrum now depends on the axial rotation (i.e., depends on K), although such rotation produces no dipole change. Figure 2.11 illustrates methyl fluoride for (*a*) $K = 0$, no axial rotation, and (*b*) $K > 0$, the molecule rotating about the symmetry axis. We see, from the much exaggerated diagram, that axial rotation widens the HCH angles and stretches the C—H bonds. The distorted molecule (*b*) has a different moment of inertia for end-over-end rotation from (*a*). If we write Eq. (2.42) as:

$$\bar{\nu}_{JK} = 2(J+1)[B - 2D_J(J+1)^2 - D_{JK}K^2] \quad \text{cm}^{-1}$$

we can see more clearly that the centrifugal distortion constants D_J and D_{JK} can be considered as correction terms to the rotational constant B, and hence as perturbing the moment of inertia I_B.

Since each value of J is associated with $2J + 1$ values of K, we see that each line characterized by a certain J value must have $2J + 1$ components.

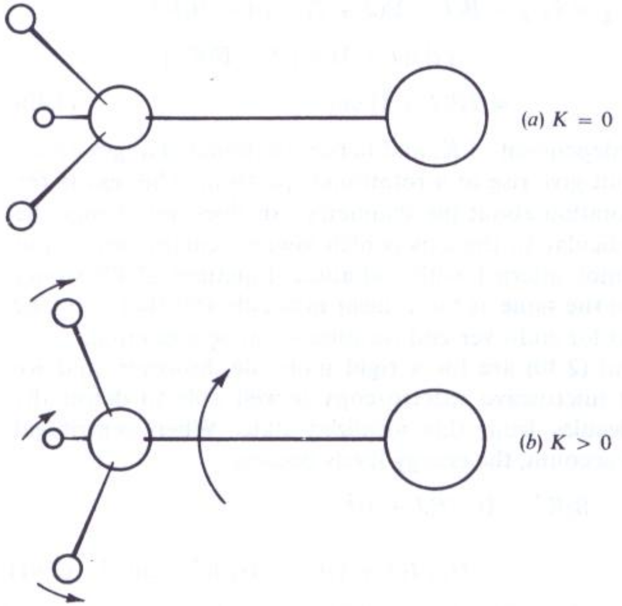

Figure 2.11 The influence of axial rotation on the moment of inertia of a symmetric top molecule, e.g., methyl fluoride, CH_3F. In (*a*) there is no axial rotation ($K = 0$), and in (*b*) $K > 0$.

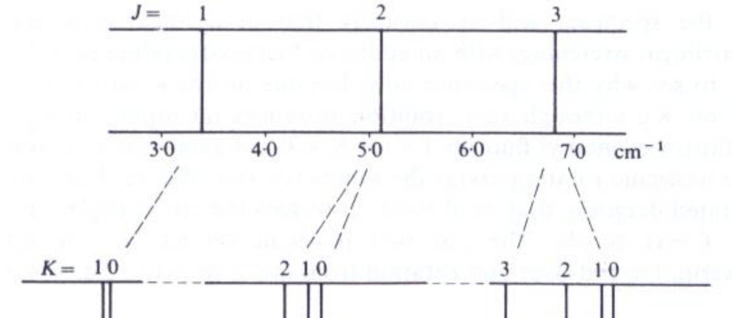

Figure 2.12 A diagrammatic representation of the rotational spectrum of the symmetric top molecule methyl fluoride, CH_3F.

However, since K only appears as K^2 in Eq. (2.42), there will be only $J + 1$ *different* frequencies, all those with $K > 0$ being doubly degenerate. We may tabulate a few lines as follows:

$$\begin{array}{rll} J = 0, K = 0 & \bar{\nu}_{JK} = 2B - 4D_J \quad \mathrm{cm}^{-1} & \\ J = 1, K = 0 & \bar{\nu}_{JK} = 4B - 32D_J & \\ K = \pm 1 & \bar{\nu}_{JK} = 4B - 32D_J - 4D_{JK} & \\ J = 2, K = 0 & \bar{\nu}_{JK} = 6B - 108D_J & \\ K = \pm 1 & \bar{\nu}_{JK} = 6B - 108D_J - 6D_{JK} & \\ K = \pm 2 & \bar{\nu}_{JK} = 6B - 108D_J - 24D_{JK}, \quad \text{etc.} & \end{array} \tag{2.43}$$

Let us now compare these with the observed spectrum of methyl fluoride. This is shown as a line diagram in Fig. 2.12, and the frequencies are tabulated in Table 2.3. Fitting these data to equations such as (2.43) leads directly to:

$$B = 0{\cdot}851\,204 \ \mathrm{cm}^{-1}$$

$$D_J = 2{\cdot}00 \times 10^{-6} \ \mathrm{cm}^{-1}$$

$$D_{JK} = 1{\cdot}47 \times 10^{-5} \ \mathrm{cm}^{-1}$$

The calculated frequencies of Table 2.3 show how precisely such measurements may now be made.

Once again each spectrum examined yields only one value of B, but the spectra of isotopic molecules can, in principle, give sufficient information for the calculation of all the bond lengths and angles of symmetric top molecules, together with estimates of the force constant of each bond.

Table 2.3 Microwave spectrum of methyl fluoride

J	K	$\bar{\nu}_{\text{obs.}}$ †(cm^{-1})	$\bar{\nu}_{\text{calc.}}$ (cm^{-1})
1	0	3·404 75	3·404 752
	1	3·404 70	3·404 693
2	0	5·107 01	5·107 008
	1	5·106 92	5·106 920
	2	5·106 65	5·106 655
3	0	6·809 12	6·809 120
	1	6·809 00	6·809 002
	2	6·808 65	6·808 649
	3	6·808 06	6·808 062

† Taken from W. Gordy, *Physical Review*, **93**, 406 (1954), by kind permission of the author.

Table 2.4 Some molecular data determined by microwave spectroscopy

Molecule	Type	Bond length (nm)	Bond angle (deg.)	Dipole moment† (debyes)
NaCl	Diatomic	0·236 06 ± 0·000 01	—	8·5 ± 0·2
COS	Linear	0·116 4 ± 0·000 1 (CO) 0·155 9 ± 0·000 1 (CS)	—	0·712 ± 0·004
HCN	Linear	0·106 317 ± 0·000 005 (CH) 0·115 535 ± 0·000 006 (CN)	—	2·986 ± 0·004
NH_3	Sym. Top	0·100 8 ± 0·000 4	107·3 ± 0·2	1·47 ± 0·01
CH_3Cl	Sym. Top	0·109 59 ± 0·000 05 (CH) 0·178 12 ± 0·000 05 (CCl)	108·0 ± 0·2 (HCH)	1·871 ± 0·005
H_2O	Asym. Top	0·095 84 ± 0·000 05	104·5 ± 0·3	1·846 ± 0·005
O_3	Asym. Top	0·127 8 ± 0·000 2	116·8 ± 0·5	0·53 ± 0·02

† Measured from the Stark effect, cf. Sec. 2.5.2.

2.4.3 Asymmetric Top Molecules

Since spherical tops show no microwave spectrum (cf. Sec. 2.1(3)) the only other class of molecule of interest here is the asymmetric top which has (Sec. 2.1(4)) all three moments of inertia different. These molecules will not detain us long since their rotational energy levels and spectra are very complex—in fact, no analytical expressions can be written for them corresponding to Eqs (2.24) and (2.28) for linear or Eqs (2.41) and (2.42) for symmetric top molecules. Each molecule and spectrum must, therefore, be treated as a separate case, and much tedious computation is necessary before structural parameters can be determined. The best method of attack so far has been to consider the asymmetric top as falling somewhere between the oblate and prolate symmetric top; interpolation between the two sets of energy levels of the latter leads to a first approximation of the energy levels—and hence spectrum—of the asymmetric molecule. It suffices to say that arbitrary methods such as this have been quite successful, and much very precise structural data have been published.

In order to give an idea of the precision of such measurements, we collect in Table 2.4 some molecular data determined by microwave methods, including examples from diatomic and linear molecules, symmetric tops, and asymmetric tops.

2.5 TECHNIQUES AND INSTRUMENTATION

2.5.1 Outline

It is not proposed here to give more than a brief outline of the techniques of microwave spectroscopy since detailed accounts are available in some of the books listed in the bibliography. Microwave spectroscopy, of course, follows the usual pattern: source, monochromator, beam direction, sample, and detector. We shall discuss each in turn.

1. *The source and monochromator.* The usual source in this region is the klystron valve which, since it emits radiation of only a very narrow frequency range, is called 'monochromatic' and acts as its own monochromator. The actual emission frequency is variable electronically and hence a spectrum may be scanned over a limited range of frequencies using a single klystron.

   One slight disadvantage of this source is that the total energy radiated is very small—of the order of milliwatts only. However, since all this is concentrated into a narrow frequency band a sharply tuned detector can be sufficiently activated to produce a strong signal.
2. *Beam direction.* This is achieved by the use of 'waveguides'—hollow tubes of copper or silver, usually of rectangular cross-section—inside which the radiation is confined. The waveguides may be gently tapered or bent to allow focusing and directing of the radiation. Atmospheric absorption of the beam is considerable, so the system must be efficiently evacuated.
3. *Sample and sample space.* In almost all microwave studies so far the sample has been gaseous. However, pressures of 0·01 mmHg are sufficient to give a reasonable absorption spectrum, so many substances which are usually thought of as solid or liquid may be examined provided their vapour pressures are above this value. The sample is retained by very thin mica windows in a piece of evacuated waveguide.
4. *Detector.* It is possible to use an ordinary superheterodyne radio receiver as detector, provided this may be tuned to the appropriate high frequency; however, a simple crystal detector is found to be more sensitive and easier to use. This detects the radiation focused upon it by the waveguide, and the signal it gives is amplified electronically for display on an oscilloscope, or for permanent record on paper.

2.5.2 The Stark Effect

We cannot leave the subject of microwave spectroscopy without a brief description of the Stark effect and its applications. A more detailed discussion is to be found in the books by Kroto and by Townes and Schawlow mentioned in the bibliography.

Experimentally the Stark effect requires the placing of an electric field, either perpendicular or parallel to the direction of the radiation beam, across the sample. Practically it is simpler to have a perpendicular field. We shall consider three advantages of this field.

1. A molecule exhibiting a rotational spectrum must have an electric dipole moment, and so its rotational energy levels will be perturbed by the

application of an exterior field since interaction will occur. Put simply, the absorption lines of the spectrum will be shifted by an amount depending on the extent of the interaction, and thus depending on both E, the applied field, and μ, the dipole moment. For a linear molecule the shift is found to be:

$$\Delta\nu \propto (\mu E)^2 \qquad \text{(linear molecule)}$$

while for a symmetric top:

$$\Delta\nu \propto \mu E \qquad \text{(symmetric top)}$$

Thus we have immediately a very accurate method of determining dipole moments, simply by observation of the Stark shift. More important, the measurement is made on very dilute gas samples, so the dipole moment observed may be taken to be that of the actual molecule, uncomplicated by molecular interactions, solvent effects, etc. Some values determined in this way are included in Table 2.4.

2. The second valuable application of the Stark effect is in the assignment of observed spectral lines to particular J values. We have seen that, in the absence of marked departure from rigidity and good resolving power, the assignment of J values is not always obvious. The line of lowest frequency which we observe *may* happen to correspond with $J = 0$, or it may be that it is the first observable line of a series, either because earlier lines are intrinsically very weak or because of limitations in the apparatus used. However, we have seen that each line is $2J + 1$ degenerate because rotations can occur in $2J + 1$ orientations in space without violating quantum laws. In the absence of any orienting effect these transitions have precisely the same frequency, but a Stark field constitutes an orienting effect, and splits the degeneracy; thus multiplet structure is observed for all lines with $J > 0$. The number of components depends on J, and hence unambiguous assignments can be made.
3. The final application is purely an instrumental one, but is especially interesting in that it has its counterpart in other spectral regions. We have already referred to the concept of signal-to-noise ratio in Chapter 1; that part of the noise which arises from random fluctuations in the background radiation may be removed by modulating the beam by means of the Stark effect as explained below.

Imagine the application of a Stark field in a periodic manner such as the 'square-wave' variation of Fig. 2.13; while the field is switched on the signal is modified in the way described in 1 and 2 above. If we arrange the modulation frequency to be some 100 to 1000 Hz, and construct the amplifier so that it amplifies only the component of the signal which has the modulated frequency, stray radiation which has not been through the modulating field will be completely ignored. This results in a great improvement of the signal-to-noise ratio.

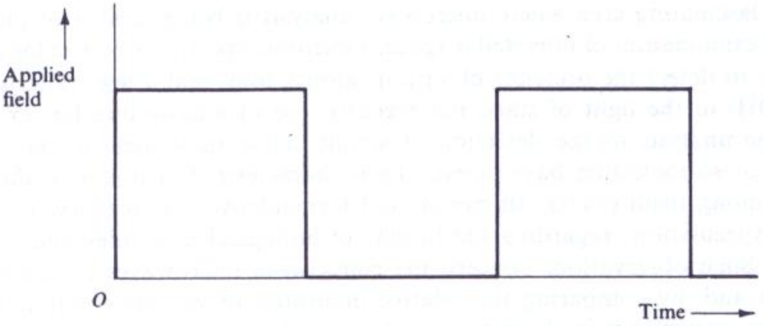

Figure 2.13 A 'square wave' potential as used for Stark modulation.

A further refinement is to arrange for both the modulated and unmodulated parts to be amplified separately and displayed on the same oscilloscope—the modulated part on the upper half, say, and the unmodulated on the lower. This much facilitates the measurement of the Stark splittings discussed in 1 and 2 above.

2.6 CHEMICAL ANALYSIS BY MICROWAVE SPECTROSCOPY

Improvements and simplifications in the techniques of microwave spectroscopy are now allowing it to move away from being purely a specialist research instrument towards becoming a technique for routine analysis. Even though effectively limited to gaseous samples, it has much to offer in this respect, since it is a highly sensitive (0·01 mmHg pressure is adequate) and specific analytical tool.

The microwave spectrum of a substance is very rich in lines since many rotational levels are populated at room temperatures, but since the lines are very sharp and their positions can be measured with great accuracy, observation of just a few of them is sufficient, after comparison with tabulated data, to establish the presence of a previously examined substance in a sample. And the technique is quantitative, since the intensity of a spectrum observed under given conditions is directly dependent on the amount of substance present. Thus mixtures can be readily analysed.

It is the *whole* molecule, by virtue of its moment(s) of inertia, which is examined by microwave spectroscopy. This means that the technique cannot detect the presence of particular molecular groupings in a sample, like $-OH$ or $-CH_3$ (cf. the chapters on infra-red, raman, and magnetic resonance spectroscopy later), but it can readily distinguish the presence of isotopes in a sample, and it can even detect different conformational isomers, provided they have different moments of inertia.

One fascinating area where microwave analysis is being used is in the chemical examination of interstellar space. Electronic spectroscopy has long been able to detect the presence of various atoms, ions, and a few radicals (e.g., —OH) in the light of stars, but recently, use of microwaves has extended the analysis to the detection of simple stable molecules in space. Some 30 or so molecules have already been characterized in this way, the earliest among them (water, ammonia, and formaldehyde) giving new impetus to speculations regarding the origins of biological molecules and of life itself. Such observations concern the emission of microwaves by these molecules and, by comparing the relative intensities of various rotational transitions, particularly in the spectrum of ammonia, accurate estimates can be made of the temperature of interstellar material.

BIBLIOGRAPHY

Chantry, G. W.: *Modern Aspects of Microwave Spectroscopy*, Academic Press, 1979.

Gordy, W., and R. L. Cook: *Microwave Molecular Spectra (Techniques of Organic Chemistry*, vol. 9), John Wiley, 1970.

Gordy, W., W. V. Smith, and R. Trambarulo: *Microwave Spectroscopy*, John Wiley, 1966.

Ingram, D. J. E.: *Spectroscopy at Radio and Microwave Frequencies*, 2nd ed., Butterworth, 1967.

Kroto, H. W.: *Molecular Rotation Spectra*, Wiley Interscience, 1975.

Sugden, T. M., and N. C. Kenney: *Microwave Spectroscopy of Gases*, Van Nostrand, 1965.

Townes, C. H. and A. L. Schawlow: *Microwave Spectroscopy*, McGraw-Hill, 1955.

Wollrab, J. E.: *Rotational Spectra and Molecular Structure*, Academic Press, 1967.

PROBLEMS

(Useful constants: $h = 6{\cdot}626 \times 10^{-34}$ J s; $k = 1{\cdot}381 \times 10^{-23}$ J K^{-1}; $c = 2{\cdot}998 \times 10^{8}$ m s^{-1}; $8\pi^2 = 78{\cdot}956$; atomic masses: $^{1}\mathrm{H} = 1{\cdot}673 \times 10^{-27}$ kg; $^{2}\mathrm{D} = 3{\cdot}344 \times 10^{-27}$ kg; $^{19}\mathrm{F} = 31{\cdot}55 \times 10^{-27}$ kg; $^{35}\mathrm{Cl} = 58{\cdot}06 \times 10^{-27}$ kg; $^{37}\mathrm{Cl} = 61{\cdot}38 \times 10^{-27}$ kg; $^{79}\mathrm{Br} = 131{\cdot}03 \times 10^{-27}$ kg.)

2.1 The rotational spectrum of $^{79}\mathrm{Br}^{19}\mathrm{F}$ shows a series of equidistant lines spaced 0·714 33 cm^{-1} apart. Calculate the rotational constant B, and hence the moment of inertia and bond length of the molecule. Determine the wavenumber of the $J = 9 \rightarrow J = 10$ transition, and find which transition gives rise to the most intense spectral line at room temperature (say 300 K).

2.2 Using your answers to Prob. 2.1, calculate the number of revolutions per second which the BrF molecule undergoes when in (*a*) the $J = 0$ state, (*b*) the $J = 1$ state, and (*c*) the $J = 10$ state.

Hint: Use $E = \frac{1}{2}I\omega^2$ in conjunction with Eqs (2.10) and (2.13), but remember that here ω is in *radians* per second.

2.3 The rotational constant for $\mathrm{H}^{35}\mathrm{Cl}$ is observed to be 10·5909 cm^{-1}. What are the values of B for $\mathrm{H}^{37}\mathrm{Cl}$ and for $^{2}\mathrm{D}^{35}\mathrm{Cl}$?

2.4 Three consecutive lines in the rotational spectrum of $\mathrm{H}^{79}\mathrm{Br}$ are observed at 84·544, 101·355 and 118·112 cm^{-1}. Assign the lines to their appropriate $J'' \rightarrow J'$ transitions, then deduce values for B and D, and hence evaluate the bond length and approximate vibrational frequency of the molecule.

2.5 Sketch a diagram similar to that of Fig. 2.7, using $B = 5$ cm^{-1} and a temperature of 1600 K.

Note: Find the maximum and calculate only two or three points on either side—don't attempt to carry out the calculation for every value of J.

2.6 The bond lengths of the linear molecule H—C≡N are given in Table 2.4. Calculate I and B for HCN and for DCN, using relative atomic masses of H = 1, D = 2, C = 12 and N = 14.

2.7 The diatomic molecule HCl has a B value of 10·593 cm^{-1} and a centrifugal distortion constant D of $5{\cdot}3 \times 10^{-4}$ cm^{-1}. Estimate the vibrational frequency and force constant of the molecule. The observed vibrational frequency is 2991 cm^{-1}; explain the discrepancy.

CHAPTER

THREE

INFRA-RED SPECTROSCOPY

We saw in the previous chapter how the elasticity of chemical bonds led to anomalous results in the rotational spectra of rapidly rotating molecules—the bonds stretched under centrifugal forces. In this chapter we consider another consequence of this elasticity—the fact that atoms in a molecule do not remain in fixed relative positions but vibrate about some mean position. We consider first the case of a diatomic molecule and the spectrum which arises if its only motion is vibration; then we shall deal with the more practical case of a diatomic molecule undergoing vibration and rotation simultaneously; finally we shall extend the discussion to more complex molecules.

3.1 THE VIBRATING DIATOMIC MOLECULE

3.1.1 The Energy of a Diatomic Molecule

When two atoms combine to form a stable covalent molecule (e.g., HCl gas) they may be said to do so because of some internal electronic rearrangement. This is not the place to discuss the detailed mechanisms of chemical bond formation; we may simply look on the phenomenon as a balancing of forces. On the one hand there is a repulsion between the positively charged nuclei of both atoms, and between the negative electron 'clouds'; on the other there is an attraction between the nucleus of one atom and the electrons of the other, and vice versa. The two atoms settle at a mean

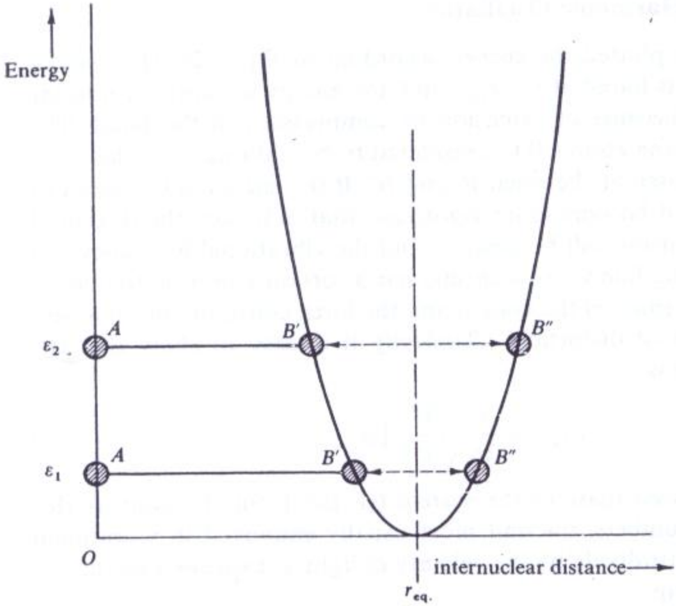

Figure 3.1 Parabolic curve of energy plotted against the extension or compression of a spring obeying Hooke's law.

internuclear distance such that these forces are just balanced and the energy of the whole system is at a minimum. Attempt to squeeze the atoms more closely together and the repulsive force rises rapidly; attempt to pull them further apart and we are resisted by the attractive force. In either case an attempt to distort the bond requires an input of energy and so we may plot energy against internuclear distance as in Fig. 3.1. At the minimum the internuclear distance is referred to as the equilbrium distance $r_{eq.}$, or more simply, as the bond length.

The compression and extension of a bond may be likened to the behaviour of a spring and we may extend the analogy by assuming that the bond, like a spring, obeys Hooke's law. We may then write

$$f = -k(r - r_{eq.}) \tag{3.1}$$

where f is the restoring force, k the force constant, and r the internuclear distance. In this case the energy curve is parabolic and has the form

$$E = \tfrac{1}{2}k(r - r_{eq.})^2 \tag{3.2}$$

This model of a vibrating diatomic molecule—the so-called simple harmonic oscillator model—while only an approximation, forms an excellent starting point for the discussion of vibrational spectra.

3.1.2 The Simple Harmonic Oscillator

In Fig. 3.1 we have plotted the energy according to Eq. (3.2). The zero of curve and equation is found at $r = r_{\text{eq.}}$, and any energy in excess of this, for example, ε_1, arises because of extension or compression of the bond. The figure shows that if one atom (A) is considered to be stationary on the $r = 0$ axis, the other will oscillate between B' and B''. If the energy is increased to ε_2 the oscillation will become more vigorous—that is to say, the degree of compression or extension will be greater—but the vibrational frequency will not change. An elastic bond, like a spring, has a certain vibration frequency dependent upon the mass of the system and the force constant, but independent of the amount of distortion. Classically it is easy to show that the oscillation frequency is:

$$\omega_{\text{osc.}} = \frac{1}{2\pi}\sqrt{\frac{k}{\mu}} \quad \text{Hz} \tag{3.3}$$

where μ is the reduced mass of the system (cf. Eq. (2.9)). To convert this frequency to wavenumbers, the unit most usually employed in vibrational spectroscopy, we must divide by the velocity of light, c, expressed in cm s^{-1} (cf. Sec. 1.1), obtaining:

$$\bar{\omega}_{\text{osc.}} = \frac{1}{2\pi c}\sqrt{\frac{k}{\mu}} \quad \text{cm}^{-1} \tag{3.4}$$

Vibrational energies, like all other molecular energies, are quantized, and the allowed vibrational energies for any particular system may be calculated from the Schrödinger equation. For the simple harmonic oscillator these turn out to be:

$$E_v = (v + \tfrac{1}{2})h\omega_{\text{osc.}} \quad \text{joules} \qquad (v = 0, 1, 2, \ldots) \tag{3.5}$$

where v is called the *vibrational quantum number*. Converting to the spectroscopic units, cm^{-1}, we have:

$$\varepsilon_v = \frac{E_v}{hc} = (v + \tfrac{1}{2})\bar{\omega}_{\text{osc.}} \quad \text{cm}^{-1} \tag{3.6}$$

as the only energies allowed to a simple harmonic vibrator. Some of these are shown in Fig. 3.2.

In particular we should notice that the *lowest* vibrational energy, obtained by putting $v = 0$ in Eq. (3.5) or (3.6), is

$$E_0 = \tfrac{1}{2}h\omega_{\text{osc.}} \quad \text{joules} \qquad [\omega_{\text{osc.}} \text{ in Hz}]$$

or

$$\varepsilon_0 = \tfrac{1}{2}\bar{\omega}_{\text{osc.}} \quad \text{cm}^{-1} \qquad [\bar{\omega}_{\text{osc.}} \text{ in cm}^{-1}] \tag{3.7}$$

The implication is that the diatomic molecule (and, indeed, *any* molecule) can never have zero vibrational energy; the atoms can never be completely

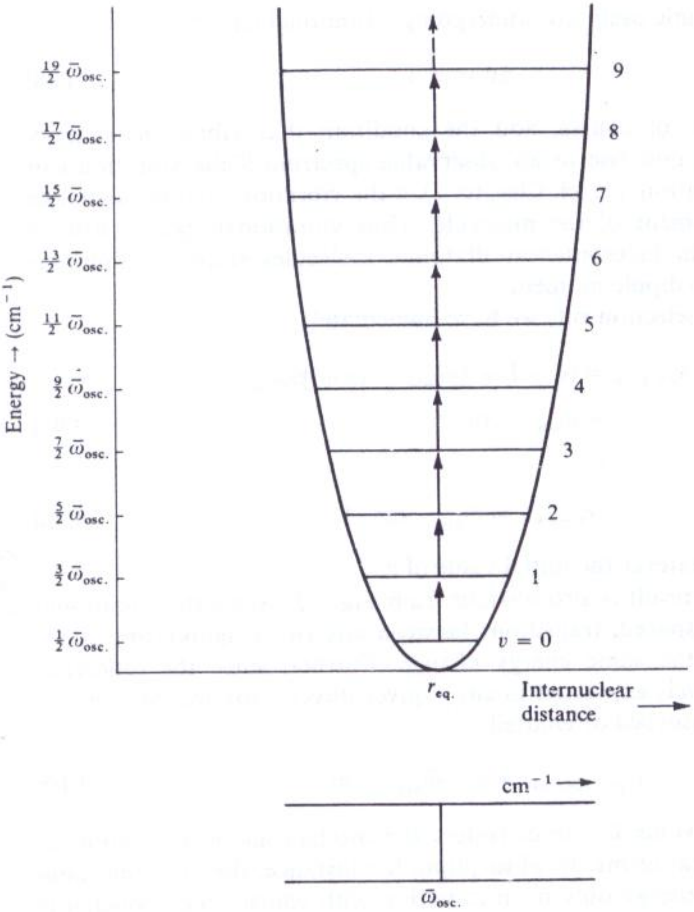

Figure 3.2 The allowed vibrational energy levels and transitions between them for a diatomic molecule undergoing simple harmonic motion.

at rest relative to each other. The quantity $\frac{1}{2}h\omega_{\text{osc.}}$ joules or $\frac{1}{2}\bar{\omega}_{\text{osc.}}$ cm^{-1} is known as the zero-point energy; it depends only on the classical vibration frequency and hence (Eq. (3.3) or (3.4)) on the strength of the chemical bond and the atomic masses.

The prediction of zero-point energy is the basic difference between the wave mechanical and classical approaches to molecular vibrations. Classical mechanics could find no objection to a molecule possessing no vibrational energy but wave mechanics insists that it must always vibrate to some extent; the latter conclusion has been amply borne out by experiment.

Further use of the Schrödinger equation leads to the simple *selection* *rule* for the harmonic oscillator undergoing vibrational changes:

$$\Delta v = \pm 1 \tag{3.8}$$

To this we must, of course, add the condition that vibrational energy changes will only give rise to an observable spectrum if the vibration can interact with radiation, i.e. (cf. Chapter 1), if the vibration involves a change in the dipole moment of the molecule. Thus vibrational spectra will be observable only in heteronuclear diatomic molecules since homonuclear molecules have no dipole moment.

Applying the selection rule we have immediately:

$$\begin{aligned} \varepsilon_{v+1 \to v} &= (v + 1 + \tfrac{1}{2})\bar{\omega}_{\text{osc.}} - (v + \tfrac{1}{2})\bar{\omega}_{\text{osc.}} \\ &= \bar{\omega}_{\text{osc.}} \quad \text{cm}^{-1} \end{aligned} \tag{3.9a}$$

for emission and

$$\varepsilon_{v \to v+1} = \bar{\omega}_{\text{osc.}} \quad \text{cm}^{-1} \tag{3.9b}$$

for absorption, whatever the initial value of v.

Such a simple result is also obvious from Fig. 3.2—since the vibrational levels are equally spaced, transitions between any two neighbouring states will give rise to the same energy change. Further, since the difference between energy levels expressed in cm^{-1} gives directly the wavenumber of the spectral line absorbed or emitted

$$\bar{v}_{\text{spectroscopic}} = \varepsilon = \bar{\omega}_{\text{osc.}} \quad \text{cm}^{-1} \tag{3.10}$$

This, again, is obvious if one considers the mechanism of absorption or emission in classical terms. In absorption, for instance, the vibrating molecule will absorb energy only from radiation with which it can coherently interact (cf. Fig. 1.8) and this must be radiation of its own oscillation frequency.

3.1.3 The Anharmonic Oscillator

Real molecules do not obey exactly the laws of simple harmonic motion; real bonds, although elastic, are not so homogeneous as to obey Hooke's law. If the bond between atoms is stretched, for instance, there comes a point at which it will break—the molecule dissociates into atoms. Thus although for small compressions and extensions the bond may be taken as perfectly elastic, for larger amplitudes—say greater than 10 per cent of the bond length—a much more complicated behaviour must be assumed. Figure 3.3 shows, diagrammatically, the shape of the energy curve for a typical diatomic molecule, together with (dashed) the ideal, simple harmonic parabola.

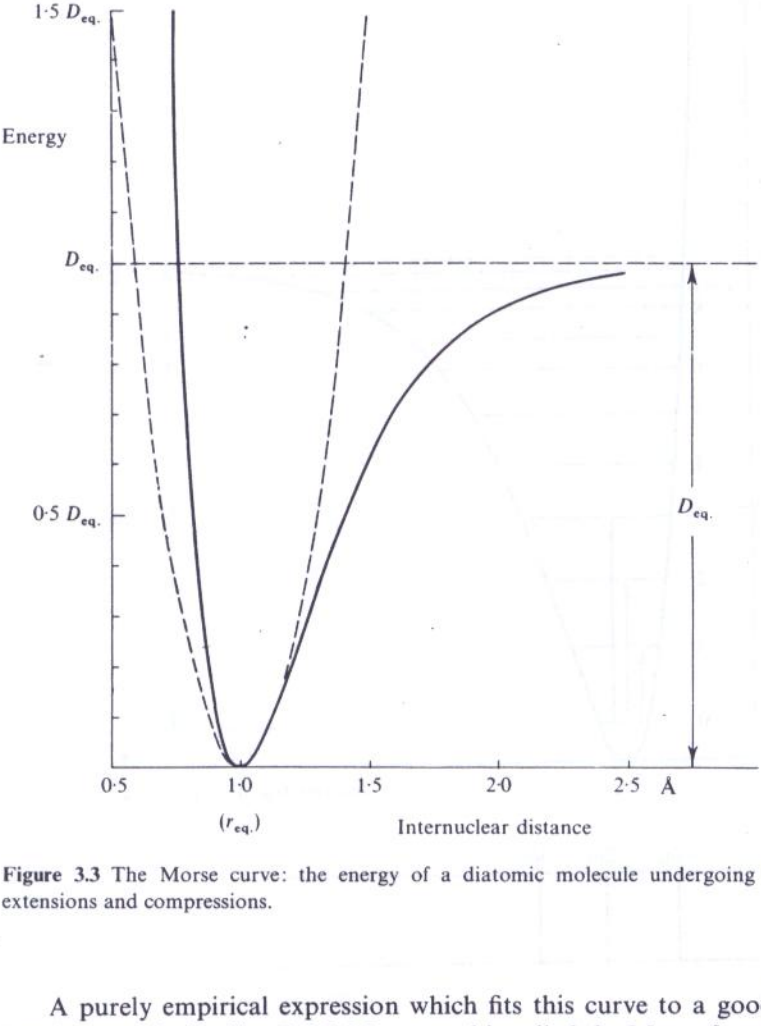

Figure 3.3 The Morse curve: the energy of a diatomic molecule undergoing anharmonic extensions and compressions.

A purely empirical expression which fits this curve to a good approximation was derived by P. M. Morse, and is called the Morse function:

$$E = D_{eq.}[1 - \exp\{a(r_{eq.} - r)\}]^2 \tag{3.11}$$

where a is a constant for a particular molecule and $D_{eq.}$ is the dissociation energy.

When Eq. (3.11) is used instead of Eq. (3.2) in the Schrödinger equation, the pattern of the allowed vibrational energy levels is found to be:

$$\varepsilon_v = (v + \tfrac{1}{2})\bar{\omega}_e - (v + \tfrac{1}{2})^2\bar{\omega}_e x_e \quad \text{cm}^{-1} \qquad (v = 0, 1, 2, \ldots) \tag{3.12}$$

where $\bar{\omega}_e$ is an oscillation frequency (expressed in wavenumbers) which we shall define more closely below, and x_e is the corresponding anharmonicity constant which, for bond stretching vibrations, is always small and positive

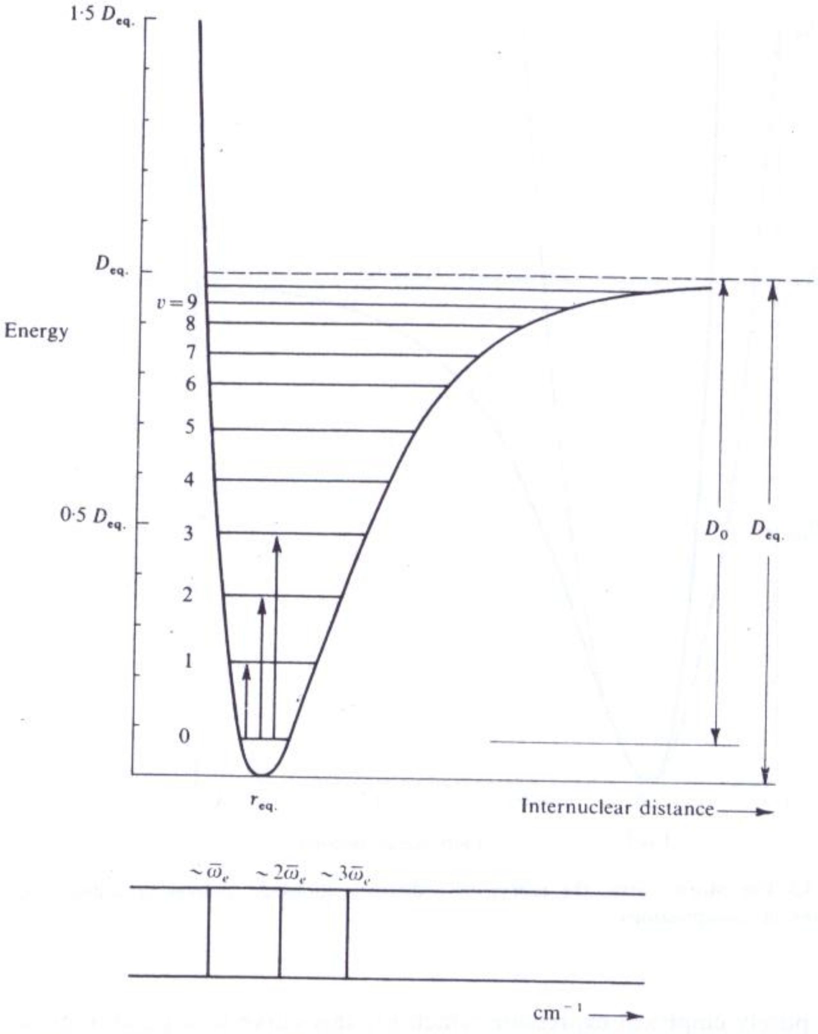

Figure 3.4 The allowed vibrational energy levels and some transitions between them for a diatomic molecule undergoing anharmonic oscillations.

($\approx +0{\cdot}01$), so that the vibrational levels crowd more closely together with increasing v. Some of these levels are sketched in Fig. 3.4.

It should be mentioned that Eq. (3.12), like (3.11), is an approximation only; more precise expressions for the energy levels require cubic, quartic, etc., terms in $(v + \frac{1}{2})$ with anharmonicity constants y_e, z_e, etc., rapidly diminishing in magnitude. These terms are important only at large values of v, and we shall ignore them.

If we rewrite Eq. (3.12), for the anharmonic oscillator, as:

$$\varepsilon_v = \bar{\omega}_e\{1 - x_e(v + \tfrac{1}{2})\}(v + \tfrac{1}{2}) \tag{3.13}$$

and compare with the energy levels of the *harmonic* oscillator (Eq. (3.6)), we see that we can write:

$$\bar{\omega}_{\text{osc.}} = \bar{\omega}_e\{1 - x_e(v + \tfrac{1}{2})\} \tag{3.14}$$

Thus the anharmonic oscillator behaves like the harmonic oscillator but with an oscillation frequency which decreases steadily with increasing v. If we now consider the hypothetical energy state obtained by putting $v = -\frac{1}{2}$ (at which, according to Eq. (3.13), $\varepsilon = 0$) the molecule would be at the equilibrium point with zero vibrational energy. Its oscillation frequency (in cm^{-1}) would be:

$$\bar{\omega}_{\text{osc.}} = \bar{\omega}_e$$

Thus we see that $\bar{\omega}_e$ may be defined as the (hypothetical) *equilibrium oscillation frequency* of the anharmonic system—the frequency for infinitely small vibrations about the equilibrium point. For any real state specified by a positive integral v the oscillation frequency will be given by Eq. (3.14). Thus in the ground state ($v = 0$) we would have:

$$\bar{\omega}_0 = \bar{\omega}_e(1 - \tfrac{1}{2}x_e) \quad \text{cm}^{-1}$$

and

$$\varepsilon_0 = \tfrac{1}{2}\bar{\omega}_e(1 - \tfrac{1}{2}x_e) \quad \text{cm}^{-1}$$

and we see that the zero point energy differs slightly from that for the harmonic oscillator (Eq. (3.7)).

The selection rules for the anharmonic oscillator are found to be:

$$\Delta v = \pm 1, \pm 2, \pm 3, \ldots$$

Thus they are the same as for the harmonic oscillator, with the additional possibility of larger jumps. These, however, are predicted by theory and observed in practice to be of rapidly diminishing probability and normally only the lines of $\Delta v = \pm 1, \pm 2$, and ± 3, at the most, have observable intensity. Further, the spacing between the vibrational levels is, as we shall shortly see, of order $10^3\ \text{cm}^{-1}$ and, at room temperature, we may use the Boltzmann distribution (Eq. (1.12)) to show

$$\frac{N_{v=1}}{N_{v=0}} = \exp\left\{-\frac{6{\cdot}63 \times 10^{-34} \times 3 \times 10^{10} \times 10^3}{1{\cdot}38 \times 10^{-23} \times 300}\right\}$$

$$\approx \exp(-4{\cdot}8) \approx 0{\cdot}008.$$

In other words, the population of the $v = 1$ state is nearly 0·01 or some one per cent of the ground state population. Thus, to a very good approximation, we may ignore all transitions originating at $v = 1$ or more and restrict ourselves to the three transitions:

1. $v = 0 \rightarrow v = 1$, $\Delta v = +1$, with considerable intensity.

$$\begin{aligned}\Delta\varepsilon &= \varepsilon_{v=1} - \varepsilon_{v=0}\\ &= (1+\tfrac{1}{2})\bar{\omega}_e - x_e(1+\tfrac{1}{2})^2\bar{\omega}_e - \{\tfrac{1}{2}\bar{\omega}_e - (\tfrac{1}{2})^2 x_e\bar{\omega}_e\}\\ &= \bar{\omega}_e(1-2x_e) \quad \text{cm}^{-1} \end{aligned} \tag{3.15a}$$

2. $v = 0 \rightarrow v = 2$, $\Delta v = +2$, with small intensity.

$$\begin{aligned}\Delta\varepsilon &= (2+\tfrac{1}{2})\bar{\omega}_e - x_e(2+\tfrac{1}{2})^2\bar{\omega}_e - \{\tfrac{1}{2}\bar{\omega}_e - (\tfrac{1}{2})^2 x_e\bar{\omega}_e\}\\ &= 2\bar{\omega}_e(1-3x_e) \quad \text{cm}^{-1} \end{aligned} \tag{3.15b}$$

3. $v = 0 \rightarrow v = 3$, $\Delta v = +3$, with normally negligible intensity.

$$\begin{aligned}\Delta\varepsilon &= (3+\tfrac{1}{2})\bar{\omega}_e - \{\tfrac{1}{2}\bar{\omega}_e - (\tfrac{1}{2})^2 x_e\bar{\omega}_e\}\\ &= 3\bar{\omega}_e(1-4x_e) \quad \text{cm}^{-1} \end{aligned} \tag{3.15c}$$

These three transitions are shown in Fig. 3.4. To a good approximation, since $x_e \approx 0{\cdot}01$, the three spectral lines lie very close to $\bar{\omega}_e$, $2\bar{\omega}_e$, and $3\bar{\omega}_e$. The line near $\bar{\omega}_e$ is called the *fundamental absorption*, while those near $2\bar{\omega}_e$ *and* $3\bar{\omega}_e$ are called the *first* and *second overtones*, respectively. The spectrum of HCl, for instance, shows a very intense absorption at 2886 cm^{-1}, a weaker one at 5668 cm^{-1}, and a very weak one at 8347 cm^{-1}. If we wish to find the equilibrium frequency of the molecule from these data, we must solve any two of the three equations (cf. Eqs. (3.15)):

$$\begin{aligned}\bar{\omega}_e(1-2x_e) &= 2886\\ 2\bar{\omega}_e(1-3x_e) &= 5668\\ 3\bar{\omega}_e(1-4x_e) &= 8347 \text{ cm}^{-1}\end{aligned}$$

and we find $\bar{\omega}_e = 2990$ cm^{-1}, $x_e = 0{\cdot}0174$. Thus we see that, whereas for the ideal harmonic oscillator the spectral absorption occurred *exactly* at the classical vibration frequency, for real, anharmonic molecules the observed fundamental absorption frequency and the equilibrium frequency may differ considerably.

The force constant of the bond in HCl may be calculated directly from Eq. (2.22) by inserting the value of $\bar{\omega}_e$:

$$\begin{aligned}k &= 4\pi^2\bar{\omega}_e^2c^2\mu \quad \text{N m}^{-1}\\ &= 516 \text{ N m}^{-1}\end{aligned}$$

when the fundamental constants and the reduced mass are inserted. These data, together with that for a few of the very many other diatomic molecules studied by infra-red techniques, are collected in Table 3.1.

Table 3.1 Some molecular data for diatomic molecules determined by infra-red spectroscopy

Molecule	Vibration (cm^{-1})	Anharmonicity constant, x_e	Force constant ($\mathrm{N\ m}^{-1}$)	Internuclear distance $r_{\mathrm{eq.}}$ (nm)
HF	4138·5	0·0218	966	0·0927
HCl†	2990·6	0·0174	516	0·1274
HBr	2649·7	0·0171	412	0·1414
HI	2309·5	0·0172	314	0·1609
CO	2169·7	0·0061	1902	0·1131
NO	1904·0	0·0073	1595	0·1151
ICl†	384·2	0·0038	238	0·2321

† Data refers to the ^{35}Cl isotope.

Although we have ignored transitions from $v = 1$ to higher states, we should note that, if the temperature is raised or if the vibration has a particularly low frequency, the population of the $v = 1$ state may become appreciable. Thus at, say, 600 K (i.e., about 300°C) $N_{v=1}/N_{v=0}$ becomes $\exp(-2{\cdot}4)$ or about 0·09, and transitions from $v = 1$ to $v = 2$ will be some 10 per cent the intensity of those from $v = 0$ to $v = 1$. A similar increase in the excited state population would arise if the vibrational frequency were 500 cm^{-1} instead of 1000 cm^{-1}. We may calculate the wavenumber of this transition as:

4. $v = 1 \rightarrow v = 2$, $\Delta v = +1$, normally very weak,

$$\begin{aligned}\Delta\varepsilon &= 2\tfrac{1}{2}\bar{\omega}_e - 6\tfrac{1}{4}x_e\bar{\omega}_e - \{1\tfrac{1}{2}\bar{\omega}_e - 2\tfrac{1}{4}x_e\bar{\omega}_e\}\\ &= \bar{\omega}_e(1 - 4x_e)\quad \mathrm{cm}^{-1} \qquad (3.15d)\end{aligned}$$

Thus, should this weak absorption arise, it will be found close to and at slightly *lower* wavenumber than the fundamental (since x_e is small and positive). Such weak absorptions are usually called *hot bands* since a high temperature is one condition for their occurrence. Their nature may be confirmed by raising the temperature of the sample when a true hot band will increase in intensity.

We turn now to consider a diatomic molecule undergoing simultaneous vibration and rotation.

3.2 THE DIATOMIC VIBRATING-ROTATOR

We saw in Chapter 2 that a typical diatomic molecule has rotational energy separations of 1–10 cm^{-1}, while in the preceding section we found that the vibrational energy separations of HCl were nearly 3000 cm^{-1}. Since the energies of the two motions are so different we may, as a first approximation, consider that a diatomic molecule can execute rotations and vibrations quite independently. This, which we shall call the Born–Oppenheimer approximation (although, cf. Eq. (6·1), this strictly includes electronic energies), is tantamount to assuming that the combined rotational–vibrational energy is simply the sum of the separate energies:

$$E_{\text{total}} = E_{\text{rot.}} + E_{\text{vib.}} \quad \text{(joules)}$$

$$\varepsilon_{\text{total}} = \varepsilon_{\text{rot.}} + \varepsilon_{\text{vib.}} \quad (\text{cm}^{-1}) \tag{3.16}$$

We shall see later in what circumstances this approximation does not apply.

Taking the separate expressions for $\varepsilon_{\text{rot.}}$ and $\varepsilon_{\text{vib.}}$ from Eqs (2.26) and (3.12) respectively, we have:

$$\begin{aligned} \varepsilon_{J,v} &= \varepsilon_J + \varepsilon_v \\ &= BJ(J+1) - DJ^2(J+1)^2 + HJ^3(J+1)^3 + \dots \\ &\quad + (v+\tfrac{1}{2})\bar{\omega}_e - x_e(v+\tfrac{1}{2})^2\bar{\omega}_e \quad \text{cm}^{-1} \end{aligned} \tag{3.17}$$

Initially, we shall ignore the small centrifugal distortion constants D, H, etc., and hence write

$$\varepsilon_{\text{total}} = \varepsilon_{J,v} = BJ(J+1) + (v+\tfrac{1}{2})\bar{\omega}_e - x_e(v+\tfrac{1}{2})^2\bar{\omega}_e \tag{3.18}$$

Note, however, that it is not logical to ignore D since this implies that we are treating the molecule as rigid, yet vibrating! The retention of D would have only a very minor effect on the spectrum.

The rotational levels are sketched in Fig. 3.5 for the two lowest vibrational levels, $v = 0$ and $v = 1$. There is, however, no attempt at scale in this diagram since the separation between neighbouring J values is, in fact, only some 1/1000 of that between the v values. Note that since the rotational constant B in Eq. (3.18) is taken to be the same for all J and v (a consequence of the Born–Oppenheimer assumption), the separation between two levels of given J is the same in the $v = 0$ and $v = 1$ states.

It may be shown that the selection rules for the combined motions are the same as those for each separately; therefore we have:

$$\Delta v = \pm 1, \pm 2, \text{etc.} \qquad \Delta J = \pm 1 \tag{3.19}$$

Strictly speaking we may also have $\Delta v = 0$, but this corresponds to the purely rotational transitions already dealt with in Chapter 2. Note carefully, however, that a *diatomic* molecule, except under very special and rare circumstances, may *not* have $\Delta J = 0$; in other words a vibrational change *must* be accompanied by a simultaneous rotational change.

In Fig. 3.6 we have drawn some of the relevant energy levels and transitions, designating rotational quantum numbers in the $v = 0$ state as J'' and in the $v = 1$ state as J'. The use of a single prime for the upper state

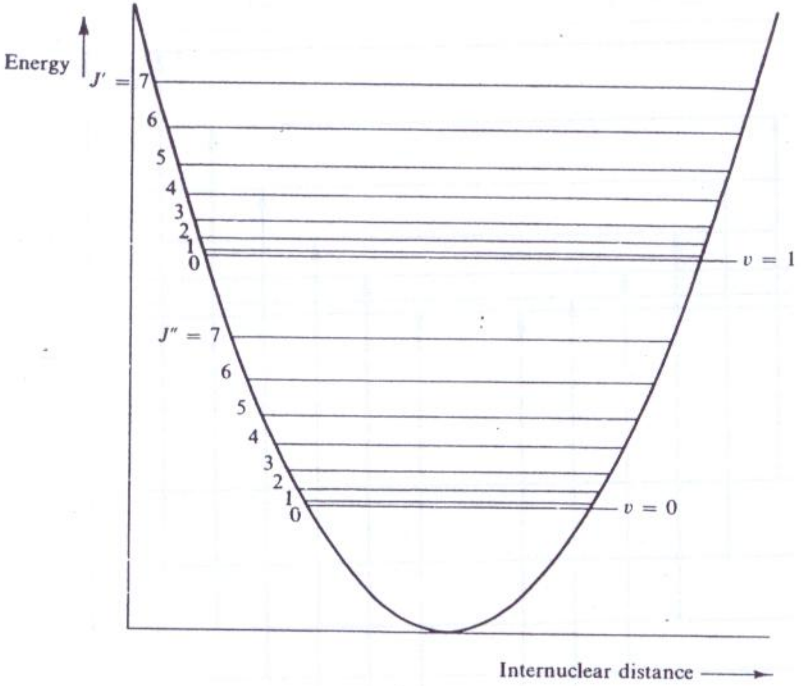

Figure 3.5 The rotational energy levels for two different vibrational states of a diatomic molecule.

and a double for the lower state is conventional in all branches of spectroscopy.

Remember (and cf. Eq. (2.20)) that the rotational levels J'' are filled to varying degrees in any molecular population, so the transitions shown will occur with varying intensities. This is indicated schematically in the spectrum at the foot of Fig. 3.6.

An analytical expression for the spectrum may be obtained by applying the selection rules (Eq. (3.19)) to the energy levels (Eq. (3.18)). Considering only the $v = 0 \rightarrow v = 1$ transition we have in general:

$$\begin{aligned}\Delta\varepsilon_{J,v} &= \varepsilon_{J',v=1} - \varepsilon_{J'',v=0}\\ &= BJ'(J'+1) + 1\tfrac{1}{2}\bar{\omega}_e - 2\tfrac{1}{4}x_e\bar{\omega}_e - \{BJ''(J''+1) + \tfrac{1}{2}\bar{\omega}_e - \tfrac{1}{4}x_e\bar{\omega}_e\}\\ &= \bar{\omega}_o + B(J'-J'')(J'+J''+1) \quad \text{cm}^{-1}\end{aligned}$$

where, for brevity, we write $\bar{\omega}_o$ for $\bar{\omega}_e(1 - 2x_e)$.

We should note that taking B to be identical in the upper and lower vibrational states is a direct consequence of the Born–Oppenheimer approximation—rotation is unaffected by vibrational changes.

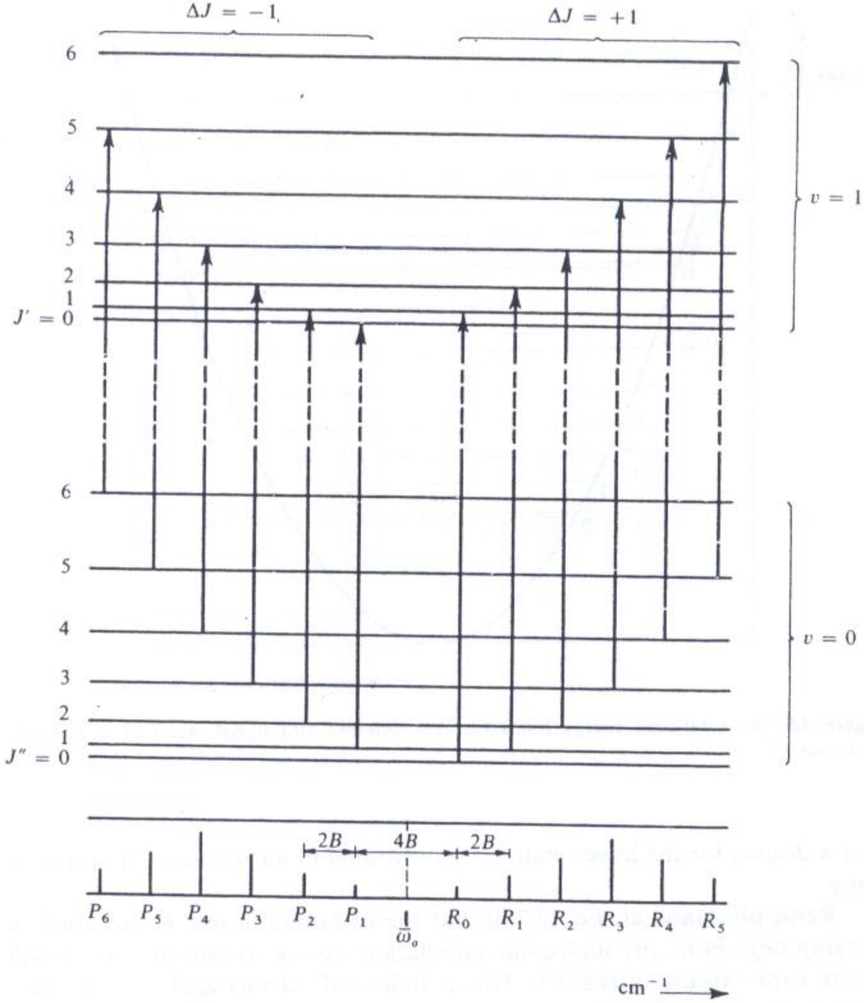

Figure 3.6 Some transitions between the rotational–vibrational energy levels of a diatomic molecule together with the spectrum arising from them.

Now we can have:

1. $\Delta J = +1$, i.e., $J' = J'' + 1$ or $J' - J'' = +1$; hence

$$\Delta\varepsilon_{J,v} = \bar{\omega}_o + 2B(J'' + 1)\ \text{cm}^{-1} \qquad J'' = 0, 1, 2, \ldots \tag{3.20a}$$

2. $\Delta J = -1$, i.e., $J'' = J' + 1$ or $J' - J'' = -1$; and

$$\Delta\varepsilon_{J,v} = \bar{\omega}_o - 2B(J' + 1)\ \text{cm}^{-1} \qquad J' = 0, 1, 2, \ldots \tag{3.20b}$$

These two expressions may conveniently be combined into:

$$\Delta\varepsilon_{J,v} = \bar{\nu}_{\text{spect.}} = \bar{\omega}_o + 2Bm \quad \text{cm}^{-1} \qquad m = \pm 1, \pm 2, \ldots \qquad (3.20c)$$

where m, replacing $J'' + 1$ in Eq. (3.20*a*) and $J' + 1$ in Eq. (3.20*b*) has positive values for $\Delta J = +1$ and is negative if $\Delta J = +1$. Note particularly that *m cannot be zero* since this would imply values of J' or J'' to be -1. The frequency $\bar{\omega}_o$ is usually called the *band origin* or *band centre*.

Equation (3.20*c*), then, represents the combined vibration–rotation spectrum. Evidently it will consist of equally spaced lines (spacing $= 2B$) on each side of the band origin $\bar{\omega}_o$, but, since $m \neq 0$, the *line at $\bar{\omega}_o$ itself will not appear*. Lines to the low-frequency side of $\bar{\omega}_o$, corresponding to negative m (that is, $\Delta J = -1$) are referred to as the *P branch*, while those to the high-frequency side (m positive, $\Delta J = +1$) are called the *R branch*. This apparently arbitrary notation may become clearer if we state here that later, in other contexts, we shall be concerned with ΔJ values of 0 and ± 2, in addition to ± 1 considered here; the labelling of line series is then quite consistent:

Lines arising from $\Delta J =$	-2	-1	0	$+1$	$+2$	
called:	*O*	*P*	*Q*	*R*	*S*	branch

The *P* and *R* notation, with the *lower J* (J'') value as a suffix, is illustrated on the diagrammatic spectrum of Fig. 3.6. This is the conventional notation for such spectra.

It is readily shown that the inclusion of the centrifugal distortion constant D leads to the following expression for the spectrum:

$$\Delta\varepsilon = \bar{\nu}_{\text{spect.}} = \bar{\omega}_o + 2Bm - 4Dm^3 \quad \text{cm}^{-1} \qquad (m = \pm 1, \pm 2, \pm 3, \ldots) \qquad (3.21)$$

But we have seen in Chapter 2 that B is some 10 cm^{-1} or less, while D is only some 0·01 per cent of B. Since a good infra-red spectrometer has a resolving power of about 0·5 cm^{-1} it is obvious that D is negligible to a very high degree of accuracy.

The anharmonicity factor, on the other hand, is not negligible. It affects not only the position of the band origin (since $\bar{\omega}_o = \bar{\omega}_e(1 - 2x_e)$), but, by extending the selection rules to include $\Delta v = \pm 2, \pm 3$, etc., also allows the appearance of overtone bands having identical rotational structure. This is illustrated in Fig. 3.7(*a*), where the fundamental absorption and first overtone of carbon monoxide are shown. From the band centres we can calculate, as shown in Sec. 1.3, the equilibrium frequency $\bar{\omega}_e$ and the anharmonicity constant x_e.

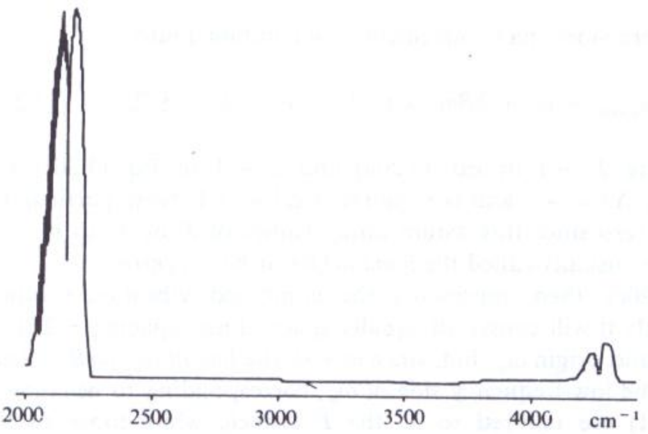

Figure 3.7(*a*) The fundamental absorption (centred at about 2143 cm^{-1}) and the first overtone (centred at about 4260 cm^{-1}) of carbon monoxide. The fine structure of the *P* branch in the fundamental is partially resolved. (Gas pressure 650 mmHg in a 10 cm cell.)

3.3 THE VIBRATION–ROTATION SPECTRUM OF CARBON MONOXIDE

In Fig. 3.7(*b*) we show the fundamental vibration–rotation band of carbon monoxide under high resolution, with some lines in the *P* and *R* branches numbered according to their J'' values. Table 3.2 gives the observed wavenumbers of the first five lines in each branch. We shall discuss shortly the slight decrease in separation between the rotational lines as the wavenumber increases; this decrease is apparent from the table and from a close inspection of the 'wings' of the spectrum.

From the table we see that the band centre is at about 2143 cm^{-1} while the average line separation near the centre is 3·83 cm^{-1}. This immediately gives:

$$2B = 3{\cdot}83\ \text{cm}^{-1} \qquad B = 1{\cdot}915\ \text{cm}^{-1}$$

Table 3.2 Part of the infra-red spectrum of carbon monoxide

Line	$\bar{\nu}$	Separation $\Delta\bar{\nu}$	Line	$\bar{\nu}$	Separation $\Delta\bar{\nu}$
$P_{(1)}$	2139·43		$R_{(0)}$	2147·08	
		3·88			3·78
$P_{(2)}$	2135·55		$R_{(1)}$	2150·86	
		3·92			3·73
$P_{(3)}$	2131·63		$R_{(2)}$	2154·59	
		3·95			3·72
$P_{(4)}$	2127·68		$R_{(3)}$	2158·31	
		3·98			3·66
$P_{(5)}$	2123·70		$R_{(4)}$	2161·97	

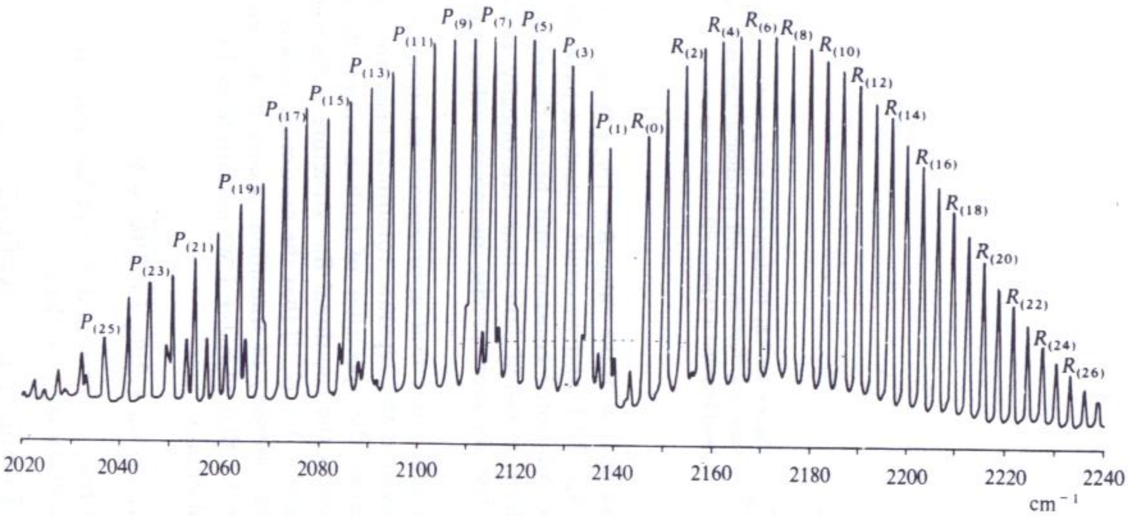

Figure 3.7(*b*) The centre of the fundamental band of carbon monoxide under higher resolution than in (*a*). (Gas pressure 100 mmHg in a 10 cm cell.) The lines are labelled according to their J'' values. The P branch is complicated by the presence of a band centred at about 2100 cm^{-1} due to the one per cent of ^{13}CO in the sample; some of the rotational lines from this band appear between P branch lines, others are overlapped by a P branch line and give it an enhanced intensity (e.g., lines $P_{(16)}$, $P_{(17)}$, $P_{(23)}$, and $P_{(24)}$).

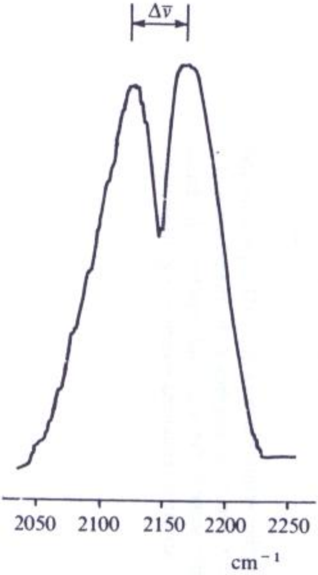

Figure 3.8 The fundamental band of Fig. 3.7(*b*) under very low resolution. All rotational fine structure has been lost and a typical PR contour is seen.

This is in satisfactory agreement with the value $B = 1{\cdot}921\,18\ cm^{-1}$ derived by microwave studies (cf. Sec. 2.3.1) and we could, therefore, have obtained quite good values for the rotational constant and hence the moment of inertia and bond length from infra-red data alone. Historically, of course, the infra-red values came first, the more precise microwave values following much later.

It is worth noting at this point that approximate rotational data is obtainable from spectra even if the separate rotational lines are not resolved. Thus Fig. 3.8 shows the spectrum of carbon monoxide under much poorer resolution, when the rotational fine structure is blurred out to an envelope. Now we saw in Eq. (2.21) that the maximum population of levels, and hence maximum intensity of transition, occurs at a J value of $\sqrt{kT/2Bhc} - \frac{1}{2}$. Remembering that $m = J + 1$ we substitute in Eq. (3.20*c*) $m = \pm\sqrt{kT/2Bhc} + \frac{1}{2}$ and obtain:

$$\bar{\nu}_{\text{max. intensity}} = \bar{\omega}_0 \pm 2B\left(\sqrt{kT/2Bhc} + \tfrac{1}{2}\right)$$

where the + and − signs refer to the R and P branches, respectively. The *separation* between the two maxima, $\Delta\bar{\nu}$, is then:

$$\Delta\bar{\nu} = 4B\left(\sqrt{kT/2Bhc} + \tfrac{1}{2}\right) = \sqrt{8kTB/hc} + 2B$$

or, since B is small compared with $\Delta\bar{\nu}$, we can write

$$\Delta\bar{\nu} \approx \sqrt{8kTB/hc}, \qquad B \approx hc(\Delta\bar{\nu})^2/8kT \quad cm^{-1}$$

where c is expressed in cm s^{-1}. In the case of carbon monoxide the separation is about 55 cm^{-1} (Fig. 3.8), while the temperature at which the spectrum was obtained was about 300 K. We are led, then, to a B value of about 1·8 cm^{-1} which is in fair agreement with the earlier values, but much less precise.

From Table 3.2 we see that the band origin, at the midpoint of $P_{(1)}$ and $R_{(0)}$, is at 2143·26 cm^{-1}. This, then, is the fundamental vibration frequency of carbon monoxide, if anharmonicity is ignored. The latter can be taken into account, however, since the first overtone is found to have its origin at 4260·04 cm^{-1}. We have:

$$\bar{\omega}_e(1 - 2x_e) = \bar{\omega}_o = 2143{\cdot}26$$

$$2\bar{\omega}_e(1 - 3x_e) = 4260{\cdot}04$$

from which $\omega_e = 2169{\cdot}74$ cm^{-1}, $x_e = 0{\cdot}0061$.

3.4 BREAKDOWN OF THE BORN–OPPENHEIMER APPROXIMATION: THE INTERACTION OF ROTATIONS AND VIBRATIONS

So far we have assumed that vibration and rotation can proceed quite independently of each other. A molecule vibrates some 10^3 times during the course of a single rotation, however, so it is evident that the bond length (and hence the moment of inertia and B constant) also changes continually during the rotation. If the vibration is simple harmonic the mean bond length will be the same as the equilibrium bond length and it will not vary with vibrational energy; this is seen in Fig. 3.1. However, the rotational constant B depends on $1/r^2$ and, as shown by an example in Sec. 2.3.4, the average value of this quantity is not the same as $1/r_{\text{eq.}}^2$ where $r_{\text{eq.}}$ is the equilibrium length. Further an increase in the vibrational energy is accompanied by an increase in the vibrational amplitude and hence the value of B will depend on the v quantum number.

In the case of anharmonic vibrations the situation is rather more complex. Now an increase in vibrational energy will lead to an increase in the average bond length—this is perhaps most evident from Fig. 3.4. The rotational constant then varies even more with vibrational energy.

In general, it is plain that, since $r_{\text{av.}}$ *increases* with the vibrational energy, B is *smaller* in the upper vibrational state than in the lower. In fact an equation of the form:

$$B_v = B_e - \alpha(v + \tfrac{1}{2}) \tag{3.22}$$

gives, to a high degree of approximation, the value of B_v, the rotational constant in vibrational level v, in terms of the equilibrium value B_e and α, a small positive constant for each molecule.

Here we restrict our discussion to the fundamental vibrational change, i.e., the change $v = 0 \rightarrow v = 1$, and we may take the respective B values as B_0 and B_1 with $B_0 > B_1$. For this transition:

$$\Delta\varepsilon = \varepsilon_{J', v=1} - \varepsilon_{J'', v=0}$$

$$= \bar{\omega}_o + B_1 J'(J' + 1) - B_0 J''(J'' + 1) \text{ cm}^{-1}$$

where, as before, $\bar{\omega}_o = \bar{\omega}_e(1 - 2x_e)$.

We then have the two cases:

1. $$\Delta J = +1 \qquad J' = J'' + 1$$

$$\Delta\varepsilon = \bar{\nu}_R = \bar{\omega}_o + (B_1 + B_0)(J'' + 1) + (B_1 - B_0)(J'' + 1)^2 \text{ cm}^{-1}$$

$$(J'' = 0, 1, 2, \ldots) \quad (3.23a)$$

and

2. $$\Delta J = -1 \qquad J'' = J' + 1$$

$$\Delta\varepsilon = \bar{\nu}_P = \bar{\omega}_o - (B_1 + B_0)(J' + 1) + (B_1 - B_0)(J' + 1)^2 \text{ cm}^{-1}$$

$$(J' = 0, 1, 2, \ldots) \quad (3.23b)$$

where we have written $\bar{\nu}_P$ and $\bar{\nu}_R$ to represent the wavenumbers of the P and R branch lines respectively. These two equations can be combined into the expression:

$$\bar{\nu}_{P,R} = \bar{\omega}_o + (B_1 + B_0)m + (B_1 - B_0)m^2 \quad \text{cm}^{-1} \qquad (m = \pm 1, \pm 2, \ldots) \quad (3.23c)$$

where positive m values refer to the R branch and negative to P.

We see that ignoring vibration–rotation interaction involves setting $B_1 = B_0$, when Eq. (3.23*c*) immediately simplifies to (3.20*c*). Since $B_1 < B_0$ the last term of (3.23*c*) is always negative, irrespective of the sign of m, and the effect on the spectrum of a diatomic molecule is to crowd the rotational lines more closely together with increasing m on the R branch side, while the P branch lines become more widely spaced as (negative) m increases. Normally B_1 and B_0 differ only slightly and the effect is marked only for high m values. This is exactly the situation shown in the spectrum of carbon monoxide, Fig. 3.7(*b*).

In Table 3.3 some of the data for carbon monoxide are tabulated, together with the positions of lines calculated from the equation:

$$\bar{\nu}_{\text{spect.}} = 2143{\cdot}28 + 3{\cdot}813m - 0{\cdot}0175m^2 \quad \text{cm}^{-1}.$$

From this we see that, for this molecule:

$$B_1 = 1{\cdot}898 \text{ cm}^{-1} \qquad B_0 = 1{\cdot}915 \text{ cm}^{-1}$$

Table 3.3 Observed and calculated wavenumbers of some lines in the spectrum of carbon monoxide

m	J''	$\bar{\nu}_{\text{obs.}}$	$\bar{\nu}_{\text{calc.}}$†
30	29	2241·64	2241·91
25	24	2227·63	2227·65
20	19	2212·62	2212·54
15	14	2196·66	2196·53
10	9	2179·77	2179·66
5	4	2161·97	2161·90
0	—	(Band centre)	2143·28
−5	5	2123·70	2123·78
−10	10	2103·27	2103·40
−15	15	2082·01	2082·15
−20	20	2059·91	2060·02
−25	25	2037·03	2037·02
−30	30	2013·35	2013·14

† Values calculated from: $\bar{\nu} = 2143{\cdot}28 + 3{\cdot}813m - 0{\cdot}0175m^2$.

and hence, using Eq. (3.22), we have:

$$\alpha = 0{\cdot}018 \qquad B_e = 1{\cdot}924 \text{ cm}^{-1}$$

Further, we can calculate the equilibrium bond length and the bond lengths in the $v = 0$ and $v = 1$ states (cf. pp. 46–47) to be:

$$r_{\text{eq.}} = 0{\cdot}1130 \text{ nm} \qquad r_0 = 0{\cdot}1133 \text{ nm} \qquad r_1 = 0{\cdot}1136 \text{ nm}$$

3.5 THE VIBRATIONS OF POLYATOMIC MOLECULES

In this section and the next, just as in the corresponding one dealing with the pure rotational spectra of polyatomic molecules, we shall find that although there is an increase in the complexity, only slight and quite logical extensions to the simple theory are adequate to give us an understanding of the spectra. We shall need to discuss:

1. The number of fundamental vibrations and their symmetry
2. The possibility of overtone and combination bands
3. The influence of rotation on the spectra.

3.5.1 Fundamental Vibrations and their Symmetry

Consider a molecule containing N atoms: we can refer to the position of each atom by specifying three coordinates (e.g., the x, y, and z cartesian coordinates). Thus the total number of coordinate values is $3N$ and we say the molecule has $3N$ *degrees of freedom* since each coordinate value may be specified quite independently of the others. However, once all $3N$ coordinates have been fixed, the bond distances and bond angles of the molecule are also fixed and no further arbitrary specifications can be made.

Now the molecule is free to move in three-dimensional space, as a whole, without change of shape. We can refer to such movement by noting the position of its centre of gravity at any instant—to do this requires a statement of three coordinate values. This translational movement uses three of the $3N$ degrees of freedom leaving $3N - 3$. In general, also, the rotation of a non-linear molecule can be resolved into components about three perpendicular axes (cf. Sec. 1.1). Specification of these axes also requires three degrees of freedom, and the molecule is left with $3N - 6$ degrees of freedom. The only other motion allowed to it is internal vibration, so we know immediately that a non-linear N-atomic molecule can have $3N - 6$ different internal vibrations:

$$\text{Non-linear:}\quad 3N - 6 \text{ fundamental vibrations} \tag{3.24a}$$

If, on the other hand, the molecule is linear, we saw in Chapter 2 that there is no rotation about the bond axis; hence only two degrees of rotational freedom are required, leaving $3N - 5$ degrees of vibrational freedom—one more than in the case of a non-linear molecule:

$$\text{Linear:}\quad 3N - 5 \text{ fundamental vibrations} \tag{3.24b}$$

In both cases, since an N-atomic molecule has $N - 1$ bonds (for acyclic molecules) between its atoms, $N - 1$ of the vibrations are bond-stretching motions, the other $2N - 5$ (non-linear) or $2N - 4$ (linear) are bending motions.

Let us look briefly at examples of these rules. First, we see that for a diatomic molecule (perforce linear) such as we have already considered in this chapter: $N = 2$, $3N - 5 = 1$ and thus there can be only one fundamental vibration. Note, however, that the $3N - 5$ rule says nothing about the presence, absence, or intensity of overtone vibrations—these are governed solely by anharmonicity.

Next, consider water, H_2O. This (Fig. 3.9) is non-linear and triatomic. Also in the figure are the $3N - 6 = 3$ allowed vibrational modes, the arrows attached to each atom showing the direction of its motion during half of the vibration. Each motion is described as stretching or bending depending on the nature of the change in molecular shape.

These three vibrational motions are also referred to as the *normal modes of vibration* (or *normal vibrations*) of the molecule; in general a normal vibration is defined as a molecular motion in which all the atoms move in phase and with the same frequency.

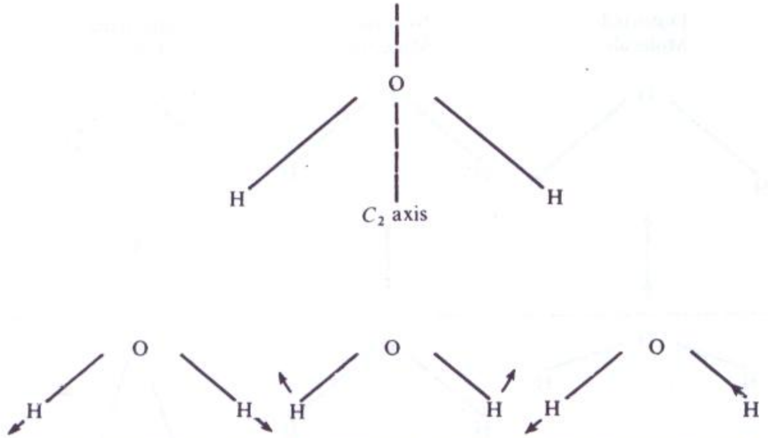

(*a*) symmetric stretching
3651·7 cm^{-1}
ν_1, parallel (‖)

(*b*) symmetric bending
1595·0 cm^{-1}
ν_2, parallel (‖)

(*c*) antisymmetric stretch
3755·8 cm^{-1}
ν_3, perpendicular (⊥)

Figure 3.9 The symmetry of the water molecule and its three fundamental vibrations. The motion of the oxygen atom, which must occur to keep the centre of gravity of the molecule stationary, is here ignored.

Further each motion of Fig. 3.9 is labelled either symmetric or antisymmetric. It is not necessary here to go far into the matter of general molecular symmetry since other excellent texts already exist for the interested student, but we can see quite readily that the water molecule contains some elements of symmetry. In particular consider the dashed line at the top of Fig. 3.9 which bisects the HOH angle; if we rotate the molecule about this axis by 180° its final appearance is identical with the initial one. This axis is thus referred to as a C_2 axis since twice in every complete revolution the molecule presents an identical aspect to an observer. This particular molecule has only the one rotational symmetry axis, and it is conventional to refer the molecular vibrations to this axis. Thus consider the first vibration, Fig. 3.9(*a*). If we rotate the *vibrating* molecule by 180° the vibration is quite unchanged in character—we call this a symmetric vibration. The bending vibration, ν_2, is also symmetric. Rotation of the stretching motion of Fig. 3.9(*c*) about the C_2 axis, however, produces a vibration which is in antiphase with the original and so this motion is described as the antisymmetric stretching mode.

In order to be infra-red active, as we have seen, there must be a dipole change during the vibration and this change may take place either along the line of the symmetry axis (parallel to it, or ‖) or at right angles to the line (perpendicular, ⊥). Figure 3.10 shows the nature of the dipole changes for the three vibrations of water, and justifies the labels parallel or perpen-

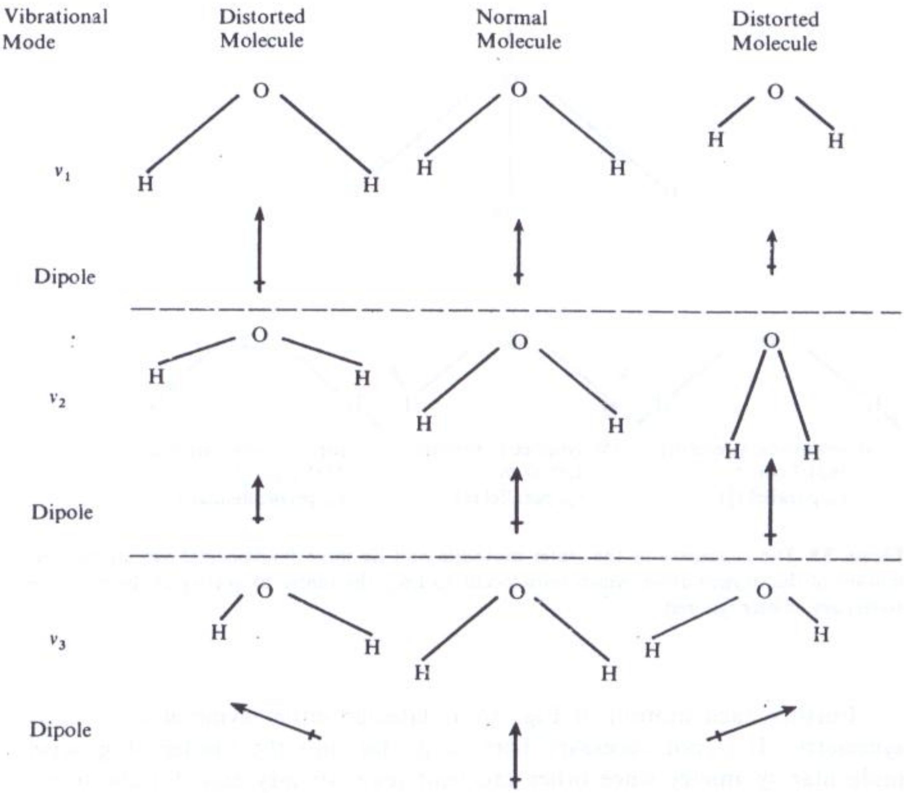

Figure 3.10 The change in the electric dipole moment produced by each vibration of the water molecule. This is seen to occur either along (‖) or across (⊥), the symmetry axis. The amplitudes are greatly exaggerated for clarity.

dicular attached to them in Fig. 3.9. We shall see later that the distinction is important when considering the influence of *rotation* on the spectrum.

Finally the vibrations are labelled in Fig. 3.9 as ν_1, ν_2, and ν_3. By convention it is usual to label vibrations in decreasing frequency within their symmetry type. Thus the symmetric vibrations of H_2O are labelled ν_1 for the highest fully symmetric frequency (3651·7 cm^{-1}), and ν_2 for the next highest (1595·0 cm^{-1}); the antisymmetric vibration at 3755·8 cm^{-1} is then labelled ν_3.

Our final example is of the linear triatomic molecule CO_2, for which the normal vibrations are shown in Fig. 3.11. For this molecule there are two different sets of symmetry axes. There is an infinite number of twofold axes (C_2) passing through the carbon atom at right angles to the bond direction, and there is an ∞-fold axis (C_∞) passing through the bond axis

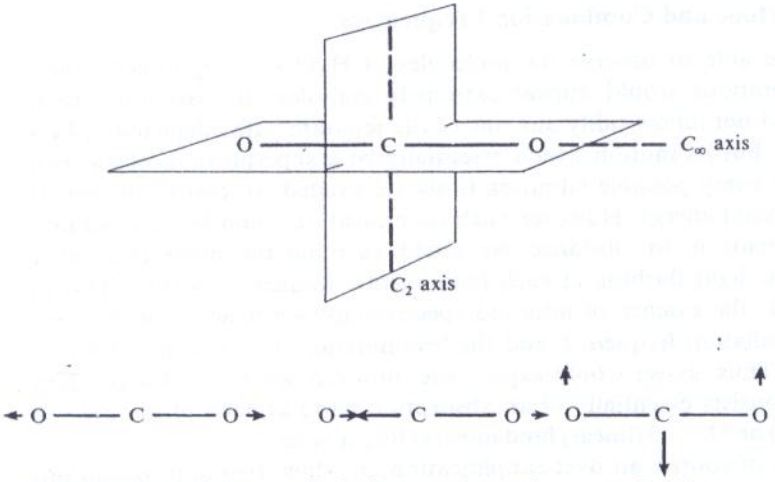

(*a*) Symmetric stretching
~1330 cm^{-1}
ν_1, ∥

(*b*) Antisymmetric stretch
2349·3 cm^{-1}
ν_3, ∥

(*c*) Bending
667·3 cm^{-1}
ν_2, ⊥

Figure 3.11 The symmetry and fundamental vibrations of the carbon dioxide molecule.

itself (this is referred to as ∞-fold since rotation of the molecule about the bond axis through *any* angle gives an identical aspect). The names symmetric stretch and antisymmetric stretch are self-evident, but it should be noted that the symmetric stretch produces no change in the dipole moment (which remains zero) so that this vibration is not infra-red active; the vibration frequency may be obtained in other ways, however, which we shall discuss in the next chapter.

For linear triatomic molecules, $3N - 5 = 4$, and we would expect four vibrational modes instead of the three shown in Fig. 3.11. However, consideration shows that ν_2 in fact consists of *two* vibrations—one in the plane of the paper as drawn, and the other in which the oxygen atoms move simultaneously into and out of the plane. The two sorts of motion are, of course, identical in all respects except direction and are termed *degenerate*; they must, nevertheless, be considered as separate motions, and it is always in the degeneracy of a bending mode that the extra vibration of a linear molecule over a non-linear one is to be found.

It might be thought that ν_2 of H_2O (Fig. 3.9(*b*)) could occur by the hydrogens moving simultaneously in and out of the plane of the paper. Such a motion is not a vibration, however, but a *rotation*. As the molecule approaches linearity this rotation degenerates into a vibration, and the molecule loses one degree of rotational freedom in exchange for one of vibration.

3.5.2 Overtone and Combination Frequencies

If one were able to observe the molecules of H_2O or CO_2 directly their overall vibrations would appear extremely complex; in particular, each atom would not follow tidily any one of the separate paths depicted in Figs 3.9 or 3.11, but its motion would essentially be a superposition of all such paths, since every possible vibration is always excited, at least to the extent of its zero point energy. However, such superposition could be resolved into its components if, for instance, we could examine the molecules under stroboscopic light flashing at each fundamental frequency in turn. This is, so to speak, the essence of infra-red spectroscopy—instead of flashing we have the radiation frequency, and the 'examination' is a sensing of dipole alteration. Thus, as we would expect, the infra-red spectrum of a complex molecule consists essentially of an absorption band at each of the $3N - 6$ (non-linear) or $3N - 5$ (linear) fundamental frequencies.

This is, of course, an over-simplification, in which two approximations are implicit: (1) that each vibration is simple harmonic, (2) that each vibration is quite independent and unaffected by the others. We shall consider (2) in more detail later; for the moment we can accept it as a good working approximation.

When the restriction to simple harmonic motion is lifted we have again, as in the case of the diatomic molecule (Sec. 3.1.3), the possibility of first, second, etc., overtones occurring at frequencies near $2\nu_1$, $3\nu_1$, $\ldots$, $2\nu_2$, $3\nu_2$, $\ldots$, $2\nu_3$, $\ldots$, etc., where each ν_i is a fundamental mode. The intensities fall off rapidly. However, in addition, the selection rules now permit *combination bands* and *difference bands*. The former arise simply from the addition of two or more fundamental frequencies or overtones. Such combinations as $\nu_1 + \nu_2$, $2\nu_1 + \nu_2$, $\nu_1 + \nu_2 + \nu_3$, etc., become allowed, although their intensities are normally very small. Similarly the difference bands, for example, $\nu_1 - \nu_2$, $2\nu_1 - \nu_2$, $\nu_1 + \nu_2 - \nu_3$, have small intensities but are often to be found in a complex spectrum.

The intensities of overtone or combination bands may sometimes be considerably enhanced by a resonance phenomenon. It may happen that two vibrational modes in a particular molecule have frequencies very close to each other—they are described as *accidentally* degenerate. Note that we are not here referring to identical vibrations, such as the two identical ν_2's of CO_2 (Fig. 3.11), but rather to the possibility of two quite different modes having similar energies. Normally the fundamental modes are quite different from each other and accidental degeneracy is found most often between a fundamental and some overtone or combination. A simple example is to be found in CO_2 where ν_1, described as at about 1330 cm^{-1}, is very close to that of $2\nu_2 = 1334\ \text{cm}^{-1}$. (As mentioned earlier, these bands are not observable in the infra-red, but both may be seen in the Raman spectrum discussed in the next chapter; the principles of resonance apply equally to both techniques.) Quantum mechanics shows that two such bands may interfere with each other in such a way that the higher is raised in frequency, the lower depressed—and in fact the Raman spectrum shows two bands, one at 1285 cm^{-1}, the other at 1385 cm^{-1}. Their mean is plainly at about 1330 cm^{-1}.

Note, however, that one of these bands arises from a fundamental mode (ν_1), the other from the overtone $2\nu_2$, and we would normally expect the former to be much more intense than the latter. In fact, they are found to be of about the same intensity—the overtone has gained intensity at the expense of the fundamental. This is an extreme case—normally the overtone takes only a small part of the intensity from the fundamental. The situation is often likened to that of two pendulums connected to a common bar—when the pendulums have quite different frequencies they oscillate independently; when their frequencies are similar they can readily exchange energy, one with the other, and an oscillation given to one is transferred to and fro between them. They are said to resonate. Similarly two close molecular vibrational frequencies resonate and exchange energy—the phenomenon being known as *Fermi resonance* when a fundamental resonates with an overtone. In the spectrum of a complex molecule exhibiting many fundamentals and overtones, there is a good chance of accidental degeneracy, and Fermi resonance, occurring. However, it should be mentioned that not all such degeneracies lead to resonance. It is necessary, also, to consider the molecular symmetry and the type of degenerate vibrations; we shall not, however, pursue the topic further here.

3.6 THE INFLUENCE OF ROTATION ON THE SPECTRA OF POLYATOMIC MOLECULES

In Sec. 3.2 we found that the selection rule for the simultaneous rotation and vibration of a diatomic molecule was

$$\Delta v = \pm 1, \pm 2, \pm 3, \ldots \qquad \Delta J = \pm 1 \qquad \Delta J \neq 0$$

and that this gave rise to a spectrum consisting of approximately equally spaced line series on each side of a central minimum designated as the band centre.

Earlier in the present section we showed that the vibrations of complex molecules could be subdivided into those causing a dipole change either (1) parallel or (2) perpendicular to the major axis of rotational symmetry. The purpose of this distinction, and the reason for repeating it here, is that the selection rules for the *rotational* transitions of complex molecules depend, rather surprisingly, on the type of *vibration*, ∥ or ⊥, which the molecule is undergoing. Less surprisingly, the selection rules and the energies depend on the *shape* of the molecule also. We shall deal first with the linear molecule as the simplest, and then say a few words about the other types of molecule.

3.6.1 Linear Molecules

Parallel vibrations The selection rule for these is identical with that for diatomic molecules, i.e.,

$$\Delta J = \pm 1 \qquad \Delta v = \pm 1 \qquad \text{for simple harmonic motion} \qquad (3.25a)$$

$$\Delta J = \pm 1 \qquad \Delta v = \pm 1, \pm 2, \pm 3, \ldots \qquad \text{for anharmonic motion} \qquad (3.25b)$$

(This is, in fact, as expected, since a diatomic molecule is linear and can undergo only parallel vibrations.) The spectra will thus be similar in appearance, consisting of *P* and *R* branches with lines about equally spaced on each side, no line occurring at the band centre. Now, however, the moment of inertia may be considerably larger, the *B* value correspondingly smaller, and the *P* or *R* line spacing will be less. Figure 3.12 shows part of the spectrum of HCN, a linear molecule whose structure is H—C≡N. The band concerned is the symmetric stretching frequency at about 3310 cm^{-1}, (corresponding to the ν_1 mode of CO_2 in Fig. 3.11), and the spacing is observed to be about 2·8–3·0 cm^{-1} near the band centre. This is to be compared, for example, with the spacing of about 4·0 cm^{-1} in the case of CO.

For still larger molecules the value of *B* may be so small that separate lines can no longer be resolved in the *P* and *R* branches. In this case the situation is exactly analogous to that shown previously in Fig. 3.8 and the same remarks apply as to the possibility of deriving a rough value of *B* from the separation between the maxima of the *P* and *R* envelopes. We shall shortly see that a non-linear molecule cannot give rise to this type of band

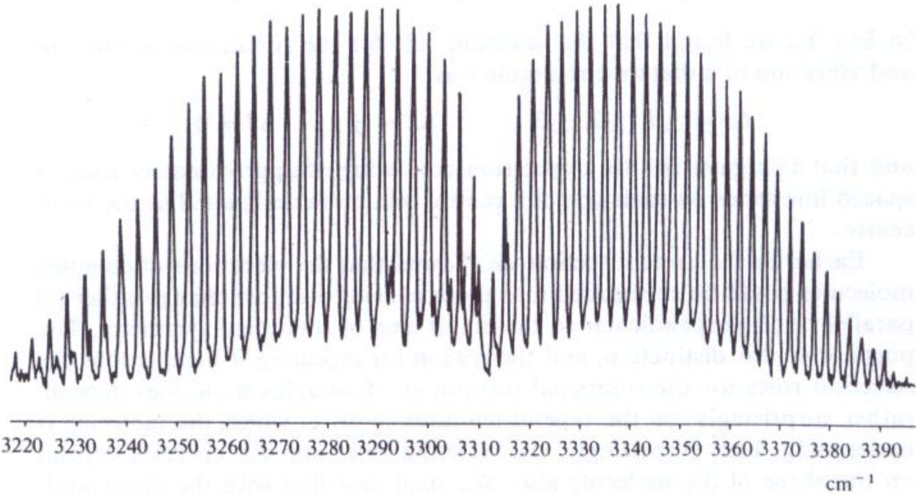

Figure 3.12 Spectrum of the symmetric stretching vibration of the HCN molecule showing the *P* and *R* branch lines.

shape, so its observation somewhere within a spectrum is sufficient proof that a linear, or nearly linear, molecule is being studied.

Perpendicular vibrations For these the selection rule is found to be:

$$\Delta v = \pm 1 \qquad \Delta J = 0, \pm 1 \qquad \text{for simple harmonic motion} \qquad (3.26)$$

which implies that now, for the first time, a vibrational change can take place with *no simultaneous rotational transition*. The result is illustrated in Fig. 3.13, which shows the same energy levels and transitions as Fig. 3.6

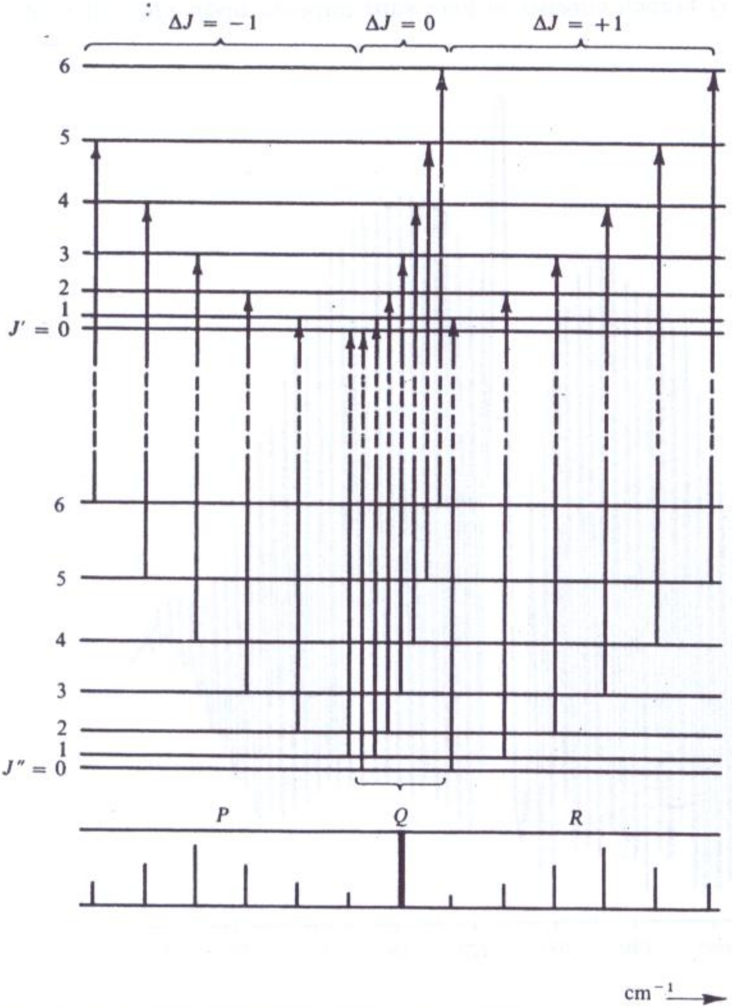

Figure 3.13 The rotational energy levels for two vibrational states showing the effect on the spectrum of transitions for which $\Delta J = 0$.

with the addition of $\Delta J = 0$ transitions. If the oscillation is taken as simple harmonic the energy levels are identical with those of Eq. (3.18) and the *P* and *R* branch lines are given, as before, by Eqs (3.20) or (3.21). Transitions with $\Delta J = 0$, however, correspond to a *Q branch* whose lines may be derived from the equations:

$$\begin{aligned}\Delta\varepsilon &= \varepsilon_{J,v+1} - \varepsilon_{J,v} \\ &= 1\tfrac{1}{2}\bar{\omega}_e - 2\tfrac{1}{4}x_e\bar{\omega}_e + BJ(J+1) - \{\tfrac{1}{2}\bar{\omega}_e - \tfrac{1}{4}x_e\bar{\omega}_e + BJ(J+1)\} \\ &= \bar{\omega}_o \quad \text{cm}^{-1} \qquad \text{for all } J \end{aligned} \tag{3.27}$$

Thus the *Q* branch consists of lines superimposed upon each other at

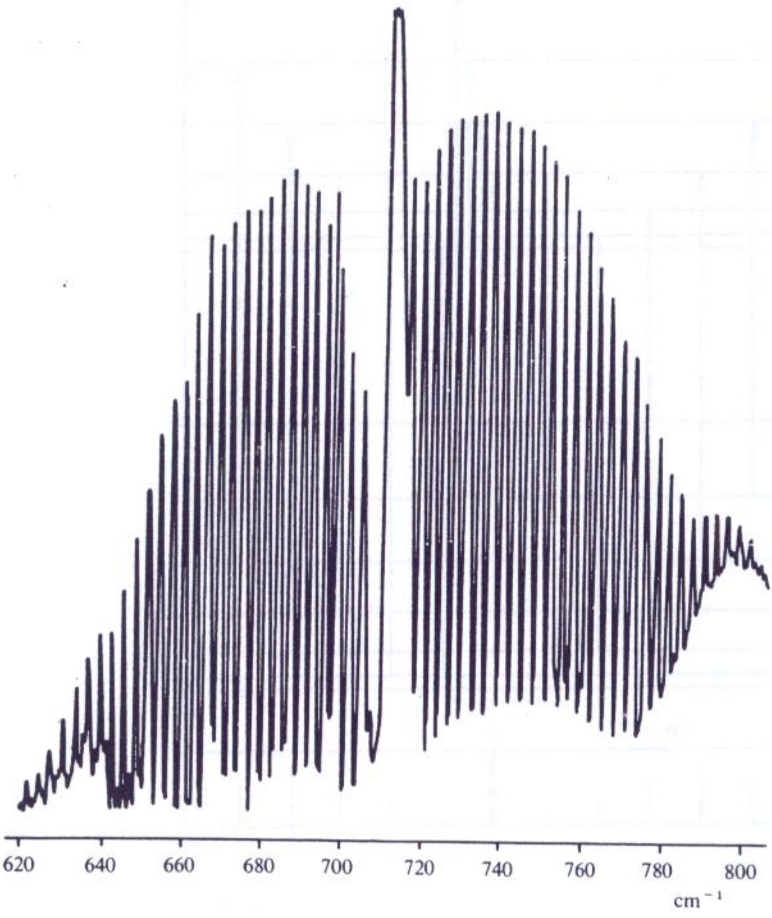

Figure 3.14 Spectrum of the bending mode of the HCN molecule showing the *PQR* structure. The broad absorption centred at 800 cm^{-1} is due to an impurity.

the band centre $\bar{\omega}_o$, one contribution arising for each of the populated J values. The resultant line is usually very intense.

If we take into account the fact that the B values differ slightly in the upper and lower vibrational states (cf. Sec. 3.4), we would write instead:

$$\begin{aligned}\Delta\varepsilon &= \varepsilon_{J,v+1} - \varepsilon_{J,v} \\ &= 1\tfrac{1}{2}\bar{\omega}_e - 2\tfrac{1}{4}x_e\bar{\omega}_e + B'J(J+1) - \{\tfrac{1}{2}\bar{\omega}_e - \tfrac{1}{4}x_e\bar{\omega}_e + B''J(J+1)\} \\ &= \bar{\omega}_o + J(J+1)(B' - B''). \end{aligned} \tag{3.28}$$

Further, if $B' < B''$, we see that the Q branch line would become split into a series of lines on the *low*-frequency side of $\bar{\omega}_o$ (since $B' - B''$ is negative). Normally, however, $B' - B''$ is so small that the lines cannot be resolved, and the Q branch appears as a somewhat broad absorption centred around $\bar{\omega}_o$. This is illustrated in Fig. 3.14, which is a spectrum of the bending mode of HCN (corresponding to ν_2 of CO_2 in Fig. 3.11). Finally, if the rotational fine structure is unresolved, this type of band has the distinctive contour shown in Fig. 3.15.

It should be remembered (see Chapter 2) that polyatomic molecules with zero dipole moment do not give rise to pure rotation spectra in the microwave region (for example, CO_2, $HC{\equiv}CH$, CH_4). Such molecules do, however, show vibrational spectra in the infra-red region (or Raman, cf. Chapter 4) and, if these spectra exhibit resolved fine structure, the moment of inertia of the molecule can be obtained.

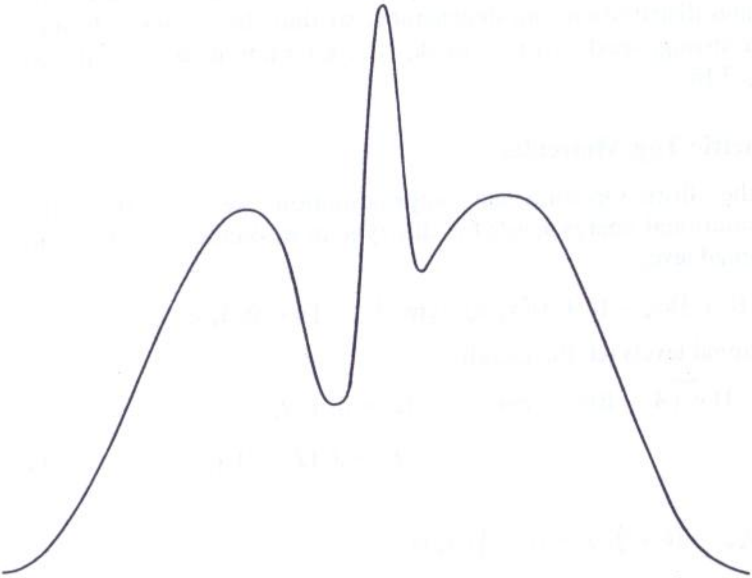

Figure 3.15 The contour of a *PQR* band under low resolution.

3.6.2 The Influence of Nuclear Spin

It is necessary here to say a brief word about the spectrum of carbon dioxide and other linear molecules possessing a centre of symmetry. A centre of symmetry means that identical atoms are symmetrically disposed with respect to the centre of gravity of the molecule. Thus, plainly both CO_2 [O=C=O] and acetylene [H—C≡C—H] possess a centre of symmetry, while HCN, or N_2O [N≡N=O] do not.

The reader may have noticed that, although we used CO_2 as an example of a vibrating molecule in Fig. 3.11, we did not use it to illustrate real spectra in the subsequent discussion. This is because the centre of symmetry has an effect on the intensity of alternate lines in the P and R branches. The effect is due to the existence of nuclear spin (cf. Chapter 7) and is an additional factor determining the populations of rotational levels. In the case of CO_2 every alternate rotational level is completely unoccupied and so alternate lines in the P and R branches have zero intensity. This leads to a line-spacing of $4B$ instead of the usual $2B$ discussed above. That the spacing is indeed $4B$ (and not $2B$ with an unexpectedly large value of B) can be shown in several ways, perhaps the most convincing of which is to examine the spectrum of the isotopic molecule $^{18}O—C—^{16}O$. Here there is no longer a centre of symmetry, nuclear spin does not now affect the spectrum and the line-spacing is found to be just half that for 'normal' CO_2.

In the case of acetylene, alternate levels have populations which differ by a factor of 3 : 1 (this, due to nuclear spin alone, is superimposed on the normal thermal distribution and degeneracy) so that the P and R branch lines show a strong, weak, strong, weak, . . . alternation in intensity, as shown in Fig. 3.16.

3.6.3 Symmetric Top Molecules

Following the Born–Oppenheimer approximation we can take the vibrational–rotational energy levels for this type of molecule to be the sum of the vibrational levels:

$$\varepsilon_{\text{vib.}} = (v + \tfrac{1}{2})\bar{\omega}_e - (v + \tfrac{1}{2})^2 x_e \bar{\omega}_e \quad \text{cm}^{-1} \qquad [v = 0, 1, 2, 3, \ldots]$$

and the rotational levels (cf. Eq. (2.38)),

$$\varepsilon_{\text{rot.}} = BJ(J+1) + (A - B)K^2 \quad \text{cm}^{-1} \qquad [J = 0, 1, 2, \ldots; \quad K = J, (J-1), (J-2), \ldots, -J]$$

thus

$$\varepsilon_{J,v} = \varepsilon_{\text{vib.}} + \varepsilon_{\text{rot.}} = (v + \tfrac{1}{2})\bar{\omega}_e - (v + \tfrac{1}{2})^2 x_e \bar{\omega}_e + BJ(J+1) + (A - B)K^2 \quad \text{cm}^{-1} \tag{3.29}$$

This equation assumes, of course, that centrifugal distortion is negligible.

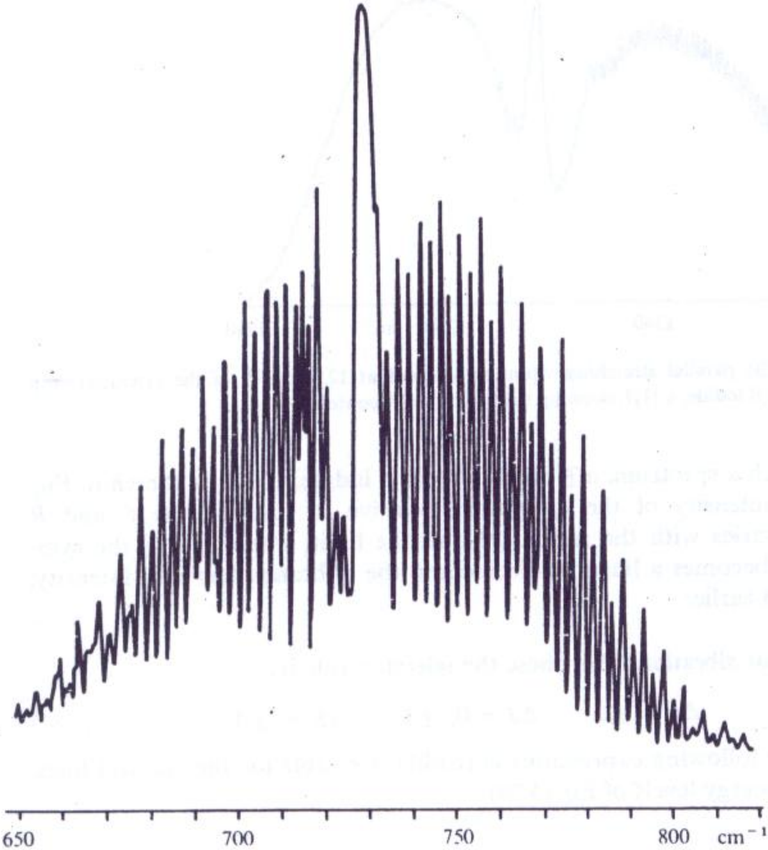

Figure 3.16 The spectrum of a bending mode of acetylene, HC≡CH, showing the strong, weak, strong, weak, ... intensity alternation in the rotational fine structure due to the nuclear spin of the hydrogen atoms.

Again it is necessary to divide the vibrations into those which change the dipole (1) parallel and (2) perpendicular to the main symmetry axis—which is nearly always the axis about which the 'top' rotates. The rotational selection rules differ for the two types.

Parallel vibrations Here the selection rule is:

$$\Delta v = \pm 1 \qquad \Delta J = 0, \pm 1 \qquad \Delta K = 0 \tag{3.30}$$

Since here $\Delta K = 0$, terms in K will be identical in the upper and lower state and so the spectral frequencies will be independent of K. Thus the situation will be identical to that discussed for the *perpendicular* vibrations of a linear molecule. The spectrum will contain P, Q, and R branches with a P, R line spacing of $2B$ (which is unlikely to be resolved) and a strong central Q

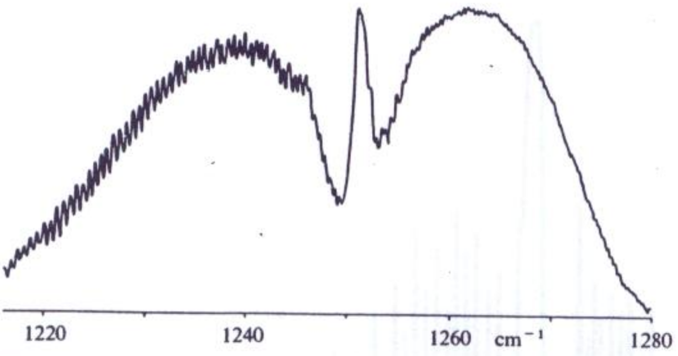

Figure 3.17 The parallel stretching vibration, centred at 1251 cm^{-1}, of the symmetric top molecule methyl iodide, CH_3I, showing the typical *PQR* contour.

branch. Such a spectrum, a ∥ band of methyl iodide, CH_3I, is shown in Fig. 3.17. The intensity of the Q branch (relative to lines in the P and R branches) varies with the ratio I_A/I_B; in the limit, when $I_A \to 0$, the symmetric top becomes a linear molecule and the Q branch has zero intensity, as discussed earlier.

Perpendicular vibrations For these the selection rule is:

$$\Delta v = \pm 1 \qquad \Delta J = 0, \pm 1 \qquad \Delta K = \pm 1 \tag{3.31}$$

Each of the following expressions is readily derivable for the spectral lines, taking the energy levels of Eq. (3.29).

(1) $\Delta J = +1, \Delta K = \pm 1$ (R branch lines):

$$\Delta \varepsilon = \bar{\nu}_{\text{spect.}} = \bar{\omega}_o + 2B(J+1) + (A-B)(1 \pm 2K) \quad \text{cm}^{-1} \tag{3.32a}$$

(2) $\Delta J = -1, \Delta K = \pm 1$ (P branch lines):

$$\bar{\nu}_{\text{spect.}} = \bar{\omega}_o - 2B(J+1) + (A-B)(1 \pm 2K) \quad \text{cm}^{-1} \tag{3.32b}$$

(3) $\Delta J = 0, \Delta K = \pm 1$ (Q branch lines):

$$\bar{\nu}_{\text{spect.}} = \bar{\omega}_o + (A-B)(1 \pm 2K) \quad \text{cm}^{-1} \tag{3.32c}$$

We see, then, that this type of vibration gives rise to many sets of P and R branch lines since for each J value there are many allowed values of K ($K = J, J-1, \ldots, -J$). The wings of the spectrum will thus be quite complicated and will not normally be resolvable into separate lines. The Q branch is also complex, since it too will consist of a series of lines on both

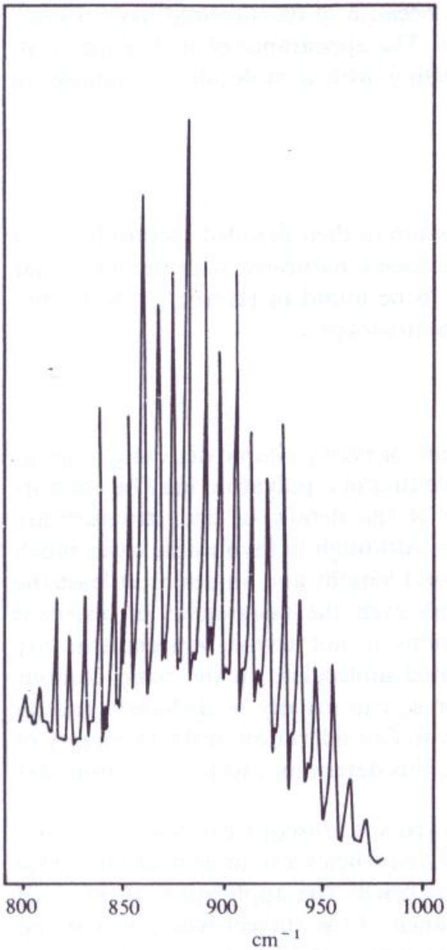

Figure 3.18 A perpendicular stretching vibration of methyl iodide showing the typical Q branch sequence.

sides of $\bar{\omega}_o$ separated by $2(A - B)$. This latter term may not be small (and is equal to zero only for *spherical top* molecules which have all their moments of inertia equal). For $A \gg B$ (for example, CH_3I) the Q branch lines will be well separated and will appear as a series of maxima above the P, R envelope. This spectrum is shown in Fig. 3.18.

It will be noted in this figure that the lines have a distinct periodical variation in intensity—strong, weak, weak, strong, weak, weak, ... This behaviour reminds us of CO_2 and C_2H_2, discussed earlier, in which the presence or absence of nuclear spin altered the relative populations of the rotational levels. In that case, where the molecule had a twofold axis of symmetry, the periodicity also was two—strong, weak, strong, weak, ... It is not surprising, therefore, that the threefold periodicity, strong, weak,

weak, strong, ... seen in CH_3I, arises because of its threefold axis of symmetry to rotations about the C—I axis. The appearance of such a spectrum confirms immediately that we are dealing with a molecule containing an XY_3 grouping.

Other Polyatomic Molecules

We shall not go further with the discussion of their detailed spectra here—it suffices to state that the complexity increases, naturally, with the molecular complexity. An excellent treatment is to be found in Herzberg's book, but the subject is not for the beginner in spectroscopy.

Summary

We have seen that the infra-red spectrum of even a simple diatomic molecule may contain a great many lines, while that of a polyatom may be extraordinarily complex, even though some of the details of fine structure are blurred by insufficient resolving power. Although in favourable cases much information may be obtained about bond lengths and angles or at least the general shape of a molecule, in others even the assignment of observed bands to particular molecular vibrations is not trivial. Assignments are based mainly on experience with related molecules, on the band contour (from which the type of vibration, $\parallel$ or $\perp$, can usually be deduced), and on the use of Raman spectra (see Chapter 4). Consideration of the symmetry of the molecule is also important because this determines which vibrations are likely to be infra-red active.

Fortunately the usefulness of infra-red spectroscopy extends far beyond the measurement of precise vibrational frequencies and molecular structural features. In the next section we discuss briefly the application of infra-red techniques to chemical analysis—a branch of the subject where it is by no means essential always to be able to assign observed bands precisely.

3.7 ANALYSIS BY INFRA-RED TECHNIQUES

Because of the $3N - 6$ and $3N - 5$ rules it is evident that a complex molecule is likely to have an infra-red spectrum exhibiting a large number of normal vibrations. Each normal mode involves some displacement of all, or nearly all, the atoms in the molecule, but while in some of the modes all atoms may undergo approximately the same displacement, in others the displacements of a small group of atoms may be much more vigorous than those of the remainder. Thus we may divide the normal modes into two classes: the *skeletal vibrations*, which involve all the atoms to much the same extent, and the *characteristic group vibrations*, which involve only a small portion of the molecule, the remainder being more or less stationary. We deal with these classes separately.

Skeletal frequencies usually fall in the range 1400–700 cm^{-1} and arise from linear or branched chain structures in the molecule. Thus such groups as

$-\mathrm{C}-\mathrm{O}-\mathrm{C}-$

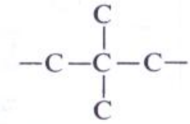

$-\mathrm{C}-\overset{\overset{\mathrm{C}}{|}}{\underset{\underset{\mathrm{C}}{|}}{\mathrm{C}}}-\mathrm{C}-$

etc., each give rise to several skeletal modes of vibration and hence several absorption bands in the infra-red. It is seldom possible to assign particular bands to specific vibrational modes, but the whole complex of bands observed is highly typical of the molecular structure under examination. Further, changing a substituent (on the chain, or in the ring) usually results in a marked change in the pattern of the absorption bands. Thus these bands are often referred to as the 'fingerprint' bands, because a molecule or structural moiety may often be recognized merely from the appearance of this part of the spectrum. An excellent example of this is shown in Fig. 3.19(*a*) which compares the infra-red spectra of natural and synthetic thymidine. The remarkably exact correlation between the spectra shows that the synthetic product cannot differ in the slightest degree from the natural substance.

Group frequencies, on the other hand, are usually almost independent of the structure of the molecule as a whole and, with a few exceptions, fall in the regions well above and well below that of the skeletal modes; Table 3.4 collects some of the data, of which a much more complete selection is to be found in the books by Bellamy and Nakamoto mentioned in the bibliography at the end of this chapter. We see that the vibrations of light atoms in terminal groups (for example, $-\mathrm{CH}_3$, $-\mathrm{OH}$, $-\mathrm{C}{\equiv}\mathrm{N}$, $>\mathrm{C}{=}\mathrm{O}$, etc.) are of high frequency, while those of heavy atoms ($-\mathrm{C}-\mathrm{Cl}$, $-\mathrm{C}-\mathrm{Br}$, metal–metal, etc.) are low in frequency. Their frequencies, and consequently their spectra, are highly characteristic of the group, and can be used for analysis. For example, the $-\mathrm{CH}_3$ group gives rise to a symmetric C—H stretching absorption invariably falling between 2850 and 2890 cm^{-1}, an asymmetric stretching frequency at 2940–2980 cm^{-1}, a symmetric deformation (i.e., the opening and closing of the 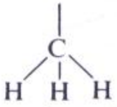 'umbrella') at about 1375 cm^{-1}, and an asymmetric deformation at about 1470 cm^{-1}. Again, the $>\mathrm{C}{=}\mathrm{O}$ group shows a very sharp and intense absorption between 1600 and 1750 cm^{-1}, depending largely on the other substituents of the group. An example of the application of group frequency data is shown in Fig. 3.19(*b*); this is the spectrum of thioacetic acid—acetic acid in which one oxygen atom has been

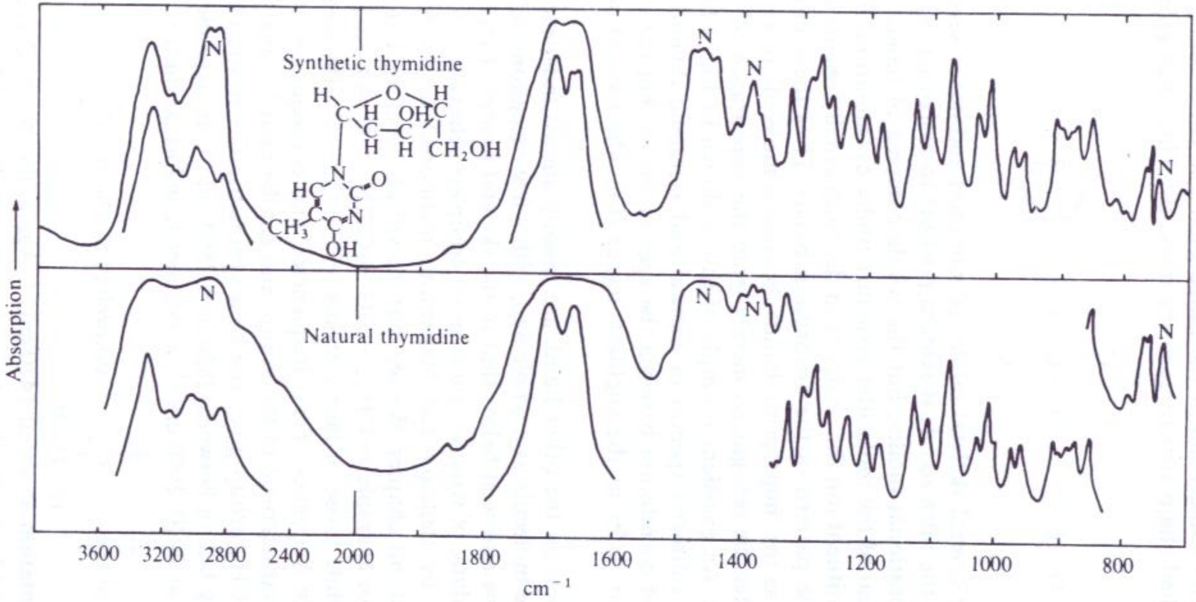

Figure 3.19(*a*) Comparison of the infra-red spectra of natural and synthetic thymidine, to show the use of the fingerprint region. (N = absorption from liquid paraffin (nujol) in which the solid thymidine is suspended.) *(These spectra and that of Fig. 3.19(b) are reproduced by kind permission of Professor N. Sheppard of the University of East Anglia, Norwich.)*

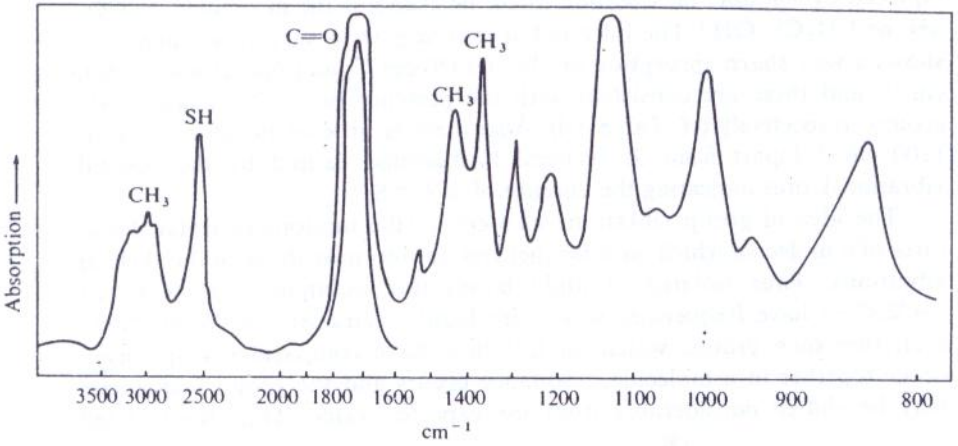

Figure 3.19(*b*) The spectrum of thiocetic acid, $CH_3CO.SH$.

Table 3.4 Characteristic stretching frequencies of some molecular groups

Group	Approximate frequency (cm^{-1})	Group	Approximate frequency (cm^{-1})
—OH	3600	>C=O	1750–1600
$-NH_2$	3400	>C=C<	1650
≡CH	3300	>C=N—	1600
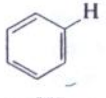	3060	⩾C—C⩽ ⩾C—N< ⩾C—O—	1200–1000
$=CH_2$	3030		
		>C=S	1100
$-CH_3$	2970 (asym. stretch)		
	2870 (sym. stretch)	⩾C—F	1050
	1460 (asym. deform.)		
	1375 (sym. deform.)	⩾C—Cl	725
$-CH_2-$	2930 (asym. stretch)	⩾C—Br	650
	2860 (sym. stretch)		
	1470 (deformation)	⩾C—I	550
—SH	2580		
—C≡N	2250		
—C≡C—	2220		

replaced by sulphur; the question might be asked: is the molecule $CH_3CO.SH$, or $CH_3CS.OH$? The infra-red spectrum gives a very clear answer. It shows a very sharp absorption at about 1730 cm^{-1}, and one at about 2600 cm^{-1}, and these are consistent with the presence of $>C{=}O$ and $-SH$ groups, respectively (cf. Table 3.4). Also there is little or no absorption at 1100 cm^{-1} (apart from the general background caused by the skeletal vibrations), thus indicating the absence of $>C{=}S$.

The idea of group vibrations also covers the motions of isolated features of a molecule which have frequencies not too near those of the skeletal vibrations. Thus isolated multiple bonds (for example, $>C{=}C<$ or $-C{\equiv}C-$) have frequencies which are highly characteristic. When, however, two such groups which, in isolation, have comparable frequencies, occur together in a molecule, resonance occurs and the group frequencies may be shifted considerably from the expected value. Thus the isolated carbonyl in a ketone 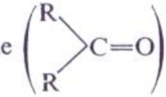 $\left(\begin{matrix}R\\ \\R\end{matrix}\!\!>C{=}O\right)$ and the $>C{=}C<$ double bond, have group frequencies of 1715 and 1650 cm^{-1} respectively; however, when the grouping 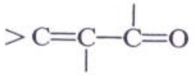 $>C{=}\underset{|}{C}-\overset{|}{C}{=}O$ occurs, their separate frequencies are shifted to 1675 and about 1600 cm^{-1} respectively and the intensity of the $>C{=}C<$ absorption increases to become comparable with that of the inherently strong $>C{=}O$ band (cf. Fermi resonance, p. 97). Closer coupling of the two groups, as in the ketene radical, $>C{=}C{=}O$, gives rise to absorptions at about 2100 and 1100 cm^{-1}, which are very far removed from the 'characteristic' frequencies of the separate groups.

Shifts in group frequencies can arise in other ways too, particularly as the result of interactions between different molecules. Thus the $-OH$ stretching frequency of alcohols is very dependent on the degree of hydrogen bonding, which lengthens and weakens the $-OH$ bond, and hence lowers its vibrational frequency. If the hydrogen bond is formed between the $-OH$ and, say, a carbonyl group, then the latter frequency is also lowered, although to a less extent than the $-OH$, since hydrogen bonding weakens the $>C{=}O$ linkage also. However, shifts in group frequency position caused by resonance or intermolecular effects are in themselves highly characteristic and very useful for diagnostic purposes.

In a similar way a change of physical state may cause a shift in the frequency of a vibration, particularly if the molecule is rather polar. In general the more condensed phase gives a lower frequency: $\nu_{\text{gas}} > \nu_{\text{liquid}} \approx \nu_{\text{solution}} > \nu_{\text{solid}}$. Thus in the relatively polar molecule HCl there is a shift of some 100 cm^{-1} in passing from vapour to liquid and a further decrease of 20 cm^{-1} on solidification. Non-polar CO_2, on the other hand, shows negligible shifts in its symmetric vibrations (Fig. 3.11(*a*) and (*b*)) but a lowering of some 60 cm^{-1} in ν_3 on solidification.

Examination of Table 3.4 shows that there are logical trends in group frequencies, since Eq. (3.4):

$$\bar{\omega} = \frac{1}{2\pi c}\sqrt{\frac{k}{\mu}} \quad \text{cm}^{-1}$$

is approximately obeyed. Thus we see that increasing the mass of the atom undergoing oscillation within the group (i.e., increasing μ) tends to decrease the frequency—cf. the series CH, CF, CCl, CBr, or the values for $>$C=O and $>$C=S. Also, increasing the strength of the bond, and hence increasing the force constant k, tends to increase the frequency, e.g., the series —C—X, —C=X, —C≡X, where X is C, N, or (in the first two fragments) O.

We should at this point consider very briefly the intensities of infra-red bands. We have seen that an infra-red spectrum only appears if the vibration produces a change in the permanent electric dipole of the molecule. It is reasonable to suppose, then, that the more polar a bond, the more intense will be the infra-red spectrum arising from vibrations of that bond. This is generally borne out in practice. Thus the intensities of the $>$C=O, $>$C=N—, and $>$C=C$<$ bands decrease in that order, as do those of the —OH, $>$NH, and $\geqslant$CH bands. For this reason, too, the vibrations of ionic crystal lattices often give rise to very strong absorptions. We shall see in the next chapter that the reverse is true in Raman spectroscopy—there the less polar (and hence usually more *polarizable*) bonds give the most intense spectral lines.

In summary, then, experience coupled with comparison spectra of known compounds enables one to deduce a considerable amount of structural information from an infra-red spectrum. It should perhaps be mentioned that the *complete* interpretation of the spectrum of a complex molecule can be a very difficult or impossible task. One is usually content to assign the strongest bands and to be able to explain some of the weaker ones as overtones or combinations.

3.8 TECHNIQUES AND INSTRUMENTATION

3.8.1 Outline

We first deal briefly with each component of the spectrometer as it is usually assembled for infra-red work.

1. *Source.* The source is always some form of filament which is maintained at red- or white-heat by an electric current. Two common sources are the Nernst filament, consisting of a spindle of rare-earth oxides about 1 inch long and 0·1 inch in diameter, and the 'globar' filament, a rod of carborundum, somewhat thicker and longer than the Nernst. The Nernst

requires to be pre-heated before it will conduct electricity, but once red-heat is reached the temperature is maintained by the current.

2. *Optical path and monochromator*. The beam is guided and focused by mirrors silvered on their surfaces. Normally a focus is produced at the point where the sample is to be placed. Ordinary lenses and mirrors are not suitable as glass absorbs strongly over most of the frequencies used. Any windows which are essential (e.g., to contain a sample, or to protect the detector) must be made of mineral salts transparent to infra-red radiation (NaCl and KBr are much used) which have been highly polished in order to reduce scattering to a minimum.

   Similarly, the monochromator in some instruments is made of a rock salt or potassium bromide prism, which is rotatable to produce the required frequency in a manner similar to that of Fig. 1.11 (except, of course, that the lens is replaced by a condensing mirror). Modern instruments, however, use a rotatable grating instead of a prism, since this gives much better resolving power.

3. *Detector*. Two main types are in common use, one sensing the heating effect of the radiation, the other depending on photoconductivity. In both the greater the effect (temperature or conductivity rise) at a given frequency, the greater the transmittance (and the less the absorbance) of the sample at that frequency.

   An example of the temperature method is to be found in the Golay cell which is pneumatic in operation. The radiation falls on to a very small cell containing air, and temperature changes are measured in terms of pressure changes within the cell which can be recorded directly as 'transmittance'. Alternative examples of this type of detector are small, sensitive thermocouples or bolometers.

   The phenomenon of conductivity in substances is thought to arise as a consequence of the movement of loosely held electrons through the lattice; insulators, on the other hand, have no such loosely bound electrons. Semiconductors are essentially midway between these materials, having no loosely bound electrons in the normal state, but having 'conduction bands' or raised electron energy levels into which electrons may be readily excited by the absorption of energy from an outside source. Photoconductors are a particular class of semiconductor in which the energy required comes from incident radiation, and some materials, such as lead sulphide, have been found sufficiently sensitive to infra-red radiation (although only above some 3500 cm^{-1}) that they make excellent detectors. The conductivity of the material can be measured continuously by a type of Wheatstone bridge network and, when plotted against frequency, this gives directly the transmittance of the sample.

4. *Sample*. For reasons just stated, the sample is held between plates of polished mineral salt rather than glass. Pure liquids are studied in thicknesses of about 0·01 mm, while solutions are usually 0·1–10 mm thick,

depending on the dilution. Gas samples at pressures of up to 1 atmosphere or greater are usually contained in glass cells either 5 or 10 cm long, closed at their ends with rock salt windows. Special long-path cells, in which the radiation is repeatedly reflected up and down the cell, may be used for gases at low pressure, perhaps less than 100 mmHg.

Solid samples are more difficult to examine because the particles reflect and scatter the incident radiation and transmittance is always low. If the solid cannot be dissolved in a suitable solvent, it is best examined by grinding it very finely in paraffin oil (nujol) and thus forming a suspension, or 'mull'. This can then be held between salt plates in the same way as a pure liquid or solvent. Provided the refractive indices of liquid and solid phase are not very different, scattering will be slight.

Another technique for handling solids is to grind them very finely with potassium bromide. Under very high pressure this material will flow slightly, and the mixture can usually be pressed into a transparent disk. This may then be placed directly in the infra-red beam in a suitable holder. Although superficially attractive the method is not generally recommended because of the difficulty in obtaining really reproducible results.

A further technique which is often used to study otherwise intractible samples is known as attenuated total reflectance (atr) spectroscopy. Consider a trapezoidal block of a transparent material, as in Fig. 3.20(*a*). If the chamfer angle is properly chosen, radiation shone into one end will strike the flat surfaces at less than the critical angle and so will undergo total internal reflection to emerge, only slightly diminished in intensity, at the far end, as in Fig. 3.20(*b*). Now, although the internal reflection is conventionally called 'total', in fact the radiation beam penetrates slightly beyond the surface of the block during each reflection. If sample material is pressed closely to the outside of the block (Fig. 3.20(*c*)) the beam will travel a small distance through the sample at each reflection and so, on emerging at the far end of the block, it will 'carry' the absorption spectrum of the sample—the internal reflection is *attenuated*, or diminished by sample absorption, hence the name of this type of spectroscopy. The amount of penetration into the sample depends on the wavelength of the radiation and the angle of incidence, but it is of the order of 10^{-4} to 10^{-3} cm for infra-red waves. During its passage through the block it may undergo some 10–20 reflections, so the total path length through the sample is 10^{-3}–10^{-2} cm, which is a short, but often perfectly adequate, path length for the production of a reasonable spectrum.

The block must be of material which is infra-red transparent, and must have a refractive index higher than that of the sample, otherwise internal reflection will not occur. Suitable materials are silver chloride, thallium halides, or germanium, and the block is typically some 5 cm long, 2 cm

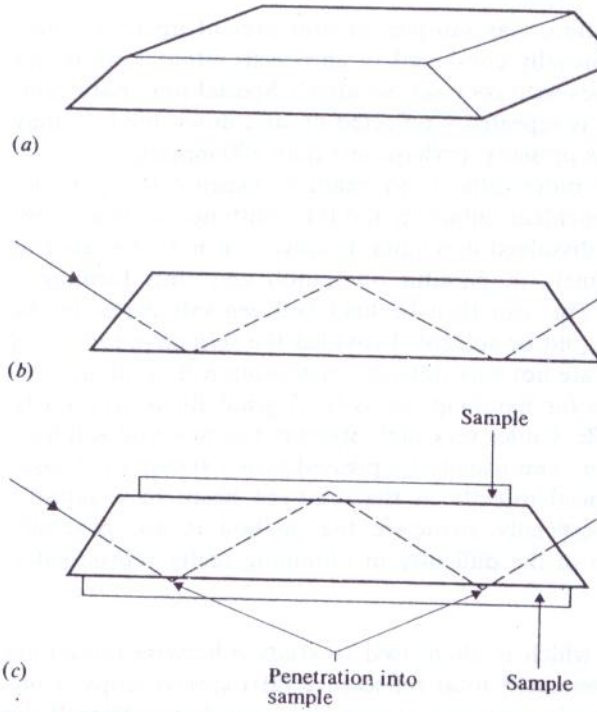

Figure 3.20 Attenuated total reflection. (*a*) the transparent block, (*b*) internal reflection in the block, and (*c*) penetration into the sample pressed against the block.

wide, and 0·5 cm thick. The sample material can be in any form (except gaseous, for which a path length of 10^{-2} cm is far too short) provided it can be kept in very close contact with the block, but the technique is usually reserved for samples difficult to study by ordinary means. Thus, it is virtually impossible to study fibrous material by transmission—the rough surface scatters all the radiation falling on it; but if the fibres are clamped firmly to the outside of an atr block, quite acceptable spectra result. And it is an excellent method of studying surface coatings, since it is only the surface of the sample which is penetrated by the radiation. Further, since the depth of penetration can, to some extent, be changed by varying the angle of incidence of the beam, the change in composition of a surface with depth can be studied. Thus one can measure the degree of oxidation of a polymer surface, or the diffusion of materials into a surface.

3.8.2 Double- and Single-Beam Operation

Figure 3.21 shows the spectrum of the atmosphere between 4000 and 400 cm^{-1} taken with a path length of some 2 m—this is not abnormally long

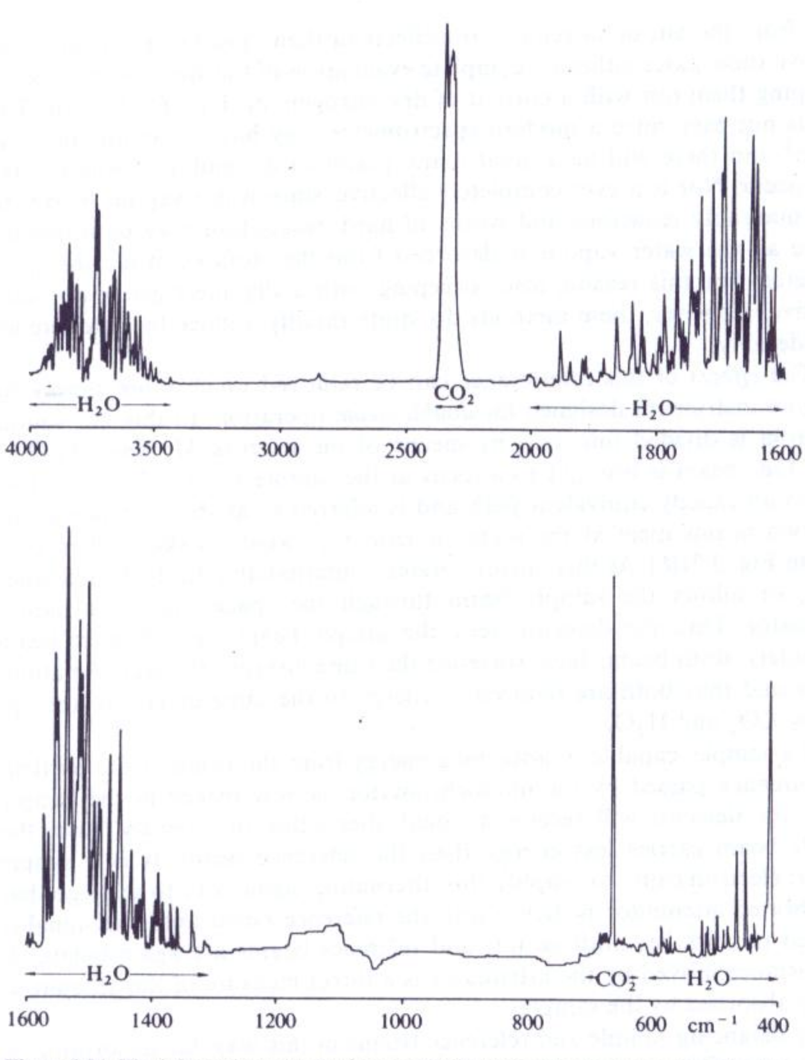

Figure 3.21 The infra-red spectrum of atmospheric water vapour and carbon dioxide.

for the beam paths in a spectrometer. It is evident that, although H_2O and CO_2 occur in air only in small percentages, their absorbance over much of the spectrum is considerable. Not only would this absorbance have to be subtracted from the spectrum of any sample run under comparable conditions but, since the percentage of water vapour in the atmosphere is variable, such a 'background' spectrum as Fig. 3.21 would have to be run afresh for each sample.

If the regions of these absorbances are not to be denied us in spectroscopic studies, some action must be taken either to remove the H_2O and

CO_2 from the air, or to remove the effects of their spectra. It is possible to remove these gases either by complete evacuation of the spectrometer, or by sweeping them out with a current of dry nitrogen, or dry CO_2-free air. The first is not easy since a modern spectrometer may have a volume of some 0·3 m^3 and there will be a great many places in its container where leaks may occur. Nor is it ever completely effective, since water vapour proves to be remarkably tenacious and weeks of hard evacuation may be necessary before all the water vapour is desorbed from the surfaces inside the spectrometer. For this reason, also, sweeping with a dry inert gas is not very effective. However, these methods do, quite rapidly, reduce the interference considerably.

The *effects* of this interference can be removed much more simply by using an instrument designed for *double-beam* operation. In this, the source radiation is divided into two by means of the mirrors M_1 and M_2 (Fig. 3.22). One beam is brought to a focus at the sample space, while the other follows an exactly equivalent path and is referred to as the reference beam. The two beams meet at the sector mirror M_3, which is sketched in plan view in Fig. 3.21(*b*). As this mirror rotates it alternately reflects the reference beam, or allows the sample beam through the spaces, into the monochromator. Thus the detector 'sees' the sample beam and reference beam alternately. Both beams have travelled the same distance through the atmosphere and thus both are reduced in energy to the same extent by absorption by CO_2 and H_2O.

If a sample, capable of absorbing energy from the beam at the particular frequency passed by the monochromator, is now placed in the sample beam, the detector will receive a signal alternating in intensity, since the sample beam carries less energy than the reference beam. It is a simple matter, electronically, to amplify this alternating signal and to arrange that a calibrated attenuator is driven into the reference beam until the signal is reduced to zero, i.e., until sample and reference beams are again balanced. The distance moved by the attenuator is a direct measure of the amount of energy absorbed by the sample.

By balancing sample and reference beams in this way, the absorption of atmospheric CO_2 and H_2O do not appear in the infra-red spectra since both beams are reduced in energy to the same extent. The double-beam spectrometer has other advantages, however.

Firstly, it is much simpler to amplify the alternating signal produced than the d.c. signal resulting from a single-beam detector.

Secondly, the sector mirror acts as a modulator (cf. p. 68) since it interrupts the beam periodically and, by amplifying only that component of the signal having the sector mirror frequency (usually 10–100 rotations per second), a great improvement in the signal-to-noise ratio results.

Thirdly, when examining the spectra of solutions, one can put a cell containing the appropriate quantity of pure solvent into the reference beam,

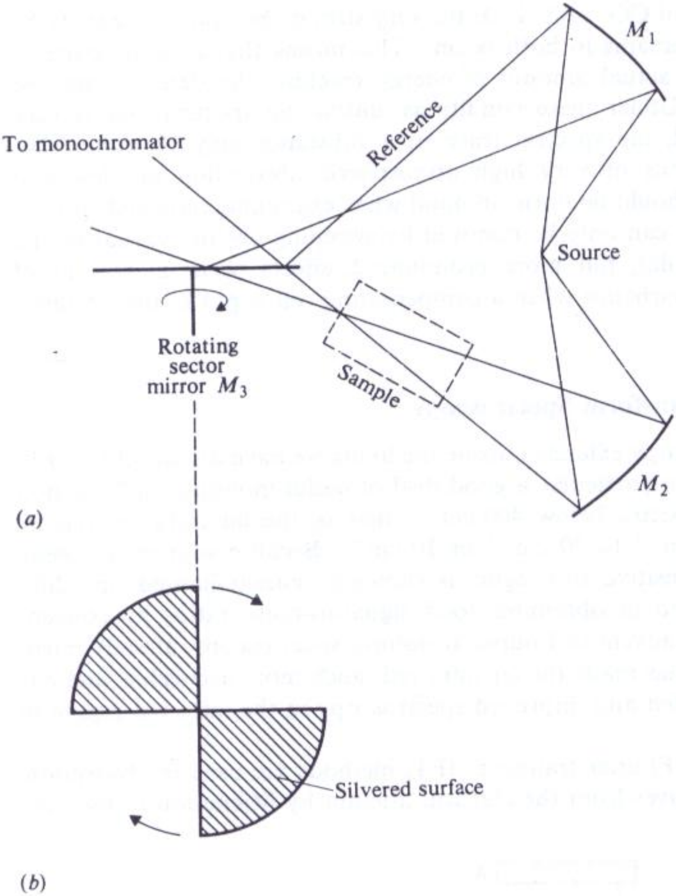

Figure 3.22 (*a*) Schematic diagram of a double-beam infra-red spectrometer. (*b*) A plan view of the rotating sector mirror M_3.

thus eliminating the solvent spectrum from the final trace. On a single-beam instrument the solvent spectrum must be taken separately and 'subtracted' from the solution spectrum in order to arrive at the spectrum of the substance of interest.

It should be pointed out, however, that a double-beam instrument is never *completely* effective in removing traces of water vapour or CO_2 from the spectra. No matter how carefully the instrument is assembled small differences occur in the beam paths and a small residual spectrum results. This can usually be removed, however, by sweeping with dry, inert gas as well as using the double-beam principle.

A further, more serious disadvantage which is not always appreciated by users of spectrometers is that the double-beam instrument only removes the spectral trace of CO_2 and H_2O; the very strong absorption of energy by these gases still remains in both beams. This means that at some parts of the spectrum the actual amount of energy reaching the detector may be extremely small. Under these conditions, unless the spectrometer is very carefully operated, the spectral trace of a substance may be quite false. Fortunately, regions of very high atmospheric absorption are few and narrow but they should be borne in mind when examining infra-red spectra. This disadvantage can only be removed by sweeping out or evacuating the spectrometer. Similar, but more pronounced, effects occur in regions of strong solvent absorbance when a compensating cell is put in the reference beam.

3.8.3 Fourier Transform Spectroscopy

Infra-red spectroscopy extends outside the limits we have discussed so far in this chapter, and in particular a good deal of useful molecular information is contained in spectra below 400 cm^{-1}, that is, the far infra-red region, from about 400 cm^{-1} to 20 cm^{-1} or 10 cm^{-1}. Because sources are weak and detectors insensitive, this region is known as 'energy-limited' and difficulty is experienced in obtaining good signal-to-noise ratios by conventional means. The advent of Fourier transform spectroscopy, already introduced in Sec. 1.8, has made the far infra-red much more accessible, and has considerably speeded and improved spectroscopy in the infra-red region in in general.

In this region Fourier transform (FT) methods are used in absorption. The apparatus derives from the classical attempt by Michelson to measure

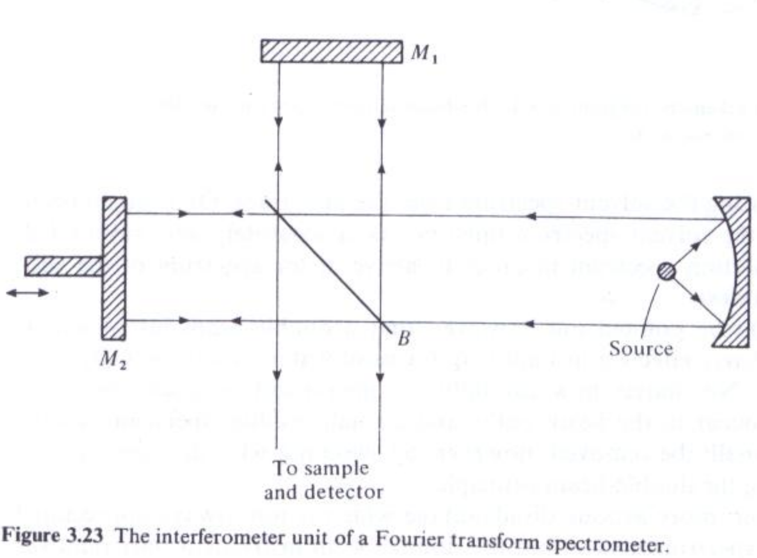

Figure 3.23 The interferometer unit of a Fourier transform spectrometer.

the 'ether wind' by determining the velocity of light in two perpendicular directions. A parallel beam of radiation is directed from the source to the interferometer, consisting of a beam splitter B and two mirrors M_1 and M_2 (Fig. 3.23). The beam splitter is a plate of suitably transparent material (e.g., potassium bromide) coated so as to reflect just 50 per cent of the radiation falling on it. Thus half the radiation goes to M_1, and half to M_2, returns from both these mirrors along the same path, and is then recombined to a single beam at the beam splitter (clearly half the total radiation is sent back to the source, but this is immaterial).

Now it is well known (and the essence of the Michelson experiment) that if *monochromatic* radiation is emitted by the source, the recombined beam leaving B shows constructive or destructive interference, depending on the relative path lengths B to M_1 and B to M_2. Thus if the path lengths are identical or differ by an integral number of wavelengths, constructive interference gives a bright beam leaving B, whereas if the difference is a half-integral number of wavelengths, the beams cancel at B. As the mirror M_2 is moved smoothly towards or away from B, therefore, a detector sees radiation alternating in intensity. It is fairly easy to imagine that if the source emits *two* separate monochromatic frequencies, ν_1 and ν_2, then the interference pattern (beat pattern) of ν_1 and ν_2 would overlay the interference caused by M_1 and M_2; the detector would see a more complicated intensity fluctuation as M_2 is moved, but computing the Fourier transform of the resultant signal is a very rapid way of obtaining the original frequencies and intensities emitted by the source. Taking the process further, even 'white' radiation emitted by the source produces an interference pattern which can be transformed back to the original frequency distribution.

Clearly then, if the recombined beam from such a source is directed through a *sample* before reaching the detector, sample absorptions will show up as gaps in the frequency distribution which, after transformation, yields a normal absorption spectrum. The production of a spectrum, then, may be thought of as follows: mirror M_2 is moved smoothly over a period of time (e.g., one second) through about 1 cm distance, while the detector signal—the interferogram—is collected into a multi-channel computer (it may be, for instance, that the detector signal is monitored every thousandth of a second during the mirror traverse, and each piece of information put serially into one of 1000 different storage points in the computer); the computer then carries out Fourier transformation on the stored data, and replaces the 'proper' spectrum piecemeal into the same 1000 locations, ready for plotting out on to paper.

The great advantage of FT spectroscopy is its speed. Since the whole spectrum is contained in the interferogram, which is recorded in the computer within one second, this is effectively the scan time. Even adding the computing and plotting time of, say, 15 seconds, the overall time to obtain a spectrum is very short compared with the 10 minutes or so required by conventional methods to obtain similar resolution. Essentially, to achieve a given resolution each element, or observation point, of the spectrum must be examined for a given time; in the conventional method each element is examined *consecutively*, whereas in the interferometer all the elements are examined *simultaneously* and later sorted out by rapid computation; the advantage of the latter is obvious.

Other advantages are also offered by the FT technique; briefly these are:

1. In a conventional instrument the radiation is invariably brought to a focus on a slit, and it is essentially the image of the slit which is seen by the detector; a very fine slit gives good resolving power since only a narrow spread of frequencies falls on the detector at any one moment, but the total amount of energy passing through the instrument is severely limited, requiring high-gain and hence 'noisy' amplifiers. In FT work parallel beams are used throughout, and there is no need to bring the radiation to a focus except for convenience at the sample and at the detector—no slit is required and *all* the source energy passes through the instrument; consequently amplifiers are less critical and the resolving power is governed solely by the mirror traverse and computer capacity. It is for this reason that FT instruments were first developed for use in the energy-limited far infra-red region.
2. The resolving power of an FT instrument is constant over the entire spectrum; in a grating or prism instrument the resolving power depends on the angle which that component makes with the radiation beam, and hence varies with frequency—in particular it is usually especially poor at the ends of the spectrum.
3. The presence of a computer for FT work means that other jobs can be carried out automatically; thus several scans of the same sample may be added into the computer store in order to improve the signal-to-noise ratio; the spectrum output may be modified to suit the user by removing solvent peaks, correcting baseline drift, expanding parts of the spectrum, offsetting window absorptions, etc. It is even possible for calculation of peak intensities or sample concentrations to be made on a routine basis.

3.8.4 The Carbon Dioxide Laser

Currently the only laser which seems to have some potential for use in routine infra-red spectroscopy is that made from a mixture of carbon dioxide and nitrogen, the so-called CO_2 laser. The primary excitation step in this is the excitation of nitrogen molecules into their first excited vibrational level, which, as Fig. 3.24 shows, is at about 2360 cm^{-1} above the ground state. This happens to be very close in energy to ν_3, the asymmetric stretching vibration of CO_2 at 2350 cm^{-1}, and so resonance excitation of CO_2 to

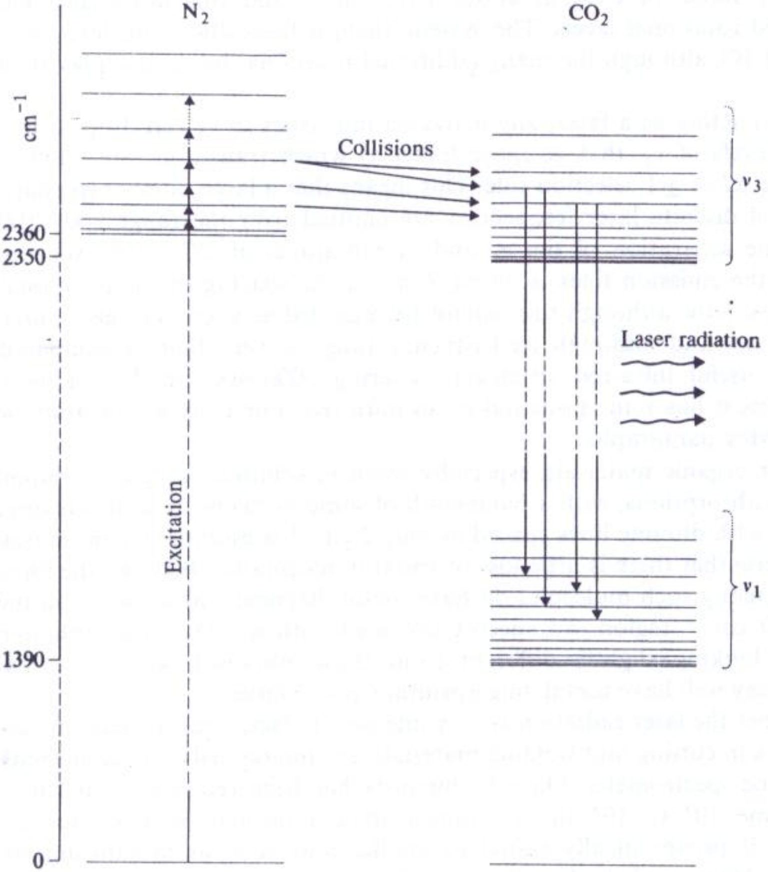

Figure 3.24 The energy levels of nitrogen and of carbon dioxide involved in the CO_2 laser.

this level occurs by collision with excited N_2. Now both N_2 and CO_2 have rotational states associated with these vibrational energies, which are also indicated (schematically and not to scale) in Fig. 3.24. This means that many different rotational levels of N_2 will be populated in the initial excitation, and consequently many rotational levels of the ν_3 vibration of CO_2 will be collisionally activated. In fact, levels up to some 200 cm^{-1} above the lowest state of ν_3 are effectively populated in this way.

The excited CO_2 can, and of course does, decay spontaneously and directly to the ground state, liberating energy as heat. For this reason some helium is incorporated into the gas mixture, to help in transferring the heat to the walls of the containing tube, and the laser is normally operated in the pulsed mode, although pulses can be as high as several per second. In addition, however, stimulated emission is possible to ν_1, the symmetric stretching mode of CO_2 at about 1390 cm^{-1}, and this mode also has associated rotational levels. The system, then, is basically a four-level laser (cf. Sec. 1.10), although the many additional rotational levels also play their part.

When acting as a laser, any activated molecules in ν_3 can drop to any *allowed* levels of ν_1, that is, those levels to which transitions are allowed under the $\Delta J = \pm 1$ selection rule. This means that a large number (perhaps 80–100) of discrete laser frequencies are emitted over the range 900–1100 cm^{-1}—the separation of the ν_1 and ν_3 vibrations of CO_2. The spacing between the emission lines is about 2 cm^{-1}, the spacing of the rotational transitions. Now although this cannot be regarded as a 'continuous' source of radiation, and although its frequency range is very limited compared with the useful infra-red spectrum (covering 3000–400 cm^{-1} or lower), nonetheless it has some potential as an infra-red source, as we illustrate in the following paragraphs.

Most organic materials, especially when in solution, have fairly broad infra-red absorptions, with a bandwidth of some 5–20 cm^{-1}; in this respect a source with discrete lines spaced at only 2 cm^{-1} is essentially continuous, in the sense that there is little loss of spectral information between the lines. Equally, many such molecules do have useful diagnostic absorptions in the 900–1100 cm^{-1} region. So spectra obtained with a CO_2 laser, although perhaps looking slightly different from those obtained with a normal source, may well have useful 'fingerprinting' possibilities.

Further the laser radiation is very intense—in fact, since its main industrial use is in cutting and welding materials, an unmodified CO_2 laser tends to melt the spectrometer. Once its intensity has been reduced so that it is 'only' some 10^3 to 10^5 times stronger than a normal infra-red source, however, it proves ideally suited to applications such as monitoring air pollution. Here one is looking for parts-per-million quantities of pollutants, and the best method is to shine the infra-red beam through a very long path of the material. Clearly an intense beam that does not diverge over a large distance is exactly what is required.

Finally, quantitative measurements of materials are most accurately obtained by using monochromatic radiation, and in this respect one of the emission lines from the CO_2 laser, selected by the use of a normal dispersion grating, is ideal, and potentially very useful for continuous monitoring of production materials.

BIBLIOGRAPHY

Alpert, N. A., W. E. Keiser, and H. A. Szymanski: *Theory and Practice of Infra-Red Spectroscopy*, Plenum Press, 1970.

Barnes, A. J., and W. J. Orville-Thomas (eds): *Vibrational Spectroscopy—Modern Trends*, Elsevier, 1977.

Bellamy, L. J.: *The Infra-Red Spectra of Complex Molecules*, Chapman and Hall, 1975.

Bellamy, L. J.: *Advances in Infra-Red Group Frequencies*, Methuen, 1968.

Ferraro, J. R., and L. J. Basile: *Fourier Transform Infra-Red Spectroscopy: Applications to Chemical Systems*, Academic Press; vol. 1, 1978; vol. 2, 1979.

Finch, A., F. N. Dickson, and F. F. Bentley: *Chemical Applications of Far Infra-Red Spectroscopy*, Academic Press, 1970.

Herzberg, G.: *Molecular Structure and Molecular Spectra:* vol. 1, *Spectra of Diatomic Molecules*, 2nd ed., Van Nostrand, 1950.

Herzberg, G.: *Molecular Spectra and Molecular Structure:* vol. 2, *Infra-Red and Raman Spectra of Polyatomic Molecules*, Van Nostrand, 1945.

Meloan, C. E.: *Elementary Infra-Red Spectroscopy*, Macmillan, 1963.

Nakamoto, K.: *Infra-Red Spectra of Inorganic and Co-ordination Compounds*, 3rd ed., John Wiley, 1978.

Ross, S. D.: *Inorganic Infra-Red and Raman Spectra*, McGraw-Hill, 1972.

Sherwood, P. M. A.: *Vibrational Spectroscopy of Solids*, Cambridge University Press, 1972.

Siesler, H. W., and K. Holland-Moritz: *Infra-Red and Raman Spectroscopy of Polymers*, Marcel Dekker Inc., 1980.

Smith, A. L.: *Applied Infra-Red Spectroscopy*, Wiley, 1979.

Steele, D.: *The Interpretation of Vibrational Spectra*, Chapman and Hall, 1971.

Williams, D. H., and I. Fleming: *Spectroscopic Methods in Organic Chemistry*, 3rd ed., McGraw-Hill, 1980.

PROBLEMS

(Useful constants: $h = 6{\cdot}626 \times 10^{-34}$ J s; $c = 2{\cdot}998 \times 10^{8}$ m s^{-1}; $N = 6{\cdot}023 \times 10^{23}$ mol^{-1}; $k = 1{\cdot}381 \times 10^{-23}$ J K^{-1}; $4\pi^2 = 39{\cdot}478$; 1 cm$^{-1} \equiv 11{\cdot}958$ J mol^{-1}; atomic masses: $^{14}\mathrm{N} = 23{\cdot}25 \times 10^{-27}$ kg; $^{16}\mathrm{O} = 26{\cdot}56 \times 10^{-27}$ kg.)

3.1 The fundamental and first overtone transitions of $^{14}\mathrm{N}^{16}\mathrm{O}$ are centred at 1876·06 cm^{-1} and 3724·20 cm^{-1} respectively. Evaluate the equilibrium vibration frequency, the anharmonicity, the exact zero point energy, and the force constant of the molecule. Assuming that in Eq. (3.12) v is a continuous variable, use calculus to determine the maximum value of ε_v, and hence calculate a value for the dissociation energy of NO. Criticize this method.

3.2 The vibrational wavenumbers of the following molecules in their $v = 0$ states are: HCl: 2885 cm^{-1}; DCl: 1990 cm^{-1}; D_2: 2990 cm^{-1}; and HD: 3627 cm^{-1}. Calculate the energy change, in kJ mol^{-1} of the reaction

$$\mathrm{HCl} + \mathrm{D_2} \rightarrow \mathrm{DCl} + \mathrm{HD}$$

and determine whether energy is liberated or absorbed.

Hint: Consider the zero point energies of the four molecules concerned.

3.3 The equilibrium vibration frequency of the iodine molecule I_2 is 215 cm^{-1}, and the anharmonicity constant x is 0·003; what, at 300 K, is the intensity of the 'hot band' ($v = 1 \rightarrow v = 2$ transition) relative to that of the fundamental ($v = 0 \rightarrow v = 1$)?

3.4 An infra-red spectrum of OCS is obtained in which the rotational fine structure is not resolved. Using data from Table 2.2, calculate the separation between the P and R branch maxima at $T = 300$ K.

3.5 How many normal modes of vibration are possible for (*a*) HBr, (*b*) OCS (linear), (*c*) SO_2 (bent), and (*d*) C_6H_6?

3.6 Estimate, using data from Table 3.4, the vibrational wave-number of (*a*) – OD, (*b*)  . (Relative atomic masses are: H = 1, D = 2, C = 12, O = 16, S = 32.)

CHAPTER

FOUR

RAMAN SPECTROSCOPY

4.1 INTRODUCTION

When a beam of light is passed through a transparent substance, a small amount of the radiation energy is scattered, the scattering persisting even if all dust particles or other extraneous matter are rigorously excluded from the substance. If monochromatic radiation, or radiation of a very narrow frequency band, is used the scattered energy will consist almost entirely of radiation of the incident frequency (the so-called *Rayleigh scattering*) but, in addition, certain discrete frequencies above and below that of the incident beam will be scattered; it is this which is referred to as *Raman scattering*.

4.1.1 Quantum Theory of Raman Effect

The occurrence of Raman scattering may be most easily understood in terms of the quantum theory of radiation. This treats radiation of frequency ν as consisting of a stream of particles (called photons) having energy $h\nu$ where h is Planck's constant. Photons can be imagined to undergo collisions with molecules and, if the collision is perfectly elastic, they will be deflected unchanged. A detector placed to collect energy at right angles to an incident beam will thus receive photons of energy $h\nu$, that is, radiation of frequency ν.

However, it may happen that energy is exchanged between photon and molecule during the collision: such collisions are called 'inelastic'. The molecule can gain or lose amounts of energy only in accordance with the quantal laws; i.e., its energy change, ΔE joules, must be the difference in energy between two of its allowed states. That is to say, ΔE must represent a change in the vibrational and/or rotational energy of the molecule. If the molecule *gains* energy ΔE, the photon will be scattered with energy $h\nu - \Delta E$ and the equivalent radiation will have a frequency $\nu - \Delta E/h$. Conversely if the molecule *loses* energy ΔE, the scattered frequency will be $\nu + \Delta E/h$.

Radiation scattered with a frequency lower than that of the incident beam is referred to as Stokes' radiation, while that at higher frequency is called anti-Stokes'. Since the former is accompanied by an *increase* in molecular energy (which can always occur, subject to certain selection rules) while the latter involves a *decrease* (which can only occur if the molecule is originally in an excited vibrational or rotational state), Stokes' radiation is generally more intense than anti-Stokes'. Overall, however, the total radiation scattered at any but the incident frequency is extremely small, and sensitive apparatus is needed for its study.

4.1.2 Classical Theory of the Raman Effect; Molecular Polarizability

The classical theory of the Raman effect, while not wholly adequate, is worth consideration since it leads to an understanding of a concept basic to this form of spectroscopy—the polarizability of a molecule. When a molecule is put into a static electric field it suffers some distortion, the positively charged nuclei being attracted towards the negative pole of the field, the electrons to the positive pole. This separation of charge centres causes an *induced electric dipole moment* to be set up in the molecule and the molecule is said to be *polarized*. The size of the induced dipole, μ, depends both on the magnitude of the applied field, E, and on the ease with which the molecule can be distorted. We may write

$$\mu = \alpha E \tag{4.1}$$

where α is the *polarizability* of the molecule.

Consider first a diatomic molecule, such as H_2, shown at Fig. 4.1(*a*). The polarizability is *anisotropic*, i.e., the electrons forming the bond are more easily displaced by an electric field applied along the bond axis than one across this direction: this may be confirmed experimentally, for example by a study of the absolute intensity of lines in the Raman spectrum, when it is found that the induced dipole moment for a given field applied along the axis is approximately twice as large as that induced by the same field applied across the axis; fields in other directions induce intermediate dipole moments. We can represent the polarizability in various directions most conveniently by drawing a *polarizability ellipsoid*, as in Fig. 4.1(*b*),

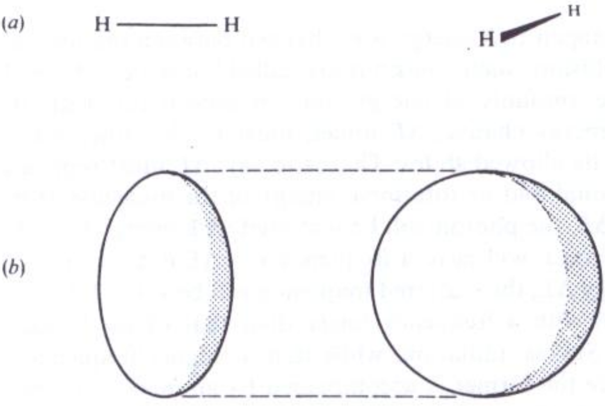

Figure 4.1 The hydrogen molecule and its polarizability ellipsoid seen from two directions at right angles.

where the ellipsoid is a three-dimensional surface whose distance from the electrical centre of the molecule (here the centre of gravity also) is proportional to $1/\sqrt{\alpha_i}$, where α_i is the polarizability along the line joining point i on the ellipsoid with the electrical centre. Thus where the polarizability is greatest the axis of the ellipsoid is least, and vice versa. (This representation is chosen because of an analogy with the momentum of a body—the momental ellipsoid is defined similarly using $1/\sqrt{I_i}$, where I_i is the moment of inertia about an axis i.)

Since the polarizability of a diatomic molecule is the same for all directions at right angles to the bond axis, the ellipsoid has a circular cross-section in this direction; thus it is shaped rather like a tangerine. All diatomic molecules, for example CO, HCl, and linear polyatomic molecules, for example CO_2, HC≡CH, etc., having ellipsoids of the same general shape, differing only in the relative sizes of their major and minor axes.

When a sample of such molecules is subjected to a beam of radiation of frequency ν the electric field experienced by each molecule varies according to the equation (cf. Eq. (1.1)):

$$E = E_0 \sin 2\pi\nu t \tag{4.2}$$

and thus the induced dipole also undergoes oscillations of frequency ν:

$$\mu = \alpha E = \alpha E_0 \sin 2\pi\nu t \tag{4.3}$$

Such an oscillating dipole emits radiation of its own oscillation frequency and we have immediately in Eq. (4.3) the classical explanation of Rayleigh scattering.

If, in addition, the molecule undergoes some internal motion, such as vibration or rotation, which *changes the polarizability* periodically, then the oscillating dipole will have superimposed upon it the vibrational or rotational oscillation. Consider, for example, a vibration of frequency $\nu_{\text{vib.}}$ which changes the polarizability: we can write

$$\alpha = \alpha_0 + \beta \sin 2\pi\nu_{\text{vib.}}t \tag{4.4}$$

where α_0 is the equilibrium polarizability and β represents the rate of change of polarizability with the vibration. Then we have:

$$\mu = \alpha E = (\alpha_0 + \beta \sin 2\pi\nu_{\text{vib.}}t)E_0 \sin 2\pi\nu t$$

or, expanding and using the trigonometric relation,

$$\sin A \sin B = \tfrac{1}{2}\{\cos (A - B) - \cos (A + B)\}$$

we have

$$\mu = \alpha_0 E_0 \sin 2\pi\nu t + \tfrac{1}{2}\beta E_0\{\cos 2\pi(\nu - \nu_{\text{vib.}})t - \cos 2\pi(\nu + \nu_{\text{vib.}})t\} \tag{4.5}$$

and thus the oscillating dipole has frequency components $\nu \pm \nu_{\text{vib.}}$ as well as the exciting frequency ν.

It should be carefully noted, however, that if the vibration does not alter the polarizability of the molecule (and we shall later give examples of such vibrations) then $\beta = 0$ and the dipole oscillates only at the frequency of the incident radiation; the same is true of a rotation. Thus we have the general rule:

> In order to be Raman active a molecular rotation or vibration must cause some change in a component of the molecular polarizability. A change in polarizability is, of course, reflected by a change in either the *magnitude* or the *direction* of the polarizability ellipsoid.

(This rule should be contrasted with that for infra-red and microwave activity, which is that the molecular motion must produce a change in the electric dipole of the molecule.)

Let us now consider briefly the shapes of the polarizability ellipsoids of more complicated molecules, taking first the bent triatomic molecule H_2O shown at Fig. 4.2(*a*). By analogy with the discussion for H_2 given above, we might expect the polarizability surface to be composed of *two* similar ellipsoids, one for each bond. While this may be correct in minute detail, we must remember that the oscillating electric field which we wish to apply for Raman spectroscopy is usually that of radiation in the visible or ultra-violet region, i.e., having a wavelength of some 1 μm–10 nm (cf. Fig. 1.4); molecular bonds, on the other hand, have dimensions of only some 0·1 nm, so we cannot expect our radiation to probe the finer details of bond polarizability—even the hardest of X-rays can scarcely do that. Instead the radiation can only sense the average polarizability in various directions through the molecule, and the polarizability ellipsoid, it may be shown, is

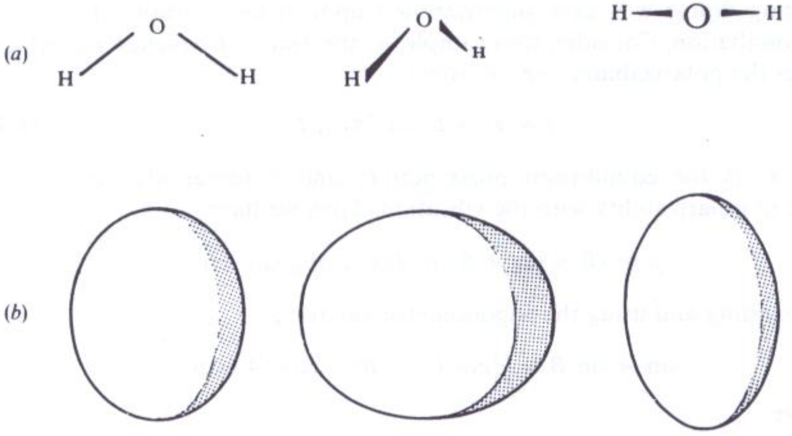

Figure 4.2 The water molecule and its polarizability ellipsoid seen along the three coordinate axes.

always a true ellipsoid—i.e., a surface having *all* sections elliptical (or possibly circular). In the particular case of H_2O the polarizability is found to be different along all three of the major axes of the molecule (which lie along the line in the molecular plane bisecting the HOH angle, at right angles to this in the plane, and perpendicularly to the plane), and so all three of the ellipsoidal axes are also different; the ellipsoid is sketched in various orientations in Fig. 4.2(*b*). Other such molecules, for example, H_2S or SO_2, have similarly shaped ellipsoids but with different dimensions.

Symmetric top molecules, because of their axial symmetry, have polarizability ellipsoids rather similar to those of linear molecules, i.e., with a circular cross-section at right angles to their axis of symmetry. It should be stressed, however, that sections in other planes are truly *elliptical*. For a molecule such as chloroform, $CHCl_3$ (Fig. 4.3(*a*)), where the chlorine atoms are bulky, the usual tendency is to draw the polarizability surface as egg-shaped, fatter at the chlorine-containing end. This is not correct; the polarizability ellipsoid for chloroform is shown at Fig. 4.3(*b*) where it will be seen that, since the polarizability is greater across the symmetry axis, the *minor* axis of the ellipsoid lies in this direction. Similar molecules are, for example, CH_3Cl and NH_3, etc. (although the latter fortuitously has a virtually spherical 'ellipsoid').

Finally, spherical top molecules, such as CH_4, CCl_4, SiH_4, etc., have spherical polarizability surfaces, since they are completely isotropic as far as incident radiation is concerned.

We are now in a position to discuss in detail the Raman spectra of various types of molecule. Since we shall be dealing with rotational and vibrational changes it is evident that expressions for the energy levels and

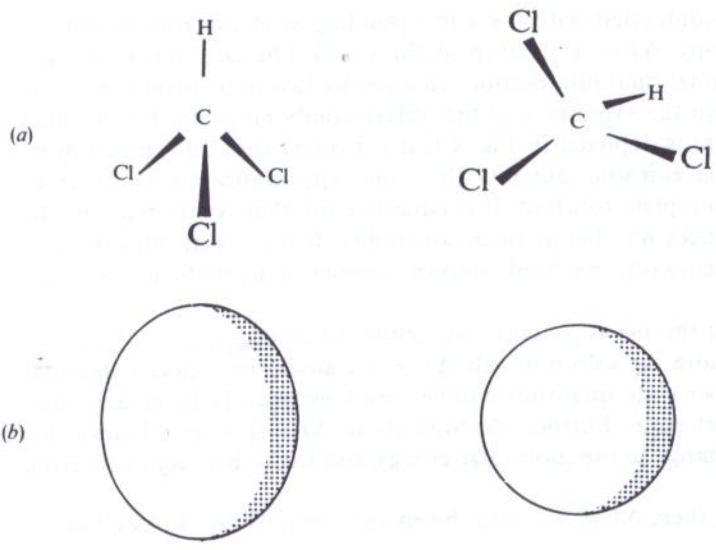

Figure 4.3 The chloroform molecule, $CHCl_3$, and its polarizability ellipsoid from across and along the symmetry axis.

for many of the allowed transitions will be identical with those already discussed in the previous two chapters. For clarity we shall repeat any such expressions but not rederive them, being content to give a cross-reference to where their derivation may be found.

4.2 PURE ROTATIONAL RAMAN SPECTRA

4.2.1 Linear Molecules

The rotational energy levels of linear molecules have already been stated (cf. Eq. (2.24)):

$$\varepsilon_J = BJ(J+1) - DJ^2(J+1)^2 \text{ cm}^{-1} \qquad (J = 0, 1, 2, \ldots)$$

but, in Raman spectroscopy, the precision of the measurements does not normally warrant the retention of the term involving *D*, the centrifugal distortion constant. Thus we take the simpler expression:

$$\varepsilon_J = BJ(J+1) \text{ cm}^{-1} \qquad (J = 0, 1, 2, \ldots) \tag{4.6}$$

to represent the energy levels.

Transitions between these levels follow the formal selection rule:

$$\Delta J = 0, \text{ or } \pm 2 \text{ only} \tag{4.7}$$

which is to be contrasted with the corresponding selection rule for microwave spectroscopy, $\Delta J = \pm 1$, given in Eq. (2.17). The fact that in Raman work the rotational quantum number changes by two units rather than one is connected with the symmetry of the polarizability ellipsoid. For a linear molecule, such as is depicted in Fig. 4.1, it is evident that during end-over-end rotation the ellipsoid presents the same appearance to an observer *twice* in every complete rotation. It is equally clear that rotation about the bond axis produces no change in polarizability, hence, as in infra-red and microwave spectroscopy, we need concern ourselves only with end-over-end rotations.

If, following the usual practice, we define ΔJ as $(J_{\text{upper state}} - J_{\text{lower state}})$ then we can ignore the selection rule $\Delta J = -2$ since, for a pure rotational change, the upper state quantum number must necessarily be greater than that in the lower state. Further the 'transition' $\Delta J = 0$ is trivial since this represents no change in the molecular energy and hence Rayleigh scattering only.

Combining, then, $\Delta J = +2$ with the energy levels of Eq. (4.6) we have:

$$\begin{aligned}\Delta\varepsilon &= \varepsilon_{J'=J+2} - \varepsilon_{J''=J} \\ &= B(4J+6)\ \text{cm}^{-1} \qquad (4.8)\end{aligned}$$

Since $\Delta J = +2$, we may label these lines S branch lines (cf. Sec. 3.2) and write

$$\Delta\varepsilon_S = B(4J+6)\ \text{cm}^{-1} \qquad (J = 0, 1, 2, \ldots) \qquad (4.9)$$

where J is the rotational quantum number in the *lower* state.

Thus if the molecule gains rotational energy from the photon during collision we have a series of S branch lines to the low wavenumber side of the exciting line (Stokes' lines), while if the molecule loses energy to the photon the S branch lines appear on the high wavenumber side (anti-Stokes' lines). The wavenumbers of the corresponding spectral lines are given by:

$$\bar{\nu}_S = \bar{\nu}_{\text{ex.}} \pm \Delta\varepsilon_S = \bar{\nu}_{\text{ex.}} \pm B(4J+6)\ \text{cm}^{-1} \qquad (4.10)$$

where the plus sign refers to anti-Stokes' lines, the minus to Stokes', and $\bar{\nu}_{\text{ex.}}$ is the wavenumber of the exciting radiation.

The allowed transitions and the Raman spectrum arising are shown schematically in Fig. 4.4. Each transition is labelled according to its lower J value and the relative intensities of the lines are indicated assuming that the population of the various energy levels varies according to Eq. (2.21) and Fig. 2.7. In particular it should be noted here that Stokes' and anti-Stokes' lines have comparable intensity because many rotational levels are populated and hence downward transitions are approximately as likely as upward ones.

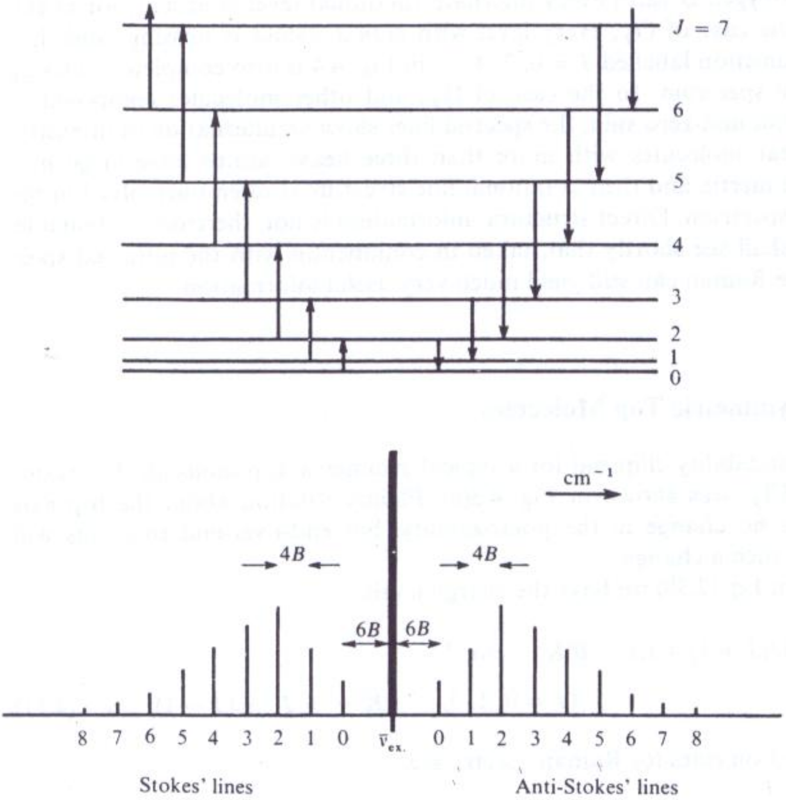

Figure 4.4 The rotational energy levels of a diatomic molecule and the rotational Raman spectrum arising from transitions between them. Special lines are numbered according to their lower J values.

When the value $J = 0$ is inserted into Eq. (4.10) it is seen immediately that the separation of the first line from the exciting line is $6B$ cm^{-1}, while the separation between successive lines is $4B$ cm^{-1}. For diatomic and light triatomic molecules the rotational Raman spectrum will normally be resolved and we can immediately obtain a value of B, and hence the moment of inertia and bond lengths for such molecules. If we recall that homonuclear diatomic molecules (for example, O_2, H_2) give no infra-red or microwave spectra since they possess no dipole moment, whereas they *do* give a rotational Raman spectra, we see that the Raman technique yields structural data unobtainable from the techniques previously discussed. It is thus complementary to microwave and infra-red studies, not merely confirmatory.

It should be mentioned that, if the molecule has a centre of symmetry (as, for example, do H_2, O_2, CO_2), then the effects of nuclear spin will be observed in the Raman as in the infra-red. Thus for O_2 and CO_2 (since the spin of oxygen is zero) every alternate rotational level is absent; for example, in the case of O_2, every level with *even* J values is missing, and thus every transition labelled $J = 0, 2, 4, \ldots$ in Fig. 4.4 is also completely missing from the spectrum. In the case of H_2, and other molecules composed of nuclei with non-zero spin, the spectral lines show an alternation of intensity.

Linear molecules with more than three heavy atoms have large moments of inertia and their rotational fine structure is often unresolved in the Raman spectrum. Direct structural information is not, therefore, obtainable, but we shall see shortly that, taken in conjunction with the infra-red spectrum, the Raman can still yield much very useful information.

4.2.2 Symmetric Top Molecules

The polarizability ellipsoid for a typical symmetric top molecule, for example, $CHCl_3$, was shown in Fig. 4.3(*b*). Plainly rotation about the top axis produces no change in the polarizability, but end-over-end rotations will produce such a change.

From Eq. (2.38) we have the energy levels:

$$\varepsilon_{J,K} = BJ(J+1) + (A-B)K^2 \quad \text{cm}^{-1}$$
$$(J = 0, 1, 2, \ldots; K = \pm J, \pm(J-1), \ldots) \qquad (4.11)$$

The selection rules for Raman spectra are:

$$\left.\begin{array}{ll}\Delta K = 0 & \\ \Delta J = 0, \pm 1, \pm 2 & \text{(except for } K = 0 \text{ states} \\ & \text{when } \Delta J = \pm 2 \text{ only)}\end{array}\right\} \qquad (4.12)$$

K, it will be remembered, is the rotational quantum number for axial rotation, so the selection rule $\Delta K = 0$ implies that changes in the angular momentum about the top axis will not give rise to a Raman spectrum—such rotations are, as mentioned previously, Raman inactive. The restriction of ΔJ to ± 2 for $K = 0$ states means effectively that ΔJ cannot be ± 1 for transitions involving the ground state ($J = 0$) since $K = \pm J$, $\pm(J-1), \ldots, 0$. Thus for all J values other than zero, K also may be different from zero and $\Delta J = \pm 1$ transitions are allowed.

Restricting ourselves, as before, to positive ΔJ we have the two cases:

1. $\Delta J = +1$ (*R* branch lines)

$$\Delta\varepsilon_R = \varepsilon_{J'=J+1} - \varepsilon_{J''=J}$$
$$= 2B(J+1) \text{ cm}^{-1} \qquad (J = 1, 2, 3, \ldots \text{ (but } J \neq 0)) \qquad (4.13a)$$

2. $\Delta J = +2$ (*S* branch lines)

$$\begin{aligned}\Delta\varepsilon_S &= \varepsilon_{J'=J+2} - \varepsilon_{J''=J} \\ &= B(4J+6)\ \text{cm}^{-1} \quad (J = 0, 1, 2, \ldots).\end{aligned} \tag{4.13b}$$

Thus we shall have two series of lines in the Raman spectrum:

$$\left.\begin{aligned}\bar{\nu}_R &= \bar{\nu}_{\text{ex.}} \pm \Delta\varepsilon_R = \bar{\nu}_{\text{ex.}} \pm 2B(J+1)\ \text{cm}^{-1} \qquad (J = 1, 2, \ldots) \\ \bar{\nu}_S &= \bar{\nu}_{\text{ex.}} \pm \Delta\varepsilon_S = \bar{\nu}_{\text{ex.}} \pm B(4J+6)\ \text{cm}^{-1} \qquad (J = 0, 1, 2, \ldots)\end{aligned}\right\} \tag{4.14}$$

These series are sketched separately in Fig. 4.5(*a*) and (*b*), where each line is labelled with its corresponding *lower J* value. In the *R* branch, lines appear

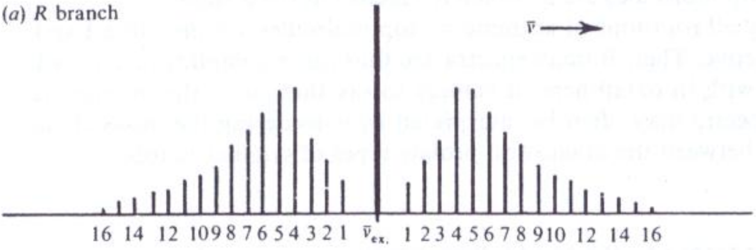
(*a*) *R* branch

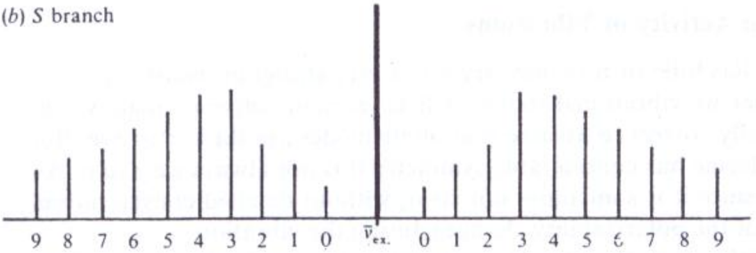
(*b*) *S* branch

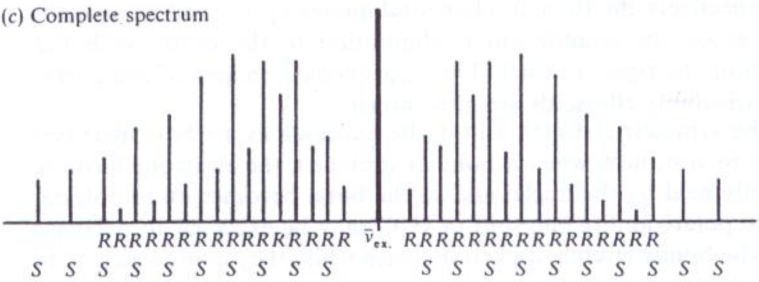
(*c*) Complete spectrum

Figure 4.5 Rotational Raman spectrum of a symmetric top molecule. The *R* and *S* branch lines are shown separately in (*a*) and (*b*) respectively, with the total spectrum in (*c*).

at $4B$, $6B$, $8B$, $10B$, ... cm^{-1} from the exciting line, while the S branch series occurs at $6B$, $10B$, $14B$, ... cm^{-1}. The complete spectrum, shown at Fig. 4.5(*c*) illustrates how every alternate R line is overlapped by an S line. Thus a marked intensity alternation is to be expected which, it should be noted, is not connected with nuclear spin statistics.

4.2.3 Spherical Top Molecules; Asymmetric Top Molecules

Examples of spherical top molecules are those with tetrahedral symmetry such as methane, CH_4, or silane, SiH_4. The polarizability ellipsoid for such molecules is a spherical surface and it is evident that rotation of this ellipsoid will produce no change in polarizability. Therefore the pure rotations of spherical top molecules are completely inactive in the Raman.

Normally *all* rotations of asymmetric top molecules, on the other hand, are Raman active. Their Raman spectra are thus quite complicated and will not be dealt with in detail here; it suffices to say that, as in the microwave region, the spectra may often be interpreted by considering the molecule as intermediate between the oblate and prolate types of symmetric top.

4.3 VIBRATIONAL RAMAN SPECTRA

4.3.1 Raman Activity of Vibrations

If a molecule has little or no symmetry it is a very straightforward matter to decide whether its vibrational modes will be Raman active or inactive: in fact, it is usually correct to assume that *all* its modes are Raman active. But when the molecule has considerable symmetry it is not always easy to make the decision, since it is sometimes not clear, without detailed consideration, whether or not the polarizability changes during the vibration.

We consider first the simple asymmetric top molecule H_2O whose polarizability ellipsoid was shown in Fig. 4.2. In Fig. 4.6 we illustrate at (*a*), (*b*), and (*c*) respectively the three fundamental modes ν_1, ν_2, and ν_3, sketching for each mode the equilibrium configuration in the centre with the extreme positions to right and left. The approximate shapes of the corresponding polarizability ellipsoids are also shown.

During the symmetric stretch, in (*a*), the molecule as a whole increases and decreases in size; now when a bond is stretched, the electrons forming it are less firmly held by the nuclei and so the bond becomes more polarizable. Thus the polarizability ellipsoid of H_2O may be expected to decrease in size while the bonds stretch, and to increase while they compress, but to maintain an approximately constant shape. On the other hand while undergoing the bending motion, in (*b*), it is the shape of the ellipsoid which changes most; thus if we imagine vibrations of very large amplitude, at one

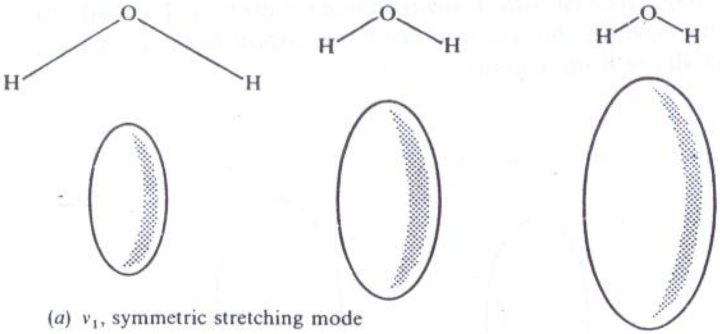

(*a*) ν_1, symmetric stretching mode

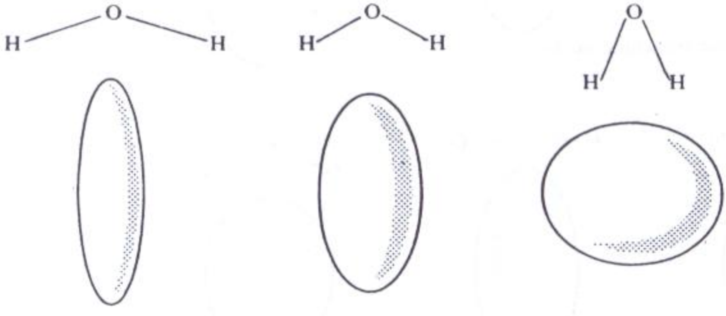

(*b*) ν_2, bending mode

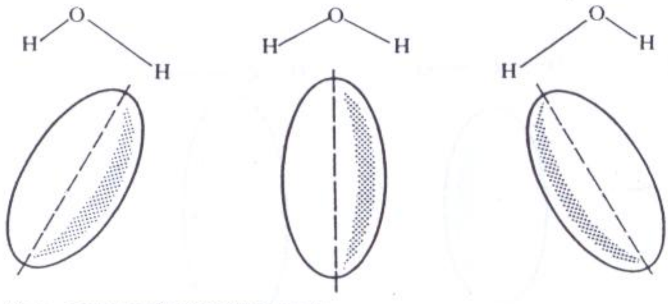

(*c*) ν_3, asymmetric stretching mode

Figure 4.6 The change in size, shape, or direction of the polarizability ellipsoid of the water molecule during each of its three vibrational modes. The centre column shows the equilibrium position of the molecule while to right and left are the extremes of each vibration.

extreme (on the left) the molecule approaches the linear configuration with a horizontal axis, while at the other extreme (on the right) it approximates to a diatomic molecule (if the two H atoms are almost coincidental) with a vertical axis. Finally in (*c*) we have the asymmetric stretching motion, ν_3, where both the size and shape remain approximately constant, but the direction of the major axis (shown dashed) changes markedly. Thus all three vibrations involve obvious changes in at least one aspect of the polarizability ellipsoid, and all are Raman *active*.

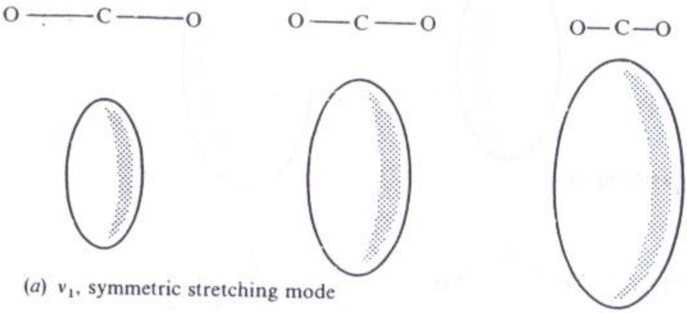

(*a*) ν_1, symmetric stretching mode

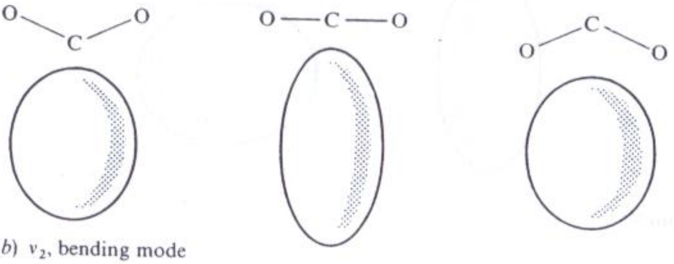

(*b*) ν_2, bending mode

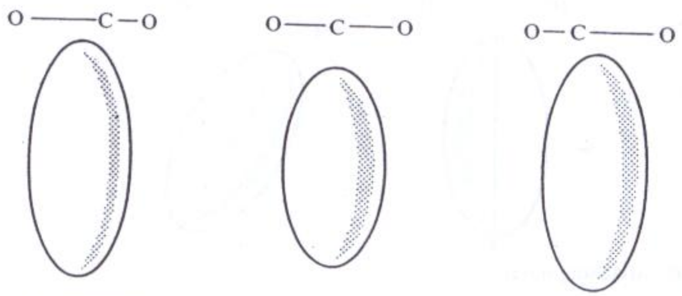

(*c*) ν_3, asymmetric stretching mode

Figure 4.7 The shape of the polarizability ellipsoid of the carbon dioxide molecule during its vibrations.

Now consider the linear triatomic molecule CO_2, whose three fundamental vibrational modes have been shown in Fig. 3.11; in Fig. 4.7 we illustrate the extreme and equilibrium configurations of the molecule and their approximate polarizability ellipsoids. The question of the Raman behaviour of the symmetric stretching mode, ν_1, is easily decided—during the motion the molecule changes size, and so there is a corresponding fluctuation in the size of the ellipsoid; the motion is thus Raman *active*. It might be thought that the ν_2 and ν_3 vibrations are also Raman active, because the molecule changes shape during each vibration and hence, presumably, so does the ellipsoid; however, both these modes are observed to be Raman *inactive*. We must, then, consider this example rather more carefully.

To do this it is usual to discuss the change of polarizability with some *displacement coordinate*, normally given the symbol ξ; thus for a stretching motion, ξ is a measure of the extension (positive ξ) or compression (negative ξ) of the bond under consideration; while for a bending mode, ξ measures the displacement of the bond angle from its equilibrium value, positive and negative ξ referring to opposite displacement directions.

Consider, as an example, the ν_1 stretch of carbon dioxide sketched in Fig. 4.7(*a*). If the equilibrium value of the polarizability is α_0 (centre picture) then, when the bonds stretch (ξ positive), α increases (remember that the extent of the ellipsoid measures the *reciprocal* of α), while when the bonds contract (negative ξ) α decreases. Thus we can sketch the variation of α with ξ as in Fig. 4.8(*a*). The details of the curve are not important since we are concerned only with *small* displacements; it is plain that near the equilibrium position ($\xi = 0$) the curve has a distinct slope, that is $d\alpha/d\xi \neq 0$ at $\xi = 0$. Thus for small displacements the motion produces a change in polarizability and is therefore Raman *active*.

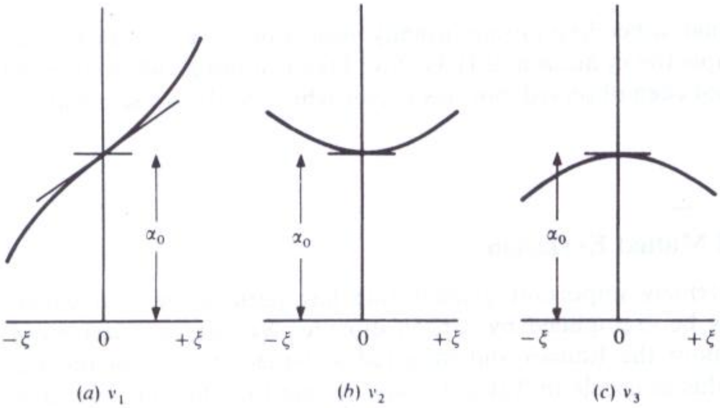

(*a*) ν_1 (*b*) ν_2 (*c*) ν_3

Figure 4.8 The variation of the polarizability, α, with the displacement coordinate, ξ, during the three vibrational modes of the carbon dioxide molecule.

If we now consider the situation for ν_2, the bending motion of Fig. 4.7(*b*), we can count a downwards displacement of the oxygen atoms as negative ξ and an upwards displacement as positive. Although it is not clear from the diagrams whether the motion causes an increase or a decrease in polarizability (actually it is an *increase*) it *is* plain that the change is exactly the same for both positive and negative ξ. Thus we can plot α against ξ as in Fig. 4.8(*b*) with, as before, $\alpha = \alpha_0$ at $\xi = 0$. Now for small displacements we evidently have $d\alpha/d\xi = 0$ and hence for *small displacements* there is effectively no change in the polarizability and the motion is Raman *inactive.*

Exactly the same argument applies to the asymmetric stretch, ν_3, shown at Fig. 4.7(*c*). Here the polarizability decreases equally for positive and negative ξ, so the plot of polarizability against ξ has the appearance of Fig. 4.8(*c*). Again $d\alpha/d\xi = 0$ for small displacements and the motion is Raman *inactive.*

We could have followed the same reasoning for the three vibrations of water discussed previously. In each case we would have discovered that the α versus ξ curve has the general shape of Fig. 4.8(*a*) or its mirror image; in other words, in each case $d\alpha/d\xi \neq 0$ and the motion is Raman *active.* In general, however, the slopes of the three curves would be different at $\xi = 0$, that is, $d\alpha/d\xi$ would have different values. Since we have seen that the Raman spectrum is forbidden for $d\alpha/d\xi = 0$ but allowed for $d\alpha/d\xi \neq 0$ we can imagine that the 'degree of allowedness' varies with $d\alpha/d\xi$. Thus if the polarizability curve has a large slope at $\xi = 0$ the Raman line will be strong; if the slope is small it will be weak; and if zero, not allowed at all. From this stems the following very useful general rule:

> symmetric vibrations give rise to intense Raman lines; non-symmetric ones are usually weak and sometimes unobservable.

In particular, a bending motion usually yields only a very weak Raman line; for example the ν_2 motion of H_2O (Fig. 3.6(*b*)), although allowed in the Raman, has not been observed, nor has ν_3, for which $d\alpha/d\xi$ is also small.

4.3.2 Rule of Mutual Exclusion

A further extremely important general rule has been established whose operation may be exemplified by carbon dioxide. We can summarize our conclusions about the Raman and infra-red activities of the fundamental vibrations of this molecule in Table 4.1, and we see that, for this molecule, no vibration is simultaneously active in both Raman and infra-red. The corresponding general rule is:

Table 4.1 Raman and infra-red activities of carbon dioxide

Mode of vibration of CO_2	Raman	Infra-red
ν_1: symmetric stretch	Active	Inactive
ν_2: bend	Inactive	Active
ν_3: asymmetric stretch	Inactive	Active

> *Rule of mutual exclusion.* If a molecule has a *centre of symmetry* then Raman active vibrations are infra-red inactive, and vice versa. If there is no centre of symmetry then some (but not necessarily all) vibrations may be both Raman and infra-red active.

The converse of this rule is also true, i.e., the observance of Raman and infra-red spectra showing no common lines implies that the molecule has a centre of symmetry; but here caution is necessary since, as we have already seen, a vibration may be Raman active but too weak to be observed. However, if some vibrations are observed to give coincident Raman and infra-red absorptions it is certain that the molecule has no centre of symmetry. Thus extremely valuable structural information is obtainable by comparison of the Raman and infra-red spectra of a substance; we shall show examples of this in Sec. 4.5.

4.3.3 Overtone and Combination Vibrations

Without detailed consideration of the symmetry of a molecule and of its various modes of vibration, it is no easy matter to predict the activity, either in Raman or infra-red, of its overtone and combination modes. The nature of the problem can be seen by considering ν_1 and ν_2 of carbon dioxide; the former is Raman active only, the latter infra-red active. What, then, of the activity of $\nu_1 + \nu_2$? In fact it is only infra-red active, but this is not at all obvious merely from considering the dipole or polarizability changes during the motions. Again, when discussing Fermi resonance (Sec. 3.5.2) we chose as an example the resonance of ν_1 and $2\nu_2$ of carbon dioxide in the *Raman* effect. Thus $2\nu_2$ is Raman active although the fundamental ν_2 is only infra-red active.

We shall not attempt here to discuss this matter further, being content to leave the reader with a warning that the activity or inactivity of a fundamental in a particular type of spectroscopy does not necessarily imply corresponding behaviour of its overtones or combinations, particularly if the molecule has considerable symmetry. A more detailed discussion is to be found in Herzberg's book *Infra-red and Raman Spectra* and others mentioned in the bibliography.

4.3.4 Vibrational Raman Spectra

The structure of vibrational Raman spectra is easily discussed. For every vibrational mode we can write an expression of the form:

$$\varepsilon = \bar{\omega}_e(v + \tfrac{1}{2}) - \bar{\omega}_e x_e(v + \tfrac{1}{2})^2 \text{ cm}^{-1} \qquad (v = 0, 1, 2, \ldots) \tag{4.15}$$

where, as before (cf. Eq. (3.12)), $\bar{\omega}_e$ is the equilibrium vibrational frequency expressed in wavenumbers and x_e is the anharmonicity constant. Such an expression is perfectly general, whatever the shape of the molecule or the nature of the vibration. Quite general, too, is the selection rule:

$$\Delta v = 0, \pm 1, \pm 2, \ldots \tag{4.16}$$

which is the same for Raman as for infra-red spectroscopy, the probability of $\Delta v = \pm 2, \pm 3, \ldots$ decreasing rapidly.

Particularizing, now, to Raman active modes, we can apply the selection rule (4.16) to the energy level expression (4.15) and obtain the transition energies (cf. Eq. (3.15)):

$$\left.\begin{aligned} v = 0 \rightarrow v = 1&: \Delta\varepsilon_{\text{fundamental}} = \bar{\omega}_e(1 - 2x_e) \quad \text{cm}^{-1} \\ v = 0 \rightarrow v = 2&: \Delta\varepsilon_{\text{overtone}} = 2\bar{\omega}_e(1 - 3x_e) \quad \text{cm}^{-1} \\ v = 1 \rightarrow v = 2&: \Delta\varepsilon_{\text{hot}} = \bar{\omega}_e(1 - 4x_e) \quad \text{cm}^{-1} \quad \text{etc.} \end{aligned}\right\} \tag{4.17}$$

Since the Raman scattered light is, in any case, of low intensity we can ignore completely all the weaker effects such as overtones and 'hot' bands, and restrict our discussion merely to the fundamentals. This is not to say that active overtones and hot bands cannot be observed, but they add little to the discussion here.

We would expect Raman lines to appear at distances from the exciting line corresponding to each active fundamental vibration. In other words we can write:

$$\bar{\nu}_{\text{fundamental}} = \bar{\nu}_{\text{ex.}} \pm \Delta\varepsilon_{\text{fundamental}} \quad \text{cm}^{-1} \tag{4.18}$$

where the minus sign represents the Stokes' lines (i.e., for which the molecule has gained energy at the expense of the radiation) and the plus sign refers to the anti-Stokes' lines. The latter are often too weak to be observed, since as we saw earlier (cf. p. 79) very few of the molecules exist in the $v = 1$ state at normal temperatures.

The vibrational Raman spectrum of a molecule is, then, basically simple. It will show a series of reasonably intense lines to the low-frequency side of the exciting line with a much weaker, mirror-image series on the high-frequency side. The separation of each line from the centre of the exciting line gives immediately the Raman active fundamental vibration frequencies of the molecule.

As an example we illustrate the Raman spectrum of chloroform, $CHCl_3$, a symmetric top molecule (Fig. 4.9(*a*)). The exciting line in this case is the

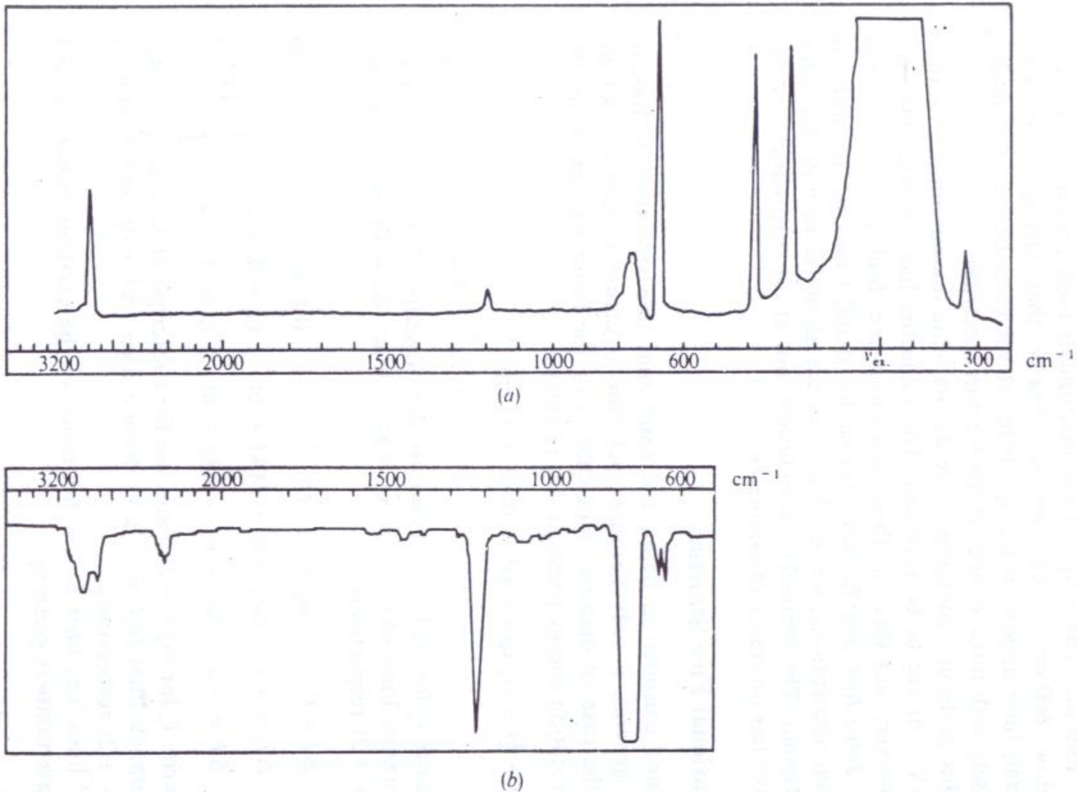

(a)

(b)

Figure 4.9 Comparison between (*a*) the Raman and (*b*) the infra-red spectra of chloroform, $CHCl_3$, demonstrating the coincidence of bands. In both spectra there is a scale change at 2000 cm^{-1}. The weak absorption at about 2400 cm^{-1} in the infra-red is an overtone of the very strong 1200 cm^{-1} band. *(Thanks are due to Dr. Riley of the Brighton Polytechnic for assistance in obtaining the above Raman spectrum.)*

very intense mercury line at 4358·3 Å, and a wavenumber scale is drawn from this line as zero. Raman lines appear at 262, 366, 668, 761, 1216, and 3019 cm^{-1} on the low-frequency (Stokes') side of the exciting line while the line at 262 cm^{-1} on the high-frequency (anti-Stokes') side is included for a comparison of its intensity.

For comparison also we show at Fig. 4.9(*b*) the *infra-red* spectrum of the same molecule. The range of the instrument used precluded measurements below 600 cm^{-1}, but we see clearly that strong (and hence fundamental) lines appear in the spectrum at wavenumbers corresponding very precisely with those of lines in the Raman spectrum.

For this molecule, containing five atoms, nine fundamental vibrations (that is, $3N - 6$) are to be expected. The molecule has considerable symmetry, however, and three of these vibrations are doubly degenerate (see Herzberg: *Infra-Red and Raman Spectra* for details) leaving six different fundamental absorptions; we see that these are all active in both the infra-red and Raman. The immediate conclusion, not at all surprisingly, is that the molecule has no centre of symmetry.

4.3.5 Rotational Fine Structure

We need not consider in detail the rotational fine structure of Raman spectra in general, if only because such fine structure is rarely resolved, except in the case of diatomic molecules. For the latter we can write the vibration–rotation energy levels (cf. Eq. (3.18)) as:

$$\varepsilon_{J,v} = \bar{\omega}_e(v + \tfrac{1}{2}) - \bar{\omega}_e x_e(v + \tfrac{1}{2})^2 + BJ(J + 1)\ \text{cm}^{-1}$$

$$(v = 0, 1, 2, \ldots,\ J = 0, 1, 2, \ldots) \qquad (4.19)$$

where we write $\bar{\nu}_o$ for $\bar{\omega}_e(1 - 2x_e)$ and use the subscripts O, Q, and S to refer to the O branch lines ($\Delta J = -2$), Q branch lines ($\Delta J = 0$), and S branch lines ($\Delta J = +2$), respectively.

$$\Delta J = 0: \quad \Delta\varepsilon_Q = \bar{\nu}_o \quad \text{cm}^{-1} \qquad (\text{for all } J) \qquad (4.20)$$

$$\left.\begin{aligned} \Delta J = +2: \quad \Delta\varepsilon_S &= \bar{\nu}_o + B(4J + 6) \qquad (J = 0, 1, 2, \ldots) \\ \Delta J = -2: \quad \Delta\varepsilon_O &= \bar{\nu}_o - B(4J + 6) \qquad (J = 2, 3, 4, \ldots) \end{aligned}\right\} \quad (4.21)$$

where we write $\bar{\nu}_o$ for $\bar{\omega}_e(1 - 2x_e)$ and use the subscripts O, Q, and S to refer to the O branch lines ($\Delta J = -2$), Q branch lines ($\Delta J = 0$), and S branch lines ($\Delta J = +2$), respectively.

Stokes' lines (i.e., lines to *low* frequency of the exciting radiation) will occur at wavenumbers given by:

$$\bar{\nu}_Q = \bar{\nu}_{\text{ex.}} - \Delta\varepsilon_Q = \bar{\nu}_{\text{ex.}} - \bar{\nu}_o \quad \text{cm}^{-1} \qquad (\text{for all } J)$$

$$\bar{\nu}_O = \bar{\nu}_{\text{ex.}} - \Delta\varepsilon_O = \bar{\nu}_{\text{ex.}} - \bar{\nu}_o + B(4J + 6)\ \text{cm}^{-1} \qquad (J = 2, 3, 4, \ldots)$$

$$\bar{\nu}_S = \bar{\nu}_{\text{ex.}} - \Delta\varepsilon_S = \bar{\nu}_{\text{ex.}} - \bar{\nu}_o - B(4J + 6)\ \text{cm}^{-1} \qquad (J = 0, 1, 2, \ldots).$$

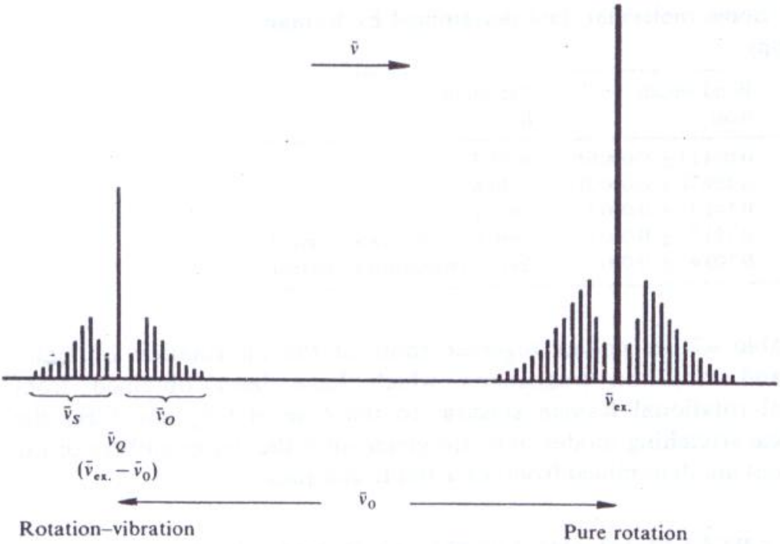

Figure 4.10 The pure rotation and the rotation–vibration spectrum of a diatomic molecule having a fundamental vibration frequency of $\tilde{\nu}_0$ cm^{-1}. Stokes' lines only are shown.

The spectrum arising is sketched in Fig. 4.10 where, for completeness, the pure rotation lines in the immediate vicinity of the exciting line are also shown. The presence of the strong *Q* branch in the Raman spectrum is to be noted and compared with the *P* and *R* branches only which occur for a diatomic molecule in the infra-red (cf. the spectrum of carbon monoxide in Fig. 3.7). The analysis of the *O* and *S* branches in the Raman spectrum to give a value for *B* and hence for the moment of inertia and bond length is straightforward.

Much weaker anti-Stokes' lines will occur at the same distance from, but to high frequency of, the exciting line.

The resolution of Raman spectra is not sufficient to warrant the inclusion of finer details such as centrifugal distortion or the breakdown of the Born–Oppenheimer approximation which were discussed in Chapter 3 for the corresponding infra-red spectra.

For larger molecules we can, in fact, ignore the rotational fine structure altogether since it is not resolved. Even the *O* and *S* (or *O*, *P*, *R*, and *S*) band contours are seldom observed since they are very weak compared with the *Q* branch. Thus, while the infra-red spectrum of chloroform, shown in Fig. 4.9(*b*) shows distinct *PR* or *PQR* structure on some bands, the Raman spectrum, with the possible exception of the band at 760 cm^{-1}, shows only the strong *Q* branches. While some information is denied us in Raman spectra because of this, it does represent a considerable simplification of the overall appearance of such spectra.

Table 4.2 Some molecular data determined by Raman spectroscopy

Molecule	Bond length (nm)	Vibration (cm^{-1})
H_2	0·074 13 ± 0·000 01	4395·2
N_2	0·109 76 ± 0·000 01	2359·6
F_2	0·141 8 ± 0·000 1	802·1
CS_2	0·155 3 ± 0·000 5	656·6 (symmetrical stretch)
CH_4	0·109 4 ± 0·000 1	2914·2 (symmetrical stretch)

In Table 4.2 we collect together some of the information on bond lengths and vibration frequencies which have been obtained from vibrational–rotational Raman spectra. In the case of CS_2 and CH_4 the symmetrical stretching modes only are given since the wavenumbers of the other modes are determined from infra-red techniques.

4.4 POLARIZATION OF LIGHT AND THE RAMAN EFFECT

4.4.1 The Nature of Polarized Light

It is well known that when a beam of light is passed through a Nicol prism or a piece of crystal filter (e.g., polaroid) the only light passing has its electric (or magnetic) vector confined to a particular plane; it is *plane polarized light.* Although superficially this light is indistinguishable from ordinary (or unpolarized) light, it has a very important property which can be demonstrated by using a second Nicol prism or crystal filter. When previously polarized light falls on the second polarizing device (now called the 'analyser') it will be passed with undiminished intensity only if the polarizing axes of the two prisms or crystal sheets are parallel to each other. At any other orientation of these axes the intensity passed will decrease until, when the axes are perpendicular, no light at all passes through the analyser. Thus the analyser serves both to detect polarized light and to determine its plane of polarization.

If the light incident upon the analyser is only partially polarized—i.e., if the majority, but not all, of the rays have their electric vectors parallel to a given plane—then the light will not be *completely* extinguished at any orientation of the analyser; its intensity will merely go through a minimum when the analyser is perpendicular to the plane of maximum polarization. We could, then, measure the degree of polarization in terms of the intensity of light transmitted parallel and perpendicular to this plane; it is more convenient, however, to measure the *degree of depolarization*, ρ, as:

$$\rho = I_{\perp}/I_{\parallel} \tag{4.22}$$

where $I_{\parallel}$ is the maximum and $I_{\perp}$ the minimum intensity passed by the analyser. Thus for completely plane-polarized light $I_{\perp} = 0$ and hence the degree of depolarization is zero also; for completely unpolarized (i.e., ordinary) light, $I_{\perp} = I_{\parallel}$ and $\rho = 1$. For intermediate degrees of polarization ρ lies between 0 and 1.

The relevance of this to Raman spectroscopy is that lines in some Raman spectra are found to be plane-polarized to different extents even though the exciting radiation is completely depolarized. The reason for this is most easily seen if we consider the vibrations of spherical top molecules.

4.4.2 Vibrations of Spherical Top Molecules

The tetrahedral molecule methane, CH_4, is a good example of a spherical top and we can see, from Fig. 4.11, that its polarizability ellipsoid is spherical. During the vibration known as the symmetric stretch all four C—H distances increase and diminish in phase so that the polarizability ellipsoid contracts and expands but *remains spherical.* For this reason the motion is often referred to as the 'breathing frequency'; it is plainly Raman active.

Let us now consider a beam of unpolarized radiation falling on this molecule, and let us designate the direction of this exciting radiation as the z axis. Since all diameters of a sphere are equal the molecule is equally polarizable in all directions; hence the induced dipole in the molecule will lie along the direction of greatest electric vector in the exciting radiation, i.e., perpendicular to the direction of propagation. Thus the induced dipole will lie in the xy plane whatever the plane of the incident radiation. This behaviour is illustrated in Fig. 4.12, where we show an incident beam with its electric vector in (*a*) the vertical (zy) plane and (*b*) some other plane making an angle α with the horizontal. In both cases the induced dipole is

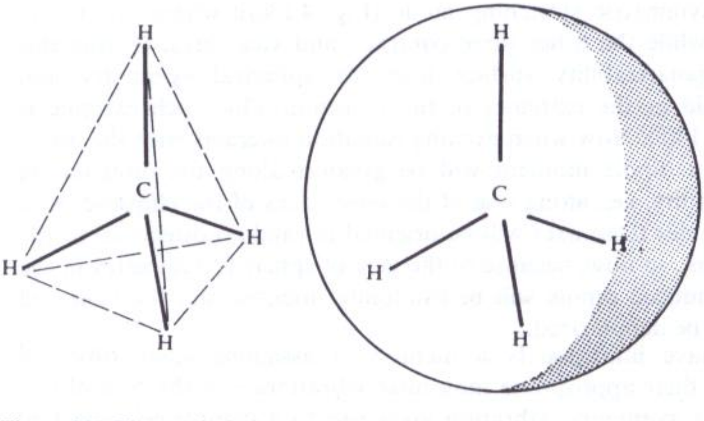

Figure 4.11 The tetrahedral structure of methane, CH_4, and the spherical polarizability ellipsoid of the molecule.

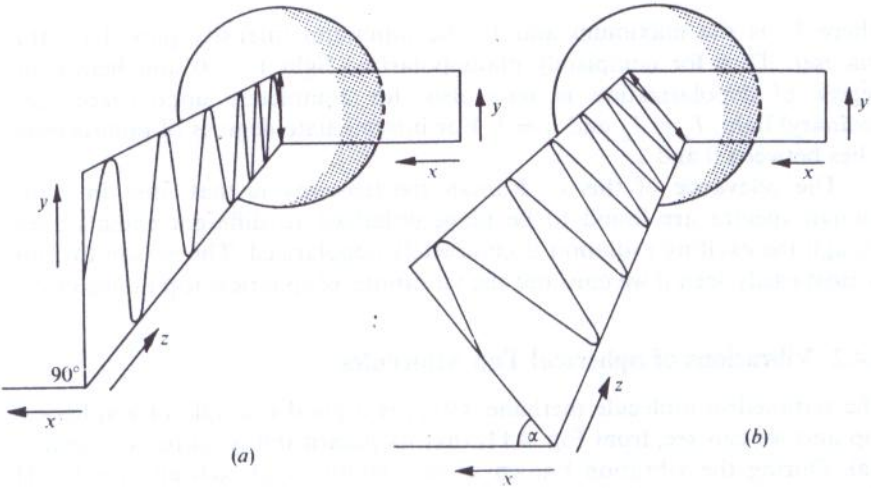

Figure 4.12 To illustrate the plane polarization of Raman scattering from the symmetric vibration ('breathing vibration') of a spherical top molecule.

in the xy plane. A non-polarized incident beam will contain components having all values α.

To an observer studying the scattered radiation at right angles to the incident beam, i.e., along the x axis, the oscillating dipole emitting the radiation is confined to the xy plane—the radiation is plane-polarized. When the molecule undergoes the breathing vibration, the polarizability ellipsoid remains spherical and the dipole change remains in the xy plane. Thus for this vibration the Raman line will be completely plane-polarized, and $\rho = 0$, quite irrespective of the nature of the exciting radiation.

We will now consider a less symmetric vibration of this molecule, for example, the asymmetric stretching mode (Fig. 4.13(*a*)) where one C—H bond stretches while the other three contract, and vice versa. During this vibration the polarizability surface loses its spherical symmetry and becomes ellipsoid at the extremes of the vibration. One such extreme is shown in Fig. 4.13(*b*). Now when exciting radiation interacts with the molecule the induced dipole moment will be greatest along the direction of easiest polarizability, i.e., along one of the *minor* axes of the ellipsoid. In a sample of molecules these axes will be oriented in random directions to the incident radiation, so now, because of the lack of spherical symmetry in the vibration, the induced dipole will be randomly oriented and the observed Raman line will be depolarized.

Thus we have immediately a method of assigning some observed Raman lines to their appropriate molecular vibrations—in the case of methane the totally symmetric vibration gives rise to a completely polarized Raman line whereas the non-symmetric vibrations give depolarized lines.

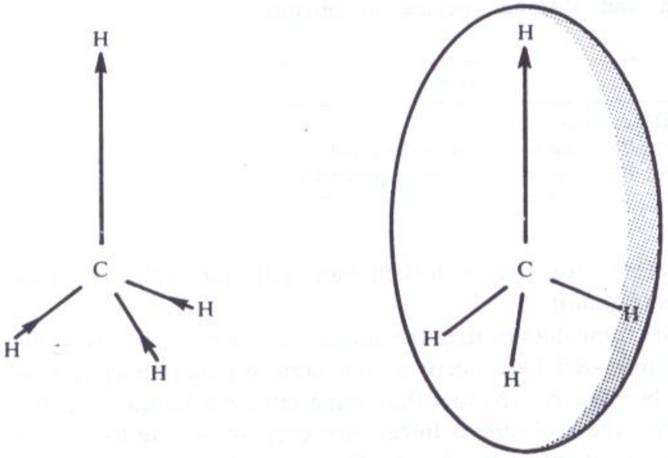

(a) (b)

Figure 4.13 An asymmetrical stretching vibration of a spherical top molecule together with the polarizability ellipsoid resulting at the extreme of the motion.

The degree of polarization of spectral lines can be readily estimated by noting how the intensity of each line varies when a piece of polaroid or other analyser is put into the scattered radiation first with its polarizing axis parallel to the xy plane (where z is defined by the direction of the incident beam) and secondly perpendicular to this plane.

4.4.3 Extension to Other Types of Molecule

Precise calculation, rather than the somewhat pictorial argument used above, shows that Raman scattering may be to some extent polarized when emitted by molecules with less symmetry than the tetrahedral ones. In general it can be stated that a symmetric vibration gives rise to a polarized or partially polarized Raman line while a non-symmetric vibration gives a depolarized line. Theoretically, if the degree of depolarization, ρ, is less than or equal to $\frac{6}{7}$, then the vibration concerned is symmetric and the Raman line is described as 'polarized', while if $\rho > \frac{6}{7}$ the line is 'depolarized' and the vibration non-symmetric. If we can speak loosely of molecules with increasing symmetry—e.g., linear molecules are less symmetric than symmetric tops which, in turn, are less symmetric than spherical tops—then the higher the molecular symmetry the smaller will be the degree of depolarization of the Raman line for a particular type of vibration.

We can see the usefulness of polarization measurements by considering a simple example. The molecule nitrous oxide has the formula N_2O. Knowing nothing about the structure of this molecule we might turn for help to its infra-red and Raman spectra. The strongest lines in these spectra

Table 4.3 Infra-red and Raman spectra of nitrous oxide

$\bar{\nu}$ (cm^{-1})	Infra-red	Raman
589	Strong; *PQR* contour	—
1285	Very strong; *PR* contour	Very strong; polarized
2224	Very strong; *PR* contour	Strong; depolarized

are collected in Table 4.3 together with their band contours (infra-red) and state of polarization (Raman).

The data tells us immediately that the molecule has no centre of symmetry (Raman and infra-red lines occur at the same wavenumber) and so the structure is *not* N—O—N. The fact that some infra-red bands have *PR* contour indicates that the molecule is linear, however, so we are led to the conclusion that the structure is N—N—O. Such a molecule should have $3N - 5 = 4$ fundamental modes but two of these (the bending modes) will be degenerate; all three different fundamental frequencies should be both infra-red and Raman active but we note that the perpendicular infra-red band (plainly to be associated with the bending mode) does not appear in the Raman. This accords with expectations—bending modes are often weak and even unobservable in the Raman.

We are left with the assignment of the 1285 and 2224 cm^{-1} bands to the symmetric and asymmetric stretching modes. Both infra-red bands have the same *PR* (parallel) contour, but we note that only the 1285 cm^{-1} is Raman polarized. This, then, we assign to the symmetric mode, leaving the 2224 cm^{-1} band as the asymmetric.

The analysis would not normally rest there. The overtone and combination bands would also be studied to ensure that their activities and contours are in agreement with the molecular model proposed; the fine structure of the infra-red bands also supports the structure; and finally isotopic substitution leads to changes in vibrational frequencies in excellent agreement with the model and assignments.

In this rather simple case polarization data were hardly essential to the analysis, but certainly useful. In more complicated molecules it can give very valuable information indeed.

4.5 STRUCTURE DETERMINATION FROM RAMAN AND INFRA-RED SPECTROSCOPY

In this section we shall discuss some examples of the combined use of Raman and infra-red spectroscopy to determine the shape of some simple molecules. The discussion must necessarily be limited and the molecules considered (CO_2, N_2O, SO_2; NO_3^-, ClO_3^-, and ClF_3) have been chosen to

Table 4.4 Infra-red and Raman bands of sulphur dioxide

Wavenumber	Infra-red contours	Raman
519	∥ type band	Polarized
1151	∥ type band	Polarized
1361	⊥ type band	Depolarized

illustrate the principles used; extension to other molecular types should be obvious.

Dealing first with the triatomic AB_2 molecules, the questions to be decided are whether each molecule is linear or not and, if linear, whether it is symmetrical ($B—A—B$) or asymmetrical ($B—B—A$). In the case of carbon dioxide and nitrous oxide, both molecules give rise to some infra-red bands with PR contours; they must, therefore, be linear. The mutual exclusion rule (cf. Sec. 4.3.2) shows that CO_2 has a centre of symmetry (O—C—O) while N_2O has not (N—N—O), since only the latter has bands common to both its infra-red and Raman spectra. Thus the structures of these molecules are completely determined.

The infra-red and Raman absorptions of SO_2 are collected in Table 4.4. We see immediately that the molecule has no centre of symmetry, since all three fundamentals are both Raman and infra-red active. In the infra-red all three bands show very complicated rotational fine structure, and it is evident that the molecule is non-linear—no band shows the simple PR structure of, say, carbon dioxide. The molecule has, then, the bent shape.

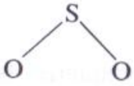

The AB_3 type molecules require rather more discussion. In general we would expect $3N - 6 = 6$ fundamental vibrations for these four-atomic molecules. However, if the molecular shape has some symmetry this number will be reduced by degeneracy. In particular, for the symmetric planar and symmetric pyramidal shapes, one stretching mode and one angle deformation mode are each doubly degenerate and so only four different fundamental frequencies should be observed. These are sketched in Table 4.5 where their various activities and band contours or polarizations are also collected. Both molecular shapes are in fact symmetric tops with the main (threefold) axis passing through atom A perpendicular to the B_3 plane. It is with respect to this axis that the vibrations can be described as ∥ or ⊥. The symmetric modes of vibration are parallel and Raman polarized while the asymmetric are perpendicular and depolarized. All the vibrations of the pyramidal molecule change both the dipole moment and the polarizability, hence all are both infra-red and Raman active. The symmetric stretching mode (ν_1) of the planar molecule, however, leaves the dipole moment unchanged (it remains zero throughout) and so is infra-red inactive, while the

Table 4.5 Activities of vibrations of planar and pyramidal AB_3 molecules

Symmetric planar	Activity (R = Raman, I = infra-red)	Vibration	Pyramidal	Activity (R = Raman, I = infra-red)
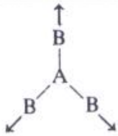	R: active (pol.) strong I: inactive	ν_1 symmetric stretch	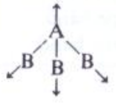	R: active (pol.) strong I: active ∥
 (⊕ = upwards ⊖ = downwards)	R: inactive I: active ∥	ν_2 out-of-plane symmetric deformation	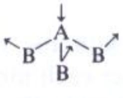	R: active (pol.) strong I: active ∥
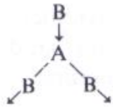	R: active (depol.) weak I: active ⊥	ν_3 asymmetric stretch	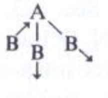	R: active (depol.) weak I: active ⊥
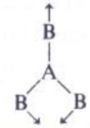	R: active (depol.) weak I: active ⊥	ν_4 asymmetric deformation	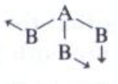	R: active (depol.) weak I: active ⊥

symmetric bending mode does not change the polarizability (cf. the discussion of the bending mode of CO_2 in Sec. 4.3.1) and so ν_2 is Raman inactive for planar AB_3.

The overall pattern of the spectra, then, should be as follows:

Planar AB_3: 1 vibration Raman active only (ν_1)
1 infra-red active only (ν_2)
2 vibrations both Raman and infra-red active (ν_3, ν_4).
Pyramidal AB_3: All four vibrations both Raman and infra-red active.
Non-symmetric AB_3: Possibly more than four different fundamental frequencies.

With this pattern in mind we can consider the spectra of NO_3^- and ClO_3^- ions. The spectroscopic data are summarized in Table 4.6. Without considering any assignment of the various absorption bands to particular vibrations, we can see immediately that the nitrate ion fits the expected pattern for a planar system, while the chlorate ion is pyramidal. Detailed assignments follow by comparison with Table 4.5. Thus for the nitrate ion,

Table 4.6 Infra-red and Raman spectra of NO_3^- and ClO_3^-

Nitrate ion (NO_3)			Chlorate ion (ClO_3^-)		
Raman (cm^{-1})	Infra-red (cm^{-1})	Assignment	Raman (cm^{-1})	Infra-red (cm^{-1})	Assignment
690	680 ⊥	ν_4	450 (depol.)	434 ⊥	ν_4
—	830 ∥	ν_2	610 (pol.)	624 ∥	ν_2
1049	—	ν_1	940 (depol.)	950 ⊥	ν_3
1355	1350 ⊥	ν_3	982 (pol.)	994 ∥	ν_1

the band which is Raman active only is obviously ν_1 while that which appears only in the infra-red is ν_2. If we make the very reasonable assumption that stretching frequencies are larger than bending, then the assignment of ν_3 and ν_4 is self-evident. This same assumption, coupled with polarization and band contour data, gives the assignment shown in the table for the chlorate ion.

Finally we consider the spectroscopic data for ClF_3. This is found to have no less than *six* strong (and hence fundamental) infra-red absorptions, some of which also occur in the Raman. We know immediately, then, that the molecule is neither symmetric planar nor pyramidal. A complete analysis is not possible from the Raman and infra-red spectra alone, but the use of microwave spectroscopy shows that the molecule is T-shaped with bond angles of nearly 90°.

4.6 TECHNIQUES AND INSTRUMENTATION

Raman spectroscopy is essentially emission spectroscopy, and the bulk of the instrumentation is simply a typical visible-region spectrometer; the distinguishing characteristic of Raman work, of course, is the exciting source. The advent of accessible and relatively inexpensive laser sources during the past few years has caused a minor revolution in Raman techniques, by largely displacing the traditional mercury discharge lamp as an exciting source. Formerly the process of obtaining a good Raman spectrum of anything but the most straightforward samples involved as much art as science, required 10–20 ml of sample, and was often a very time-consuming operation; now Raman spectra of virtually all samples can be run on a completely routine basis using one millilitre or less of sample and taking a few minutes only.

In fact the laser is almost ideal as a Raman source; it gives a very narrow, highly monochromatic beam of radiation, which may be focused very finely into a small sample, and which packs a relatively large power—

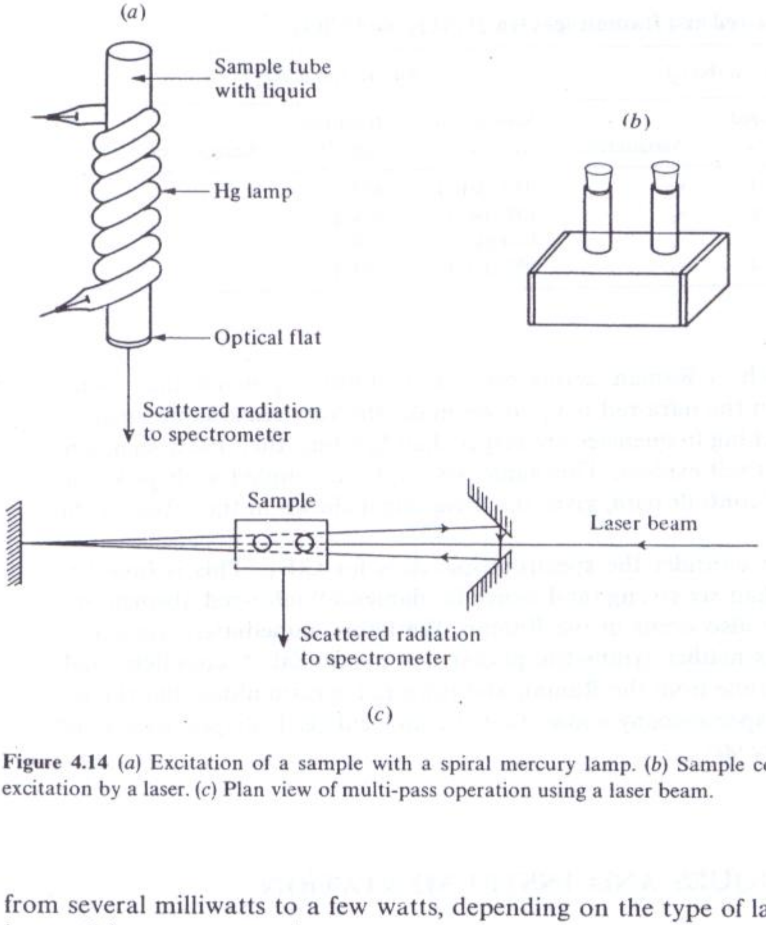

Figure 4.14 (*a*) Excitation of a sample with a spiral mercury lamp. (*b*) Sample container for excitation by a laser. (*c*) Plan view of multi-pass operation using a laser beam.

from several milliwatts to a few watts, depending on the type of laser—into its small frequency spread.

Figure 4.14 compares the two excitation techniques. In part (*a*) the mercury discharge lamp is shown in the form of a spiral round the sample; this form of excitation pumps a good deal of energy into the sample, but it is spread over the many emission lines of the mercury vapour—notably 435·8 and 253·6 nm—and it suffers from three main disadvantages. Firstly, the extended source allows a good deal of the exciting radiation to be scattered directly into the spectrometer where it masks all the Raman lines less than some 100 cm^{-1} from the exciting frequency; secondly the sample tube needs to be about 20–30 cm long and 1–2 cm in diameter, so that a considerable quantity of sample is required; thirdly, the relatively high frequency of the mercury radiation often causes the sample to fluoresce (cf. Sec. 6.3.3), and the resulting fluorescence spectrum swamps the very weak Raman spectrum. Nonetheless the mercury lamp is often still preferred for gaseous samples, where a large sample tube can have a very carefully tailored mercury lamp built round it, and thus collect the exciting radiation with maximum efficiency.

Figure 4.14(*c*) illustrates how the laser beam is directed through a sample and, by means of mirrors, caused to undergo multiple passes; only three such passes are shown but, by careful alignment of the mirrors up to 10 passes may be achieved, thus enhancing the Raman signal. The standard sample container is a 'box' of quartz, as shown in Fig. 4.14(*b*), about 2 cm long and 0·5 cm^2 in cross-section, provided with filling ports; its capacity is thus 1 ml. The quantity of sample required can be reduced considerably, however, by using a thin capillary tube, filled with sample and sealed at one end, with the laser beam directed along its length; in this case the multiple traverse facility cannot be used, but nonetheless a few microlitres of liquid give a spectrum of about 60 per cent of the intensity of that from a 1 ml sample with multiple traverse. Solids, in powder or transparent block form, are equally suitable for laser excitation. Further, lasers typically operate at frequencies lower than that of the mercury lamp (e.g., the He–Ne laser at 632·8 nm and the argon laser at 514·5 and 488·0 nm), and are thus very much less likely to cause the sample to fluoresce; also if one particular laser does produce fluorescence, it is a simple matter technically (although perhaps not financially) to switch to another laser and run a successful Raman spectrum. Finally, the Rayleigh scattering is much diminished with the very confined laser beam, and it is routine to detect Raman scattering to within some 20 cm^{-1} of the exciting line.

Radiation scattered from the sample is directed, via mirrors, into a spectrometer operating in the visible region; the monochromator is either a quartz prism or a grating, and the radiation is detected, in the case of a laser instrument, by a photoelectric detector with its output fed to an amplifier and pen recorder. Instruments using a mercury discharge lamp as exciting source may also use a photomultiplier and pen recorder, but they have, in addition, provision for the insertion of a photographic plate as detector, since the very weakest of Raman lines may be observed by allowing the exposure to continue for many hours, or even several days.

BIBLIOGRAPHY

Anderson, A.: *The Raman Effect*: vol. 1 *Principles*, Marcel Dekker Inc., 1971.
Anderson, A.: *The Raman Effect*: vol. 2 *Applications*, Marcel Dekker Inc., 1973.
Barnes, A. J., and W. J. Orville-Thomas (eds): *Vibrational Spectroscopy—Modern Trends*, Elsevier, 1977.
Gilson, T. R., and P. J. Hendra: *Laser Raman Spectroscopy*, Wiley, 1970.
Herzberg, G.: *Molecular Structure and Molecular Spectra*: vol. 1, *Spectra of Diatomic Molecules*, 2nd ed., Van Nostrand, 1950.
Herzberg, G.: *Molecular Spectra and Molecular Structure*: vol. 2, *Infra-Red and Raman Spectra of Polyatomic Molecules*, Van Nostrand, 1945.
Loader, J.: *Basic Laser Raman Spectroscopy*, Heyden & Son Ltd., 1970.

Ross, S. D.: *Inorganic Infra-Red and Raman Spectra*, McGraw-Hill, 1972.
Siesler, H. W., and K. Holland-Moritz: *Infra-Red and Raman Spectroscopy of Polymers*, Marcel Dekker Inc., 1980.
Tobin, M. C.: *Laser Raman Spectroscopy*, Wiley-Interscience, 1971.
Williams, D. H., and I. Fleming: *Spectroscopic Methods in Organic Chemistry*, 3rd ed., McGraw-Hill, 1980.

PROBLEMS

(Useful constants: $h = 6{\cdot}626 \times 10^{-34}$ J s; $c = 2{\cdot}998 \times 10^{8}$ m s^{-1}; $8\pi^2 = 78{\cdot}957$; mass of H atom $= 1{\cdot}673 \times 10^{-27}$ kg.)

4.1 With which type of spectroscopy would one observe the pure rotation spectrum of H_2? If the bond length of H_2 is 0·074 17 nm, what would be the spacing of the lines in the spectrum?

4.2 The spin of the hydrogen nucleus is $\frac{1}{2}$; does this make any difference to your answer to Prob. 4.1?

4.3 A molecule A_2B_2 has infra-red absorptions and Raman spectral lines as in the following table:

cm^{-1}	Infra-red	Raman
3374	—	Strong
3287	Very strong; *PR* contour	—
1973	—	Very strong
729	Very strong; *PQR* contour	—
612	—	Weak

Deduce what you can about the structure of the molecule and assign the observed vibrations to particular molecular modes as far as possible.

Hint: Use data from Table 3.4 to help with your answer.

4.4 A molecule AB_2 has the following infra-red and Raman spectra:

cm^{-1}	Infra-red	Raman
3756	Very strong: perpendicular	—
3652	Strong; parallel	Strong; polarized
1595	Very strong; parallel	—

The rotational fine structure of the infra-red bands is complex and does not show simple *PR* or *PQR* characteristics. Comment on the molecular structure, and assign the observed lines to specific molecular vibrations as far as possible.

4.5 Both N_2O and NO_2 exhibit three different fundamental vibrational frequencies, and for the two molecules some modes are observed in both the infra-red and the Raman. The bands in N_2O show only simple *PR* structure (no *Q* branches) while those in NO_2 show complex rotational structure. What can be deduced about the structure of each molecule?

CHAPTER

FIVE

ELECTRONIC SPECTROSCOPY OF ATOMS

5.1 THE STRUCTURE OF ATOMS

5.1.1 Electronic Wave Functions

It is well known that an atom consists of a central, positively charged nucleus, which contributes nearly all the mass to the system, surrounded by negatively charged electrons in sufficient number to balance the nuclear charge. Hydrogen, the smallest and simplest atom, has a nuclear charge of $+1$ units (where the unit is the electronic charge, $1{\cdot}60 \times 10^{-19}$ coulomb) and one electron; each succeeding atom increases the nuclear charge and electron total by unity, up to atoms with 100 or more electrons.

Modern theories have long ceased to regard the electron as a particle which obeys the laws of classical mechanics applicable to massive, everyday objects; instead, in common with all entities of subatomic size, we consider that it obeys the laws of quantum mechanics (or wave mechanics) as embodied in the Schrödinger wave equation. In principle, this equation may be used to determine many things: e.g., the way in which electrons group themselves about a nucleus when forming an atom, the energy which each electron may have, the way in which it can undergo transitions between energy states, etc. In practice the application of the Schrödinger equation to these problems presents difficulties which can only be overcome in the case of the simplest atoms or by the use of gross approximations. Here, however, we shall be concerned only with the results obtained—and then only in qualitative terms—rather than the mathematical theory of the process.

The Schrödinger theory can be used to predict the *probability* of an electron with a particular energy being at a particular point in space, and it expresses this probability in terms of a very important algebraic expression called the *wave function* of the electron. The wave function is given the Greek symbol ψ. Quite simply, the probability of finding an electron, whose wave function is ψ, within unit volume at a given point in space, is proportional to the value of ψ^2 at that point:

$$\text{Relative probability density} = \psi^2 \tag{5.1}$$

Let us see what this means. Electronic wave functions consist of three elements: (1) some fundamental *physical constants* (π, h, c, m, e, etc.—where m and e are the mass and charge, respectively, of the electron); (2) *parameters* peculiar to the system under discussion—e.g., for atoms, distance from the nucleus, either radially (r) or along some coordinate axes (x, y, z); and (3) one or more *quantum numbers.* These latter are by no means arbitrarily introduced into the problem in order to make the predictions match experiment; they *belong* to the solution of the Schrödinger equation in the sense that ψ represents a sensible physical situation *only if* the quantum numbers have certain values.

As an example we may quote here the expression for a set of wave functions, ψ_n, which are solutions to the Schrödinger equation for the hydrogen atom:

$$\psi_n = f\left(\frac{r}{a_0}\right) \exp\left(-\frac{r}{na_0}\right) \tag{5.2}$$

where $a_0 = h^2/4\pi^2me^2$, r is radial distance from the nucleus, $f(r/a_0)$ is a power series of degree $(n-1)$ in r/a_0, and n is the *principal quantum number*, which can have only integral values, 1, 2, 3, ..., ∞. The constant a_0 has dimensions of length (and is, in fact, about 53 nm) and so the quantity r/a_0 is a pure number. Thus for particular values of r and n, ψ_n and ψ_n^2 are also simply numbers, and ψ_n^2 represents the probability of finding the electron at our chosen distance r from the nucleus when it is in the state represented by the given n value.

It is found that the electronic wave functions of all atoms require the introduction of only four quantum numbers. We shall describe these briefly here, leaving a more thorough discussion to later sections.

5.1.2 The Shape of Atomic Orbitals; Atomic Quantum Numbers

Table 5.1 lists the four quantum numbers, gives the allowed values of each, and states what is the function of each. The *principal quantum number*, as stated earlier, can take integral values from one to infinity. It governs the

Table 5.1 The atomic quantum numbers

Quantum No.	Allowed values	Function
Principal, n	1, 2, 3, ...	Governs the energy and size of the orbital
Orbital, l	$(n-1), (n-2), \ldots, 0$	Governs the shape of the orbital and the electronic angular momentum
Magnetic, m	$\pm l, \pm(l-1), \ldots, 0$	Governs the direction of an orbital and the electrons' behaviour in a magnetic field
Spin, s	$+\frac{1}{2}$	Governs the axial angular momentum of the electron

energy of the electron mainly (although we shall see later that the other quantum numbers also affect this energy to some extent). The table shows that n also governs the size of the electronic *orbital*; this latter is a term used to represent the space within which an electron can move according to the Schrödinger theory—it corresponds approximately to the earlier idea of Bohr that electrons move in circular or elliptical *orbits* like planets round a sun. Energy and size of the orbital are connected in that the smaller the orbital the closer to the nucleus the electron will be and hence the more firmly bound..

The *orbital* (or *azimuthal*) *quantum number* l, also has integral values only, but these must be less than n. Thus for $n = 3$, l can be 2, 1, or 0. It governs the shape of the orbital (cf. Fig. 5.1) and the angular momentum of the electron as it circulates about the nucleus in its orbital.

The *magnetic quantum number* m takes integral values which depend on l. Thus for $l = 2$, m can be $+2$, $+1$, 0, -1, -1, or -2; in general there are $2l + 1$ values of m. Besides denoting the behaviour of electrons in orbitals when the atom is placed in a magnetic field, the m quantum number can also be used to specify the direction of a particular orbital.

The *spin quantum number* s is of magnitude $+\frac{1}{2}$ only (but cf. Sec. 5.2.2). It measures the spin angular momentum which the electron possesses whether it is present in an atom or in free space.

Since wave functions represent only a probability distribution of an electron it is difficult to define precisely the shape and size of an orbital. From Eq. (5.2) we see that even at very large values of r, ψ_n (and hence ψ_n^2) still has a value, even though small. Thus an orbital tails off to infinity (although, because of the smallness of a_0, 'infinity' on the atomic scale might be taken as 10^{-4} or 10^{-5} cm) in all directions. However, the difficulty can be overcome if we agree to draw a three-dimensional shape *within* which the electron spends, say, 95 per cent or some other fraction of its time. This can be taken as the effective boundary of the electron's domain and it can be called *the orbital*.

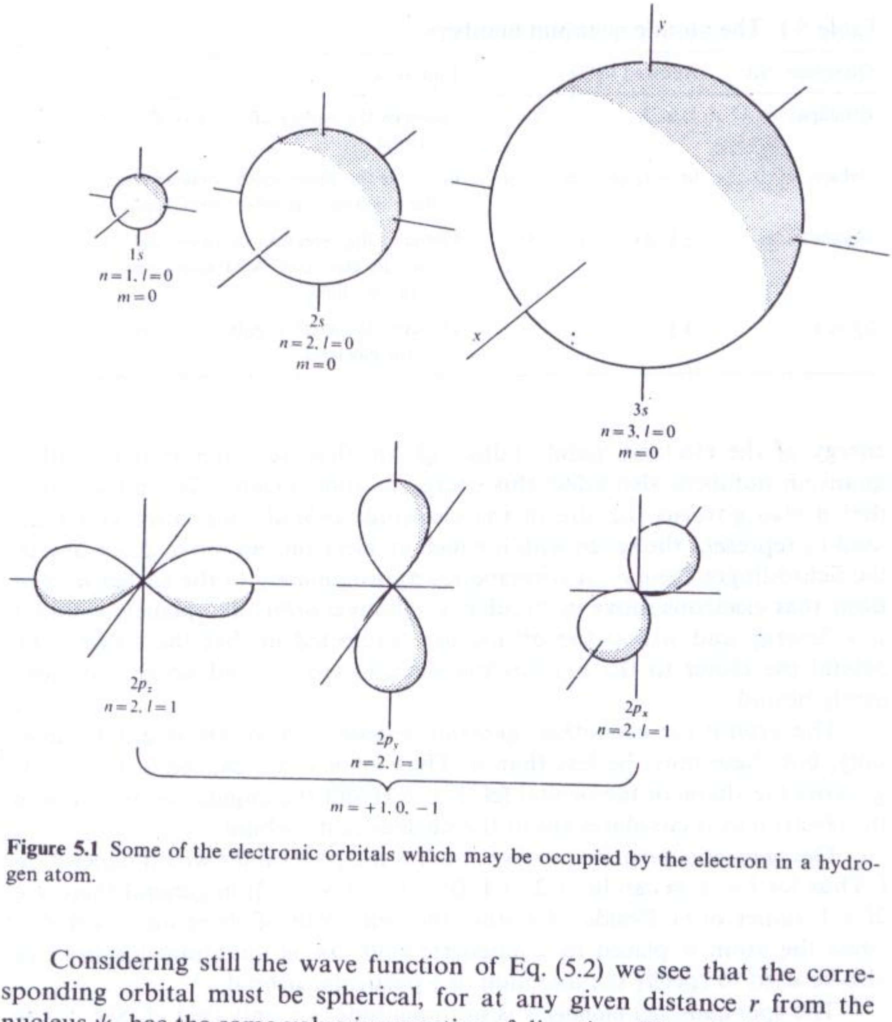

Figure 5.1 Some of the electronic orbitals which may be occupied by the electron in a hydrogen atom.

Considering still the wave function of Eq. (5.2) we see that the corresponding orbital must be spherical, for at any given distance r from the nucleus ψ_n has the same value irrespective of direction. Thus the 95 per cent boundary will be spherical. For larger n the function tails off less rapidly with distance and so the electron can spend proportionately more of its time further from the nucleus; thus the 95 per cent sphere will increase in size with n. We have drawn the cases $n = 1$, 2, and 3 at the top of Fig. 5.1. These spherical orbitals, it so happens, are associated with an l value of zero (and hence $m = 0$) and they are referred to as *s orbitals*. (Although it is perhaps helpful to connect *s* with 'spherical'—in fact the label arose historically because of the alleged particular *sharpness* of spectral lines arising from transition of electrons occupying *s* orbitals—the connection which should be remembered is between *s* orbitals and $l = 0$.) The *s* orbitals are labelled according to their n quantum numbers: 1*s*, 2*s*, …, *ns*.

Orbitals with $l = 1$ (and hence $n \geq 2$) also arise as solutions to the Schrödinger equation for the hydrogen atom. These are twin-lobed and have the approximate shape shown for $n = 2$ in the lower half of Fig. 5.1. Orbitals with $n = 3$, $l = 1$ are larger but have the same shape. Such orbitals are labelled p (historically their transitions were thought to be 'principal') and we see that, for a given n, there are *three* of them, one along each coordinate axis. They can be distinguished as np_x, np_y, and np_z, if necessary. The fact that there are three of them is connected with the three values of m, $m = +1$, 0, and -1, allowed for $l = 1$ states. It is conventional to associate the value $m = 0$ with the np_z orbitals but, for good physical reasons which lie outside the scope of this book, it is not then possible to associate the other m values with either np_x or np_y. Other representations of these orbitals can be drawn, however, in such a way that there is a one-to-one correspondence between each m value and an orbital; these representations are less convenient for the descriptive purposes of this book and we shall not discuss them here.

We can go further: for $l = 2$ (hence $n \geq 3$) we have a set of *d orbitals* (historically 'diffuse'), and $l = 3 (n \geq 4)$ *f orbitals* (historically 'fundamental'): there are five of the former ($m = \pm 2$, ± 1 or 0) and seven of the latter ($m = \pm 3$, ± 2, ± 1 or 0). Sketches of d orbitals show that they have four lobes, while the f have six, but we shall not attempt to reproduce these here. Orbitals with higher l values, $l = 4, 5, 6, \ldots$, are of less importance and we shall not consider them further; if necessary they are labelled alphabetically after f, that is, $l = 4$, g; $l = 5$, h, etc.

5.1.3 The Energies of Atomic Orbitals; Hydrogen Atom Spectrum

However large an atom its electrons take up orbitals of the $s, p, d, \ldots$ type (according to very specific laws which we shall discuss later) and so the overall shape of each electron's domain is unaltered. The *energy* of each orbital, on the other hand, varies considerably from atom to atom. There are two main contributions to this energy: (1) attraction between electrons and nucleus, (2) repulsion between electrons in the same atom.

We consider first the case of hydrogen in some detail: this is the simplest because, having only one electron, factor (2) is completely absent. We shall later see how the picture should be modified for larger atoms.

Because of the absence of interelectronic effects all orbitals with the same n value have the same energy in hydrogen. Thus the $2s$ and $2p$ orbitals, for instance, are degenerate, as are the $3s$, $3p$, and $3d$. However the energies of the $2s$, $3s$, $4s$, ... orbitals differ considerably. For the s orbitals given by Eq. (5.2):

$$\psi_{ns} = f\left(\frac{r}{a_0}\right) \exp\left(-\frac{r}{na_0}\right)$$

the Schrödinger equation shows that the energy is:

$$E_n = -\frac{me^4}{8h^2\varepsilon_o^2 n^2} \text{ J}$$

$$\varepsilon_n = -\frac{me^4}{8h^3 c\varepsilon_o^2 n^2} = -\frac{R}{n^2} \text{ cm}^{-1} \qquad (n = 1, 2, 3, \ldots) \qquad (5.3)$$

where ε_o is the vacuum permittivity, and where the fundamental constants have been collected together and given the symbol R, called the Rydberg constant. Since *p*, *d*, ... orbitals have the same energies as the corresponding *s* (for hydrogen *only*), Eq. (5.3) represents *all* the electronic energy levels of this atom.

The lowest value of ε_n is plainly $\varepsilon_n = -R$ cm^{-1} (when $n = 1$), and so this represents the most stable (or ground) state. ε_n increases with increasing n, reaching a limit, $\varepsilon_n = 0$ for $n = \infty$. This represents complete removal of the electron from the nucleus, i.e., the state of ionization. We sketch these energy levels for $n = 1$ to 5 and $l = 0$, 1, and 2 only in Fig. 5.2. (Some

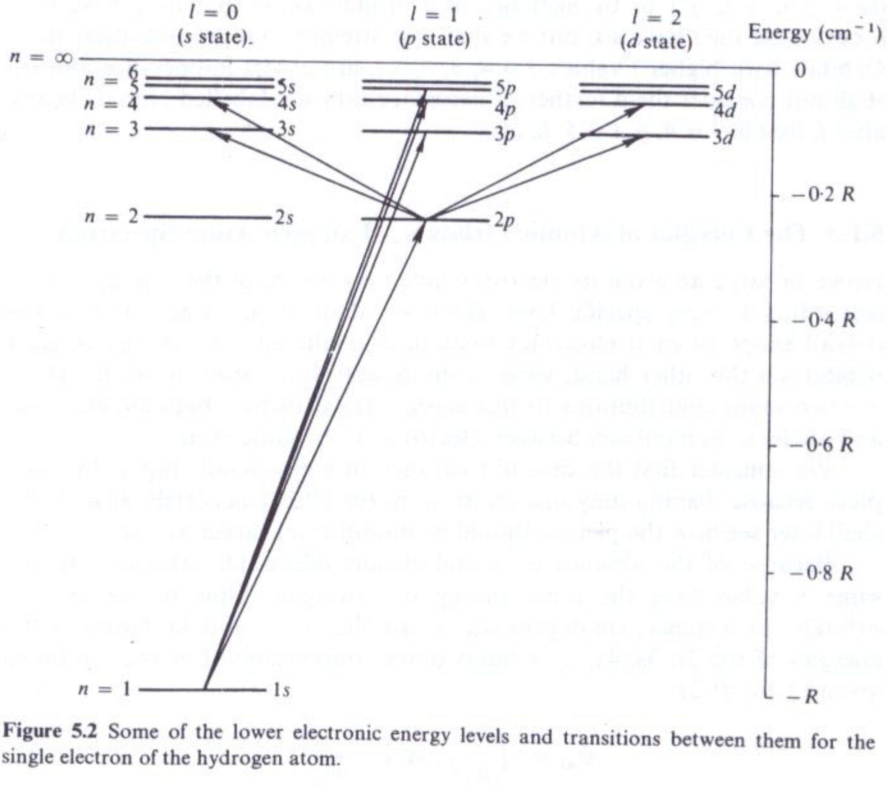

Figure 5.2 Some of the lower electronic energy levels and transitions between them for the single electron of the hydrogen atom.

possible transitions, also shown, will be discussed shortly.) The three p states and five d states for each n are degenerate and not shown separately.

Equation (5.3) and Fig. 5.2, then, represent the energy levels of the atom; in order to discuss the spectra which may arise we need the selection rules governing transitions. The Schrödinger equation shows these to be:

$$\Delta n = \text{anything} \qquad \text{and} \qquad \Delta l = \pm 1 \text{ only} \tag{5.4}$$

From these selection rules we see immediately that an electron in the ground state (the $1s$) can undergo a transition into any p state:

$$1s \rightarrow np \qquad (n \geq 2)$$

while a $2p$ electron can have transitions either into an s state or a d state:

$$2p \rightarrow ns \quad \text{or} \quad nd$$

Since s and d orbitals are here degenerate the energy of both these transitions will be identical. These transitions are sketched in Fig. 5.2.

In general an electron in a lower state n'', can undergo a transition into a higher state n', with absorption of energy:

$$\Delta\varepsilon = \varepsilon_{n'} - \varepsilon_{n''} \quad \text{cm}^{-1}$$

$$\therefore\ \bar{\nu}_{\text{spect.}} = -\frac{R}{n'^2} - \left(-\frac{R}{n''^2}\right) = R\left\{\frac{1}{n''^2} - \frac{1}{n'^2}\right\} \quad \text{cm}^{-1} \tag{5.5}$$

An identical spectral line will be produced in emission if the electron falls from state n' to state n''. In both cases l must change by unity. Let us consider a few of these transitions, restricting ourselves to absorption for simplicity.

Transitions $1s \rightarrow n'p$, $n' = 2, 3, 4, \ldots$. For these

$$\bar{\nu}_{\text{Lyman}} = R\left\{\frac{1}{1} - \frac{1}{n'^2}\right\} = R - \frac{R}{n'^2} \quad \text{cm}^{-1}$$

$$= \frac{3R}{4}, \frac{8R}{9}, \frac{15R}{16}, \frac{24R}{25}, \ldots \quad \text{cm}^{-1} \quad (\text{for } n' = 2, 3, 4, 5, \ldots)$$

Hence we expect a series of lines at the wavenumbers given above. Just such a series is indeed observed in the atomic hydrogen spectrum, and it is called the Lyman series after its discoverer. The appearance of this spectrum is sketched in Fig. 5.3 together with a scale in units of R and in wavenumbers. We can see that the spectrum converges to the point R cm^{-1}, and from the observed spectrum the very precise value $R = 109\,677{\cdot}581$ cm^{-1} is obtained. This convergence limit, which arises when $n' = \infty$, is shown dashed on the figure. It plainly represents complete removal of the electron—i.e., ionization—and the energy required to ionize the atom is given, in cm^{-1}, by the value of R. Using the conversion factor 1 cm^{-1} = $1{\cdot}987 \times 10^{-23}$ J,

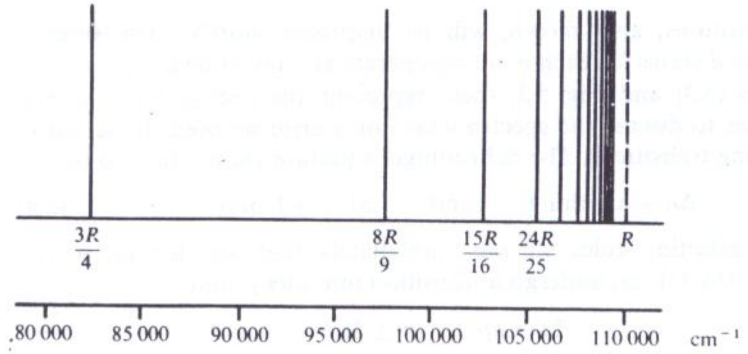

Figure 5.3 Representation of part of the Lyman series of the hydrogen atom showing the convergence (ionization) point.

we have a very precise measure of the *ionization potential* from the ground (1*s*) state: $2{\cdot}1781 \times 10^{-18}$ J (which may be more familiar in non-SI units as 13·595 eV).

Another set of transitions arises from an electron initially in the 2*s* or 2*p* states: $2s \rightarrow n'p$ or $2p \rightarrow n's, n'd$. For these we write:

$$\bar{\nu}_{\text{Balmer}} = R\left\{\frac{1}{4} - \frac{1}{n'^2}\right\} \quad \text{cm}^{-1}$$

$$= \frac{5R}{36}, \frac{3R}{16}, \frac{21R}{100}, \ldots \quad \text{cm}^{-1} \qquad (\text{for } n' = 3, 4, 5, \ldots)$$

Thus we expect another series of lines converging to $\frac{1}{4}R$ cm^{-1} ($n' = \infty$); this series, called the Balmer series after its discoverer, is observed and the value of $\frac{1}{4}R$ obtained from its convergence limit—which represents the ionization potential from the first excited state—is in excellent agreement with the value of R from the Lyman series.

Other similar line series (called the Paschen, Brackett, Pfund, etc., series) are observed for $n'' = 3, 4, 5, \ldots$; indeed these spectra were observed long before the modern theory of atomic structure had been developed. The spectral lines were correlated empirically by Rydberg, and he showed that an equation of the form given in Eq. (5.5) described the wavenumbers of each. It is after him that the Rydberg constant is named.

It should be mentioned that each line series discussed above shows a *continuous absorption* or *emission* to high wavenumbers of the convergence limits. The convergence limit represents the situation where the atomic electron has absorbed just sufficient energy from radiation to escape from the nucleus with zero velocity. It can, however, absorb more energy than this and hence escape with higher velocities and since the kinetic energy of an electron moving in free space is *not* quantized, *any* energy above the ionization energy can be absorbed. Hence the spectrum in this region is continuous.

This completes our discussion of what might be termed the coarse structure of the hydrogen atom spectrum. In order to consider the fine structure we need to know how the other quantum numbers, besides n, affect the electronic energy levels.

5.2 ELECTRONIC ANGULAR MOMENTUM

5.2.1 Orbital Angular Momentum

An electron moving in its orbital about a nucleus possesses *orbital* angular momentum, a measure of which is given by the l value corresponding to the orbital. This momentum is, of course, quantized, and it is usually expressed in terms of the unit $h/2\pi$, where h is Planck's constant. We may write:

$$\text{Orbital angular momentum} = \sqrt{l(l+1)} \cdot \frac{h}{2\pi} = \sqrt{l(l+1)} \text{ units} \quad (5.6)$$

Now angular momentum is a *vector* quantity, by which we mean that its *direction* is important as well as its magnitude—the axis of a spinning top, for instance, points in a particular direction. Conventionally, vectors may be represented by arrows, and the angular momentum vector is represented by an arrow based at the centre of the top, along the top axis, and of length proportional to the magnitude of the angular momentum. Such an arrow can lie in two different directions, at 180° to each other; these directions are associated, depending on the sign convention used, with clockwise and anticlockwise rotations of the top. Mathematically we can ignore the spinning body and deal merely with the properties of the arrow.

It is usual to distinguish vector quantities by the use of *bold-face* type and we shall accordingly represent orbital angular momentum by the symbol $\mathbf{l}$ where:

$$\mathbf{l} = \sqrt{l(l+1)} \text{ units} \quad (5.7)$$

In this equation l is always zero or positive and hence so is $\mathbf{l}$. Since $\mathbf{l}$ and l are so closely connected they are often loosely used interchangeably: thus we speak of an electron having 'an angular momentum of 2' when we strictly mean that $l = 2$ and $\mathbf{l} = \sqrt{2 \times 3} = 2{\cdot}44$ units.

We might at first think that the angular momentum vector of an electron could point in an infinite number of different directions. This, however, would be to reckon without the quantum theory. In fact, once a reference direction has been specified (and this may be done in many ways, either externally, such as by applying an electric or magnetic field, or internally, perhaps in terms of the angular momentum vector of one particular

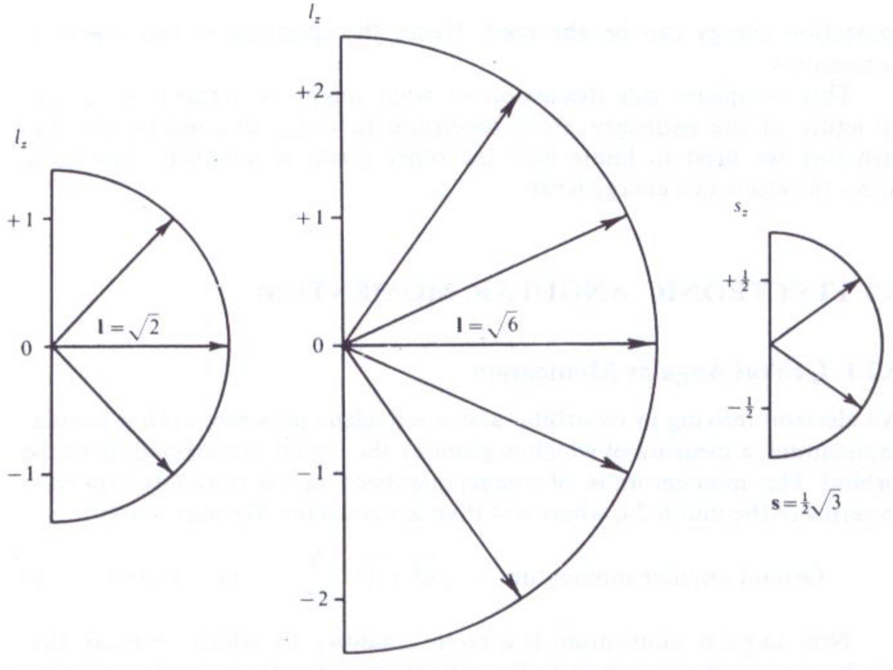

(*a*) $l = 1$ (*b*) $l = 2$ (*c*) $s = \frac{1}{2}$

Figure 5.4 The allowed directions of the electronic angular momentum vector for an electron in (*a*) a *p* state ($\mathbf{l} = 1$), (*b*) a *d* state ($\mathbf{l} = 2$), and (*c*) the allowed directions of the electronic spin angular momentum vector. The reference direction is taken arbitrarily as upwards in the plane of the paper.

electron), the angular momentum vector can point *only so that its components along the reference direction are integral multiples of* $h/2\pi$. Figure 5.4(*a*) and (*b*) show the situation for an electron with $l = 1$ and $l = 2$ respectively (i.e., a *p* and a *d* electron). The reference direction, here taken to be vertical in the figure, is conventionally used to define the *z* axis, and so we can write the *components* of $\mathbf{l}$ in this direction as $\mathbf{l}_z$ (note the use of bold-face type for $\mathbf{l}_z$, since the components of angular momentum are clearly vectors, having both magnitude and direction). Alternatively, since we know that the $\mathbf{l}_z$ are integral multiples of $h/2\pi$, we can represent the components in terms of an integral number l_z (not bold-face), where

$$\mathbf{l}_z = l_z \cdot \frac{h}{2\pi} \tag{5.8}$$

This latter notation is used in Fig. 5.4, and we see there that for $l = 1$, l_z takes values of $+1$, 0, and -1, while for $l = 2$ the values are $+2$, $+1$, 0, -1, and -2. In general we see that l_z has values:

$$l_z = l, l - 1, \ldots, 0, \ldots, -(l - 1), l \tag{5.9}$$

and that there are $2l + 1$ values of l_z for a given l. Plainly l_z is to be identified with the magnetic quantum number m introduced in Sec. 5.1.2:

$$l_z \equiv m$$

and this justifies our previous assertion that m governs essentially the *direction* of an orbital.

Before proceeding further let us reiterate the distinction between l, $\mathbf{l}$, $\mathbf{l}_z$, and l_z. The quantum number l is an integer, positive or zero, representing the state of an electron in an atom and determining its orbital angular momentum. The vector $\mathbf{l}$ designates the magnitude and direction of this momentum as shown by the vector arrows of Fig. 5.4. When expressed in units of $h/2\pi$, $\mathbf{l}$ is numerically equal to $\sqrt{l(l+1)}$. Once a reference direction is specified (and this is often arbitrary) $\mathbf{l}$ can point only so as to have components $\mathbf{l}_z = l_z h/2\pi$ (with l_z an integer or zero) along that direction.

Usually the orbital energy of the electron depends only on the magnitude and not the direction of its angular momentum; thus the $2l + 1$ values of l_z are all *degenerate*. But we should note that it is possible to *lift the degeneracy* (cf. Sec. 5.6) so that levels with different l_z have different energy.

5.2.2 Electron Spin Angular Momentum

Every electron in an atom can be considered to be spinning about an axis as well as orbiting about the nucleus. Its spin motion is designated by the *spin quantum number* s, which can be shown to have a value of $\frac{1}{2}$ only. Thus the spin angular momentum is given by:

$$\mathbf{s} = \sqrt{s(s+1)}\,\frac{h}{2\pi} = \sqrt{\frac{1}{2} \times \frac{3}{2}}\ \text{units}$$

$$= \tfrac{1}{2}\sqrt{3}\ \text{units} \tag{5.10}$$

The quantization law for spin momentum is that the vector can point so as to have components in the reference direction which are *half-integral* multiples of $h/2\pi$, that is, so that $\mathbf{s}_z = s_z h/2\pi$ with s_z taking the values $+\frac{1}{2}$ or $-\frac{1}{2}$ only. The two (that is, $2s + 1$) allowed directions are shown in Fig. 5.4(*c*); they are normally degenerate.

5.2.3 Total Electronic Angular Momentum

We now need to discover some means whereby the orbital and spin contributions to the electronic angular momentum may be combined. Formally we can write:

$$\mathbf{j} = \mathbf{l} + \mathbf{s} \tag{5.11}$$

where $\mathbf{j}$ is the *total angular momentum*. Since $\mathbf{l}$ and $\mathbf{s}$ are vectors, Eq. (5.11) must be taken to imply *vector addition*. Also formally, we can express $\mathbf{j}$ in terms of a total angular momentum quantum number j:

$$\mathbf{j} = \sqrt{j(j+1)}\,\frac{h}{2\pi} = \sqrt{j(j+1)} \text{ units} \tag{5.12}$$

where j is *half-integral* (since s is half-integral for a one-electron atom), and a quantal law applies equally to **j** as to **l** and **s** : **j** *can have z-components which are half-integral only*, i.e.,

$$j_z = \pm j, \pm(j-1), \pm(j-2), \ldots, \tfrac{1}{2} \tag{5.13}$$

There are two methods by which we can deduce the various allowed values of **j** for particular **l** and **s** values. We shall consider them both briefly.

1. *Vector summation.* In ordinary mechanics two forces in different directions may be added by a graphical method in which vector arrows are drawn to represent the magnitude and direction of the forces, the 'parallelogram is completed', and the magnitude and direction of the resultant given by the diagonal of the parallelogram. Exactly the same method can be used to find the resultant (**j**) of the vectors **l** and **s**. The important difference is that quantum mechanical laws restrict the angle between **l** and **s** to values such that **j** is given by Eq. (5.12) with *half-integral j*. Thus **j** can take values

   $$\tfrac{1}{2}\sqrt{3}, \tfrac{1}{2}\sqrt{15}, \tfrac{1}{2}\sqrt{35}, \ldots \qquad \text{corresponding to} \qquad j = \tfrac{1}{2}, \tfrac{3}{2}, \tfrac{5}{2}, \ldots$$

   The method is illustrated in Fig. 5.5(*a*) and (*b*) for the case $l = 1$ (that is, $\mathbf{l} = \sqrt{2}$) and $s = \frac{1}{2}$ ($\mathbf{s} = \frac{1}{2}\sqrt{3}$). In (*a*) the summation yields $\mathbf{j} = \frac{1}{2}\sqrt{15}$, which corresponds to a j value of $\frac{3}{2}$, while in (*b*) $\mathbf{j} = \frac{1}{2}\sqrt{3}$ or $j = \frac{1}{2}$. Construction or calculation shows that **l** and **s** may not be combined in any other way to give an allowed value of **j**.

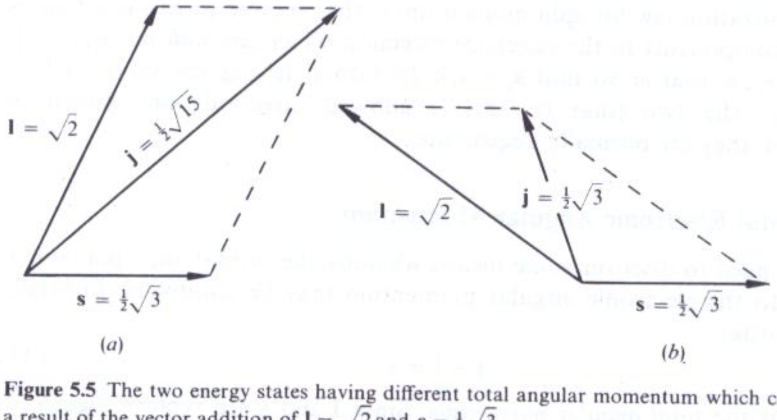

Figure 5.5 The two energy states having different total angular momentum which can arise as a result of the vector addition of $\mathbf{l} = \sqrt{2}$ and $\mathbf{s} = \frac{1}{2}\sqrt{3}$.

Note that we can get exactly the same answer by summing the *quantum numbers* l and s to get the *quantum number* j. In this example $l = 1$, $s = \frac{1}{2}$, and hence:

$$j = l + s = \tfrac{3}{2} \quad \text{or} \quad j = l - s = \tfrac{1}{2}$$

This simple approach, although adequate for systems with one electron only, is not readily extended to multi-electron systems. For these we must use the rather more fundamental method outlined below.

2. *Summation of z components.* If the components along a common direction of two vectors are added, the summation yields the component in that direction of their resultant. We have seen (cf. Eq. (5.9)) that the z components of $l = 1$ are ± 1, and 0, while those of $s = \frac{1}{2}$ are $\pm\frac{1}{2}$ only. Taking all possible sums of these quantities we have:

$$\begin{aligned} j_z &= l_z + s_z \\ \therefore\ j_z &= 1 + \tfrac{1}{2},\ 1 - \tfrac{1}{2},\ 0 + \tfrac{1}{2},\ 0 - \tfrac{1}{2},\ -1 + \tfrac{1}{2},\ -1 - \tfrac{1}{2} \\ &= \tfrac{3}{2},\ \tfrac{1}{2},\ \tfrac{1}{2},\ -\tfrac{1}{2},\ -\tfrac{1}{2},\ -\tfrac{3}{2} \end{aligned}$$

In this list of six j_z components, the maximum value is $\frac{3}{2}$, which we know (cf. Eq. (5.13)) must belong to $j = \frac{3}{2}$. Other components of $j = \frac{3}{2}$ are $\frac{1}{2}$, $-\frac{1}{2}$, and $-\frac{3}{2}$ and, striking these from the above six, we are left with $j_z = +\frac{1}{2}$ and $-\frac{1}{2}$. These values are plainly consistent with $j = \frac{1}{2}$.

Thus all the six components are accounted for if we say that the states $j = \frac{3}{2}$ and $j = \frac{1}{2}$ may be formed from $l = 1$ and $s = \frac{1}{2}$. This is, of course, in agreement with the vector summation method.

Both these methods show that for a p electron (that is, $l = 1$), the orbital and spin momenta may be combined to produce a total momentum of $\mathbf{j} = \frac{1}{2}\sqrt{15}$ when $\mathbf{l}$ and $\mathbf{s}$ reinforce (physically we would say that the angular momenta have the same *direction*) or to give $\mathbf{j} = \frac{1}{2}\sqrt{3}$ when $\mathbf{l}$ and $\mathbf{s}$ oppose each other. Thus the total momentum is different in *magnitude* in the two cases and hence we have arrived at two *different energy states* depending on whether $\mathbf{l}$ and $\mathbf{s}$ reinforce or oppose. Both energy states are p states, however (since l is 1 for both), and they may be distinguished by writing the j quantum number value as a subscript to the *state symbol P*, thus $P_{3/2}$ or $P_{1/2}$. (We here use a capital letter for the state of a whole atom and a small letter for the state of an individual electron; in the hydrogen atom, which contains only one electron, the distinction is trivial.) States such as these, split into two energies, are termed *doublet states*; their doublet nature is usually indicated by writing a superscript 2 to the state symbol, thus: ${}^2P_{3/2}$, ${}^2P_{1/2}$. The state (or term) symbols produced are to be read 'doublet P three halves' or 'doublet P one half' respectively.

All other higher l values for the electron will obviously produce doublet states when combined with $s = \frac{1}{2}$; for instance, $l = 2, 3, 4, \ldots$ will yield

$^2D_{5/2,\,3/2}$, $^2F_{7/2,\,5/2}$, $^2G_{9/2,\,7/2}$, etc. The student should satisfy himself of this, preferably by using the z-component summation method outlined above. There is, however, a slight difficulty with s states ($l = 0$). Here, since $l = 0$, it can make no contribution to the vector sum, and the only possible resultant is $\mathbf{s} = \frac{1}{2}\sqrt{3}$ or $s = \frac{1}{2}$. Remember $s = -\frac{1}{2}$ is not allowed, since the *quantum number* cannot be negative; it is only the z component of the vector which can have negative values. Thus for an s electron we would have the state symbol $S_{1/2}$ only. This is nonetheless formally written as a doublet state ($^2S_{1/2}$) for reasons which should become clear during the discussion of multiplicity in Sec. 5.4.3.

We can now consider the relevance of this discussion to atomic spectroscopy.

5.2.4 The Fine Structure of the Hydrogen Atom Spectrum

The hydrogen atom contains but one electron and so the coupling of orbital and spin momenta and consequent splitting of energy levels will be exactly as described above. We summarize the essential details of the energy levels

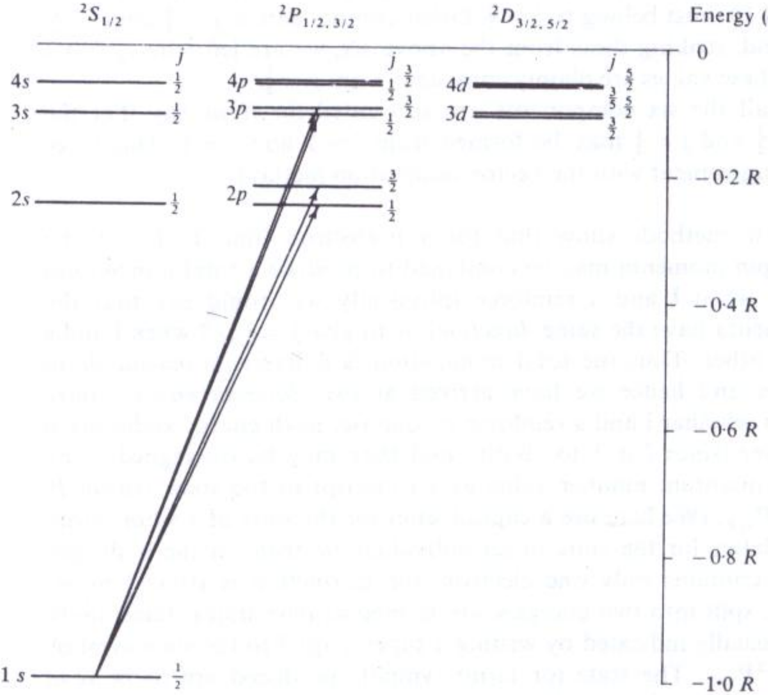

Figure 5.6 Some of the lower energy levels of the hydrogen atom showing the inclusion of j-splitting. The splitting is greatly exaggerated for clarity.

in Fig. 5.6. Each level is labelled with its n quantum number on the extreme left, and its j value on the right; the l value is indicated by the state symbols S, P, D, ... at the top of each column. There is no attempt to show the energy-level splitting of the P and D states to scale in this diagram—the separation between levels differing only in j is many thousands of times smaller than the separation between levels of different n. However, we do indicate that the j-splitting *decreases* with increasing n and with increasing l. The F, G, ... states, not shown on the diagram, follow the same pattern.

The selection rules for n and l are the same as before:

$$\Delta n = \text{anything} \qquad \Delta l = \pm 1 \text{ only} \tag{5.14}$$

but now there is a selection rule for j:

$$\Delta j = 0, \ \pm 1 \tag{5.15}$$

These selection rules indicate that transitions are allowed between any S level and any P level:

$$^2S_{1/2} \rightarrow {}^2P_{1/2} \qquad (\Delta j = 0)$$
$$^2S_{1/2} \rightarrow {}^2P_{3/2} \qquad (\Delta j = +1)$$

Thus the spectrum to be expected from the ground ($1s$) state will be identical with the Lyman series (cf. Sec. 5.1.3) except that *every line will be a doublet*. In fact the separation between the lines is too small to be readily resolved but we shall shortly consider the spectrum of sodium in which this splitting is easily observed.

Transitions between the ^2P and ^2D states are rather more complex; Fig. 5.7 shows four of the energy levels involved. Plainly the transition at lowest frequency will be that between the closest pair of levels, the $^2P_{3/2}$ and $^2D_{3/2}$. This, corresponding to $\Delta j = 0$ is allowed. The next transition, $^2P_{3/2} \rightarrow {}^2D_{5/2}$ ($\Delta j = +1$), is also allowed and will occur close to the first because the separation between the doublet D states is very small. Thirdly, and more widely spaced, will be $^2P_{1/2} \rightarrow {}^2D_{3/2}$ ($\Delta j = +1$), but the fourth transition (shown dotted) $^2P_{1/2} \rightarrow {}^2D_{5/2}$, is not allowed since for this $\Delta j = +2$.

Thus the spectrum will consist of the three lines shown at the foot of the figure. This, arising from transitions between doublet levels, is usually referred to as a 'compound doublet' spectrum.

We see, then, that the inclusion of coupling between orbital and spin momenta has led to a slight increase in the complexity of the hydrogen spectrum. In practice, the complexity will be observed only in the spectra of heavier atoms, since for them the j-splitting is larger than for hydrogen. In principle, however, all the lines in the hydrogen spectrum should be close doublets if the transitions involve s levels, or 'compound doublets' if s electrons are not involved.

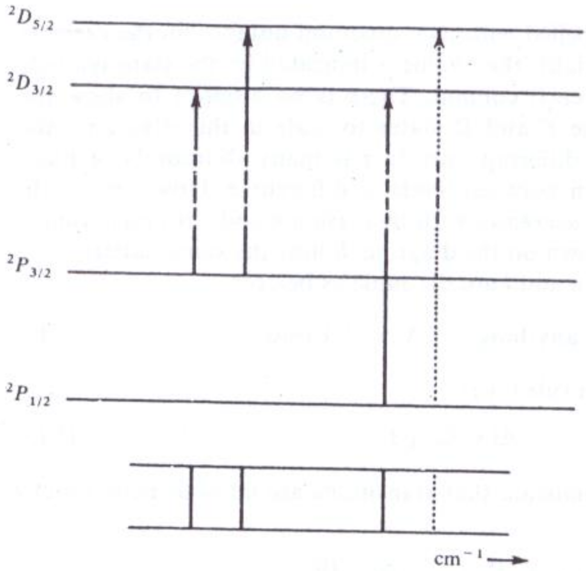

Figure 5.7 The 'compound doublet' spectrum arising as the result of transitions between ^2P and ^2D levels in the hydrogen atom.

5.3 MANY-ELECTRON ATOMS

5.3.1 The Building-up Principle

The Schrödinger equation shows that electrons in atoms occupy orbitals of the same type and shape as the *s*, *p*, *d*, ... orbitals discussed for the hydrogen atom, but that the energies of these electrons differ markedly from atom to atom. There is no general expression for the energy levels of a many-electron atom comparable to Eq. (5.3) for hydrogen; each atom must be treated as a special case and its energy levels either tabulated or shown on a diagram similar to Fig. 5.2 or Fig. 5.6.

There are three basic rules, known as the building-up rules, which determine how electrons in large atoms occupy orbitals. These may be summarized as:

1. Pauli's principle: no two electrons in an atom may have the same set of values for n, l, l_z ($\equiv m$), and s_z.
2. Electrons tend to occupy the orbital with lowest energy available.
3. Hund's principle: electrons tend to occupy degenerate orbitals singly with their spins parallel.

Rule 1 effectively limits to two the number of electrons in each orbital.

An example may make this clear: we may characterize both an orbital and an electron occupying it by specifying the n, l, and m quantum numbers. Thus a 1s orbital or 1s electron has $n = 1$, $l = 0$, and $m = l_z = 0$; the electron (but not the orbital) is further characterized by a statement of its spin direction, i.e., by specifying $s_z = +\frac{1}{2}$ or $s_z = -\frac{1}{2}$. Two electrons can together occupy the 1s orbital provided, according to rule 1, that one has the set of values $n = 1$, $l = 0$, $l_z = 0$, $s_z = +\frac{1}{2}$, and the other $n = 1$, $l = 0$, $l_z = 0$, $s_z = -\frac{1}{2}$. We talk, rather loosely, of two electrons occupying the same orbital only if their spins are *paired* (or *opposed*). A third electron cannot exist in the same orbital without repeating a set of values for n, l, l_z, and s_z already taken up. It would have to be placed into some other orbital and the choice is determined by rule 2: it would go into the next higher vacant or half-vacant orbital. In general, orbital energies in many-electron atoms increase with increasing n, as they do for hydrogen, but they also increase with increasing l, whereas we noted for hydrogen that all s, p, d, ... orbitals with the same n were degenerate. In fact the order of the energy levels for most atoms is as follows:

$$1s < 2s < 2p < 3s < 3p < 4s < 3d < 4p < 5s < 4d \cdots \qquad (5.16)$$

Thus when the 1s orbital is full (i.e., contains two electrons) the next available orbital is the 2s, and after this the 2p. Now we remember that there are *three* 2p orbitals, one along each coordinate axis, and *each* of these can contain two electrons. We may write the n, l, l_z, and s_z values as:

$$\left.\begin{array}{llll} n = 2 & l = 1 & l_z = 1 & s_z = \pm\frac{1}{2} \\ n = 2 & l = 1 & l_z = 0 & s_z = \pm\frac{1}{2} \\ n = 2 & l = 1 & l_z = -1 & s_z = \pm\frac{1}{2} \end{array}\right\} \text{total six electrons}$$

All three p orbitals remain degenerate (as do the five d orbitals, seven f, etc.) for a given n. It is rule 3 which tells us how electrons occupy these degenerate orbitals. Hund's rule states that when, for example, the $2p_x$ orbital contains an electron, the next electron will go into a *different* 2p, say $2p_y$, orbital, and a third into the $2p_z$. This may be looked upon as a consequence of repulsion between electrons. A fourth electron has no choice but to pair its spin with an electron already in one 2p orbital, while a fifth and sixth will complete the filling of the three 2p's.

On this basis we can build up the *electronic configurations* of the 10 smallest atoms, from hydrogen to neon. This is shown in Table 5.2 where each box represents an orbital occupied by one or two electrons with spin directions shown by the arrows. A convenient notation for the electronic configuration is also shown in the table.

When a set of orbitals of given n and l is filled it is referred to as a *closed shell*. Thus the $1s^2$ set of helium, the $2s^2$ set of beryllium, and the $2p^6$ set of neon are all closed shells. The convenience of this is that closed shells

Table 5.2 Electronic structure of some atoms

	1s	2s	2p			
Hydrogen	↑					$1s^1$
Helium	↑↓					$1s^2$
Lithium	↑↓	↑				$1s^2 2s^1$
Beryllium	↑↓	↑↓				$1s^2 2s^2$
Boron	↑↓	↑↓	↑			$1s^2 2s^2 2p_x^1$
Carbon	↑↓	↑↓	↑	↑		$1s^2 2s^2 2p_x^1 2p_y^1$
Nitrogen	↑↓	↑↓	↑	↑	↑	$1s^2 2s^2 2p_x^1 2p_y^1 2p_z^1$
Oxygen	↑↓	↑↓	↑↓	↑	↑	$1s^2 2s^2 p_x^2 2p_y^1 2p_z^1$
Fluorine	↑↓	↑↓	↑↓	↑↓	↑	$1s^2 2s^2 2p_x^2 2p_y^2 2p_z^1$
Neon	↑↓	↑↓	↑↓	↑↓	↑↓	$1s^2 2s^2 2p_x^2 2p_y^2 2p_z^2$

make no contribution to the orbital or spin angular momentum of the whole atom and hence they may be ignored when discussing atomic spectra. This represents a considerable simplification.

5.3.2 The Spectrum of Lithium and Other Hydrogen-like Species

The alkali metals, lithium, sodium, potassium, rubidium, and cesium, all have a single electron outside a closed-shell core (cf. lithium in Table 5.2). Superficially, then, they resemble hydrogen and this resemblance is augmented by the fact that we can ignore the angular momentum of the core and deal merely with the spin and orbital momentum of the outer electron. Thus we immediately expect the *p*, *d*, ... levels to be split into doublets because of coupling between **l** and **s**.

The energy levels of lithium are sketched in Fig. 5.8, which figure should be compared with the corresponding Fig. 5.6 for hydrogen. The two diagrams are similar except for the energy difference between the *s*, *p*, and *d* orbitals of given *n* in the case of lithium, and the fact that, for this metal, the 1*s* state is filled with electrons which do not generally take part in spectroscopic transitions, it requiring much less energy to induce the 2*s* electron to undergo a transition. Under high energy conditions, however, one or both of the 1*s* electrons may be promoted.

The selection rules for alkali metals are the same as for hydrogen, that is, $\Delta n =$ anything, $\Delta l = \pm 1$, $\Delta j = 0, \pm 1$, and so the spectra will be similar also. Thus transitions from the ground state ($1s^2 2s$) can occur to *p* levels: $2S_{1/2} \rightarrow nP_{1/2,\,3/2}$, and a series of doublets similar to the Lyman series will be formed converging to some point from which the ionization potential can be found. From the 2*p* state, however, two separate series of lines will be seen:

$$2\,{}^2P_{1/2,\,3/2} \rightarrow n\,{}^2S_{1/2}$$

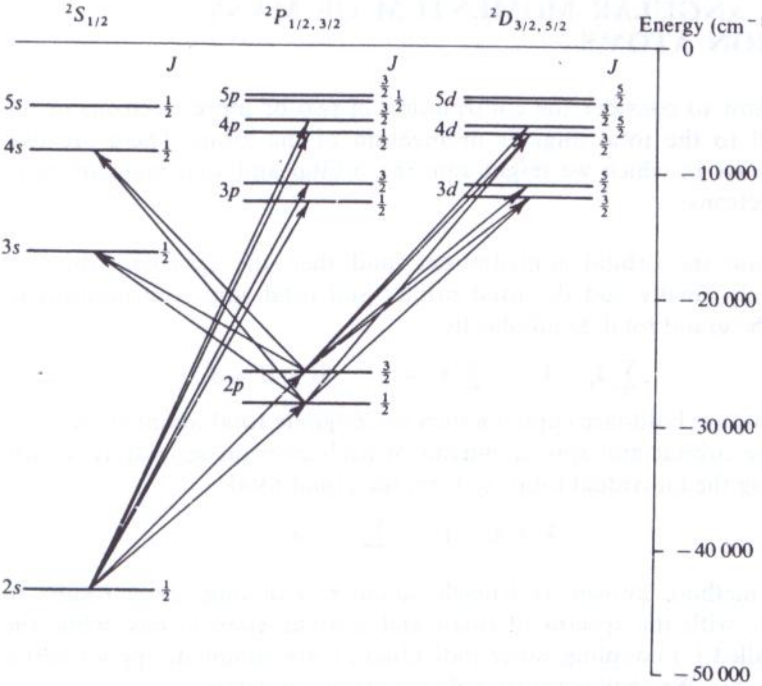

Figure 5.8 Some of the lower energy levels of the lithium atom showing the difference in energy of *s*, *p*, and *d* states with the same value of *n*. Some allowed transitions are also shown. The *j*-splitting is greatly exaggerated.

and

$$2\ {}^2P_{1/2,\,3/2} \rightarrow n\ {}^2D_{3/2,\,5/2}$$

The former will be doublets, the latter compound doublets, but their frequencies will differ because the *s* and *d* orbital energies are no longer the same.

The same remarks apply to the other alkali metals, the differences between their spectra and that of lithium being a matter of scale only. For instance the *j*-splitting due to coupling between **l** and **s** increases markedly with the atomic number. Thus the doublet separation of lines in the spectral series, which is scarcely observable for hydrogen, is less than 1 cm⁻¹ for the 2*p* level of lithium, about 17 cm⁻¹ for sodium, and over 5000 cm⁻¹ for cesium.

Any atom which has a single electron moving outside a closed shell will exhibit a spectrum of the type discussed above. Thus ions of the type He^+, Be^+, B^{2+}, etc., should, and indeed do, show what are termed 'hydrogen-like spectra'.

5.4 THE ANGULAR MOMENTUM OF MANY-ELECTRON ATOMS

We turn now to consider the contribution of two or more electrons in the outer shell to the total angular momentum of the atom. There are two different ways in which we might sum the orbital and spin momentum of several electrons:

1. First sum the orbital contributions, and then the spin contributions separately, finally add the total orbital and total spin contributions to reach the grand total. Symbolically:

   $$\sum \mathbf{l}_i = \mathbf{L} \qquad \sum \mathbf{s}_i = \mathbf{S} \qquad \mathbf{L} + \mathbf{S} = \mathbf{J}$$

   where we use bold-face capital letters to designate total momentum.
2. Sum the orbital and spin momenta of each electron separately, finally summing the individual totals to form the grand total:

   $$\mathbf{l}_i + \mathbf{s}_i = \mathbf{j}_i \qquad \sum \mathbf{j}_i = \mathbf{J}$$

The first method, known as Russell–Saunders coupling, gives results in accordance with the spectra of small and medium-sized atoms, while the second (called *j*, *j* coupling, since individual *j*'s are summed) applies better to large atoms. We shall consider only the former in detail.

5.4.1 Summation of Orbital Contributions

The orbital momenta, $\mathbf{l}_1$, $\mathbf{l}_2$, ... of several electrons may be added by the same methods as were discussed in Sec. 5.2.3 for the summation of the orbital and spin momenta of a single electron. Thus we could:

1. Add the vectors $\mathbf{l}_1$, $\mathbf{l}_2$, ... graphically remembering that their resultant **L** must be expressible by

   $$\mathbf{L} = \sqrt{L(L+1)} \qquad (L = 0, 1, 2, \ldots) \tag{5.17}$$

   where L is the total orbital momentum quantum number. Thus **L** can have values 0, $\sqrt{2}$, $\sqrt{6}$, $\sqrt{12}$, ... only. Figure 5.9 illustrates the method for a *p* and a *d* electron, $l_1 = 1$, $l_2 = 2$, hence $\mathbf{l}_1 = \sqrt{2}$, $\mathbf{l}_2 = \sqrt{6}$. There are three, and only three, ways in which the two vectors may be combined to give **L** consistent with Eq. (5.17). The three values of **L** are seen to be $\sqrt{12}$, $\sqrt{6}$, and $\sqrt{2}$, corresponding to the quantum number $L = 3$, 2, and 1 respectively.
2. Alternatively we could add the individual *quantum numbers* l_1 and l_2 to obtain the total quantum number L according to:

   $$L = l_1 + l_2 \qquad l_1 + l_2 - 1, \ldots \qquad |l_1 - l_2| \tag{5.18}$$

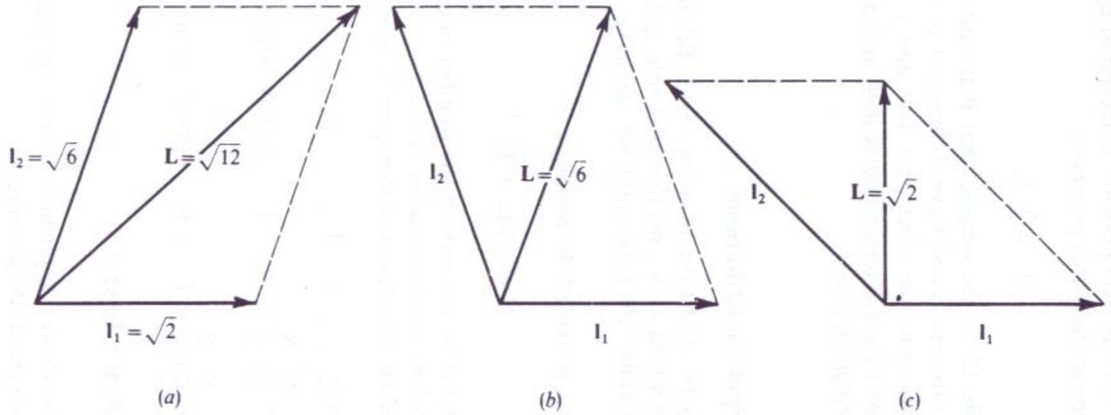

Figure 5.9 Summation of orbital angular momenta for a *p* and a *d* electron.

where the modulus sign $|\ldots|$ indicates that we are to take $l_1 - l_2$ or $l_2 - l_1$, whichever is positive. For two electrons, there will plainly be $2l_i + 1$ different values of L, where l_i is the smaller of the two l values.

3. Finally we could add the z components of the individual vectors, picking out from the result sets of components corresponding to the various allowed **L** values. Symbolically this process is:

$$L_z = \sum l_{i_z}$$

Of these methods, (2) is the simplest but it is only applicable when the individual electrons concerned have different n or different l values (these are termed *non-equivalent* electrons). If n and l are the same for two or more electrons they are termed *equivalent* and method 3 must be used. Examples will be given later.

5.4.2 Summation of Spin Contributions

The same methods may be used here as in Sec. 5.4.1. Briefly, if we write the total spin angular momentum as **S**, and the total spin quantum number as S (which is often simply called the total spin), we can have:

1. Graphical summation, provided the resultant is

$$\mathbf{S} = \sqrt{S(S+1)} \tag{5.19}$$

where S is either *integral or zero* only, if the number of contributing spins is *even*, or *half-integral* only, if the number is *odd*.

2. Summation of individual quantum numbers; for N spins we have:

$$\begin{aligned} S &= \sum s_i, \sum s_i - 1, \sum s_i - 2, \ldots \\ &= \frac{N}{2}, \frac{N}{2} - 1, \ldots, \tfrac{1}{2} \qquad \text{(for } N \text{ odd)} \\ &= \frac{N}{2}, \frac{N}{2} - 1, \ldots, 0 \qquad \text{(for } N \text{ even)} \end{aligned} \tag{5.20}$$

3. Summation of individual s_z to give S_z.

Method 2, which is *always* applicable, is the simplest. Thus for two electrons we have the two possible spin states:

$$S = \tfrac{1}{2} + \tfrac{1}{2} = 1 \qquad \text{or} \qquad S = \tfrac{1}{2} + \tfrac{1}{2} - 1 = 0$$

In the former the spins are called *parallel* and the state may be written (↑↑), while in the latter they are *paired* or *opposed* and written (↑↓).

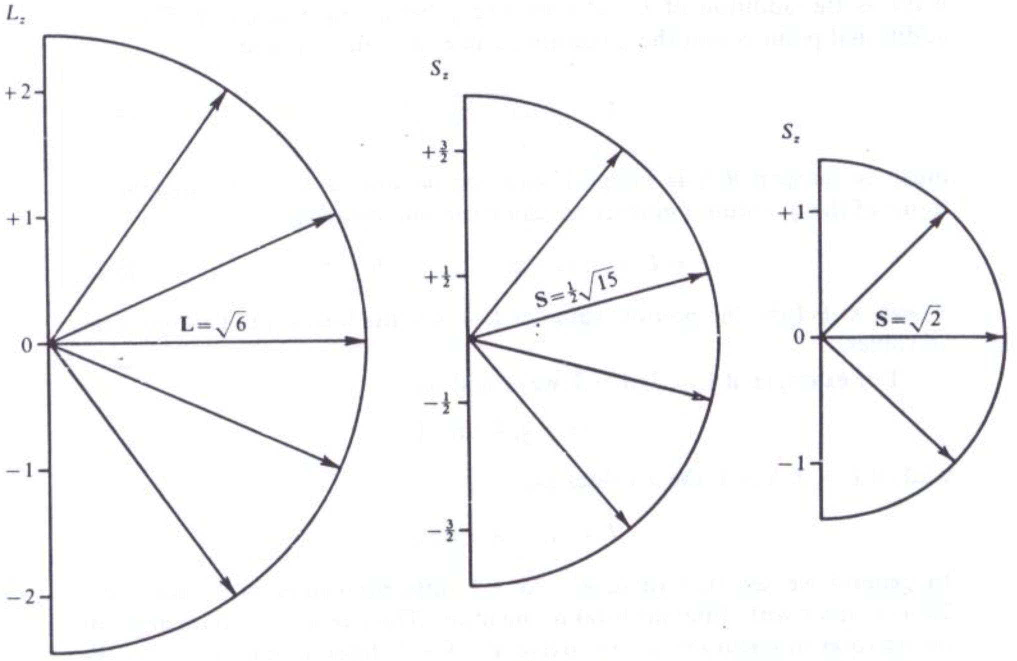

(*a*) $L=2$ (*b*) $S=\frac{3}{2}$ (*c*) $S=1$

Figure 5.10 Showing the *z* components of (*a*) an orbital angular momentum vector, (*b*) a spin vector for which *S* is half-integral, and (*c*) a spin vector for which *S* is integral.

Again, for three electrons we may have:

$$S = \tfrac{1}{2} + \tfrac{1}{2} + \tfrac{1}{2} = \tfrac{3}{2} \quad (\uparrow\uparrow\uparrow)$$

$$S = \tfrac{1}{2} + \tfrac{1}{2} + \tfrac{1}{2} - 1 = \tfrac{1}{2} \quad (\uparrow\uparrow\downarrow,\ \uparrow\downarrow\uparrow \text{ or } \downarrow\uparrow\uparrow)$$

where we see that there are three ways in which the $S = \frac{1}{2}$ state may be realized, one in which $S = \frac{3}{2}$.

As we have implied above, both **L** and **S** have *z* components along a reference direction. For **L** these components are limited to integral values by quantum laws and, as we can see from Fig. 5.10(*a*), there are, in general, $2L + 1$ of them, while for **S** the S_z will be integral only or half-integral only, depending on whether S is integral or half-integral. We show examples in Fig. 5.10(*b*) and (*c*). In both cases there are $2S + 1$ components.

5.4.3 Total Angular Momentum

The addition of the total orbital momentum **L** and the total spin momentum **S** to give the grand total momentum **J** can be carried out in the same ways as the addition of **l** and **s** to give **j**, for a single electron. The only additional point is that the quantum number J in the expression

$$\mathbf{J} = \sqrt{J(J+1)} \cdot \frac{h}{2\pi} \tag{5.21}$$

must be *integral* if S is integral, and *half-integral* if S is half-integral. In terms of the quantum numbers we can write immediately:

$$J = L + S,\ L + S - 1,\ \ldots,\ |L - S| \tag{5.22}$$

where, as before, the *positive* value of $L - S$ is the lowest limit of the series of values.

For example, if $L = 2$, $S = \frac{3}{2}$, we would have

$$J = \tfrac{7}{2}, \tfrac{5}{2}, \tfrac{3}{2}, \text{ and } \tfrac{1}{2}$$

while if $L = 2$, $S = 1$, the J values are:

$$J = 3, 2, \text{ or } 1 \text{ only}$$

In general we see that there are $2S + 1$ different values of J and hence $2S + 1$ states with different total momentum. The energy of a state depends on its total momentum, so we arrive at $2S + 1$ different energy levels, the energy of each depending on the way in which **L** and **S** are combined. The quantity $2S + 1$, which occupies a special place in atomic spectroscopy, is called the *multiplicity* of the system.

We recall that, when discussing the total angular momentum of a single electron (Sec. 5.2.3), we found that each state, except those with $l = 0$, consisted of two very slightly different energy levels owing to j-splitting; we called these 'doublet states'. We also called the $l = 0$ states doublets, although each has but one energy level since $j = \frac{1}{2}$ only. We now see that the concept of multiplicity justifies us in labelling *all* one-electron states as doublets, since for all of them $S = \frac{1}{2}$, hence $2S + 1 = 2$, and they all have a multiplicity of two.

It is a general rule that in states with $L \geq S$, whether consisting of one electron or of many, the multiplicity is equal to the actual number of levels with different J, whereas if $L < S$, then there are only $2L + 1$ different J values, which is less than the multiplicity. As an example of the latter, if $L = 1$ and $S = 2$, there are only three different J values, $J = 3$, 2, or 1, whereas the multiplicity is $2S + 1 = 5$.

It is in fact highly convenient to label states with their multiplicities rather than to show the number of different J values because, as we shall see shortly, there is a selection rule which forbids transitions between states with different multiplicities; thus designating the multiplicity of a particular state immediately indicates to which other levels in the system a transition may take place.

5.4.4 Term Symbols

In the whole of this section we have been describing the way in which the total angular momentum of an atom is built up from its various components. Using one sort of coupling only (the Russell–Saunders coupling) we arrive at vector quantities **L**, **S**, and **J** for a system which may be expressed in terms of quantum numbers L, S, and J:

$$\mathbf{L} = \sqrt{L(L+1)} \qquad \mathbf{S} = \sqrt{S(S+1)} \qquad \mathbf{J} = \sqrt{J(J+1)} \qquad (5.23)$$

where the integral L and integral or half-integral S and J are themselves combinations of individual electronic quantum numbers.

In any particular atom, then, we see that the individual electronic angular momenta may be combined in various ways to give different states each having a different total angular momentum (**J**) and hence a different energy (unless some states happen to be degenerate). Before discussing the effect of these states on the spectrum of an atom we require some symbolism which we may use to describe states conveniently. We have already introduced such *state symbols* or *term symbols* in Sec. 5.2.6, but we now consider them rather more fully.

The term symbol for a particular atomic state is written as follows:

$$\text{Term symbol} = {}^{2S+1}L_J \qquad (5.24)$$

where the numerical superscript gives the *multiplicity* of the state, the numerical subscript gives the total angular momentum quantum number J, and the value of the oribital quantum number L is expressed by a *letter*:

For $\quad L = 0, 1, 2, 3, 4, \ldots$

Symbol $\;= S, P, D, F, G, \ldots$

which symbolism is comparable with the s, p, d, ... already used for single-electron states with $l = 0, 1, 2, \ldots$.

Let us now see some examples.

1. $S = \frac{1}{2}$, $L = 2$; hence $J = \frac{5}{2}$ or $\frac{3}{2}$ and $2S + 1 = 2$. Term symbols: ${}^2D_{5/2}$ and ${}^2D_{3/2}$, which are to be read 'doublet D five halves' and 'doublet D three halves' respectively.
2. $S = 1$, $L = 1$; hence $J = 2$, 1, or 0, and $2S + 1 = 3$. Term symbols: ${}^3P_2$, ${}^3P_1$, or ${}^3P_0$ (read 'triplet P two', etc.).

   In both these examples we see that (since $L \geq S$), the multiplicity is the same as the number of different energy states.
3. $S = \frac{3}{2}$, $L = 1$; hence $J = \frac{5}{2}, \frac{3}{2}$, or $\frac{1}{2}$ and $2S + 1 = 4$. Term symbols: ${}^4P_{5/2}$, ${}^4P_{3/2}$, ${}^4P_{1/2}$ (read 'quartet P five halves', etc.) where, since $L < S$, there are only three different energy states but each is nonetheless described as *quartet* since $2S + 1 = 4$.

The reverse process is equally easy; given a term symbol for a particular atomic state we can immediately deduce the various total angular momenta of that state. Some examples:

4. ${}^3S_1$: we read immediately that $2S + 1 = 3$, hence $S = 1$, and that $L = 0$ and $J = 1$.
5. ${}^2P_{3/2}$: $L = 1$, $J = \frac{3}{2}$, $2S + 1 = 2$, hence $S = \frac{1}{2}$.

Note, however, that the term symbol tells us only the total spin, total orbital, and grand total momenta of the whole atom—it tells us nothing of the states of the individual electrons in the atoms, nor even how many electrons contribute to the total. Thus in example 5 above, the fact that $S = \frac{1}{2}$ implies that the atom has an odd number of contributing electrons, all except one of which have their spins paired. Thus a single electron (↑), three electrons (↑↑↓), five electrons (↑↓↑↓↑), etc., all form a doublet state. Similarly, the value $L = 1$ implies, perhaps, one *p* electron, or perhaps one *p* and two *s* electrons, or one of many other possible combinations.

Normally this is not important; the spectroscopist is interested only in the energy state of the atom as a whole. Should we wish to specify the energy states of individual electrons, however, we can do so by including them in the term symbol as a prefix. Thus in example 5 we might have $2p\,{}^2P_{3/2}$, or $1s2p3s\,{}^2P_{3/2}$, etc.

We can now apply our knowledge of atomic states to the discussion of the spectra of some atoms with two or more electrons. We start with the simplest, that of helium.

5.4.5 The Spectrum of Helium and the Alkaline Earths

Helium, atomic number two, consists of a central nucleus and two outer electrons. Clearly there are only two possibilities for the relative spins of the two electrons:

(1) their spins are paired; in which case if s_{1_z} is $+\frac{1}{2}$, s_{2_z} must be $-\frac{1}{2}$, hence $S_z = s_{1_z} + s_{2_z} = 0$, and so $S = 0$ and we have *singlet* states; or
(2) their spins are parallel; now $s_{1_z} = s_{2_z} = +\frac{1}{2}$, say, so that $S_z = 1$ and the states are *triplet*.

The lowest possible energy state of this atom is when both electrons occupy the 1*s* orbital; this, by Pauli's principle, is possible only if their spins are paired, so the ground state of helium must be a singlet state. Further $L = l_1 + l_2 = 0$, and hence J can only be zero. The ground state of helium, therefore, is ${}^1S_0$.

The relevant selection rules for many-electron systems are:

$$\Delta S = 0 \qquad \Delta L = \pm 1 \qquad \Delta J = 0, \pm 1 \tag{5.25}$$

(There is a further rule that a state with $J = 0$ cannot make a transition to another $J = 0$ state, but this will not concern us here.) We see immediately that, since S cannot change during a transition, the singlet ground state can undergo transitions only to other singlet states. The selection rules for L and J are the same as those for l and j considered earlier.

For the moment we shall imagine that only one electron undergoes transitions, leaving the other in the 1s orbital, and the left-hand side of Fig. 5.11 shows the energy levels for the various singlet states which arise.

Initially the $1s^2\ {}^1S_0$ state can undergo a transition only to $1s^1\ np^1$ states (abbreviated to $1snp$); in the latter $L = 1$, $S = 0$, and hence $J = 1$ only, so the transition may be symbolized:

$$1s^2\ {}^1S_0 \rightarrow 1snp\ {}^1P_1$$

or, briefly:

$${}^1S_0 \rightarrow {}^1P_1$$

From the ${}^1P_1$ state the system could either revert to ${}^1S_0$ states, as shown in the figure, or undergo transitions to the higher ${}^1D_2$ states (for these $S = 0$, $L = 2$, hence $J = 2$ only). In general, then, all these transitions will give rise to spectral series very similar to those of lithium except that here transitions are between *singlet* states only and all the spectral lines will be single.

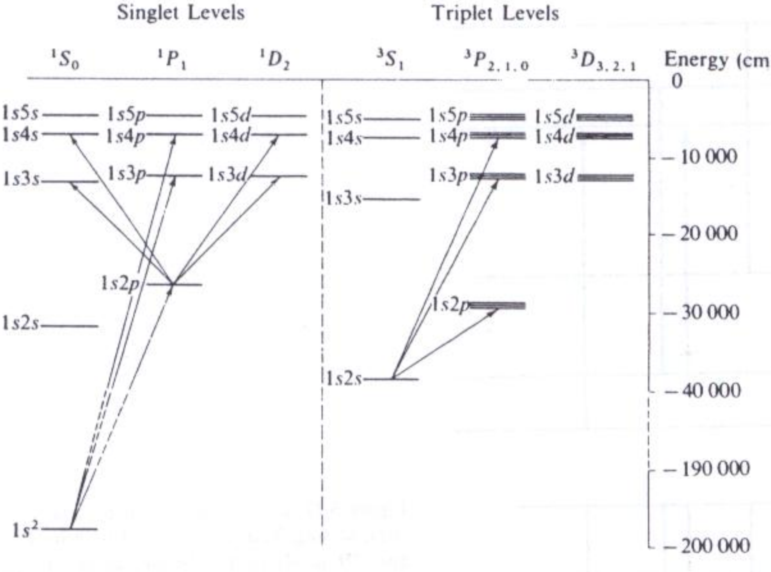

Figure 5.11 Some of the energy levels of the electrons in the helium atom together with a few allowed transitions.

Returning now to the situation in which the electron spins are parallel (case (2) the triplet states) we see that, since the electrons are now forbidden by Pauli's principle from occupying the same orbital, the lowest energy state is $1s2s$. This and other triplet energy levels are shown on the right of Fig. 5.11. The $1s2s$ state has $S = 1$, $L = 0$ and hence $J = 1$ only, and so it is ${}^3S_1$; by the selection rules of Eq. (5.25) it can only undergo transitions into the $1snp$ triplet states: these, with $S = 1$, $L = 1$, have $J = 2$, 1 or 0, and so the transitions may be written:

$${}^3S_1 \rightarrow {}^3P_2,\ {}^3P_1,\ {}^3P_0$$

All three transitions are allowed, since $\Delta J = 0$ or ± 1, so the resulting spectral lines will be *triplets*.

Transitions from the ${}^3P$ states may take place either to ${}^3S$ states (spectral series of triples) or to ${}^3D$ states. In the latter case the spectral series may be very complex if completely resolved. For ${}^3D$ we have $S = 1$, $L = 2$, hence $J = 3$, 2, or 1 and we show in Fig. 5.12 a transition between ${}^3P$ and ${}^3D$ states, bearing in mind the selection rule $\Delta J = 0, \pm 1$. We note that ${}^3P_2$ can go to each of ${}^3D_{3,2,1}$, ${}^3P_1$ can go only to ${}^3D_{2,1}$, and ${}^3P_0$ can go only to ${}^3D_1$. Thus the complete spectrum (shown at the foot of the figure) should consist of six lines. Normally, however, the very close spacing is not resolved, and only three lines are seen; for this reason the spectrum is referred to as a *compound triplet*.

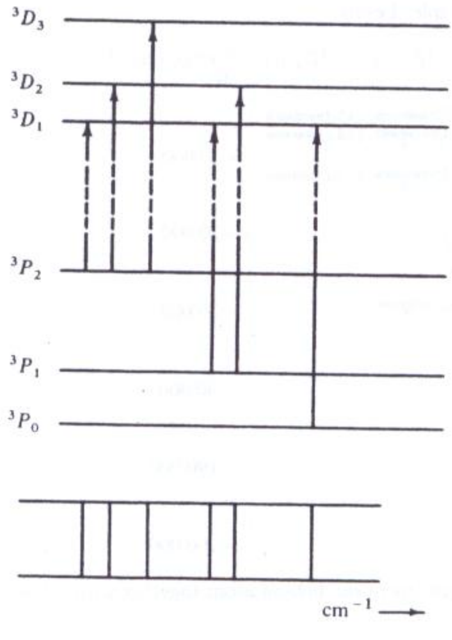

Figure 5.12 The 'compound triplet' spectrum arising from transitions between ${}^3P$ and ${}^3D$ levels in the helium atom. The separation between levels of different J is much exaggerated.

We might note in passing that Fig. 5.12 shows that levels with higher J have a higher energy in helium, and that the separation decreases from top to bottom. This is not the case with all atoms, however. If higher J is equivalent to lower energy then the separation *increases* from top to bottom and the multiplet is described as *inverted*. In helium, and other atoms with similar behaviour, the multiplet is *normal* or *regular*.

We see, then, that the spectrum of helium consists of spectral series grouped into two types which overlap each other in frequency. In one type, involving transitions between singlet levels, all the spectral lines are themselves singlets, while in the other the transitions are between triplet states and each 'line' is at least a close triplet and possibly even more complex. Because of the selection rule $\Delta S = 0$ there is a strong prohibition on transitions between singlet and triplet states, and transitions *cannot occur* between the right- and left-hand sides of Fig. 5.11. Early experimenters, noting the difference between the two types of spectral series, suggested that helium exists in two modifications, ortho- and para-helium. This is not far from the truth, although we know now that the difference between the two forms is very subtle: it is merely that one has its electron spins always opposed, and the other always parallel.

Other atoms containing two outer electrons exhibit spectra similar to that of helium. Thus the alkaline earths, beryllium, magnesium, calcium, etc., fall in this category, as do ionized species with just two remaining electrons, for example, B^+, C^{2+}, etc.

We should remind the reader at this point that the above discussion on helium has been carried through on the assumption that one electron remains in the 1*s* orbital all the time. This is a reasonable assumption since a great deal of energy would be required to excite *two* electrons simultaneously, and this would not happen under normal spectroscopic conditions. However, not all atoms have only *s* electrons in their ground state configuration, and we consider next some of the consequences.

5.4.6 Equivalent and Non-Equivalent Electrons; Energy Levels of Carbon

The ground state electronic configuration of carbon is $1s^22s^22p^2$, which indicates that both the 1*s* and 2*s* orbitals are filled (and hence contribute nothing to the angular momentum of the atom) while the 2*p* orbitals are only partially filled. The 2*p* electrons, also, are most easily removed, so it is these which normally undergo spectroscopic transitions.

Two or more electrons are referred to as *equivalent* if they have the same value of n and of l. Thus the two 2*p* electrons in the ground state of carbon are equivalent ($n_1 = n_2 = 2$, $l_1 = l_2 = 1$) while the set of 1*s*2*s* are non-equivalent ($n_1 \neq n_2$ although $l_1 = l_2$) as are, for example, 2*s*2*p* ($n_1 = n_2$ but $l_1 \neq l_2$). Special care is necessary when considering the total angular momentum of equivalent electrons since restrictions are placed on the values of the quantum numbers which each may have. Let us consider the case of $2p^2$ in some detail.

The first restriction arises from Pauli's principle (Sec. 5.3.1). Since we have $n_1 = n_2$ and $l_1 = l_2$ we cannot simultaneously choose $l_{1_z} = l_{2_z}$ *and* $s_{1_z} = s_{2_z}$.

Further restrictions follow from physical considerations. The basic principle is that electrons cannot be distinguished from each other and so if the energies of two electrons are exchanged we have no way of discovering experimentally that such exchange has taken place. The implication is that if the values of all four numbers n, l, l_z, and s_z for each of two electrons are exchanged, the initial situation is identical in every way with the final. When considering total momentum and the term symbols of atoms we are interested only in different situations and we must not count twice those systems which are interconvertible merely by an exchange of all four numbers n, l, l_z, and s_z. Consider some examples chosen from the $2p^2$ case:

1. We have $n_1 = n_2$, $l_1 = l_2$ and if we also choose $l_{1_z} = l_{2_z}$ then we know (Pauli's principle) that if $s_{1_z} = +\frac{1}{2}$, then $s_{2_z} = -\frac{1}{2}$; alternatively if $s_{1_z} = -\frac{1}{2}$ then $s_{2_z} = +\frac{1}{2}$. Now these two cases are completely identical because one can be reached from the other by exchanging n, l, l_z and s_z. Thus, while we can consider either set alone as typical of the state, we must not consider both together.
2. Similarly, if we assume $s_{1_z} = s_{2_z}$ then we know $l_{1_z} \neq l_{2_z}$. For p electrons $l = 1$ and hence $l_z = 1, 0$ or -1. So we might have:

$$\begin{array}{lll} s_{1_z} = s_{2_z}: & l_{1_z} = 1 & l_{2_z} = 0 \text{ or } -1 \\ & l_{1_z} = 0 & l_{2_z} = 1 \text{ or } -1 \\ & l_{1_z} = -1 & l_{2_z} = 1 \text{ or } 0 \end{array}$$

Note, however, that the system represented by the pair of values (1, 0) for (l_{1_z}, l_{2_z}) is identical with that for (0, 1); (0, −1) is identical with (−1, 0) and (1, −1) with (−1, 1). Thus we reduce the above six pairs to only three *different* sets:

$$\begin{array}{lll} s_{1_z} = s_{2_z}: & l_{1_z} = 1 & l_{2_z} = 0 \\ & l_{1_z} = 1 & l_{2_z} = -1 \\ & l_{1_z} = 0 & l_{2_z} = -1 \end{array}$$

3. Finally we note that if $l_{1_z} \neq l_{2_z}$ and $s_{1_z} \neq s_{2_z}$, then interchange of only *one* pair of values (for example, $s_{1_z} = +\frac{1}{2}$, $s_{2_z} = -\frac{1}{2}$, $\rightarrow s_{1_z} = -\frac{1}{2}$ $s_{2_z} = +\frac{1}{2}$) does produce a *different* situation; physically an electron

Table 5.3 Sub-states of two equivalent p electrons ($n_1 = n_2 = 2; l_1 = l_2 = 1$)

l_{1_z}	l_{2_z}	s_{1_z}	s_{2_z}	L_z $(l_{1_z} + l_{2_z})$	S_z $(s_{1_z} + s_{2_z})$	Substate
$+1$	$+1$	$+\frac{1}{2}$	$-\frac{1}{2}$	$+2$	0	(*a*)
$+1$	0	$+\frac{1}{2}$	$+\frac{1}{2}$	$+1$	$+1$	(*b*)
$+1$	0	$+\frac{1}{2}$	$-\frac{1}{2}$	$+1$	0	(*c*)
$+1$	0	$-\frac{1}{2}$	$+\frac{1}{2}$	$+1$	0	(*d*)
$+1$	0	$-\frac{1}{2}$	$-\frac{1}{2}$	$+1$	-1	(*e*)
$+1$	-1	$+\frac{1}{2}$	$+\frac{1}{2}$	0	$+1$	(*f*)
$+1$	-1	$+\frac{1}{2}$	$-\frac{1}{2}$	0	0	(*g*)
$+1$	-1	$-\frac{1}{2}$	$+\frac{1}{2}$	0	0	(*h*)
$+1$	-1	$-\frac{1}{2}$	$-\frac{1}{2}$	0	-1	(*i*)
0	0	$+\frac{1}{2}$	$-\frac{1}{2}$	0	0	(*j*)
0	-1	$+\frac{1}{2}$	$+\frac{1}{2}$	-1	$+1$	(*k*)
0	-1	$+\frac{1}{2}$	$-\frac{1}{2}$	-1	0	(*l*)
0	-1	$-\frac{1}{2}$	$+\frac{1}{2}$	-1	0	(*m*)
0	-1	$-\frac{1}{2}$	$-\frac{1}{2}$	-1	-1	(*n*)
-1	-1	$+\frac{1}{2}$	$-\frac{1}{2}$	-2	0	(*o*)

already distinguishable by its l_z value is being reversed in spin. All four numbers n, l, l_z, and s_z must be exchanged to produce and indistinguishable state.

Keeping these rules in mind we can construct Table 5.3, in which the four columns list combinations of l_{1_z}, l_{2_z}, s_{1_z}, and s_{2_z} leading to different energy states (let us call them substrates). We are interested in the *total* energy and so we show in the next two columns the values of $l_{1_z} + l_{2_z} = L_z$ and $s_{1_z} + s_{2_z} = S_z$ respectively. The final column merely supplies a convenient label to each substate for the following discussion. The 15 substates in the table constitute the z components of the various **L** and **S** vectors which may be formed from two equivalent p electrons. We can find the term symbols in the following way:

1. Note first that the largest L_z value in the table is $L_z = +2$ (substate (*a*)), and this is associated with $S_z = 0$. $L_z = +2$ must be a z component of the state $L = 2$, that is, one component of a D state, the other components of which are $L_z = +1, 0, -1$, and -2. In the table we can find several substates of the requisite L_z values, all associated with $S_z = 0$; it is immaterial which of the alternatives we choose, so let us take substates (*c*), (*g*), (*l*), and (*o*). Since $S_z = 0$ the state must be singlet, hence we have:

$$^1D = \text{substates } (a), (c), (g), (l), \text{ and } (o)$$

With $L = 2$, $S = 0$ this can only be a $^1D_2$ state.

2. Of the remaining substates the largest L_z is $+1$ associated with $S_z = +1$ (substate (*b*)). This is plainly one component of a ^3P state, the other components of which may be selected as:

^3P state: $S_z = +1$: $L_z = 1, 0,$ and -1, that is, (*b*), (*f*), (*k*)
$S_z = 0$: $L_z = 1, 0,$ and -1, that is, (*d*), (*h*), (*m*)
$S_z = -1$: $L_z = 1, 0,$ and -1, that is, (*e*), (*j*), (*n*)

Here we have considered the three components of $S = 1$, $S_z = +1, 0,$ and -1, to be associated in turn with the components of $L = 1$. The three states listed correspond to term symbols $^3P_2$, $^3P_1$, and $^3P_0$.

3. Finally the one remaining substate, (*j*), has $L_z = S_z = 0$ and this plainly comprises a $^1S_0$ state.

Overall, then, two equivalent *p* electrons give rise to the three different energy states ^1D, ^1S, and ^3P, of which the latter, being a triplet state, has three close energy levels $^3P_2$, $^3P_1$, and $^3P_0$. Hund's rule, which we quoted in Sec. 5.3.1, may be expressed for equivalent electrons as: 'The state of lowest energy for a given electronic configuration is that having the *greatest multiplicity*. If more than one state has the same multiplicity then the lowest of these is that with the greatest L value'.

Thus for carbon the ground state is the ^3P, the next in energy is the ^1D, and finally the ^1S. We note that this new expression of Hund's rule implies that electrons in degenerate orbitals tend to have their spins parallel (since this gives the greatest multiplicity, and hence lowest energy); this in turn means that electrons tend to go into separate orbitals since in the same orbital they must have paired spins. Thus we are justified in writing the electronic structures of carbon, nitrogen, and oxygen as in Table 5.2.

If now one of the $2p$ electrons of carbon is promoted to the $3p$ state we have the configuration $1s^2 2s^2 2p 3p$. This is an excited state in which the *p* electrons are non-equivalent. The interested student should show, by the method of Table 5.3, that six different term symbols can be found for this configuration, that is, ^1S, ^1P, ^1D, ^3S, ^3P, and ^3D. In this case, since $n_1 \neq n_2$, neither the Pauli principle nor the principle of indistinguishability offers restrictions to l_z and s_z values, and hence more terms result.

For non-equivalent electrons, however, it is simpler to deal directly with L and S values. Thus we have $s_1 + s_2 = 1$ or 0 depending upon whether the electron spins are parallel or opposed, while for $l_1 = l_2 = 1$ we can have $L = 2$, 1 or 0. We can then tabulate L, S, and J directly, together with their term symbols:

L	S	J	Term symbol
2	1	3, 2, or 1	$^3D_{3,2,1}$
2	0	2	$^1D_2$
1	1	2, 1 or 0	$^3P_{2,1,0}$
1	0	1	$^4P_1$
0	1	1	$^3S_1$
0	0	0	$^1S_0$

and we arrive at the six states listed previously. Note that this direct method is not applicable to equivalent electrons because summation of l to give L implies that all l_z are allowed: this, we have seen, is not true when the electrons are equivalent.

Many other electronic configurations occur, both for carbon and other atoms, in which two or more equivalent electrons contribute to the total energy. We shall not discuss these further, however, except to state that their total energies and term symbols may be discovered by the same process as exemplified above for $2p^2$ electrons.

We can, however, now conveniently discuss rather more fully the operation of the helium–neon laser which was mentioned briefly in Sec. 1.10. This is an example of a continuous laser; by means of an electric discharge the helium atoms in a mixture of helium and neon are excited and ionized. Those which are excited into singlet states decay by emitting radiation until they arrive in the ground state once more, ready for re-excitation; those excited to triplet states, however (see Fig. 5.11), can decay only as far as the $1s2s\ ^3S_1$ state, which is metastable, since the selection rule $\Delta S = 0$ prevents its reversion to the ground $1s^2\ ^1S_0$ state. The $1s2s\ ^3S_1$ state is about 160 000 cm^{-1} above the ground state.

Turning now to the other component of the mixture, neon, this has a ground state configuration $1s^22s^22p^6\ ^1S_0$; it happens that one of its excited states, the $1s^22s^22p^54s^1$, where one of the $2p$ electrons has been promoted to the $4s$ orbital, is very nearly 160 000 cm^{-1} above the ground state, so collisions between excited helium atoms and ground state neon atoms can result in a resonance exchange of energy:

$$\text{He}^* + \text{Ne} \rightarrow \text{He} + \text{Ne}^*$$

Thus the electric discharge essentially pumps *neon* atoms into an excited state. This state can undergo spontaneous decay to lower singlet states, but here the induced decay is quite important and, if radiation of about 8700 cm^{-1} is present, the decay to $1s^22s^22p^53p^1$ is induced, while radiation of 15 800 cm^{-1} results in decay to $1s^22s^22p^53s^1$—it is this latter which gives the usual 632.8 nm radiation from this laser.

The presence of radiation of the appropriate frequency is ensured by keeping the helium–neon mixture at low pressure in a tube placed between a pair of highly efficient mirrors. Thus the majority of the radiation is repeatedly reflected up and down the tube, and it is only the one per cent or so which 'escapes' through the mirrors that constitutes the useful output from the laser. Nonetheless, because all the available power is concentrated into a very narrow, highly monochromatic and coherent beam, these lasers are increasingly used as sources of light and power.

5.5 PHOTOELECTRON SPECTROSCOPY AND X-RAY FLUORESCENCE SPECTROSCOPY

5.5.1 Photoelectron Spectroscopy

The recently developed technique of Photoelectron Spectroscopy (PES) offers an excellent way of studying the electronic energy levels of atoms and—as we shall see in Sec. 6.2.5—of molecules too. Basically the method is equivalent to measuring the ionization energy of both outer (valence) electrons and the more firmly bound inner electrons; electrons are ejected from atoms or molecules essentially by giving them an energy 'kick' of known size and measuring the amount of excess energy with which each emerges from the atom or molecule.

For valence electrons the energy is usually provided by radiation from a helium lamp, in which low-pressure helium gas is excited by an electric discharge. The radiation arises when atoms excited into the $1s2p\ ^1P_1$ state (cf. Fig. 5.11) by the discharge return to the ground $1s^2\ ^1S_0$ state, and has a frequency of $5{\cdot}14 \times 10^{15}$ Hz and a wavelength of 58·4 nm. For our purposes, however, it is more convenient to think of this radiation as consisting of a stream of photons, each of energy $h\nu$, that is, $3{\cdot}41 \times 10^{-18}$ J (for those who still prefer non-SI units, this figure is equivalent to 21·2 eV). When such radiation falls on to a sample atom, one can think of a photon 'colliding' with an electron in the atom and giving up its energy. If the electron is held very firmly by its nucleus, $3{\cdot}14 \times 10^{-18}$ J may well not be enough to dislodge it, but if it is one of the outer electrons, a kick of this magnitude will certainly eject it from the atom. If its binding energy is small, say $0{\cdot}8 \times 10^{-18}$ J (or 5 eV), then it will leave with a kinetic energy equivalent to $(3{\cdot}4 - 0{\cdot}8) \times 10^{-18}\text{J} = 2{\cdot}6 \times 10^{-18}$ J, whereas if it is held with an energy of, say $3{\cdot}2 \times 10^{-18}$ J (20 eV), it will leave with a much smaller kinetic energy, only $0{\cdot}2 \times 10^{-18}$ J. We may write:

$$\text{Kinetic energy of ejection} = 3{\cdot}4 \times 10^{-18}\ \text{J} - \text{binding energy}$$

or, more generally:

$$\text{Kinetic energy} = h\nu - I \tag{5.26}$$

where $h\nu$ is the energy of the exciting radiation and I the binding energy (ionization potential) of the electron. In order to measure binding energies we clearly need a technique to estimate the kinetic energy, or velocity, of the ejected electrons.

There are two main approaches to this, both shown in Fig. 5.13. In (*a*) the radiation passes along the axis of a metal can, which contains a concentric metal grid, and which also holds the sample. Electrons ejected from sample atoms may pass through the grid and are then collected by the can, to be registered as a current by a sensitive electrometer. While the grid is uncharged, *all* the electrons emitted by the sample reach the can and the current is at its maximum. If now a negative potential is applied to the grid, slow-moving electrons will be repelled and will not reach the can, so the current falls. As the grid potential is increased from zero a curve of current (i.e., relative number of electrons reaching the can) versus grid potential (i.e., kinetic energy) can be plotted.

Figure 5.13(*b*) shows the second method. Here the electrons ejected from the sample are collimated into a beam by a slit in the can and then,

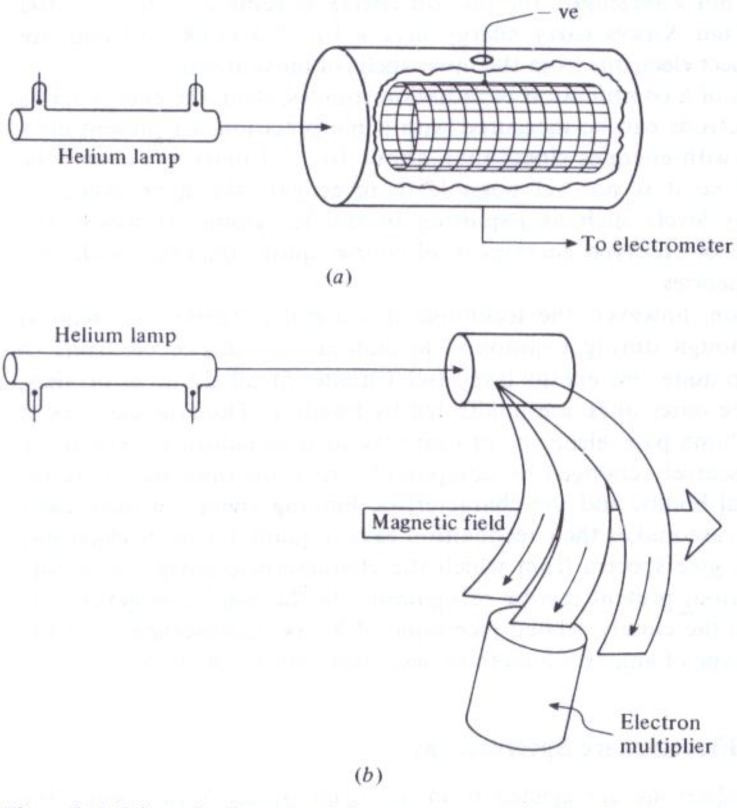

Figure 5.13 Schematic diagrams of the apparatus required for the observation of photoelectron spectra using (*a*) the electron retardation method, and (*b*) the velocity spectrometer method.

since all electrons have the same mass, they can be sorted into their velocities by a magnetic field—a simple form of velocity spectrometer akin to a mass spectrometer. The path of moving electrons is curved into a circle whose radius is directly proportional to their velocity and inversely proportional to the magnitude of the field, so that increasing the field from zero causes electrons of successively higher velocities to be recorded by the cascade electron detector.

The grid method of Fig. 5.13(*a*) has the advantage of higher sensitivity in that electrons emitted in all directions from sample atoms are collected by the can, whereas in the velocity spectrometer of Fig. 5.13(*b*) only those electrons passing through the slit are utilized. The latter method is advantageous, however, when experiments concerning the directional nature (or polarization) of the ejected electrons are undertaken.

While the 58·4 nm helium radiation is sufficiently energetic to eject valence electrons from all other elements, it cannot disturb *inner* electrons. For these the lamp may be replaced by an X-ray source; for example with X-rays of 10 nm wavelength, the photon energy is some 2×10^{-17} J (100 eV), while 1 nm X-rays carry energy of 2×10^{-16} J (1000 eV) and are sufficient to eject electrons from the inner shells of most atoms.

By means of a combination of radiation sources, then, the energy levels of atomic electrons can be measured with some precision. At present electrons ejected with energies closer than about 10^{-21} J (0·01 eV) cannot be distinguished, so it is not yet possible to investigate the finer details of atomic energy levels such as *j*-splitting in smaller atoms. However, the broad pattern of observed energies is, of course, quite consistent with current atomic theories.

In addition, however, the technique has useful potential in chemical analysis. Although during compound formation the valence electrons of atoms take up quite new energy levels (see Chapter 6), all the inner orbitals, and even some outer ones, are unaffected by bonding. Thus the energies of the so-called 'lone pair' electrons of elements such as chlorine, oxygen, or nitrogen are scarcely changed by compound formation since they play no part in normal bonds, and the characteristic binding energy of these electrons in each case makes their recognition easy. Equally for inner electrons, X-ray sources give spectra from which the characteristic energy level pattern of each atom present can be recognized. On the whole, however, it is simpler to use the closely related technique of X-ray fluorescence spectroscopy for this type of analysis, a method described very briefly in Sec. 5.5.2.

5.5.2 X-ray Fluorescence Spectroscopy

When inner electrons are ejected from an atom by an X-ray beam, the 'holes' left in the inner orbitals are rapidly filled by electrons dropping down from higher levels; much of the energy which they emit during this process appears in the X-ray region, but to lower frequency than the original exciting beam—the substance is said to *fluoresce*. The emitted secondary X-rays may be readily analysed into their component frequencies by diffraction from a crystal surface, since this forms a grating with appropriately sized spacings for the wavelengths involved. Now since the inner orbital energies are quite unaffected by external influences, and since each atom has its own quite characteristic pattern of energy levels, X-ray fluorescence spectroscopy is an excellent, rapid, and quite unambiguous method of detecting and estimating particular atoms in a sample. The technique is, for instance, widely used to estimate the composition of alloys, particularly since the analysis is sufficiently rapid for a sample to be withdrawn from the melt and analysed in time for adjustments to be made to the bulk alloy composition before casting.

5.6 THE ZEEMAN EFFECT

We have been concerned in this chapter with two sorts of electronic energy. Firstly, there is energy of *position*—energy arising by virtue of interaction between electrons and the nucleus and between electrons and other electrons in the same atom. This energy can be described in terms of the n and l quantum numbers, although we have discussed it, rather less precisely, by drawing energy level diagrams. Secondly, there is energy of *motion*—energy arising from the summed orbital and spin momenta of the electrons in the atom which depends on the l_z and s_z values of each electron and the way in which these are coupled. This gives rise to the fine structure of spectroscopic lines discussed earlier.

Angular momentum can be considered as arising from a physical movement of electrons about the nucleus and, since electrons are charged, such motion constitutes a circulating electric current and hence a magnetic field. This field can, indeed, be detected, and it is its interaction with exterior fields which is the subject of this section.

We can represent the angular momentum field by a vector $\boldsymbol{\mu}$—the magnetic dipole of the atom—and it is readily shown that $\boldsymbol{\mu}$ is directly proportional to the angular momentum $\mathbf{J}$ and has the same direction. If the electron is considered as a point of mass m and charge e, then we have:

$$\boldsymbol{\mu} = -\frac{e}{2m}\mathbf{J} \quad \mathrm{JT^{-1}}$$

(Here we use the SI unit of magnetic field, the tesla (T), which is equivalent to 10 000 gauss in electromagnetic units.) But quantum mechanics indicates that the electron is not a point charge and a more exact expression for $\boldsymbol{\mu}$ is:

$$\boldsymbol{\mu} = -\frac{ge}{2m}\mathbf{J} = -\frac{ge}{2m}\sqrt{J(J+1)}\,\frac{h}{2\pi} \quad \mathrm{J\,T^{-1}} \tag{5.27}$$

where g is a purely numerical factor, called the Landé splitting factor. This factor depends on the state of the electrons in the atom and is given by:

$$g = \frac{3}{2} + \frac{S(S+1) - L(L+1)}{2J(J+1)} \tag{5.28}$$

In general g lies between 0 and 2.

We now recall (cf. Eq. (5.13) for one electron) that **J** can have either integral or half-integral components J_z along a reference direction, depending upon whether the quantum number J is integral or half-integral. Figure 5.14(*a*) shows this for a state with $J = \frac{3}{2}$, the $2J + 1$ components being given in general by:

$$J_z = J, J-1, \ldots, \tfrac{1}{2} \text{ or } 0, \ldots, -J \tag{5.29}$$

Further, since $\boldsymbol{\mu}$ is proportional to **J**, $\boldsymbol{\mu}$ will also have components in the z direction which are given by:

$$\mu_z = -\frac{ge}{2m}\frac{h}{2\pi} J_z \tag{5.30}$$

These are shown diagrammatically at Fig. 5.14(*b*). If now an external field is applied to the atom, thus specifying the previously arbitrary z direction, the atomic dipole $\boldsymbol{\mu}$ will interact with the applied field to an extent depending on its component in the field direction. If the strength of the applied field is B_z then the extent of the interaction is simply $\mu_z B_z$:

$$\text{Interaction} = \Delta E = \mu_z B_z = -\frac{heg}{4\pi m} B_z \quad \text{J} \tag{5.31}$$

In this equation we have expressed the interaction as ΔE since the application of the field splits the originally degenerate energy levels corresponding to the $2J + 1$ values of J_z into $2J + 1$ *different* energy levels. This is shown for $J = \frac{3}{2}$ in Fig. 5.14(*c*). It is this splitting, or lifting of the degeneracy on the application of an external magnetic field, which is called the *Zeeman effect* after its discoverer.

The energy splitting is very small; the factor $he/4\pi m$ in Eq. (5.31), known as the *Bohr magneton*, has a value of $9{\cdot}27 \times 10^{-24}$ J T^{-1}; thus for $g = 1$, and for an applied field B_z of one tesla (that is, 10 000 gauss), the interaction energy is only some 10^{-23} joules, which in turn is of the order $0{\cdot}5$ cm^{-1}. This small splitting is, of course, reflected in a splitting of the spectral transitions observed when a magnetic field is applied to an atom. In order to discuss the effect on the spectrum we need one further selection rule:

$$\Delta J_z = 0, \pm 1$$

Let us consider the doublet lines in the sodium spectrum produced, as we have discussed in Sec. 5.3.2, by transitions between the $^2S_{1/2}$ states and

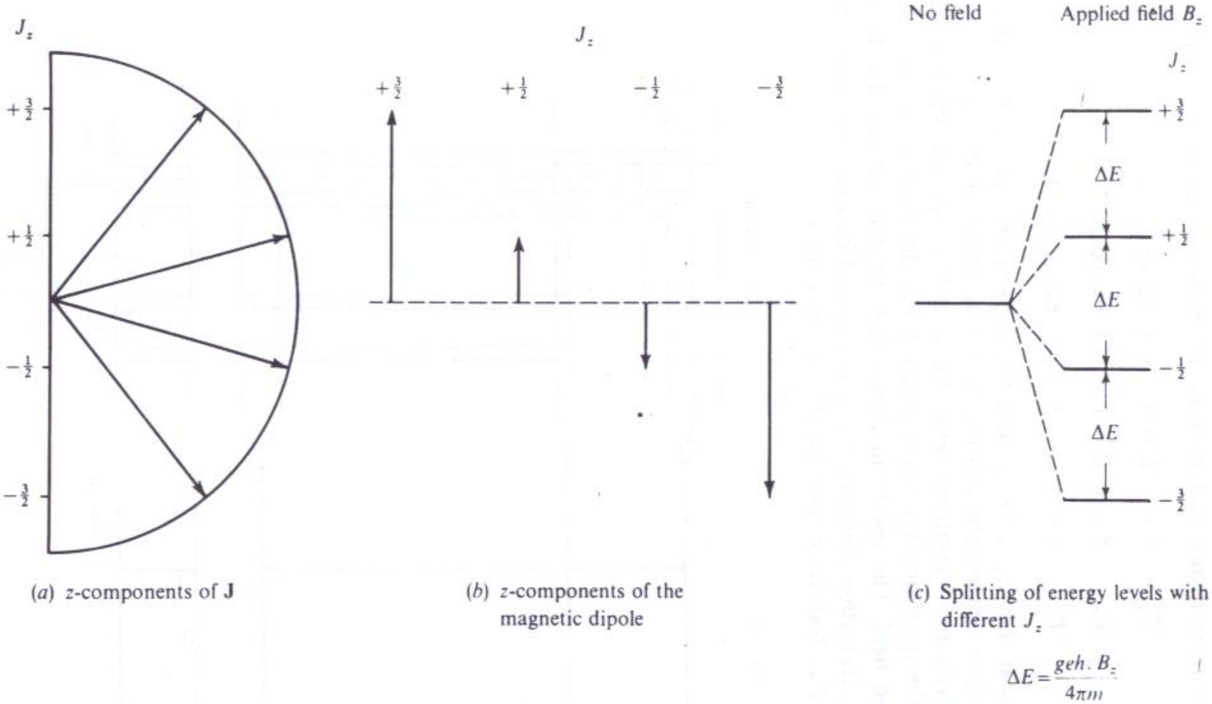

(*a*) *z*-components of **J**

(*b*) *z*-components of the magnetic dipole

(*c*) Splitting of energy levels with different J_z

$$\Delta E = \frac{geh \, . \, B_z}{4\pi m}$$

Figure 5.14 The effect of an applied magnetic field on the energy levels of an electron with $J = \frac{3}{2}$. In (*a*) the $2J + 1 = 4$ components of J are shown, and in (*b*) their corresponding magnetic moments in the reference direction. An external field splits the originally degenerate levels into four separate levels as in (*c*).

the $^2P_{1/2}$ and $^2P_{3/2}$ states. When a field B_z is applied to the atom, the $^2S_{1/2}$ and $^2P_{1/2}$ states are both split into two (since $J = \frac{1}{2}$, $2J + 1 = 2$), while the $^2P_{3/2}$ is split into four. The extent of the splitting (Eq. (5.31)) is proportional to the g factor in each state and, from Eq. (5.28) we can easily calculate:

$$^2S_{1/2}\text{:}\quad S = \tfrac{1}{2},\ L = 0,\ J = \tfrac{1}{2},\ \text{hence } g = 2$$

$$^2P_{1/2}\text{:}\quad S = \tfrac{1}{2},\ L = 1,\ J = \tfrac{1}{2},\ \text{hence } g = \tfrac{2}{3}$$

$$^2P_{3/2}\text{:}\quad S = \tfrac{1}{2},\ L = 1,\ J = \tfrac{3}{2},\ \text{hence } g = 1\tfrac{1}{3}$$

and we see that the $^2S_{1/2}$, $^2P_{1/2}$, and $^2P_{3/2}$ levels are split in the ratio of 3 : 1 : 2. We show the situation in Fig. 5.15. On the left of the figure we see the energy levels and transitions *before* the field B_z is applied; the levels are unsplit and the spectrum is a simple doublet. On the right we see the effect of the applied field. The spectrum shows that the original line due to the $^2S_{1/2} \rightarrow {}^2P_{1/2}$ transition disappears and is replaced by *four* new lines, while the $^2S_{1/2} \rightarrow {}^2P_{3/2}$ transition is replaced by *six* new lines.

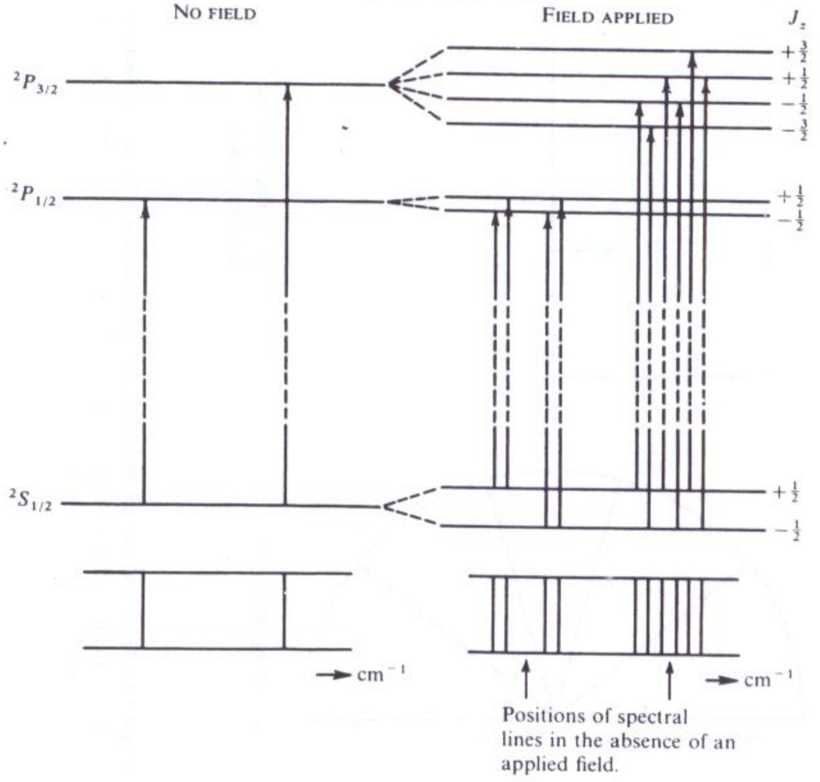

Figure 5.15 The Zeeman effect on transitions between ^2S and ^2P states. The situation before the field is applied is shown on the left, that after on the right.

The effect described above is usually referred to as the *anomalous Zeeman effect*—although, in fact, most atoms show the effect in this form. The *normal Zeeman effect* applies to transitions between singlet states only (e.g., the transitions of electrons in the helium atom shown on the left of Fig. 5.11). For singlet states we have:

$$2S + 1 = 1 \qquad \text{hence} \qquad S = 0$$

$$\therefore\ J = L \qquad \text{and} \qquad g = 1 \qquad \text{(cf. Eq. (5.28))}$$

Thus the splitting between all singlet levels is identical for a given applied field and the corresponding Zeeman spectrum is considerably simplified.

In general, the Zeeman effect can give very useful information about the electronic states of atoms. In the first place, the number of lines into which each transition becomes split when a field is applied depends on the J value of the states between which transitions arise. Next the g value, deduced from the splitting for a known applied field, gives information about the L and S values of the electron undergoing transitions. Overall, then, the term symbols for various atomic states can be deduced by Zeeman experiments. In this way all the details of atomic states, term symbols, etc., discussed above, have been amply confirmed experimentally.

5.7 THE INFLUENCE OF NUCLEAR SPIN

The nuclei of many atoms are known to be spinning about an axis. We shall discuss at some length in Chapter 7 the spectrum which this spin may give rise to in the radiofrequency region, but it is pertinent here to consider very briefly what effect such spin may have on the electronic spectra of atoms.

The nuclear spin quantum number I may be zero, integral, or half-integral depending on the particular nucleus considered. Thus the nuclear angular momentum, given by

$$\mathbf{I} = \sqrt{I(I+1)}\,\frac{h}{2\pi} = \sqrt{I(I+1)} \text{ units} \tag{5.32}$$

can have values 0, $\sqrt{3}/2$, $\sqrt{2}$, $\sqrt{15}/2$, etc.

The effect of $\mathbf{I}$ on the spectrum can be understood if we define the total momentum (electronic + nuclear) of an atom by $\mathbf{F}$:

$$\mathbf{F} = \sqrt{F(F+1)}\,\frac{h}{2\pi} = \sqrt{F(F+1)} \text{ units} \tag{5.33}$$

where F is the *total momentum quantum number*. If, as before, J is the total electronic quantum number, then we may write

$$F = J + I,\ J + I - 1,\ \ldots,\ |J - I| \tag{5.34}$$

thus giving $2J + 1$ or $2I + 1$ different energy states, whichever is the less.

The energy-level splitting due to nuclear spin is of the order 10^{-3} that due to electron spin; thus extremely fine resolving power is necessary for its observation and it is normally referred to as *hyperfine structure*.

5.8 CONCLUSION

This completes all we have to say about atomic spectroscopy. In the next chapter we extend the ideas introduced here to cover the electronic spectra of simple molecules, and we shall briefly discuss the techniques of electronic spectroscopy.

BIBLIOGRAPHY

See the Bibliography to Chapter 6 with the following important additions:

Herzberg, G.: *Atomic Spectra and Atomic Structure*, Dover, 1944.
Kuhn, M. G.: *Atomic Spectra*, Academic Press, 1962.
Shore, B. W., and D. H. Menzel: *Principles of Atomic Spectra*, Wiley, 1968.

PROBLEMS

(Useful constants: $R = 109\,677{\cdot}581$ cm^{-1}; 1 cm$^{-1} \equiv 11{\cdot}958$ J mol^{-1}.)

5.1 Calculate the first three lines in the absorption spectrum arising from transitions from the 3*s* level of the hydrogen atom; what is the ionization energy of this level?

5.2 The term symbol for a particular atomic state is quoted as $^4D_{5/2}$. What are the values of L, S, and J for this state? What is the minimum number of electrons which could give rise to this? Suggest a possible electronic configuration.

5.3 What are the term symbols for the following pairs of non-equivalent electrons: (*a*) *ss*, (*b*) *pp*, (*c*) *sd*, and (*d*) *pd*?

5.4 What are the term symbols for the following pairs of equivalent electrons: (*a*) s^2, (*b*) p^2, and (*c*) d^2?

5.5 The term symbols for particular states of three different atoms are quoted as $^4S_1$, $^2D_{7/2}$, and $^0P_1$; explain why these are erroneous.

5.6 Figure 5.7 (p. 170) shows the three transitions arising between ^2P and ^2D states; into how many lines would each of these transitions split if a magnetic field were applied? (Assume that the g-value is different for each energy level.)

5.7 Show that the p^3 configuration with equivalent electrons contains the states ^2D, ^2P, and ^4S. Which state is lowest in energy? What additional states arise if the electrons are non-equivalent?

CHAPTER

SIX

ELECTRONIC SPECTROSCOPY OF MOLECULES

In the first section of this chapter we shall discuss, in some detail, the electronic spectra of diatomic molecules. We shall find that the overall appearance of such spectra can be considered without assuming any knowledge of molecular structure, without reference to any particular electronic transition, and indeed, with little more than a formal understanding of the nature of electronic transitions within molecules. In Sec. 6.2 we shall summarize modern ideas of molecular structure and show how these lead to a classification of electronic states analogous to the classification of atomic states discussed in the previous chapter. Section 6.3 will extend the ideas of Secs 6.1 and 6.2 to polyatomic molecules and Sec. 6.4 will deal briefly with experimental techniques.

6.1 ELECTRONIC SPECTRA OF DIATOMIC MOLECULES

6.1.1 The Born–Oppenheimer Approximation

As a first approach to the electronic spectra of diatomic molecules we may use the Born–Oppenheimer approximation previously mentioned in Sec. 3.2; in the present context this may be written:

$$E_{\text{total}} = E_{\text{electronic}} + E_{\text{vibration}} + E_{\text{rotation}} \tag{6.1}$$

which implies that the electronic, vibrational, and rotational energies of a molecule are completely independent of each other. We shall see later to what extent this approximation is invalid. A change in the total energy of a molecule may then be written:

$$\Delta E_{\text{total}} = \Delta E_{\text{elec.}} + \Delta E_{\text{vib.}} + \Delta E_{\text{rot.}} \quad \text{J}$$

or

$$\Delta \varepsilon_{\text{total}} = \Delta \varepsilon_{\text{elec.}} + \Delta \varepsilon_{\text{vib.}} + \Delta \varepsilon_{\text{rot.}} \quad \text{cm}^{-1} \tag{6.2}$$

The approximate orders of magnitude of these changes are:

$$\Delta \varepsilon_{\text{elec.}} \approx \Delta \varepsilon_{\text{vib.}} \times 10^3 \approx \Delta \varepsilon_{\text{rot.}} \times 10^6 \tag{6.3}$$

and so we see that vibrational changes will produce a 'coarse structure' and rotational changes a 'fine structure' on the spectra of electronic transitions. We should also note that whereas pure rotation spectra (Chapter 2) are shown only by molecules possessing a permanent electric dipole moment, and vibrational spectra (Chapter 3) require a change of dipole during the motion, electronic spectra are given by *all* molecules since changes in the electron distribution in a molecule are always accompanied by a dipole change. This means that homonuclear molecules (for example, H_2 or N_2), which show no rotation or vibration–rotation spectra, *do* give an electronic spectrum and show vibrational and rotational structure in their spectra from which rotational constants and bond vibration frequencies may be derived.

Initially we shall ignore rotational fine structure and discuss the appearance of the vibrational coarse structure of spectra.

6.1.2 Vibrational Coarse Structure: Progressions

Ignoring rotational changes means that we rewrite Eq. (6.1) as

$$E_{\text{total}} = E_{\text{elec.}} + E_{\text{vib.}} \quad \text{J}$$

or

$$\varepsilon_{\text{total}} = \varepsilon_{\text{elec.}} + \varepsilon_{\text{vib.}} \quad \text{cm}^{-1} \tag{6.4}$$

From Eq. (3.12) we can write immediately:

$$\varepsilon_{\text{total}} = \varepsilon_{\text{elec.}} + (v + \tfrac{1}{2})\bar{\omega}_e - x_e(v + \tfrac{1}{2})^2\bar{\omega}_e \quad \text{cm}^{-1} \qquad (v = 0, 1, 2, \ldots) \tag{6.5}$$

The energy levels of this equation are shown in Fig. 6.1 for two arbitrary values of $\varepsilon_{\text{elec.}}$. As in previous chapters the lower states are distinguished by a *double* prime (v'', $\varepsilon''_{\text{elec.}}$), while the upper states carry only a *single* prime (v', $\varepsilon'_{\text{elec.}}$). Note that such a diagram cannot show correctly the relative separations between levels of different $\varepsilon_{\text{elec.}}$, on the one hand, and those with different v' or v'' on the other (cf. Eq. (6.3)), but that the spacing between the upper vibrational levels is deliberately shown to be rather smaller than that between the lower; this is the normal situation since an excited electronic state usually corresponds to a weaker bond in the molecule and hence a smaller vibrational wavenumber $\bar{\omega}_e$.

There is essentially no selection rule for v when a molecule undergoes an electronic transition, i.e., every transition $v'' \rightarrow v'$ has some probability, and a great many spectral lines would, therefore, be expected. However, the situation is considerably simplified if the *absorption* spectrum is considered from the electronic ground state. In this case, as we have seen in Sec. 3.1.3, virtually all the molecules exist in the lowest vibrational state, that is, $v'' = 0$, and so the only transitions to be observed with appreciable intensity are those indicated in Fig. 6.1. These are conventionally labelled according to their (v', v'') numbers (note: upper state *first*), that is, (0, 0), (1, 0), (2, 0), etc. Such a set of transitions is called a *band* since, under low resolution, each line of the set appears somewhat broad and diffuse, and is more particularly called a v' *progression*, since the value of v' increases by unity for each line in the set. The diagram shows that the lines in a band crowd together more closely at high frequencies; this is a direct consequence of the anharmonicity of the upper state vibration which causes the excited vibrational levels to converge.

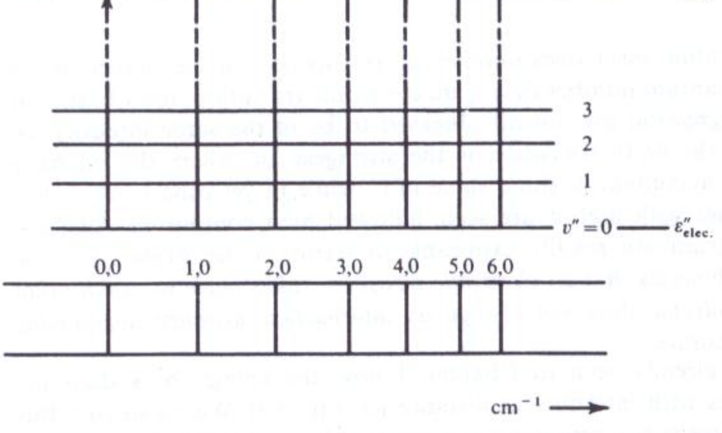

Figure 6.1 The vibrational 'coarse' structure of the band formed during electronic absorption from the ground ($v'' = 0$) state to a higher state.

An analytical expression can easily be written for this spectrum. From Eq. (6.5) we have immediately:

$$\Delta\varepsilon_{\text{total}} = \Delta\varepsilon_{\text{elec.}} + \Delta\varepsilon_{\text{vib.}}$$

$$\therefore\ \bar{\nu}_{\text{spec.}} = (\varepsilon' - \varepsilon'') + \{(v' + \tfrac{1}{2})\bar{\omega}'_e - x'_e(v' + \tfrac{1}{2})^2\bar{\omega}'_e\} - \{(v'' + \tfrac{1}{2})\bar{\omega}''_e - x''_e(v'' + \tfrac{1}{2})^2\bar{\omega}''_e\} \quad \text{cm}^{-1} \qquad (6.6)$$

and, provided some half-dozen lines can be observed in the band, values for $\bar{\omega}'_e$, x'_e, $\bar{\omega}''_e$, and x''_ε, as well as the separation between electronic states, $(\varepsilon' - \varepsilon'')$, can be calculated. Thus the observation of a band spectrum leads not only to values of the vibrational frequency and anharmonicity constant in the ground state ($\bar{\omega}''_e$ and x''_e), but also to these parameters in the excited electronic state ($\bar{\omega}'_e$ and x'_e). This latter information is particularly valuable since such excited states may be extremely unstable and the molecule may exist in them for very short times; nonetheless the band spectrum can tell us a great deal about the bond strength of such species.

We shall see later that molecules normally have many excited electronic energy levels, so that the whole absorption spectrum of a diatomic molecule will be more complicated than Fig. 6.1 suggests: the ground state can usually undergo a transition to several excited states, and each such transition will be accompanied by a band spectrum similar to Fig. 6.1.

Further, in *emission spectra* the previously excited molecule may be in one of a large number of available (ε', v') states, and has a similar multitude of (ε'', v'') states to which it may revert. Thus emission spectra are usually extremely complicated, and a great deal of care and patience is needed for a complete analysis.

6.1.3 Intensity of Vibrational–Electronic Spectra: the Franck–Condon Principle

Although quantum mechanics imposes no restrictions on the change in the vibrational quantum number during an electronic transition, the vibrational lines in a progression are not all observed to be of the same intensity. In some spectra the (0, 0) transition is the strongest, in others the intensity increases to a maximum at some value of v', while in yet others only a few vibrational lines with high v' are seen, followed by a continuum. All these types of spectrum are readily explicable in terms of the *Franck–Condon principle* which states that *an electronic transition takes place so rapidly that a vibrating molecule does not change its internuclear distance appreciably during the transition.*

We have already seen in Chapter 3 how the energy of a diatomic molecule varies with internuclear distance (cf. Fig. 3.3). We recall that this figure, the Morse curve, represents the energy when one atom is considered fixed on the $r = 0$ axis and the other is allowed to oscillate between the

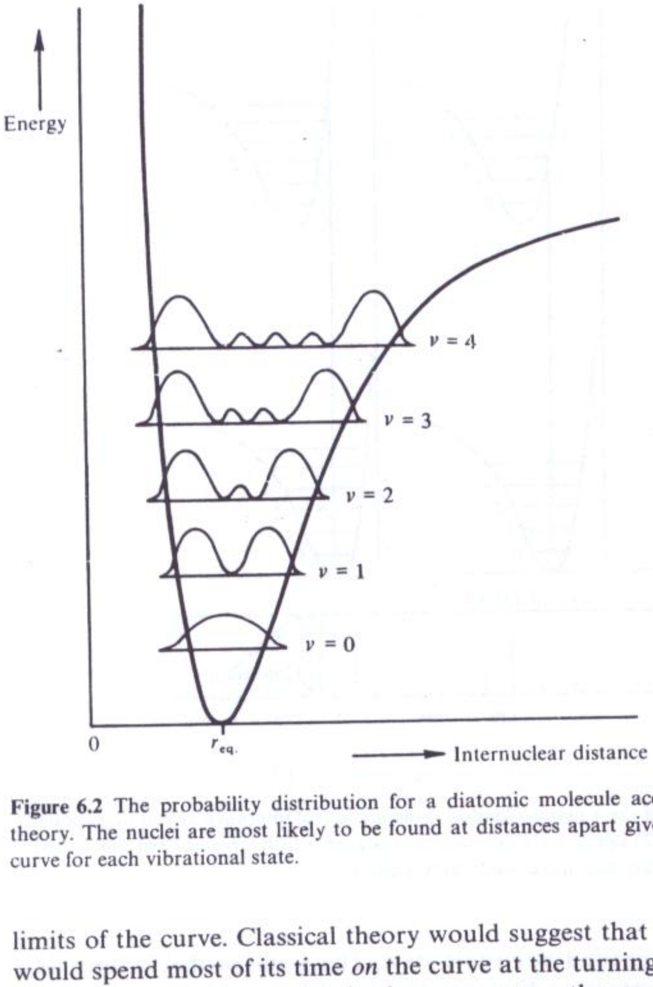

Figure 6.2 The probability distribution for a diatomic molecule according to the quantum theory. The nuclei are most likely to be found at distances apart given by the maxima of the curve for each vibrational state.

limits of the curve. Classical theory would suggest that the oscillating atom would spend most of its time *on* the curve at the turning point of its motion, since it is moving most slowly there; quantum theory, while agreeing with this view for high values of the vibrational quantum number, shows that for $v = 0$ the atom is most likely to be found at the *centre* of its motion, i.e., at the equilibrium internuclear distance $r_{\text{eq.}}$. For $v = 1, 2, 3, \ldots$ the most probable positions steadily approach the extremities until, for high v, the quantal and classical pictures merge. This behaviour is shown in Fig. 6.2 where we plot the probability distribution in each vibrational state against internuclear distance. Those who have studied quantum mechanics will realize that Fig. 6.2 shows the variation of ψ^2 with internuclear distance, where ψ is the vibrational wave function.

If a diatomic molecule undergoes a transition into an upper electronic state in which the excited molecule is stable with respect to dissociation into its atoms, then we can represent the upper state by a Morse curve similar in

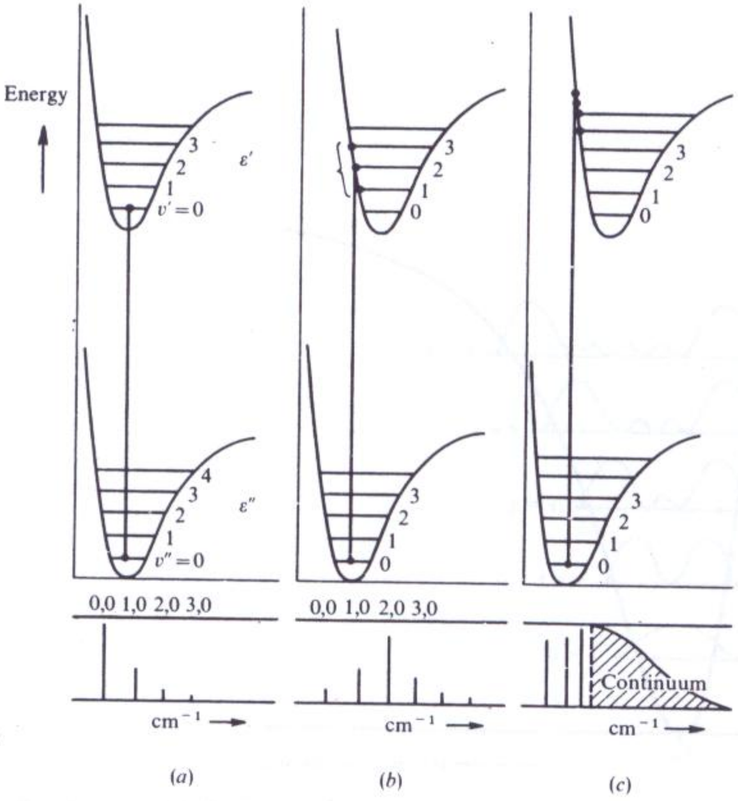

Figure 6.3 The operation of the Franck–Condon principle for (*a*) internuclear distances equal in upper and lower states, (*b*) upper-state internuclear distance a little greater than that in the lower state, and (*c*) upper-state distance considerably greater.

outline to that of the ground electronic state. There will probably (but not necessarily) be differences in such parameters as vibrational frequency, equilibrium internuclear distance, or dissocation energy between the two states, but this simply means that we should consider each excited molecule as a new, but rather similar, molecule with a different, but also rather similar, Morse curve.

Figure 6.3 shows three possibilities. In (*a*) we show the upper electronic state having the same equilibrium internuclear distance as the lower. Now the Franck–Condon principle suggests that a transition occurs *vertically* on this diagram, since the internuclear distance does not change, and so if we consider the molecule to be initially in the ground state both electronically (ε'') and vibrationally ($v''=0$), then the most probable transition is that indicated by the vertical line in Fig. 6.3(*a*). Thus the strongest spectral line of the $v''=0$ progression will be the (0, 0). However, the quantum theory only says that the *probability* of finding the oscillating atom is greatest at the equilibrium distance in the $v = 0$ state—it allows some, although small, chance of the atom being near the extremities of its vibrational motion. Hence there is some chance of the transition starting from the ends of the $v'' = 0$ state and finishing in the $v' = 1, 2,$ etc., states. The (1, 0), (2, 0), etc., lines diminish rapidly in intensity, however, as shown at the foot of Fig. 6.3(*a*).

In Fig. 6.3(*b*) we show the case where the excited electronic state has a *slightly* greater internuclear separation than the ground state. Now a vertical transition from the $v'' = 0$ level will most likely occur into the upper vibrational state $v' = 2$, transitions to lower and higher v' states being less likely; in general the upper state most probably reached will depend on the difference between the equilibrium separations in the lower and upper states. In Fig. 6.3(*c*) the upper state separation is drawn as *considerably* greater than that in the lower state and we see that, firstly, the vibrational level to which a transition takes place has a high v' value. Further, transitions can now occur to a state where the excited molecule has energy in excess of its own dissociation energy. From such states the molecule will dissociate without any vibrations and, since the atoms which are formed may take up any value of kinetic energy, the transitions are not quantized and a continuum results. This is shown at the foot of the figure. We consider the phenomenon of dissociation more fully in the next section.

The situation is rather more complex for emission spectra and for absorption from an excited vibrational state, for now transitions take place from *both ends* of the vibrational limits with equal probability; hence each progression will show two maxima which will coincide only if the equilibrium separations are the same in both states.

6.1.4 Dissociation Energy and Dissociation Products

Figure 6.4(*a*) and (*b*) shows two of the ways in which electronic excitation can lead to dissociation (a third way called *predissociation*, will be considered in Sec. 6.1.7). Part (*a*) of the figure represents the case, previously discussed, where the equilibrium nuclear separation in the upper state is considerably greater than that in the lower. The dashed line limits of the Morse curves represent the dissociation of the normal and excited molecule into atoms, the dissociation energies being D''_0 and D'_0 from the $v = 0$ state in each case. We see that the total energy of the dissociation products (i.e., atoms) from the upper state is greater by an amount called $E_{\text{ex.}}$ than that of the products of dissociation in the lower state. This energy is the *excitation energy* of one (or rarely both) of the atoms produced on dissociation.

We saw in the previous section that the spectrum of this system consists of some vibrational transitions (quantized) followed by a continuum (non-quantized transitions) representing dissociation. The lower wavenumber

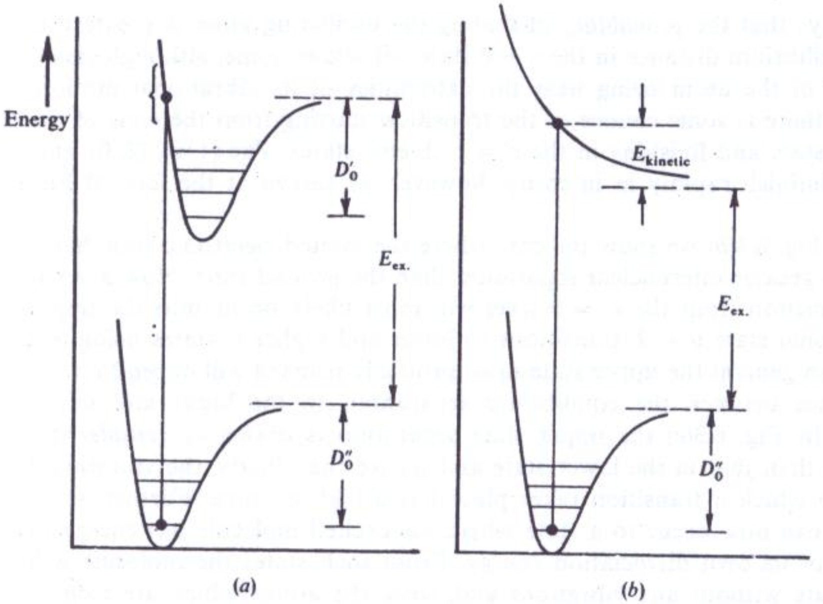

Figure 6.4 Illustrating dissociation by excitation into (*a*) a stable upper state, and (*b*) a continuous upper state.

limit of this continuum must represent just sufficient energy to cause dissociation and no more (i.e., the dissociation products separate with virtually zero kinetic energy) and thus we have

$$\bar{\nu}_{(\text{continuum limit})} = D_0'' + E_{ex.} \quad \text{cm}^{-1} \tag{6.7}$$

and we see that we can measure D_0'', the dissociation energy, if we know $E_{ex.}$, the excitation energy of the products, whatever they may be. Now, although the excitation energy of atoms to various electronic states is readily measurable by atomic spectroscopy (cf. Chapter 5), the precise *state* of dissociation products is not always obvious. There are several ways in which the total energy $D_0'' + E_{ex.}$ may be separated into its components, however; here we shall mention just two.

Firstly, thermochemical studies often lead to an approximate value of D_0'' and hence, since $D_0'' + E_{ex.}$ is accurately measurable spectroscopically, a rough value for $E_{ex.}$ is obtained. When the spectrum of the atomic products is studied, it usually happens that only one value of excitation energy corresponds at all well with $E_{ex.}$. Thus the state of the products is known, $E_{ex.}$ measured accurately, and a precise value of D_0'' deduced.

Secondly, if more than one spectroscopic dissociation limit is found, corresponding to dissociation into two or more different states of products with different excitation energies, the separations between the excitation energies are often found to correspond closely with the separations between only one set of excited states of the atoms observed spectroscopically. Thus the nature of the excited products and their energies are immediately known.

In Fig. 6.4(*b*) we illustrate the case in which the upper electronic state is *unstable*: there is no minimum in the energy curve and, as soon as a molecule is raised to this state by excitation, the molecule dissociates into products with total excitation energy $E_{\text{ex.}}$. The products fly apart with kinetic energy E_{kinetic} which represents (as shown on the figure) the excess energy in the final state above that needed just to dissociate the molecule. Since E_{kinetic} is not quantized the whole spectrum for this system will exhibit a continuum the lower limit of which (if observable) will be precisely the energy $D_0'' + E_{\text{ex.}}$. As before, if $E_{\text{ex.}}$ can be found from a knowledge of the dissociation products, D_0'' can be measured with great accuracy.

We shall see in Sec. 6.2.1 what sort of circumstances lead to the minimum in the upper state (Fig. 6.4(*a*)) on the one hand, or the *continuous* upper state (Fig. 6.4(*b*)) on the other.

In many electronic spectra no continua appear at all—the internuclear distances in the upper and lower states are such that transitions near to the dissociation limit are of negligible probability—but it is still possible to derive a value for the dissociation energy by noting how the vibrational lines converge. We have already seen in Chapter 3 (cf. Eq. (3.12)), that the vibrational energy levels may be written:

$$\varepsilon_v = (v + \tfrac{1}{2})\bar{\omega}_e - x_e(v + \tfrac{1}{2})^2\bar{\omega}_e \quad \text{cm}^{-1} \tag{6.8}$$

and so the separation between neighbouring levels, $\Delta\varepsilon$, is plainly:

$$\begin{aligned}\Delta\varepsilon &= \varepsilon_{v+1} - \varepsilon_v \\ &= \bar{\omega}_e\{1 - 2x_e(v + 1)\} \text{ cm}^{-1}\end{aligned} \tag{6.9}$$

This separation obviously decreases linearly with increasing v and the dissociation limit is reached when $\Delta\varepsilon \to 0$. Thus the maximum value of v is given by $v_{\text{max.}}$, where:

$$\bar{\omega}_e\{1 - 2x_e(v_{\text{max.}} + 1)\} = 0$$

i.e.,

$$v_{\text{max.}} = \frac{1}{2x_e} - 1 \tag{6.10}$$

We recall that the anharmonicity constant, x_e, is of the order 10^{-2}, hence $v_{\text{max.}}$ is about 50.

We saw in Sec. 3.1.3, that two vibrational transitions (in the infra-red) were sufficient to determine x_e and $\bar{\omega}_e$. Thus, an example given there for HCl yielded $\bar{\omega}_e = 2990 \text{ cm}^{-1}$, $x_e = 0{\cdot}0174$. From Eq. (6.10) we calculate $v_{\text{max.}} = 27{\cdot}74$ and the next lowest integer is $v = 27$. Replacing $v = 27$, $\bar{\omega}_e = 2990 \text{ cm}^{-1}$ and $x_e = 0{\cdot}0174$ into Eq. (6.8) gives the maximum value of the vibrational energy as 42 890 cm^{-1} or 513·0 kJ mol^{-1}. This is to be compared with a more accurate value of 427·2 kJ mol^{-1} evaluated thermochemically.

The discrepancy between these two figures arises from two causes. Firstly, the infra-red data only allows us to consider two or three vibrational transitions (the fundamental plus the first and second overtones). The electronic spectrum, as we have seen, shows many more vibrational lines (in fact the number is limited not by quantum restrictions, but by the Franck–Condon principle) and we shall get a better value of D''_0 if we make use of this extra data. Secondly, we have assumed that Eq. (6.8) applies exactly even at high values of v; this is not true because cubic and even quartic terms become important at this stage. Because of these, $\Delta\varepsilon$ decreases more rapidly than Eq. (6.9) suggests.

Both these points may be met if we plot the *separation* between vibrational transitions, $\Delta\varepsilon$, as observed in the electronic spectrum, against the

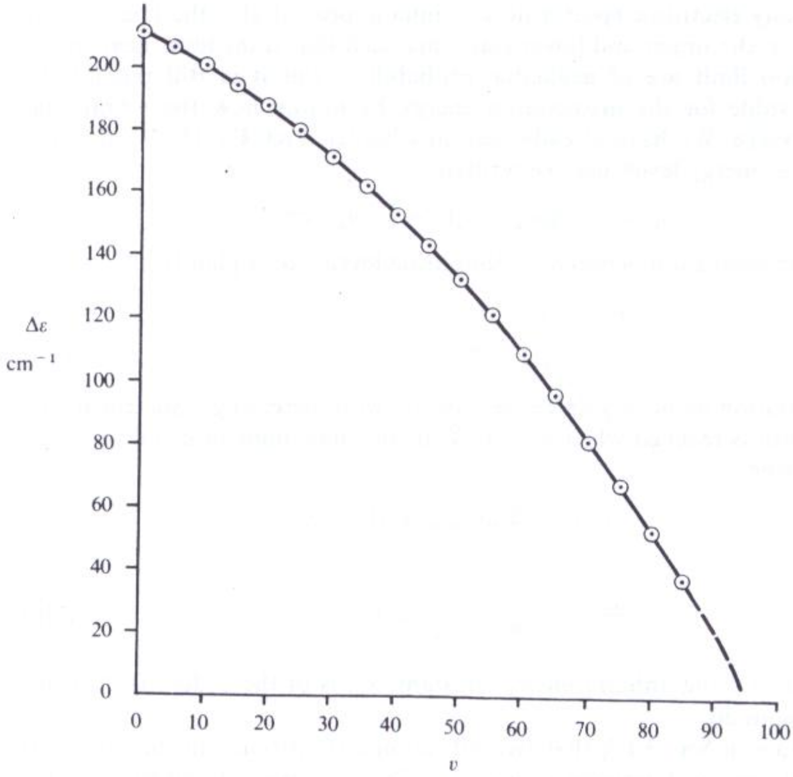

Figure 6.5 Birge–Sponer extrapolation to determine the dissociation energy of the iodine molecule, I_2. *(Taken from the data of R. D. Verma, J. Chem. Phys., vol. 32, p. 738 (1960), by kind permission of the author.)*

vibrational quantum number. Initially, Eq. (6.9) will apply quite accurately and the graph will be a straight line which may be extrapolated either to find $v_{\text{max.}}$ or, since the dissociation energy itself is simply the sum of all the increments $\Delta\varepsilon$ from $v = 0$ to $v = v_{\text{max.}}$, the *area* under the $\Delta\varepsilon$ versus v graph gives this energy directly. Such a linear extrapolation was first suggested by Birge and Sponer and is usually given their name.

On the other hand, if extensive data are available about a set of electronic–vibration transitions, the graph of $\Delta\varepsilon$ versus v will, at high v, begin to fall off more sharply as cubic and quartic terms become significant. In this case the most accurate determination of dissociation energy is obtained by extrapolating the smooth curve and finding the area beneath it. Figure 6.5 shows this process for data on iodine vapour given by R. D. Verma, *J. Chem. Phys.*, **32**, 738 (1960).

In absorption spectra it is normally the series of lines originating at $v'' = 0$ which is observed (cf. Fig. 6.1). Thus the convergence of the levels in the upper state and hence the dissociation energy of that state is normally found. While this in itself is of great interest, particularly since molecules in excited states usually revert to the ground state within fractions of a microsecond, the dissociation energy in the ground state can be found quite easily provided, as before, the dissociation products and their excitation energy are known. Thus, in Fig. 6.4(*a*), if we know $E_{\text{ex.}}$ (from atomic spectroscopy), and D'_0 (from Birge–Sponer extrapolation), and if we can measure the energy of the (0, 0) transition either directly or by calculation from the observed energy levels, we have:

$$D''_0 = \text{energy of } (0, 0) + D'_0 - E_{\text{ex.}} \quad \text{cm}^{-1} \qquad (6.11)$$

6.1.5 Rotational Fine Structure of Electronic–Vibration Transitions

So far we have seen that the electronic spectrum of a diatomic molecule consists of one or more series of convergent lines constituting the vibrational coarse structure on each electronic transition. Normally each of these 'lines' is observed to be broad and diffuse or, if the resolution is sufficiently good, each appears as a cluster of many very close lines. This is, of course, the rotational fine structure.

To a very good approximation we can ignore centrifugal distortion and we have the energy levels of a rotating diatomic molecule (cf. Eqs (2.11) and (2.12)) as:

$$\varepsilon_{\text{rot.}} = \frac{h}{8\pi^2 Ic} J(J+1) = BJ(J+1) \text{ cm}^{-1} \qquad (J = 0, 1, 2, \ldots) \quad (6.12)$$

where I is the moment of inertia, B the rotational constant, and J the rotational quantum number. Thus, by the Born–Oppenheimer approximation, the total energy (excluding kinetic of translation) of a diatomic molecule is:

$$\varepsilon_{\text{total}} = \varepsilon_{\text{elec.}} + \varepsilon_{\text{vib.}} + BJ(J + 1) \text{ cm}^{-1} \tag{6.13}$$

Changes in the total energy may be written:

$$\Delta\varepsilon_{\text{total}} = \Delta\{\varepsilon_{\text{elect.}} + \varepsilon_{\text{vib.}}\} + \Delta\{BJ(J + 1)\} \text{ cm}^{-1} \tag{6.14}$$

and the wavenumber of a spectroscopic line corresponding to such a change becomes simply:

$$\bar{\nu}_{\text{spect.}} = \bar{\nu}_{(v', v'')} + \Delta\{BJ(J + 1)\} \text{ cm}^{-1} \tag{6.15}$$

where we write $\bar{\nu}_{(v'', v'')}$ to represent the wavenumber of an electronic–vibrational transition. This plainly corresponds to any *one* of the transitions, for example, (0, 0) or (1, 0), etc., considered in previous sections. Here we are mainly concerned with $\Delta\{BJ(J + 1)\}$.

The selection rule for J depends upon the type of electronic transition undergone by the molecule. We shall discuss these in more detail in Sec. 6.2.2; for the moment we must simply state that if both the upper and lower electronic states are $^1\Sigma$ states (i.e., states in which there is no electronic angular momentum about the internuclear axis), this selection rule is:

$$\Delta J = \pm 1 \text{ only} \qquad \text{for } {}^1\Sigma \rightarrow {}^1\Sigma \text{ transitions} \tag{6.16}$$

whereas for all other transitions (i.e., provided either the upper or the lower states (or both) have angular momentum about the bond axis) the selection rule becomes:

$$\Delta J = 0, \text{ or } \pm 1 \tag{6.17}$$

For this latter case there is the added restriction that a state with $J = 0$ cannot undergo a transition to another $J = 0$ state:

$$J = 0 \nleftrightarrow J = 0 \tag{6.18}$$

Thus we see that for transitions between $^1\Sigma$ states, P and R branches only will occur, while for other transitions Q branches will appear in addition.

We can expand Eq. (6.15) as follows:

$$\bar{\nu}_{\text{spect.}} = \bar{\nu}_{(v', v'')} + B'J'(J' + 1) - B''J''(J'' + 1) \text{ cm}^{-1} \tag{6.19}$$

where B' and J' refer to the upper electronic state, B'' and J'' to the lower. When we considered vibration–rotational spectra in Chapter 3, we saw (cf. Sec. 3.4) that the difference between B values in different vibrational levels was very small and could be ignored except in explaining finer details of the spectra. But this is by no means the case in electronic spectroscopy: here we have seen, when discussing the Franck–Condon principle in Sec. 6.1.3, that equilibrium internuclear distances in the lower and upper electronic states may differ considerably, in which case the moments of inertia, and hence B values, in the two states will also differ. We cannot say a priori which of the two B values will be greater. Quite often the electron excited is one of those forming the bond between the nuclei; if this is so, the bond in the upper state will be weaker and probably longer (cf. Fig. 6.3(*b*) or (*c*)) so that the equilibrium moment of inertia increases during the transition and B decreases. Thus $B' < B''$. The reverse is sometimes true, however, e.g., when the electron is excited from an antibonding orbital (see Sec. 6.2.2).

We can discuss the rotational fine structure quite generally by applying the selection rules of Eqs (6.16), (6.17), and (6.18) to the expression for spectral lines, Eq. (6.19). We may note, in passing, that the treatment given here for the P and R branch lines is identical with that given in Sec. 3.4 for the vibration–rotation spectrum, except that there we were concerned with B_0 and B_1—B values in lower and upper *vibrational* states. Here our concern is with B values in lower and upper *electronic* states, B'' and B', and we also consider the formation of a Q branch.

Taking the P, R and Q branches in turn:

1. P branch: $\Delta J = -1, J'' = J' + 1$

$$\Delta\varepsilon = \bar{\nu}_P = \bar{\nu}_{(v', v'')} - (B' + B'')(J' + 1) + (B' - B'')(J' + 1)^2 \text{ cm}^{-1}$$

$$\text{where } J' = 0, 1, 2, \ldots \quad (6.20a)$$

2. R branch: $\Delta J = +1, J' = J'' + 1$

$$\Delta\varepsilon = \bar{\nu}_R = \bar{\nu}_{(v', v'')} + (B' + B'')(J'' + 1) + (B' - B'')(J'' + 1)^2 \text{ cm}^{-1}$$

$$\text{where } J'' = 0, 1, 2, \ldots \quad (6.20b)$$

These two equations can be combined into:

$$\bar{\nu}_{P,R} = \bar{\nu}_{(v', v'')} + (B' + B'')m + (B' - B'')m^2 \quad \text{cm}^{-1}$$

$$\text{where } m = \pm 1, \pm 2, \ldots \quad (6.20c)$$

positive m values comprising the R branch (i.e., corresponding to $\Delta J = +1$) and negative values the P branch ($\Delta J = -1$). Note that m cannot be zero (this would correspond in, e.g., the P branch, to $J' = -1$ which is impossible) so that no line from the P and R branch appears at the *band origin* $\bar{\nu}_{(v', v'')}$. We draw the appearance of the R and P branches separately in Fig. 6.6(*a*) and (*b*) respectively, taking a 10 per cent difference between the upper and lower B values and choosing $B' < B''$. Note that, *with this choice*, P branch lines occur on the *low* wavenumber side of the band origin and the spacing between the lines increases with m. On the other hand the R branch appears on the *high* wavenumber of the origin and the line spacing decreases rapidly with m—so rapidly that the lines eventually reach a maximum wavenumber and then begin to return to low wavenumbers with increasing spacing.† It will be remembered that

---

† The returning lines of the R branch coincide with earlier lines if Eq. (6.20*b*) is obeyed exactly. For real molecules cubic and quartic terms become important at high values of m.

in Sec. 3.4, a similar decrease in spacing was observed in the R branch but this was much too slow for a convergence limit to be reached; the rapid convergence here is due simply to the magnitude of $B' - B''$. The point at which the R branch separation decreases to zero is termed the *band head.*

3. Q branch: $\Delta J = 0, J' = J''$

$$\Delta\varepsilon = \bar{\nu}_Q = \bar{\nu}_{(v', v'')} + (B' - B'')J'' + (B' - B'')J''^2 \quad \text{cm}^{-1}$$

$$\text{where } J'' = 1, 2, 3, \ldots \quad (6.21)$$

Note that here $J'' = J' \neq 0$ since we have the restriction shown in Eq. (6.18). Thus again *no line will appear at the band origin.* We sketch the Q branch in Fig. 6.6(c), again for $B' < B''$ and a 10 per cent difference between the two. We see that the lines lie to *low* wavenumber of the origin and their spacing increases. The first few lines of this branch are not usually resolved.

The complete rotational spectrum is shown in Fig. 6.6(d). We have seen in Sec. 2.3.2 that many rotational levels are populated even at room temperature; consequently, a large number of the P and R (and Q, where appropriate) lines will appear in the spectrum with comparable intensity. The spectrum is usually dominated by the band head, since here several of

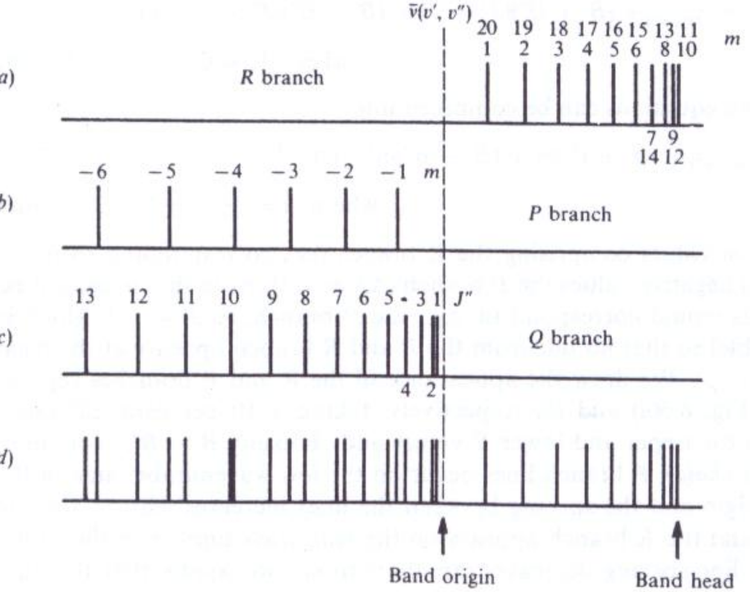

Figure 6.6 The rotational fine structure of a particular vibrational–electronic transition for a diatomic molecule. The R, P, and Q branches are shown separately at (a), (b), and (c) respectively, with the complete spectrum at (d).

the *R* branch lines crowd together; for this reason, the *Q* branch is not very apparent if it occurs.

In the situation we have been discussing ($B' < B''$), the band head appears in the *R* branch on the high wavenumber side of the origin; such a band is said to be *degraded* (or *shaded*) *towards the red*—i.e., the tail of the band where the intensity falls off points towards the red (low-frequency) end of the spectrum. If, on the other hand, $B' > B''$, then all our previous arguments are reversed. Briefly: (1) the *Q* branch spreads to *high* wavenumber, (2) the *R* branch (still, of course, on the *high* wavenumber side) consists of a series of lines with *increasing* separation, and (3) the band head appears in the *P* branch to *low* frequency of the origin. Such a band is *shaded to the violet*.

Normally, all the vibrational bands in any one electronic transition (e.g., the set of bands shown as a line spectrum in Fig. 6.1) are shaded in the same direction, while different electronic transitions in the same molecule may well show different shadings. Thus, observation of the shading may assist in the analysis of a complex spectrum. However, it may happen that different shadings are observed in bands belonging to the same electronic transition. This is because the B' and B'' values are not altogether independent of the vibrational state (as we have already seen in Sec. 3.4) so that, if $B' - B''$ is small, it may reverse sign for some higher vibrational levels. This behaviour is observed, for example, in the molecular fragment AlF, but is rare.

6.1.6 The Fortrat Diagram

We may rewrite the expressions for the *P, R*, and *Q* lines, Eq. (6.20*c*) and (6.21), with *continuously variable* parameters *p* and *q*:

$$\bar{\nu}_{P,\,R} = \bar{\nu}_{(v',\,v'')} + (B' + B'')p + (B' - B'')p^2 \qquad (6.22a)$$

$$\bar{\nu}_Q = \bar{\nu}_{(v',\,v'')} + (B' - B'')q + (B' - B'')q^2 \qquad (6.22b)$$

when we see that they each represent a parabola, *p* taking both positive and negative values, while *q* is positive only. We sketch these parabolae in Fig. 6.7 choosing, as before, $B' < B''$ and a difference of 10 per cent between them, and labelling regions of positive *p* with $\bar{\nu}_R$ and negative *p* with $\bar{\nu}_p$. These parabolae are usually referred to as the Fortrat parabolae. If we now illustrate the fact that *p* and *q* may in fact take only integral values (but not zero) by drawing circles round the allowed points on the parabolae, we can then read off the $\bar{\nu}$ values of the spectral lines directly from the graph. We show at the foot of the figure the first few lines of each branch with dotted leader lines connecting spectrum and Fortrat diagram at intervals.

A useful property of the Fortrat diagram is that the band head is plainly at the vertex of the *P, R* parabola. We may calculate the position of

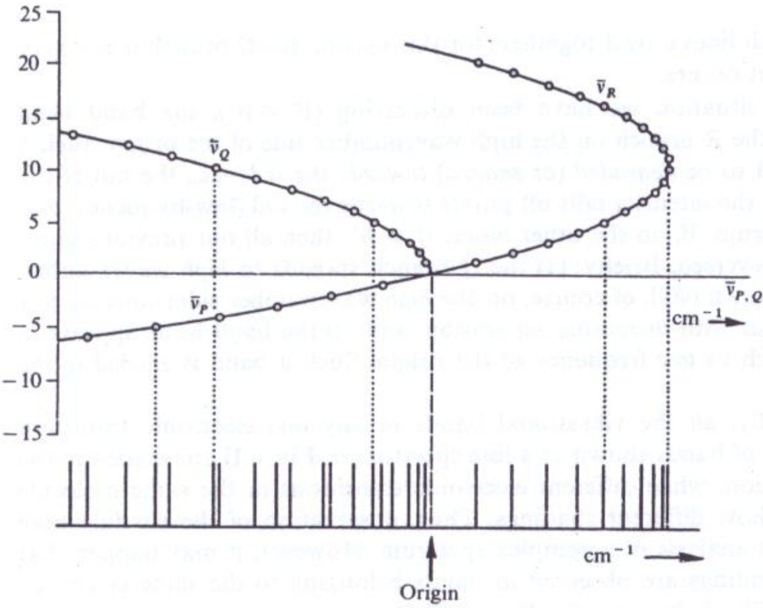

Figure 6.7 The Fortrat diagram sketched for a 10 per cent difference between B' and B'' (with $B' < B''$). The spectrum illustrated at the foot is identical with that of Fig. 6.6(*d*).

the vertex by differentiation of Eq. (6.22*a*):

$$\frac{d\bar{\nu}_{P,R}}{dp} = B' + B'' + 2(B' - B'')p = 0$$

or

$$p = -\frac{B' + B''}{2(B' - B'')} \quad \text{for band head} \qquad (6.23)$$

Thus if $B' < B''$ (upper state has longer equilibrium bond length) the band head occurs at *positive p* values (i.e., in the *R* branch), the line at maximum wavenumber being given by the nearest positive integer to *p*. Conversely, for $B' > B''$ the band head occurs in the region of *p* negative, i.e., in the *P* branch. A simple calculation shows that for a 10 per cent difference between B' and B'' the band head occurs at $p \approx 10$.

6.1.7 Predissociation

If a large number of vibrational transitions are observed for a particular molecule, it sometimes happens that the vibrational and rotational structure are quite distinct within a progression for large and small changes in the vibrational quantum number, but either the rotational structure is blurred or a complete continuum is observed for intermediate changes. A

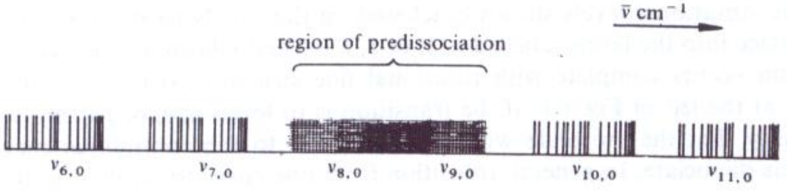

Figure 6.8 Diagrammatic illustration of the appearance of predissociation. The rotational fine structure is clearly defined for vibrational transitions both above and below the predissociation region, but in this region the fine structure becomes blurred and lost.

diagram showing the appearance of such a band is sketched in Fig. 6.8. A continuum at high wavenumber would correspond to ordinary dissociation (cf. Sec. 6.1.4) but the central continuum, occurring at energies well below the true dissociation limit, is referred to as *predissociation*.

Predissociation can arise when the Morse curves of a particular molecule in two different excited states intersect; one such possibility is shown in Fig. 6.9. One of the excited states is stable, since it has a minimum in the curve, and the other is continuous. Some of the vibrational levels are also shown, and let us suppose a transition takes place from some lower state

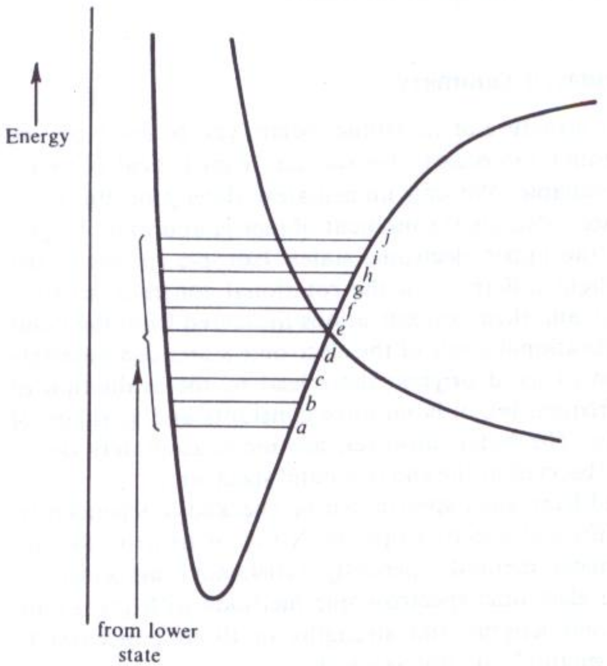

Figure 6.9 Showing the occurrence of predissociation during transitions into a stable upper state intersected by a continuous state.

into the vibrational levels shown bracketed on the left. Now if a transition takes place into the levels labelled *a*, *b*, or *c*, a normal vibrational–electronic spectrum occurs complete with rotational fine structure; two such bands appear at the left of Fig. 6.8. If the transition is to levels *d*, *e*, or *f* there is a possibility that the molecule will 'cross over' on to the continuous curve and thus dissociate. In general, transition from one curve to another in this way (a so-called *radiationless transfer* since no energy is absorbed or emitted in the process) is faster than the time taken by the molecule to rotate ($\sim 10^{-10}$ s) but usually slower than the vibrational time ($\sim 10^{-13}$ s). Thus predissociation will occur before the molecule rotates (and thus all rotational fine structure will be destroyed in the spectrum), while the vibrational structure is usually not destroyed. If the cross-over is faster than the vibrational time, then a complete continuum will occur in the spectrum as shown in Fig. 6.8.

On the other hand, transitions into levels *g*, *h*, . . . will give rise to a normal vibrational–electronic spectrum including rotational fine structure once more. As we have seen previously (Sec. 6.1.3) the molecule spends most time at the extreme ends of its vibrational motion when v is large, and very little time in between. When moving in the vibrational states *g*, *h*, . . ., the molecule spends insufficient time near the cross-over point for appreciable dissociation to occur and a normal spectrum results.

6.1.8 Diatomic Molecules: a Summary

When the rotational fine structure of electronic spectra can be resolved—as it normally can for diatomic molecules—we see that a great deal of useful information becomes available. We can immediately determine the rotational constant, and hence calculate the moment of inertia and bond length, for both the lower and the upper electronic states. Isotopic species in the molecule will cause a slight difference in the rotational constant, so such isotopes may be detected, and their concentrations measured from the band intensity. Equally, the vibrational levels of the electronic states can be determined from the position of band origins; these lead to the evaluation of fundamental vibration frequencies, of bond force constants and, perhaps, of dissociation energies too. The latter, however, are more accurately determined if a continuum is observed at the end of a band spectrum.

Where data obtained from such spectra can be checked independently, e.g., by microwave or infra-red spectroscopy, by X-ray or neutron diffraction, or by thermochemical methods, perfectly satisfactory agreement is found. Thus we can use electronic spectroscopic methods with great confidence to determine bond lengths and strengths in those molecules to which such independent methods are not applicable.

Probably the most important application of this type of spectroscopy is to the study of excited states and unstable radicals. Thus we have seen that

B values and dissociation energies are obtained for both the upper and lower electronic states—and data for the upper state are not obtainable by other means. Further, considerable amounts of energy are involved in the production of electronic spectra, and complex molecules are frequently disrupted into fragments during the process, the fragments, or free radicals, normally being very short-lived. Examples are legion, a few of the more important diatomic ones being CH, NH, C_2, OH, CN, etc. Spectra arising from these radicals can be recognized and studied, leading to the determination of bond lengths, force constants, dissociation energies, etc. Further, if the variation of the intensity of such spectra over short periods of time is studied—as in the techniques of flash photolysis—information can be obtained about the rate at which the radicals are produced and destroyed. Since the length of time during which some radicals have an independent existence is measured in microseconds or less, it is remarkable that many such 'diatomic molecules' are as well characterized as, for example, the rather more stable H_2 or CO.

6.2 ELECTRONIC STRUCTURE OF DIATOMIC MOLECULES

6.2.1 Molecular Orbital Theory

Several theories have been suggested to account for the formation of molecules from atoms. All, if taken to a sufficiently high degree of approximation, seem to agree with observed data, but the calculation involved is so extensive that complete agreement is seldom reached and then only in the simplest examples. Here we shall discuss just one of these theories—the *molecular orbital theory*; we choose this, not because it is better or simpler than others (such considerations depend upon the particular problem in hand and are, in any case, largely subjective), but because it gives a convenient pictorial representation of molecule formation which is particularly suited to the discussion of electronic transitions, and because the ideas it uses are entirely analogous to those of atomic structure which we have discussed in the previous chapter.

Thus we have seen that electrons in atoms do not occupy space haphazardly or have arbitrary energies, but that their distribution and energy are governed by well-defined natural laws. These characteristics may be calculated from the Schrödinger equation and expressed in terms of a three-dimensional wave function, or orbital, ψ, which depends on the values of three quantum numbers, n, l, and m (or l_z); the spin of the electron also contributes to the energy. Definite rules determine which orbitals are occupied in the ground state and what transitions may take place between orbitals.

Molecular orbital theory supposes orbitals to extend about, and embrace, *two or more nuclei*, the shape and energy of these orbitals being calculable from the Schrödinger equation in terms of three quantum numbers. Essentially the same rules (i.e., lowest energy first, maximum of two (paired) electrons per orbital, parallel spins in degenerate orbitals) apply to their filling as to the filling of atomic orbitals.

The situation is relatively simple for diatomic molecules where the molecular orbital embraces two nuclei only and we shall discuss these molecules in some detail first. The extension to polyatomic molecules will be outlined in Sec. 6.3.

6.2.2 The Shapes of Some Molecular Orbitals

As in atomic orbital theory (cf. Sec. 5.1.2) the shape of a molecular orbital is the space within which an electron belonging to that orbital will spend 95 per cent (or some other arbitrary fraction) of its time. While detailed computation of these shapes from the Schrödinger theory may be extremely difficult, a very good qualititative idea of their approximate shape may be obtained by considering molecular orbitals to be made up of sums and differences of the atomic orbitals of the constituent atoms—the so-called *linear combination of atomic orbitals* (LCAO) approximation. Thus for a diatomic molecule we could imagine the formation of two different molecular orbitals whose wave functions would be:

$$\psi_{\text{mo.}} = \psi_1 + \psi_2 \qquad \text{or} \qquad \psi_{\text{mo.}} = \psi_1 - \psi_2 \tag{6.24}$$

where ψ_1 and ψ_2 are the relevant atomic orbitals of the two atoms. Note that the function $\psi_2 - \psi_1$ is identical with $\psi_1 - \psi_2$, since it is $\psi^2_{\text{mo.}}$ which represents the probability of finding an electron in a particular place.

Let us consider the hydrogen molecule, H_2, as an example; the obvious atomic orbitals to use are the $1s$ orbitals of each atom. Figure 6.10(*a*) shows the situation:

$$\psi_{H_2} = \psi_{1s} + \psi_{1s} \tag{6.25}$$

We recall from the previous chapter (Eq. (5.2)) that ψ_{1s} is everywhere positive in value and so, where the atomic orbitals overlap, the value of ψ_{H_2} will be increased. This suggests (and detailed calculation confirms) that the molecular orbital of Eq. (6.25) is a simple ellipsoid, symmetrical in shape. The concentration of electronic charge between the nuclei acts as a sort of cement keeping the nuclei together and thus this orbital represents the formation of a bond between the atoms. It is called a *bonding orbital* and given the label $1s\sigma$ since it is produced from two $1s$ orbitals (we shall see later that σ has a similar significance regarding the orbital angular momenta of molecular electrons as s has for atoms).

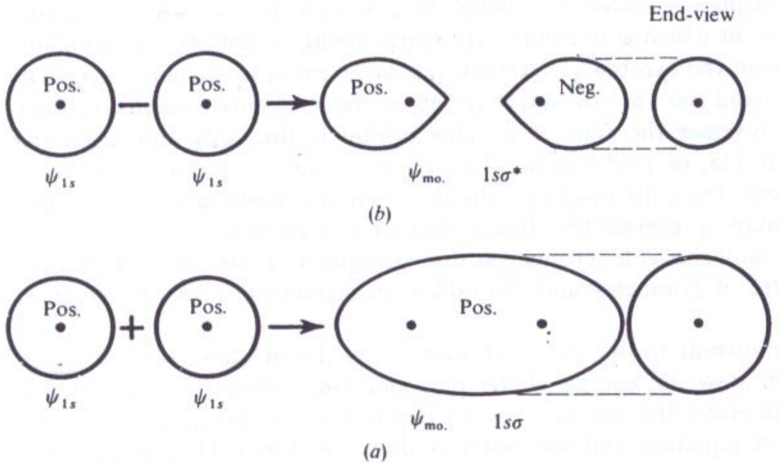

Figure 6.10 The formation of (*a*) a bonding $1s\sigma$ orbital and (*b*) an antibonding $1s\sigma^*$ orbital from two atomic $1s$ orbitals.

On the other hand, Fig. 6.10(*b*) shows the situation for

$$\psi_{\mathrm{H}_2} = \psi_{1s} - \psi_{1s} \tag{6.26}$$

Since, again, ψ_{1s} is everywhere positive, where the two separate ψ_{1s} orbitals overlap, they will cancel each other. Thus between the nuclei $\psi_{\mathrm{mo.}}$ will be zero, while it will be positive near one nucleus and negative near the other (remember that it is ψ^2 which determines probability and this is, in either case, positive). Now, however, the shape of the molecular orbital shows that electronic charge, far from being concentrated *between* the nuclei, is greatest *outside* them; thus the nuclear repulsion is enhanced and the orbital is described as *antibonding*. It leads to a state of higher energy than two separate atoms and is labelled $1s\sigma^*$, the asterisk representing high energy. Figure 6.10 also shows, at the extreme right, an end-view of these orbitals. They are both seen to have cylindrical symmetry about the bond axis; it is this property which leads to their both being described as σ orbitals although in other respects they have quite different appearances.

Another facet of orbital symmetry should be mentioned here. If the molecule considered is homonuclear (i.e., made of two *identical* atoms) then the midpoint of the bond between them is a *centre of symmetry*—starting from any point in the molecule, on or off the internuclear axis, exactly similar surroundings are encountered by proceeding to the point diagonally opposite the centre. Such a process is known as *inversion*, and such molecular properties as electron density, force fields, etc., are quite unchanged by inversion. However, we note that ψ (as opposed to ψ^2) may or may not be changed *in sign* by inversion. Thus inversion of the $1s\sigma$ molecular orbital of

Fig. 6.10(*a*) plainly causes no change in ψ since it is everywhere positive; this orbital, in which ψ is completely symmetrical, is described as *even* and usually given the symbol *g* (German: *gerade* = even) as a suffix: $1s\sigma_g$. On the other hand the $1s\sigma^*$ orbital in (*b*) of the figure is antisymmetrical, since inversion reverses the sign of ψ. This orbital is thus *odd* and given the subscript *u*, $1s\sigma_u$ or $1s\sigma_u^*$ (German: *ungerade* = odd). In the case of molecular hydrogen, then, the bonding orbital is even, the antibonding is odd; this situation may be reversed for other molecular orbitals as we shall see.

If the molecule is heteronuclear (for example, CO, HCl, etc.) then there is no centre of symmetry and the odd–even classification of orbitals does not arise.

Before turning to the shapes of other molecular orbitals, it is instructive to consider how the energy of the $1s\sigma_g$ and $1s\sigma_u^*$ orbitals varies with the distance between the nuclei. This variation may be calculated from the Schrödinger equation and the result is shown in Fig. 6.11. The $1s\sigma_g$, the

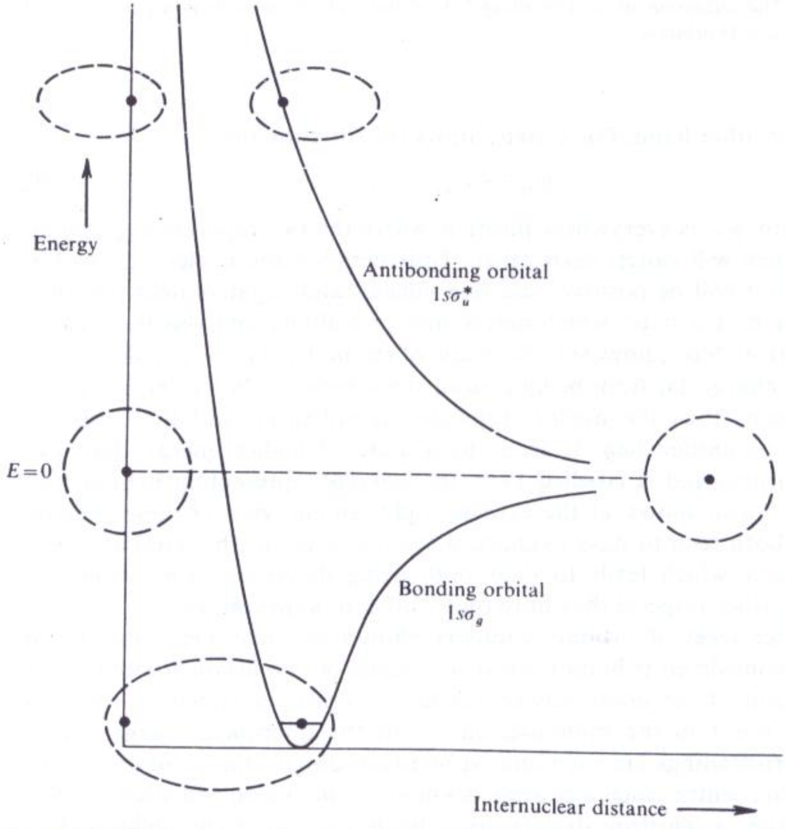

Figure 6.11 The variation of energy with internuclear distance in the bonding and antibonding orbitals, $1s\sigma_g$ and $1s\sigma_u^*$.

bonding orbital, shows a typical Morse curve for a diatomic molecule, the minimum in the curve showing that a bond is formed between the atoms. The $1s\sigma_u^*$, on the other hand, shows no minimum, but is one of the 'continuous' curves already discussed in Sec. 6.1.4. In this case the dissociation limits of the two curves coincide since the dissociation products are identical—two hydrogen atoms. The relationship of the orbitals sketched in Fig. 6.10 to the energy curve is shown by superimposing the molecular orbitals at their appropriate equilibrium internuclear distance and the separate atomic orbitals at a large distance.

Two $2s$ atomic orbitals can form $2s\sigma_g$ and $2s\sigma_u^*$ bonding and antibonding orbitals with identical shape to (but larger and with higher energy than) the $1s\sigma_g$ and $1s\sigma_u^*$ orbitals. Two $2p$-type orbitals can overlap in two different ways depending on their relative orientation. If we label the internuclear axis the z direction, then we may consider first the $2p$ orbital which lies along this axis for each atom, i.e., the $2p_z$ orbitals. Now the expression for the wave function of a $2p_z$ orbital has the form $\psi_{2p_z} = zf(r)$, where $f(r)$ is a positive function of distance from the nucleus. We see then, that for $+z$ directions ψ is also positive, while it is negative for $-z$. The two lobes of a $2p$ orbital thus have opposite signs of ψ (although, of course, ψ^2 is everywhere positive).

We draw these orbitals and indicate their signs on the left of Fig. 6.12 and it is evident that in the molecular orbital

$$\psi_{\text{mo.}} = \psi_{2p_z} + \psi_{2p_z} \tag{6.27}$$

the electron density between the nuclei is cancelled to zero and the orbital will have the shape shown at the top right of the figure. Similarly in

$$\psi_{\text{mo.}} = \psi_{2p_z} - \psi_{2p_z} \tag{6.28}$$

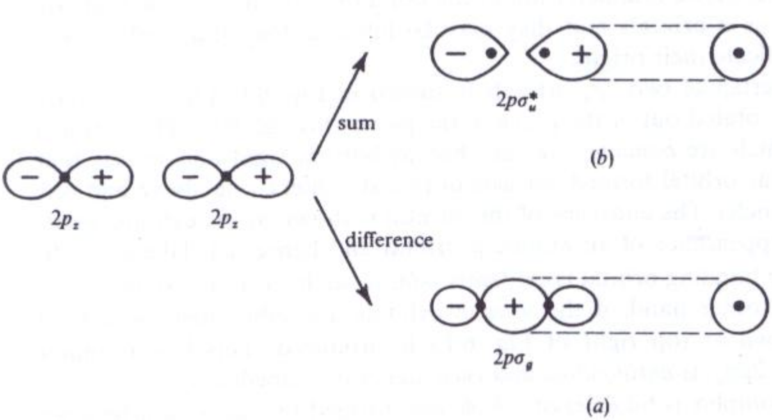

Figure 6.12 The formation of (*a*) a bonding $2p\sigma_g$ and (*b*) an antibonding $2p\sigma_u^*$ orbital from two atomic $2p_z$ orbitals, where the z axis is taken as the internuclear axis.

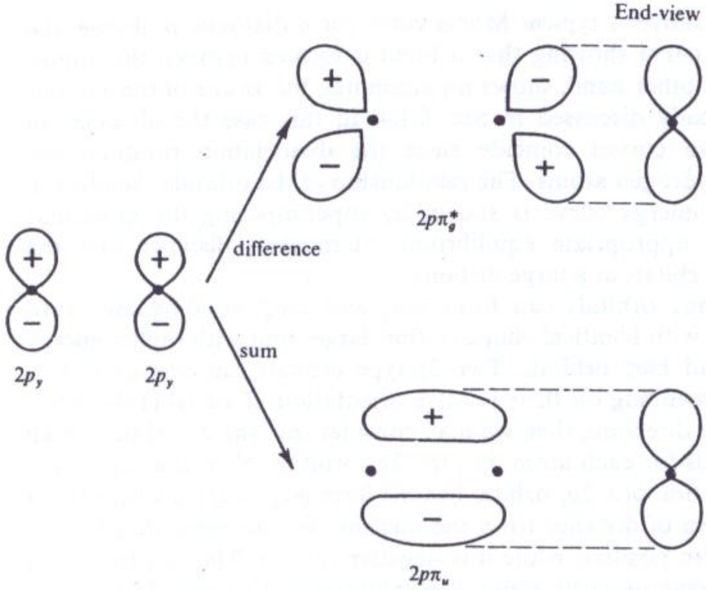

Figure 6.13 The formation of bonding ($2p\pi_u$) and antibonding ($2p\pi_g^*$) orbitals from two atomic $2p_y$ orbitals, the z axis being the internuclear axis. Atomic $2p_x$ orbitals would form identical molecular orbitals except that all lobes would be rotated through a right angle about the z axis.

the electron density increases between the nuclei and the shape is shown at the bottom right of the figure. Plainly the latter is *bonding*, and consideration of its symmetry shows that it is *even* (g), while the former is plainly *antibonding* and *odd* (u) in character. The end-view of both is the same, however, and shows symmetry about the bond axis; for this reason both are referred to as σ orbitals and they may be labelled $2p\sigma_g$ and $2p\sigma_u^*$ respectively to indicate their origin.

The overlap of two $2p_y$ orbitals is shown in Fig. 6.13 ($2p_x$ are exactly similar but rotated out of the plane of the paper through 90°). The summed orbitals, which are *bonding*, are sketched at bottom right and we see that the molecular orbital formed consists of two streamers, one above and one below the nuclei. The end-view of this orbital is shown at the extreme right; it has the appearance of an atomic p orbital and hence it is labelled π. In this case the bonding orbital is evidently *odd*, so we have a $2p\pi_u$ state.

On the other hand, if the atomic orbitals are subtracted the orbital picture shown at top right of Fig. 6.13 is produced. This has a similar end-view to $2p\pi_u$, is *antibonding* and *even*, hence it is labelled π_g^*.

More complex orbitals exist—δ, ϕ, etc., formed by interaction between d, f, etc., atomic orbitals—but they need not concern us; the simple molecules with which we shall deal use σ and π orbitals only. We do need to

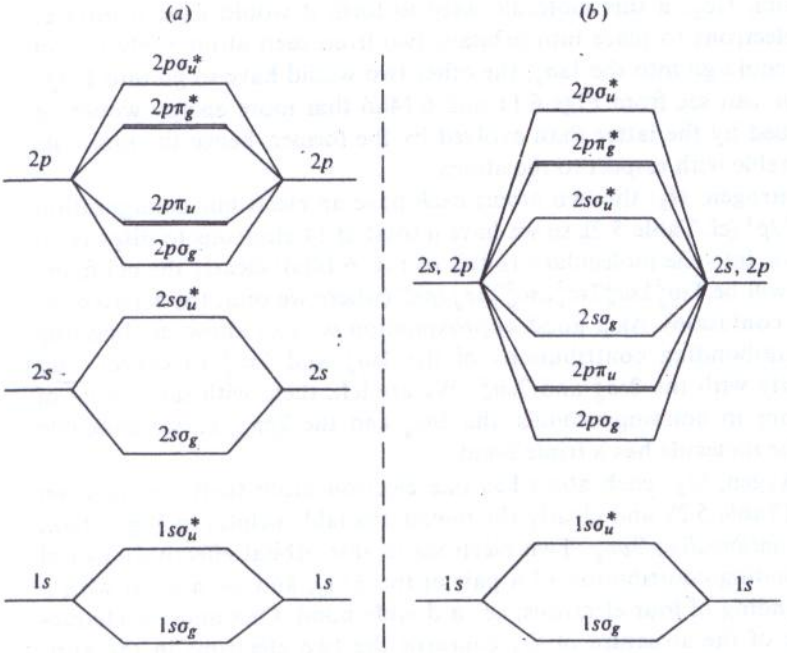

Figure 6.14 Molecular orbital energy level diagrams for (*a*) molecules other than hydrogen, and (*b*) the hydrogen molecule.

know, however, the order of increasing energy of the molecular orbitals so far discussed so that we can consider the ground states of some atoms. This we show diagrammatically (and by no means to scale) in Fig. 6.14(*a*), where we also indicate, to the right and left, the atomic orbitals which combine to form each molecular state. As drawn here the diagram represents the situation for the larger molecules such as N_2, O_2, and F_2; for smaller molecules such as Li_2, the $2p\pi_u$, $2p\sigma_g$, and $2s\sigma_u^*$ become overlapped, while for the lightest molecule of all, H_2, the situation is as shown in Fig. 6.14(*b*). Here, because in the separate atoms the 2*s* and 2*p* orbitals have identical energies, the molecular orbitals take up the order shown. Using these diagrams and the Pauli principle (not more than two electrons to each orbital) we can build up the electronic configurations of simple molecules. Some examples follow:

Firstly hydrogen, H_2: in the ground state of this molecule the two 1*s* atomic electrons, one from each atom, can both occupy the molecular $1s\sigma_g$ provided their spins are opposed. The energy of the electrons in this state, as we can see from Figs. 6.11 and 6.14(*b*), is lower than that of two separate atoms, hence the molecule is stable. We can write its configuration $1s\sigma_g^2$.

Next helium, He_2: if this molecule were to form it would have a total of four electrons to place into orbitals, two from each atom. Only two of these could go into the $1s\sigma_g$; the other two would have to go into $1s\sigma_u^*$. But we can see from Figs 6.11 and 6.14(*a*) that more energy would be absorbed by the latter than evolved by the former, hence the molecule is unstable with respect to the atoms.

Thirdly, nitrogen, N_2: the two atoms each have an electronic configuration $1s^2 2s^2 2p^3$ (cf. Table 5.2), so we have a total of 14 electrons to dispose of, in pairs, into the molecular orbitals of Fig. 6.14(*a*); clearly the configuration will be $1s\sigma_g^2 1s\sigma_u^2 2s\sigma_g^2 2s\sigma_u^2 2p\sigma_g^2 2p\pi_u^4$ (where we omit the asterisks to avoid confusion). As a good approximation we can allow the bonding and antibonding contributions of the $1s\sigma_g^2$ and $1s\sigma_u^2$ to cancel, and similarly with the $2s\sigma_g^2$ and $2s\sigma_u^2$. We are left, then, with three pairs of electrons in bonding orbitals, the $2p\sigma_g$ and the $2p\pi_u$, so we conclude that the molecule has a triple bond.

Finally, oxygen, O_2: each atom has one electron more than the nitrogen atom (Table 5.2), and clearly the lowest available orbital in Fig. 6.14(*a*) is the *antibonding* $2p\pi_g$. Two electrons in this orbital effectively cancel the bonding contribution of a pair in the $2p\pi_u$, and we are left with a net bonding of four electrons, i.e., a double bond. One unusual characteristic of the structure of O_2 concerns the two electrons in the antibonding $2p\pi_g$. Since there are here two degenerate orbitals, the electrons will occupy one each to satisfy electron repulsion; however, according to Hund's rule (p. 186) which applies to molecules just as to atoms, they will preferentially have their spins *parallel* rather than paired. Thus O_2 is a molecule containing some unpaired electrons—a structural characteristic which gives it its most unusual magnetic properties.

6.2.3 Electronic Angular Momentum in Diatomic Molecules; Classification of States

We found in Sec. 5.2, that the total energy of an electron, while depending mainly on its average distance from the nucleus (represented by the quantum number *n*) also depends on its orbital and spin angular momenta (quantum numbers *l* and *s*) and on the way in which these are coupled together (quantum number *j*). For several electrons in an atom we found that their separate energies can be combined in different ways to produce a variety of states; simple rules allow the ground state to be predicted in any particular case.

Much the same comments apply to electrons in molecules. Thus a single electron in a molecule has a quantum number *n* specifying the size of its orbital and mainly determining its energy, and a number *l* specifying its orbital angular momentum. Small letters *s*, *p*, *d*, . . . are used, as before, to designate l values of 0, 1, 2, ... However, it will be remembered that in order to discuss the components of **l** we required to invoke some reference direction called the z direction; in a diatomic molecule a reference direction is already quite obviously specified—the inernuclear axis, or bond—and it would be perverse (not to say *wrong*) to discuss the components of **l** along any other direction. Furthermore, a force-field exists along this direction due to the presence of two nuclear charges; therefore different **l** components are not degenerate but represent *different energies*.

The axial component of orbital angular momentum is of more importance in molecules than the momentum itself and for this reason it is given the special symbol λ. Formally $\lambda \equiv |l_z|$, so that λ takes *positive* integral values or is zero, and we designate the λ state of an electron in a molecule by using the small Greek letters corresponding to the s, p, d, . . . of atomic nomenclature. Thus we have, for

$$l_z = 0,\ \pm 1,\ \pm 2,\ \pm 3, \ldots$$

$$\lambda = 0, 1, 2, 3, \ldots$$

and the symbols are $\sigma, \pi, \delta, \phi, \ldots$

Since λ has positive values only, each λ state with $\lambda > 0$ is *doubly degenerate*, because it corresponds to l_z being both positive and negative. The significance of λ is that the *axial component of orbital angular momentum* $= \lambda h/2\pi$ or λ *units*.

The total orbital angular momentum of several electrons in a molecule can be discussed, as for atoms, in terms of the quantum number $L = \Sigma l$, $\Sigma l - 1$, etc., with $\mathbf{L} = \sqrt{L(L+1)}h/2\pi$, but again the axial component, denoted by Λ, is of greatest significance. Since, by definition, all individual λ_i lie along the internuclear axis, their summation is particularly simple. We have

$$\Lambda = |\Sigma\lambda_i| \tag{6.29}$$

and states are designated by capital Greek letters Σ, Π, Δ, etc., for $\Lambda = 0, 1, 2, \ldots$. We must take into account, when using Eq. (6.29), that the individual λ_i may have the same or opposite directions and all possible combinations which give a positive Λ should be considered. Thus for a π and a δ electron ($\lambda_1 = 1$, $\lambda_2 = 2$) we could have $\Lambda = 1$ or 3 (but not -1), that is, a Π or a Φ state.

Electron *spin* momentum, on the other hand, is not greatly affected by the electric field of the two nuclei—we say the spin–axial coupling is weak, whereas the orbital–axial coupling is usually strong. Normally, therefore, we use the same notation for electronic spin in molecules as in atoms; the total spin momentum **S** is given by $\sqrt{S(S+1)}$ where the total spin quantum number S is:

$$S = \Sigma S_i,\ \Sigma S_i - 1,\ \Sigma S_i - 2, \ldots, \tfrac{1}{2} \text{ or } 0 \tag{6.30}$$

The multiplicity of a molecular state is, as for atoms, $2S + 1$ and this is usually indicated as an upper prefix to the state symbol. Thus for the Π and Φ states discussed in the previous paragraph, the states would be written $^3\Pi$ or $^3\Phi$ if the individual π and δ electron spins are parallel ($S = \frac{1}{2} + \frac{1}{2} = 1$, $2S + 1 = 3$), or as $^1\Pi$ or $^1\Phi$ if the spins are paired.

When the *axial* component of a spin is required, however, it is often designated by σ for a single electron or Σ for several (corresponding to s and S for the atomic case). In this case the multiplicity is $2\Sigma + 1$.

Finally, we consider the axial component of the *total* electronic angular momentum, i.e., the sum of the axial components of spin and orbital motion. In general the total momentum is strongly coupled to the axis and its axial component is more significant than the momentum itself. If we write the axial component as Ω we have simply:

$$\Omega = |\Lambda + \Sigma| \tag{6.31}$$

but we must remember that Λ and Σ may have the same or opposite directions along the internuclear axis. Thus in the $^3\Pi$ state described above we have $\Lambda = 1$, $\Sigma = 1$, hence $\Omega = 2$ or 0. The $^1\Pi$ state has $\Lambda = 1$, $\Sigma = 0$, hence we have $\Omega = 1$ only. These states would be indicated by writing their Ω values as subscripts: $^3\Pi_2$, $^3\Pi_0$, $^3\Pi_1$.

Perhaps it will assist the student if we draw up a table (Table 6.1) showing the symbols used to designate the various sorts of angular momentum in atoms and molecules, together with their axial components, for one or more electrons.

Table 6.1 Comparison of symbols used for electronic angular momenta

	Orbital momentum	Spin momentum	Total momentum
For atoms			
Single electron	l (symbol s, p, d for $l = 0, 1, 2, \ldots$)	s	j
Single electron (z component)	l_z	s_z	j_z
Several electrons	L (symbol S, P, D for $L = 0, 1, 2, \ldots$)	S	J
Several electrons (z component)	L_z	S_z	J_z
For molecules			
Single electron	l	s	j_a (seldom used)
Single electron (axial component)	λ (symbol σ, π, δ, for $\lambda = 0, 1, 2, \ldots$)	σ	ω
Several electrons	L	S	J_a (seldom used)
Several electrons (axial component)	Λ (symbol Σ, Π, Δ, for $\Lambda = 0, 1, 2, \ldots$)	Σ	Ω

6.2.4 An Example: the Spectrum of Molecular Hydrogen

Before turning to polyatomic molecules, let us see how the above ideas may be applied to the simplest molecule, H_2. We shall consider first the nature of the ground state and some excited states of the molecule and how these relate to occupancy of the molecular orbitals of Fig. 6.14(*b*); then the energy of these states and, finally, what transitions may arise between them. The student may find it helpful to discover the many points of similarity between the discussion which follows and that given in Sec. 5.4.5 on helium.

The hydrogen molecule contains two electrons, one contributed to by each of the atoms. We would thus expect to find singlet and triplet states, depending on whether the electron spins are paired or parallel. In the *ground state* both electrons will occupy the same lowest orbital, i.e., the $1s\sigma_g$ of Fig. 6.14(*b*) and, by Pauli's principle, they must then form a singlet state. Both electrons are σ electrons (since both are in a σ orbital) hence $\lambda_1 = \lambda_2 = 0$ and $\Lambda = 0$ also; the state is thus $^1\Sigma$. We could indicate the value of Ω as a subscript ($\Omega = \Lambda + \Sigma = 0 + 0 = 0$, since $\Sigma = 0$ for singlet states) but it is more informative to specify the symmetry (g or u) of the orbital. In this case both electrons are in the same g orbital, hence the total state is $^1\Sigma_g$.

A further subdivision of Σ states is normally made, representing another facet of molecular symmetry. In any diatomic molecule (whether homo- or heteronuclear) any plane drawn through both nuclei is a *plane of symmetry*, i.e., electron density, shape, force fields, etc., are quite unchanged by reflection in the plane. However, the wave function of the electron, ψ, may either be completely unchanged (symmetrical) or changed in sign only (antisymmetrical) with respect to such a reflection (in either case, of course, ψ^2 is unchanged). The former states are distinguished by a superscript $+$ and the latter by $-$. For several reasons this division is made for Σ states only and nearly all such states are in fact $+$. Certainly all the states of hydrogen are symmetric.

Thus the ground state of molecular hydrogen can be written:

$$\text{Ground state:} \quad (1s\sigma_g)^2 \; {}^1\Sigma_g^+$$

A large number of excited singlet states also exist; let us consider some of the lower ones for which one electron only has been raised from the ground state into some higher molecular orbital, i.e., singly excited states. We can ignore promotion into any of the starred states of Fig. 6.14(*b*), since this would lead to the formation of an unstable molecule and immediate dissociation (cf. Fig. 6.11, where the placing of an electron in each of the σ_g and σ_u^* orbitals produces dissociation into two H atoms). Thus we may consider the three possible excited states $(1s\sigma_g 2s\sigma_g)$, $(1s\sigma_g 2p\sigma_g)$, and $(1s\sigma_g 2p\pi_u)$.

Taking $(1s\sigma_g 2s\sigma_g)$ first: here both electrons are σ electrons, hence $\Lambda = \lambda_1 + \lambda_2 = 0$ and, since we are considering only singlet states, $S = 0$ also.

Further, since both constituent orbitals are *even* and *symmetrical*, the overall state will be the same, and we have $(1s\sigma_g 2s\sigma_g)^1\Sigma_g^+$.

Now $(1s\sigma_g 2p\sigma_g)$: here we again have a $^1\Sigma$ state since both electrons are σ, but the overall state is now *odd* (u); this may be rationalized if we think of one electron as rising from a hydrogen atom in the *even* 1*s* state, and the other from an *odd* 2*p* state—the combination of an odd and an even state leading to an overall odd state. Thus $(1s\sigma_g 2p\sigma_g)\ ^1\Sigma_u^+$.

Finally the $(1s\sigma_g 2p\pi_u)$: now $\Lambda = \lambda_1 + \lambda_2 = 1$, since one electron is in a π state and, again since one electron originates from a 2*p* orbital, the combined state is u: $^1\Pi_u$.

The energies of these three states increase in the order of the constituent molecular orbitals, as shown in Fig. 6.14(*b*), i.e.,

$$^1\Sigma_u^+ < {}^1\Pi_u < {}^1\Sigma_g^+$$

Similar states are obtained by excitation to the 3*s* and 3*p* states, to the 4*s* and 4*p* states, etc. Also for $n = 3, 4, \ldots$ there exists the possibility of excitation to the *nd* orbital. It may be shown by methods similar to those above that interaction between 1*s* and *nd* electrons can lead to the three configurations and state symbols in increasing energy:

$$(1s\sigma\ nd\sigma)\ ^1\Sigma_g^+ < (1s\sigma\ nd\pi)\ ^1\Pi_g < (1s\sigma\ nd\delta)\ ^1\Delta_g$$

Some of these energy levels are shown at the left of Fig. 6.15. Transitions between them can occur according to the *selection rules*:

1. $$\Delta\Lambda = 0, \pm 1 \qquad (6.32)$$

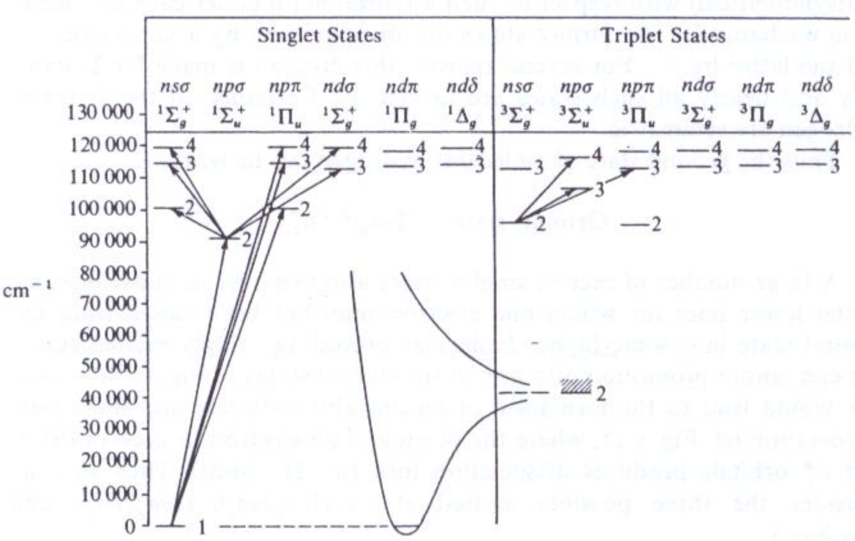

Figure 6.15 The singlet and triplet energy levels of the hydrogen molecule. One electron only is assumed to undergo transitions, the other remaining in the $1s\sigma$ state.

Thus transitions $\Sigma \leftrightarrow \Sigma$, $\Sigma \leftrightarrow \Pi$, $\Pi \leftrightarrow \Pi$, etc., are allowed, but $\Sigma \leftrightarrow \Delta$, for example, is not.

2. $$\Delta S = 0 \tag{6.33}$$

For the present we are concerned only with singlet states so this rule does not arise.

3. $$\Delta\Omega = 0, \pm 1 \tag{6.34}$$

This follows directly from 1 and 2 above.

4. There are also restrictions on symmetry changes. Σ^+ states can undergo transitions only into other Σ^+ states (or, of course, into Π states) while Σ^- go only into Σ^- (or Π). Symbolically:

$$\Sigma^+ \leftrightarrow \Sigma^+ \qquad \Sigma^- \leftrightarrow \Sigma^- \qquad \Sigma^+ \not\leftrightarrow \Sigma^- \tag{6.35}$$

And finally:

$$g \leftrightarrow u \qquad g \not\leftrightarrow g \qquad u \not\leftrightarrow u \tag{6.36}$$

We show a few allowed transitions from the ground state and the lowest excited state in Fig. 6.15.

Let us now consider some of the triplet states of molecular hydrogen, i.e., those states in which the electron spins are parallel and hence $S = 1$. Plainly both electrons cannot now occupy the same orbital so the state of lowest energy will be either $(1s\sigma_g 2s\sigma_g)$, $(1s\sigma_g 2p\sigma_g)$, or $(1s\sigma_g 2p\pi_u)$. The first two are evidently ${}^3\Sigma$ states, the third is ${}^3\Pi$, and, following the rules outlined above, we can write down their state symbols and order of energies as:

$$(1s\sigma_g 2p\sigma_g)\ {}^3\Sigma_u^+ < (1s\sigma_g 2p\pi_u)\ {}^3\Pi_u < (1s\sigma_g 2s\sigma_g)\ {}^3\Sigma_g^+$$

These energy levels are shown on the right of Fig. 6.15, together with those formed by the introduction of $3d$ and $4d$ orbitals. (The very small splitting of the levels into states with different $\Omega = \Lambda + S$ is ignored in the figure.) A few of the allowed transitions are shown from the $(1s\sigma 2s\sigma)$ state, but it should be particularly noted that, because of the selection rule $\Delta S = 0$ given in Eq. (6.33), transitions are not allowed between singlet and triplet states, i.e., between the two halves of Fig. 6.15.

Transitions are not shown from the lowest ${}^3\Sigma_u^+$ state on Fig. 6.15, that is, the lowest triplet state. This is not because transitions are forbidden, but because the state is the continuous one shown in the upper half of Fig. 6.11, the $1s\sigma_u$. Thus in this state the molecule immediately dissociates into atoms before further transitions can occur. The energy level shown for this state in Fig. 6.15 is the lower limit, i.e., the dissociation limit, and in fact the state extends continuously from this limit up to the top of the diagram. Part of Fig. 6.11 is reproduced on Fig. 6.15 to underline the relationship between them.

Thus although the hydrogen spectrum will be complicated by the presence of vibrational and rotational structure on each of the transitions sketched in the figure, basically the overall pattern consists of sets of Rydberg-like line series from which the positions of the energy levels can be found.

6.2.5 Molecular Photoelectron Spectroscopy

Photoelectron spectroscopy and its application to atoms has been described in Sec. 5.5; here we want to discuss the information which this technique can give us about diatomic molecules. To do this we shall use the oxygen molecule as an example.

Photoelectron spectroscopy relies on the ejection of an electron, and consequent formation of an ion, under the influence of a beam of radiation; two ways in which this can happen for O_2 are shown in Fig. 6.16. Part (*a*) shows the upper four energy levels of the O_2 molecule, and the way in which they are filled in the ground state (cf. the discussion on p. 222). The ionization process requiring least energy is the removal of an electron from the $2p\pi_g$ level (an antibonding electron) as shown in (*b*); the resulting O_2^+ is in its lowest possible energy state, so we may refer to it as the ground state of O_2^+. Alternatively, part (*c*) shows the removal of a bonding $2p\pi_u$ electron, requiring somewhat more energy, and resulting in the formation of an excited O_2^+. Other more highly excited states can be formed by the ejection of more firmly bound electrons (e.g., the $2p\sigma_g$ or the $2s\sigma_u$).

It should, perhaps, be mentioned here that the usual notation for O_2 and its ions describes the ground state molecule as $^3\Sigma_g$ (triplet, since $S = \frac{1}{2} + \frac{1}{2} = 1$, and Σ since the electrons' angular momenta are opposed, so $\Lambda = \lambda_1 + \lambda_2 = 1 - 1 = 0$), while the ground state of O_2^+ is $^2\Pi_g$ (doublet, since there is only one unpaired electron spin), and the excited state is $^4\Pi_g$ (three unpaired spins, hence quartet). We shall not use this notation here, however.

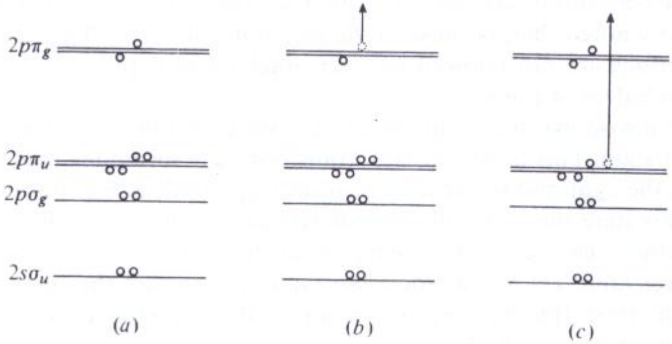

Figure 6.16 (*a*) The occupied molecular energy levels in the O_2 molecule: each circle represents an electron. The excitation of an electron (dotted) is shown in the formation of O_2^+ in (*b*) the ground state, and (*c*) the first excited state.

The observed photoelectron spectrum of O_2 confirms this pattern of energy levels, since it indicates electrons having an ionization potential of about $1{\cdot}9 \times 10^{-18}$ J (12·1 eV) and twice as many electrons with an ionization potential of about $2{\cdot}6 \times 10^{-18}$ J (16·2 eV)—clearly these correspond to the two $2p\pi_g$ electrons and the four $2p\pi_u$ electrons respectively. Higher ionization potentials are found for the more firmly held electrons. Thus photoelectron spectroscopy immediately gives us a quantitative estimate of the relative energies of the various molecular orbitals in the oxygen molecule or, of course, of any other diatomic molecule which can be studied by this technique.

The O_2^+ ions formed in this way are stable, but short-lived, molecules. That is to say, in the absence of electron capture (when they revert to O_2) they have no tendency to dissociate into O and O^+, but behave like ordinary diatomic molecules. In particular they vibrate and rotate. We illustrate the situation for O_2 and O_2^+, both in their ground states, in Fig. 6.17(*a*). Ultra-violet spectroscopy shows that the equilibrium bond lengths of these two molecules are 0·121 nm for O_2 and 0·112 nm for O_2^+ and, if we take the $v = 0$ state of O_2 as the arbitrary zero of energy, then the $v = 0$ state of O_2^+ is some $1{\cdot}9 \times 10^{-18}$ J (the ionization potential) above this. Because of

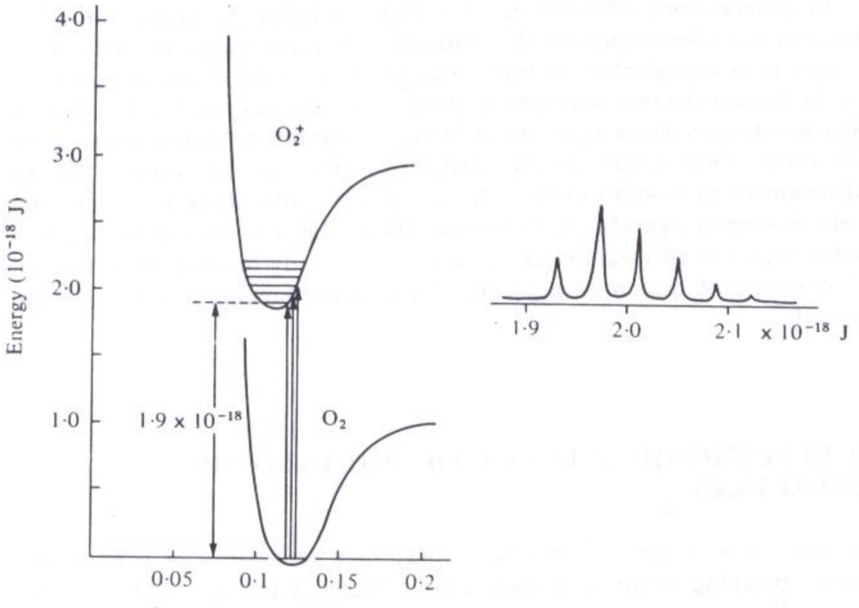

(*a*) (*b*)

Figure 6.17 (*a*) The formation of ground state O_2^+ from O_2 and (*b*) the resulting fine structure of the photoelectron spectrum.

the difference in the equilibrium internuclear distances, the Franck–Condon rule (Sec. 6.1.3) indicates that a jump from the ground vibrational state of O_2 will populate several vibrational states of O_2^+; this behaviour is confirmed by the high-resolution photoelectron spectrum, shown diagrammatically in Fig. 6.17(*b*), which shows a set of discrete ionization potentials, each corresponding to ionization into a particular vibrationally excited state of O_2^+. The spacing between the peaks, about $0{\cdot}37 \times 10^{-19}$ J (or 0·23 eV), corresponds to the spacing between the vibrational energy levels of the O_2^+ molecule, which in turn, as we remember from Chapter 3, is equal to the vibrational frequency of the molecule. Since $1000\ \text{cm}^{-1} \equiv 0{\cdot}2 \times 10^{-19}$ J, the spacing gives a vibrational frequency for O_2^+ of about $1850\ \text{cm}^{-1}$. This should be compared with the fundamental frequency of the O_2 molecule itself, determined from Raman spectroscopy, of $1580\ \text{cm}^{-1}$; we see that, very reasonably, removal of an antibonding electron to form O_2^+ in its ground state results in the formation of a stronger, shorter bond.

Similarly observation of the fine structure of the $2{\cdot}6 \times 10^{-18}$ J ionization potential reveals a vibrational splitting of some $0{\cdot}24 \times 10^{-19}$ J (0·15 eV) or $1200\ \text{cm}^{-1}$—a lower frequency than O_2 itself, consistent with the ionization of a bonding electron.

In general then, observation of a high-resolution photoelectron spectrum can give information on the vibrational frequency of diatomic molecular ions, even though their lifetimes may be of the order of microseconds or less. At present the resolving power of the technique is some 5×10^{-21} J; in other words lines closer than about $250\ \text{cm}^{-1}$ cannot be distinguished from each other. Thus *rotational* fine structure cannot yet be studied, but an improvement in resolution by a factor of 10 would allow the rotational levels of ionized hydrides (for example, HF or HCl) to be studied, while a further factor of 10 would open the way to the study of rotational states of the majority of diatomic molecules. Such developments are breathlessly awaited.

6.3 ELECTRONIC SPECTRA OF POLYATOMIC MOLECULES

We have seen in Sec. 3.7 that the vibrational frequencies of a particular atomic grouping within a molecule, for example, CH_3, C=O, C=C, etc., are usually fairly insensitive to the nature of the rest of the molecule. Other bond properties, such as length or dissociation energy, are also largely independent of the surrounding atoms in a molecule. Since all these properties depend, in the final analysis, on the electronic structure of the bond, it is plain that we may, at least as an approximation, discuss the structure, and hence the spectrum, of each bond in isolation. Bonds for which this approximation is adequate are usually said to have 'localized' molecular orbitals, i.e., orbitals embracing a pair of nuclei only; other molecules, for which this approximation is invalid, have non-localized orbitals and are often called 'conjugated'. We shall meet some examples of this latter class shortly.

When each bond may be considered in isolation, it is evident that the complete electronic spectrum of a molecule is the sum of the spectra from each bond. The result will plainly be very complex, but a great deal of information about the molecule is contained within it. Thus if some band series can be recognized for a particular bond we immediately know the vibrational frequency of that bond and probably a good estimate of its dissociation energy also. If the rotational structure is resolved, then we have the moment of inertia (from the line spacing) and hence information about the shape and size of the molecule.

Such detailed information is usually obtainable only for molecules studied in the gas phase: in pure liquids, or in solution, molecular rotation is hindered and no rotational structure will be observed. The blurring of the rotational structure often masks the vibrational line series also, and the electronic spectrum of a liquid is usually rather broad and characterless. However, as we shall discuss shortly, it may still be highly characteristic of a particular molecular grouping both in its frequency and its intensity.

Confining our attention, for the moment, to gas-phase spectra, we have already remarked that one of the more important advantages of electronic spectroscopy is that the vibrations, rotations, dissociation energies, and structures of molecules may be investigated in their *excited states*, even though a particular molecule may exist in such a state for not much longer than the time it takes to complete a few rotations. We have not the space to discuss this topic in detail, but one aspect is especially interesting—the fact that electronic excitation often leads to a change in shape of the molecule. That this happens can be seen by studying rotational fine structure in the spectra; here we briefly discuss the theoretical basis for its occurrence.

6.3.1 Change of Shape on Excitation

In Fig. 6.18 we show the orbital picture of a hydride H_2A where A is any polyvalent atom, both in its bent configuration (*a*), with a bond angle of 90°, and in a linear form (*b*), bond angle 180°. We have seen in Sec. 5.1, that the *p* orbitals of an atom are at right angles to each other, so we can readily imagine the rectangular molecule to be formed by interaction of two of these *p* orbitals with hydrogen 1*s* orbitals, leaving the third *p* orbital unaffected; the latter is called a 'non-bonding' orbital since it plays no part in bonding A and H together, and in general it will have a higher energy than bonding orbitals. In Fig. 6.18(*a*) we label the non-bonding orbital (which is out of the plane of the paper) N_1, the two bonding molecular orbitals

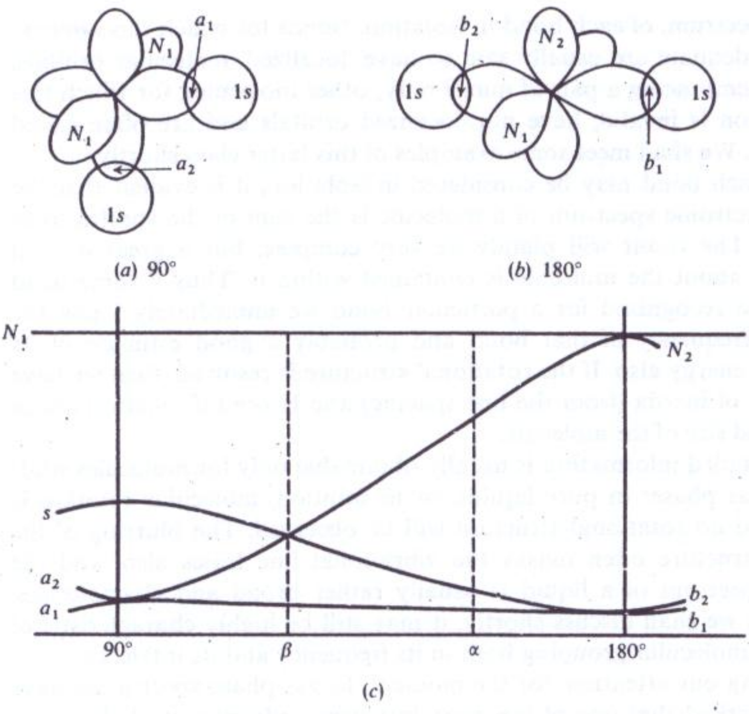

(a) 90° (b) 180°

(c)

Figure 6.18 The orbital pictures for an AH_2 molecule where the AH bonds are (*a*) at 90°, and (*b*) at 180°. In (*c*) is shown qualitatively the change in energy of the various orbitals as the bond angle changes from 90 to 180°. *(Adapted, with the kind permission of the author, from A. D. Walsh, J. Chem. Soc., 1953, p. 2262.)*

formed from the *p* and 1*s* atomic orbitals as a_1 and a_2 and the unused (and hence non-bonding) atomic orbital *s* of A simply as *s*.

In the linear molecule a new principle must be introduced—that of orbital hybridization. For this, atom A is supposed to mix its *s* orbital with one of its *p* orbitals and, from these two orbitals, to form two new orbitals—hybrids—which, it may be shown theoretically, point at 180° to each other. These *sp* hybrids form rather stronger bonds to other atoms than separate *s* and *p* orbitals, so it is energetically favourable, in certain cases, for the atom to 'prepare' hybrid orbitals at the moment of bond formation. In this configuration (Fig. 6.18(*b*)), there are now two non-bonding *p* orbitals, labelled N_1 and N_2, and two bonding orbitals formed by overlap between *sp* hybrids and hydrogen 1*s*, called b_1 and b_2.

Now, remembering that a non-bonding orbital is higher in energy than a bonding, and that an *sp*-bonding orbital is stronger (hence *lower* in energy because the molecule is more stable) than a *p*-bonding, we can plot the qualitative energy changes for a smooth transition from 90 to 180° bonding.

This we do in Fig. 6.18(*c*), which is constructed as follows:

1. The non-bonding orbital N_1 remains unchanged throughout, hence its energy is constant;
2. The bonding orbital a_1 passes over into the stronger orbital b_1, hence its energy decreases;
3. The bonding orbital a_2 becomes the non-bonding N_2, thus increasing in energy; N_1 and N_2 are identical in energy at 180°;
4. The bonding orbitals b_1 and b_2 are formed by absorption of the non-bonding *s* into a_1;
5. If we increase the bond angle beyond 180° (or decrease it below 90°) the reverse changes begin to take place, so 180 and 90° represent maxima and minima on the energy curves as shown.

Now let us see the relevance of this to molecular shapes. Consider first the molecule BeH_2, beryllium hydride. Beryllium, we have seen in Sec. 5.3.1, has the electronic ground state configuration $1s^2 2s^2$, that is, it has two outer electrons with which to form bonds, the two $1s$ electrons being too firmly held by the nucleus to take part in bonding. Each hydrogen atom contributes a further electron, so the BeH_2 molecule must dispose of four electrons into molecular orbitals, with, according to Pauli, a maximum of two electrons per orbital. The most stable state, as can be seen from Fig. 6.18(*c*), will be for two electrons to go into b_1 and two into b_2, thus producing a *linear* molecule.

When the molecule is excited electronically, the next available orbital to contain the excited electron is N_2 (or N_1), but with a configuration $b_1^2 b_2^1 N_2^1$ it is evident from the figure that the most stable state will be at a bond angle, α, somewhere between 90 and 180°—the increase in the energies of b_1 and b_2 being more than compensated for by the decrease in N_2 until equilibrium occurs at an angle α. Thus we see that the excited state is *bent*. If the electron is so excited as to be ionized completely, leaving the ion BeH_2^+, the three remaining electrons will all be in the b_1 and b_2 orbitals and hence the most stable configuration will again be *linear*.

Now consider the case of water, H_2O. The oxygen atom has an outer electron configuration $2s^2 2p^4$, and so has six electrons to dispose into molecular orbitals. As before each hydrogen contributes one, so water is formed by placing a total of four pairs of electrons into four molecular orbitals. The lowest energy state at which this can be done is shown by the angle β in the figure, which is some angle between 90 and 180° (and is observed experimentally to be about 104°). Thus water is bent in the ground state, with a configuration which may be written $a_1^2 a_2^2 s^2 N_1^2$, since the angle is not far removed from 90°. During excitation one of the N_1 electrons will undergo transitions since these, being of highest energy, are most easily removed. However, since the energy of N_1 does not change with angle, the angle of the remaining $a_1^2 a_2^2 s^2 N_1^1$ state will not change during the transition.

These arguments may be readily extended to other triatomic molecules or to larger polyatomic molecules, although the energy diagram corresponding to Fig. 6.18(*c*) is more complicated since more orbitals are involved. The results show, however, and experiment confirms, that linear molecules such as CO_2 and HC═CH become bent on excitation, the latter taking up a planar zig-zag conformation.

6.3.2 Chemical Analysis by Electronic Spectroscopy

Although rotational and sometimes vibrational fine structure do not appear in the liquid or solid state, both the position and intensity of the rather broad absorption due to an electronic transition is very characteristic of the molecular group involved. In this branch of spectroscopy the position of an absorption is almost invariably given as the *wavelength* at the point of maximum absorption, $\lambda_{\text{max.}}$, quoted either in Ångstrom units ($1\ \text{Å} = 10^{-10}$ m) or in nanometres ($1\ \text{nm} = 10^{-9}$ m), the latter being more usual. It should be particularly noted that a *large* energy change, corresponding to a high frequency or wavenumber, is represented by a *small* wavelength. For practical reasons the electronic spectrum is divided into three regions: (1) the visible region, between 400 and 750 nm (4000–7500 Å or 25 000–13 300 cm^{-1}), (2) the near ultra-violet region, between 200 and 400 nm (2000–4000 Å or 50 000–25 000 cm^{-1}), and (3) the far (or vacuum) ultra-violet, below 200 nm (below 2000 Å or above 50 000 cm^{-1}). The latter is so called because absorption by atmospheric oxygen is considerable in this region and spectra can only be obtained if the whole spectrometer is carefully evacuated. Thus commercial instruments extend only down to about 185 nm and absorptions below this range are little used for routine chemical purposes.

The *intensity* of an electronic absorption is given by the simple equation:

$$\varepsilon = \frac{1}{cl} \log_{10} \frac{I_0}{I}\ l\ \text{mol}^{-1}\ \text{cm}^{-1} \tag{6.37}$$

where c and l are the concentration and path length of the sample (in mol l^{-1} and in cm^{-1}, respectively), I_0 is the intensity of light of wavelength $\lambda_{\text{max.}}$ falling on the sample, and I is the intensity transmitted by the sample. ε is the molar extinction coefficient and ranges from some 5×10^5 for the strongest bands to 1 or less for very weak absorptions.

Electrons in the vast majority of molecules fall into one of the three classes: σ electrons, π electrons, and non-bonding electrons (called n electrons). The first two classes were discussed in Sec. 6.2.2 and the third, which plays no part in the bonding of atoms into molecules, was mentioned briefly in Sec. 6.3.1. In chemical terms a single bond between atoms, such as C—C, C—H, O—H, etc., contains only σ electrons, a multiple bond, C═C,

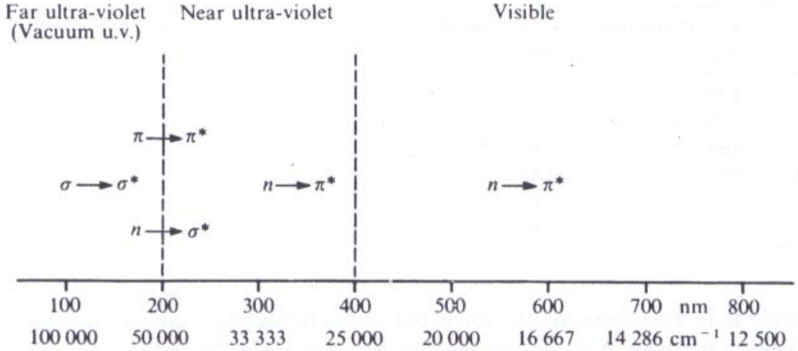

Figure 6.19 The regions of the electronic spectrum and the type of transition which occurs in each.

C≡C, C=N, etc., contains π electrons in addition, while atoms to the right of carbon in the periodic table, notably nitrogen, oxygen, and the halogens, possess n electrons. In general the σ electrons are most firmly bound to the nuclei and hence require a great deal of energy to undergo transitions, while the π and n electrons require less energy, the n electrons usually (but not invariably) requiring less than the π. Thus, in an obvious notation, $\sigma \rightarrow \sigma^*$ transitions fall into the vacuum ultra-violet, $\pi \rightarrow \pi^*$ and $n \rightarrow \sigma^*$ appear near the borderline of the near and far ultra-violet, and $n \rightarrow \pi^*$ come well into the near ultra-violet and visible regions. These generalizations are indicated schematically on Fig. 6.19, which also shows the relationship between the nanometer and wavenumber scales.

Saturated hydrocarbon molecules, then, which can only undergo $\sigma \rightarrow \sigma^*$ transitions, do not give rise to spectra with any analytic interest since they fall outside the generally available range; examples are the $\sigma \rightarrow \sigma^*$ transitions of methane CH_4, and ethane C_2H_6 which are at 122 and 135 nm respectively.

The insertion of a group containing n electrons, e.g., the NH_2 group, allows the possibility of $n \rightarrow \sigma^*$ transitions in addition and also tends to increase the wavelength of the $\sigma \rightarrow \sigma^*$ absorption; for example, CH_3NH_2: $\sigma \rightarrow \sigma^*$ 170 nm, $n \rightarrow \sigma^*$ 213 nm. It is unsaturated molecules, i.e., molecules containing multiple bonds, which give rise to the most varied and interesting spectra, however. We cannot here discuss the large mass of data in any detail but must be content to indicate a few of the more important generalizations. More detail is to be found in the books by Scott, and by Williams and Fleming, listed in the bibliography at the end of this chapter.

Consider, first, *isolated* multiple bonds within a molecule; the most important factor determining the position of the absorption maxima is, of course, the nature of the atoms which are multiply-bonded. From the following table we see that the $\pi \rightarrow \pi^*$ transitions are relatively insensitive to those atoms while the $n \rightarrow \pi^*$ transitions vary widely:

	$\pi \to \pi^*$ (strong) (nm)	$n \to \pi^*$ (weak) (nm)
>C=C<	170	—
—C≡C—	170	—
>C=O	166	280
>C=N⟍	190	300
>N=N⟋	?	350
>C=S	?	500

This behaviour is very reasonable since the *n* electrons play no part in the bonding and control of them is retained by the atom (O, N, or S) contributing them. The above data is approximate only since different substituents on the A=B group produce slight variations in the wavelength of the $n \to \pi^*$ transition. Thus, considering ketones alone, $\lambda_{\text{max.}}$ varies from 272 nm for CH_3COCH_3 to 290 nm for cyclohexanone, and even higher if halogen substituents are included. From the mass of empirical data already assembled, a great deal of information about the substituents to a particular group is obtainable from the electronic spectrum.

More pronounced changes occur, however, when two or more multiple bonds are *conjugated* in the molecule, i.e., when structures having alternate single and multiple bonds arise, for example —C=C—C=C— or —C=C—C=O. In this case the $\pi \to \pi^*$ and $n \to \pi^*$ transitions both increase considerably in wavelength and intensity, the increase being greater the more conjugate linkages there are. As a simple example we have the following approximate data for $\pi \to \pi^*$ transitions in carbon–carbon bonds:

	$\lambda_{\text{max.}}$ (nm)	ε
—C=C—	170	16 000
—C=C—C=C—	220	21 000
—C=C—C=C—C=C—	260	35 000

while for oxygen-containing molecules we have both $\pi \to \pi^*$ and $n \to \pi^*$ transitions:

	$\pi \to \pi^*$ (strong) (nm)	$n \to \pi^*$ (weak) (nm)
—C=O	166	280
—C=C—C=O	240	320
—C=C=C—C=O	270	350
	245	435

Thus we see that conjugation immediately brings the very intense $\pi \rightarrow \pi^*$ transition into the easily available region of ultra-violet spectrometers. For this reason these techniques are particularly well adapted to the study of conjugated and aromatic systems.

In the last example given above we see that the $n \rightarrow \pi^*$ absorption of *p*-benzoquinone, at 435 nm, has shifted into the blue region of the visible spectrum. When the substance is seen in the ordinary way the complementary colour—yellow—is observed. Colour in large organic molecules is invariably due to the existence of considerable conjugation raising the transition wavelength into the visible region—a fact on which the chemistry of dyestuffs is based.

Substituents on conjugated systems also perturb the ultra-violet transitions in a systematic way; a great deal of empirical data has led to the formulation of rules to predict the effects. These are inown as Woodward's rules, but they have undergone considerable modification and extension since they were first formulated by Woodward in 1941. As a simple example, consider butadiene, $CH_2{=}CH.CH{=}CH_2$, which has a strong absorption at 217 nm due to the $\pi \rightarrow \pi^*$ transition. This molecule may be considered to be the 'parent' of a whole series of molecules containing the trans conjugated  group, whether in hydrocarbon chains or in ring systems. Any substituents or modifications to this parent fragment have each been assigned a positive or negative value which must be added to the basic absorption at 217 nm in order to arrive at the expected absorption frequency of the substituted molecule. Thus the increment for a chlorine atom is 5 nm and for an $-OCH_3$ group 6 nm; if both these substituents occur together, the molecule would absorb at $217 + 5 + 6 = 228$ nm. Excellent accounts of these rules, and tabulations of the values for various substituents, etc., are to be found in the books by Scott, and by Williams and Fleming, mentioned in the bibliography.

6.3.3 The Re-Emission of Energy by an Excited Molecule

After a molecule has undergone an electronic transition into an excited state there are several processes by which its excess energy may be lost; we discuss some of these briefly below.

1. *Dissociation.* The excited molecule breaks into two fragments. This was discussed in some detail for the particular case of a diatomic molecule dissociating into atoms in Sec. 6.1.4. No spectroscopic phenomena, beyond the initial absorption spectrum, are observed unless the fragments radiate energy by one of the processes mentioned below.
2. *Re-emission.* If the absorption process takes place as shown schematically in Fig. 6.20(*a*), then the re-emission is just the reverse of this, as in (*b*) of the figure. The radiation emitted, which may be collected and displayed as an emission spectrum, is identical in frequency with that absorbed.

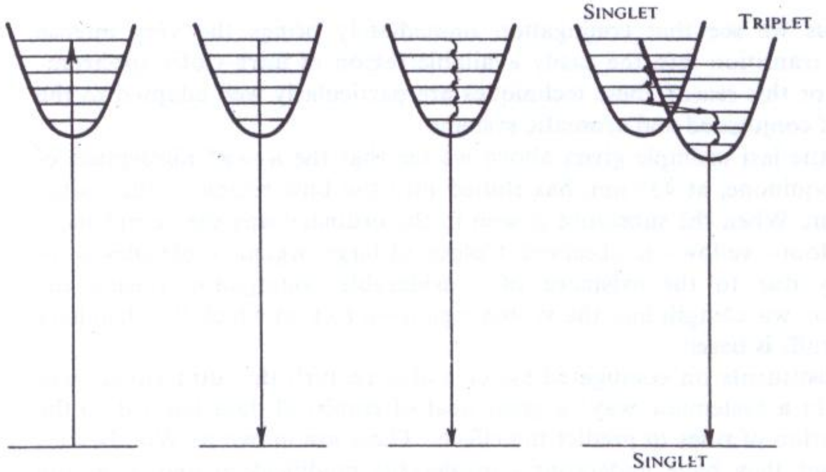

(*a*) Absorption (*b*) Re-emission (*c*) Fluorescence (*d*) Phosphorescence

Figure 6.20 Showing the various ways in which an electronically excited molecule can lose energy.

3. *Fluorescence.* If, as in Fig. 6.20(*a*), the molecule is in a high *vibrational* state after electronic excitation, then excess vibrational energy may be lost by intermolecular collisions; this is illustrated in (*c*) of the figure. The vibrational energy is converted to kinetic energy and appears as heat in the sample; such transfer between energy levels is referred to as 'radiationless'. When the excited molecule has reached a lower vibrational state (for example, $v' = 0$), it may then emit radiation and revert to the ground state; the radiation emitted, called the *fluorescence spectrum*, is normally of lower frequency than that of the initial absorption, but under certain conditions it may be of higher frequency. The time between initial absorption and return to ground state is very small, of the order of 10^{-8} s.
4. *Phosphorescence.* This can occur when two excited states of different total spin have comparable energies. Thus in Fig. 6.20(*d*), we imagine the ground state and one of the excited states to be singlets (that is, $S = 0$), while the neighbouring excited state is a triplet ($S = 1$). Although the rule $\Delta S = 0$ forbids *spectroscopic* transitions between singlet and triplet states, there is no prohibition if the transfer between the excited states occurs *kinetically*, i.e., through radiationless transitions induced by collisions. Such transfer, however, can only occur close to the cross-over point of the two potential curves (cf. Sec. 6.1.7), and once the molecule has arrived in the triplet state and undergone some loss of vibrational energy in that state, it cannot return to the excited singlet state. It will, therefore, eventually reach the $v' = 0$ level of the *triplet* state. Now al-

though a transition from here to the ground state is spectroscopically forbidden, it *may* take place but much more slowly than an allowed electronic transition. Thus it is that a phosphorescent material will continue to emit radiation seconds, minutes, or even hours after the initial absorption. The phosphorescence spectrum, as a rule, consists of frequencies lower than that absorbed.

Considerable confusion often occurs between the Raman effect, discussed in Chapter 4, and the phenomena of fluorescence or phosphorescence. The main points of difference are as follows:

(*a*) In fluorescence and phosphorescence, radiation must be absorbed by the molecule and an excited electronic state formed; in Raman spectroscopy energy is merely transferred from radiation to molecule, or vice versa, but no excited electronic state is formed.

(*b*) The exciting radiation for fluorescence or phosphorescence must be just that equivalent to the energy difference between electronic states; the exciting radiation for Raman spectroscopy can be of any frequency *except* that which would induce electronic transitions; in the latter case absorption would occur, rather than scattering.

5. *Stimulated emission.* This increasingly important mechanism for removal of excess energy can lead to the production of laser radiation, as discussed in Sec. 1.10. The helium–neon laser, which emits light in the visible region of the spectrum, was considered in Sec. 5.4.6.

6.4 TECHNIQUES AND INSTRUMENTATION

The simple techniques of electronic spectroscopy are familiar to every schoolboy studying physics—a glass prism, some sort of telescope, a bunsen burner, and a pinch of common salt are sufficient apparatus for observing part of the emission spectrum of sodium. And in fact a great deal of rapid and precise analytical work, both qualitative and quantitative, is carried out using flame spectrophotometers not very much more sophisticated in construction than this, except that a photomultiplier or photographic plate is used instead of the rather inaccurate human eye. However, for high-resolution work or for absorption studies, the practical requirements are more stringent.

The choice of a suitable source was formerly one of the main difficulties. The prime requirements of a source are that it should be *continuous* over the region of interest (i.e., there must be no wavelengths at which it does not emit) and it should be as *even* as possible (i.e., there must be no intense emission lines). In the visible region and just into the near ultraviolet—say between 350 and 800 nm—an ordinary tungsten filament lamp is quite suitable. Below this a hydrogen discharge lamp proves adequate, down to about 190 nm, while below this again discharge lamps containing rare gases, such as xenon, must be used. Thus we see that, in contrast to the other forms of spectroscopy discussed in previous chapters, no one source is suitable throughout the region.

Transparent materials for windows and sample cells present no problem, at least in the visible and near ultra-violet regions, since good quality glass or quartz transmit down to 200 nm or better. Below this region alkali fluorides, such as lithium fluoride or calcium fluoride, must be used; these are transparent down to about 100 nm. Prisms, if used, can be made of the same materials. Modern high-resolution instruments, however, employ a reflection grating rather than a prism since the former gives better dispersion and so allows more precise wavelength selection and measurement.

The detector for visible and ultra-violet studies is either a photographic plate or a photomultiplier tube. The chief disadvantage of the photographic method is that the resolving power is limited by the graininess of the image; on the other hand there is no other detector which can record the complete spectrum simultaneously in a small fraction of a second. When studying short-lived species, such as free radicals, it would be quite impossible to scan the complete spectrum using a photomultiplier. Also, at the other end of the time-scale the photographic plate is an efficient integrator of very weak signals—exposure times can be extended to many hours or even days to record a weak emission or absorption. For most routine purposes, however, where the spectrum of a stable material is to be recorded in a time of several minutes, a photomultiplier detector coupled to an amplifier and paper chart recorder is the most flexible and useful combination.

BIBLIOGRAPHY

Bingel, W. A.: *Theory of Molecular Spectra*, Wiley, 1969.

Carlson, T. A.: *Photoelectron and Auger Spectroscopy*, Plenum Press, 1975.

Herzberg, G.: *Molecular Spectra and Molecular Structure, vol. 1, Spectra of Diatomic Molecules*, 2nd ed., Van Nostrand, 1950.

Herzberg, G.: *Molecular Spectra and Molecular Structure, vol. 3, Electronic Spectra and Electronic Structure of Polyatomic Molecules*, Van Nostrand, 1967.

Scott, A. I.: *Interpretation of the Ultraviolet Spectra of Natural Products*, Pergamon Press, 1964.

Sutton, D.: *Electronic Spectra of Transition Metal Complexes*, McGraw-Hill, 1968.

Turner, D. W., C. Baker, A. D. Baker, and C. R. Brundle: *Molecular Photoelectron Spectroscopy*, Wiley-Interscience, 1970.

Williams, D. H. and I. Fleming: *Spectroscopic Methods in Organic Chemistry*, 3rd ed., McGraw-Hill, 1980.

PROBLEMS

(Useful constant: $1\ \text{cm}^{-1} \equiv 11{\cdot}958\ \text{J mol}^{-1}$.)

6.1 Using the data of Fig. 6.5 (some of which is tabulated below), estimate the dissociation energy of the I_2 molecule:

v:	0	5	10	30	50	70	75	80
$\Delta\varepsilon$:	213·3	207·2	200·7	172·1	134·7	82·3	67·0	52·3 cm^{-1}

6.2 The absorption spectrum of O_2 shows vibrational structure which becomes a continuum at 56 876 cm^{-1}; the upper electronic state dissociates into one ground state atom and one excited atom (the excitation energy of which, measured from the atomic spectrum, is 15 875 cm^{-1}). Estimate the dissociation energy of ground state O_2 in kJ mol^{-1}.

6.3 The values of $\bar{\omega}_e$ and x_e in the ground state ($^3\Pi_u$) and a particular excited state ($^3\Pi_g$) of C_2 are:

	$\bar{\omega}_e$	x_e
Ground state	1641·4 cm^{-1}	$7{\cdot}11 \times 10^{-3}$
Excited state	1788·2 cm^{-1}	$9{\cdot}19 \times 10^{-3}$

Use Eq. (6.10) to find the number of vibrational energy levels below the dissociation limit and hence the dissociation energy of C_2 in both states.

6.4 The spectrum arising from transitions between the two states of C_2 in Prob. 6.3 shows the ν_{00} line at 19 378 cm^{-1} and a convergence limit at 39 231 cm^{-1}. The dissociation is into one ground state atom and one excited atom, the excitation energy of the latter being 10 308 cm^{-1}; calculate the exact dissociation energies of the two states and compare your answers with those of Prob. 6.3. Explain any discrepancy.

6.5 The band origin of a transition in C_2 is observed at 19 378 cm^{-1}, while the rotational fine structure indicates that the rotational constants in excited and ground states are, respectively, $B' = 1{\cdot}7527$ cm^{-1} and $B'' = 1{\cdot}6326$ cm^{-1}. Estimate the position of the band head. Which state has the larger internuclear distance?

CHAPTER

SEVEN

SPIN RESONANCE SPECTROSCOPY

We have seen in earlier chapters that all electrons and some nuclei possess a property conveniently called 'spin'. Electronic spin was introduced in Chapter 5 to account for the way in which electrons group themselves about a nucleus to form atoms and we found that the spin also accounted for some fine structure, such as the doublet nature of the sodium D line, in atomic spectra. Equally, in Sec. 5.6 it was necessary to invoke a nuclear spin to account for very tiny effects, called hyperfine structure, observed in the spectra of some atoms.

In this chapter we shall consider these spins in rather more detail and discuss the sort of spectra they can given rise to directly rather than their influence on other types of spectra. After an introduction discussing the interaction of spin with an external magnetic field we shall consider in some detail the spectra of particles with a spin of $\frac{1}{2}$ (that is, electrons, and some nuclei such as hydrogen, fluorine, or phosphorus), then a brief discussion of some other nuclei whose spins are greater than $\frac{1}{2}$, and finally a few words on the techniques involved in producing electronic and nuclear spin spectra.

7.1 SPIN AND AN APPLIED FIELD

7.1.1 The Nature of Spinning Particles

We have seen that all electrons have a spin of $\frac{1}{2}$, that is, they have an angular momentum of $\sqrt{\frac{1}{2}(\frac{1}{2}+1)}(h/2\pi) = \sqrt{3}/2$ units. Many nuclei also

GENERAL BIBLIOGRAPHY

Some of the general texts on spectroscopy, each covering a wide range of techniques, are listed below:

Bingel, W. A.: *Theory of Molecular Spectra*, Wiley, 1969.

Brand, J. C. D., and J. C. Speakman: *Molecular Structure: The Physical Approach*, 2nd ed., Edward Arnold, 1975.

Brittain, E. F., W. O. George, and C. H. Wells: *Introduction to Molecular Spectroscopy, Theory and Experiment*, Academic Press, 1970.

Browning, D. R. (ed.): *Spectroscopy*, McGraw-Hill, 1969.

Chang, R.: *Basic Principles of Spectroscopy*, Krieger, 1978.

Cottrell, T. L.: *Dynamic Aspects of Molecular Energy States*, Oliver and Boyd, 1965.

Crooks, J. E.: *The Spectrum in Chemistry*, Academic Press, 1978.

Dunford, H. B.: *Elements of Diatomic Molecular Spectroscopy*, Addison-Wesley, 1968.

Steinfeld, J. I.: *Molecules and Radiation: An Introduction to Modern Molecular Spectroscopy*, Harper & Row, 1974.

Straughan, B. P., and S. Walker: *Spectroscopy*, Vols. 1–3, Chapman and Hall, 1976.

Wheatley, P. J.: *The Chemical Consequences of Nuclear Spin*, North-Holland Pub. Co., 1970.

Williams, D. H., and I. Fleming: *Spectroscopic Methods in Organic Chemistry*, 3rd ed., McGraw-Hill, 1980.

ANSWERS TO PROBLEMS

Chapter 1

1.1 $v = 2{\cdot}998 \times 10^{13}$ Hz; $\bar{v} = 10^{3}\ \text{cm}^{-1}$; $\Delta E = 1{\cdot}987 \times 10^{-20}\ \text{J mol}^{-1}$ or $\Delta E = 1{\cdot}196 \times 10^{4}$ J mol^{-1}; $\lambda = 5\ \mu\text{m}$ (that is, half as large).

1.2 (*a*) HBr only; (*b*) HBr and CS_2 (for the asymmetric stretch and the bend only).

1.3 (*a*) $\delta E \approx 10^{-33}$ J; $\delta v \approx 10^{-2}$ Hz. (*b*) $\delta E \approx 10^{-31}$ J; $\delta v \approx 1$ Hz.

1.4 For $4{\cdot}005 \times 10^{-22}$ J: (*a*) 368; (*b*) 818; (*c*) 905; (*d*) 990. For $4{\cdot}005 \times 10^{-21}$ J: (*a*) 0; (*b*) 135; (*c*) 368; (*d*) 905.

Chapter 2

2.1 $B = 0{\cdot}357\,17\ \text{cm}^{-1}$; $I = 7{\cdot}837 \times 10^{-42}\ \text{kg m}^2$; $r = 1{\cdot}756 \times 10^{-10}$ m. For $J = 9 \rightarrow \text{J} = 10$ the value of $\Delta\varepsilon$ is $7{\cdot}1434\ \text{cm}^{-1}$; the maximum population is at $J = 17$.

2.2 In general, $\omega/2\pi = 2Bc\sqrt{J(J+1)}$ r/s, hence (*a*) zero; (*b*) $3{\cdot}02 \times 10^{10}$; (*c*) $11{\cdot}24 \times 10^{10}$ r/s.

2.3 H^{37} Cl: $B = 10{\cdot}5739\ \text{cm}^{-1}$; D^{35}Cl: $B = 5{\cdot}446\ \text{cm}^{-1}$.

2.4 The quickest way to evaluate J, B, and D is to note that the separations between the given lines are about $16{\cdot}8\ \text{cm}^{-1}$; this suggests that $2B$ is about $17\ \text{cm}^{-1}$, from which the first line, at $84{\cdot}544\ \text{cm}^{-1}$, obviously corresponds to the $J = 4 \rightarrow J = 5$ transition. Using this, B and D can be calculated from two of the lines and checked using the third. Hence: $B = 8{\cdot}473\ \text{cm}^{-1}$; $D = 3{\cdot}71 \times 10^{4}\ \text{cm}^{-1}$; $r = 1{\cdot}414 \times 10^{-10}$ m; $\bar{\omega} = 2560\ \text{cm}^{-1}$, approx.

2.5 Maximum population is at $J = 10$; some other points on the graph are:

J	Approx. relative population	J	Approx. relative population
0	1·0	12	12·4
2	4·9	14	11·3
4	8·2	16	9·7
6	10·7	18	8·0
8	12·2	20	6·2
10	12·8		

2.6 For HCN: $I = 19{\cdot}005 \times 10^{-47}$ kg m^2; $B = 1{\cdot}4728$ cm^{-1}; for DCN: $I = 23{\cdot}254 \times 10^{-47}$ kg m^2; $B = 1{\cdot}2037$ cm^{-1}.

2.7 Vibrational frequency is about 2995 cm^{-1}.

Chapter 3

3.1 $\bar{\omega}_e = 1903{\cdot}98$ cm^{-1}; $\bar{\omega}_e x_e = 13{\cdot}96$ cm^{-1} (or $x_e = 7{\cdot}332 \times 10^{-3}$); zero point energy, $\varepsilon_0 = 948{\cdot}51$ cm^{-1}; force constant, $k = 1595{\cdot}0$ kg s^{-2} (or 1595·0 N m^{-1}); dissociation energy = 744·4 kJ mol^{-1} (inaccurate because cubic and quartic terms in $(v + \frac{1}{2})$ are ignored and these become important at large v—see Sec. 6.1.4 for details).

3.2 Zero point energy for $(\mathrm{HCl} + \mathrm{D_2}) = 2937{\cdot}5$ cm^{-1}, while that for $(\mathrm{DCl} + \mathrm{HD})$ is 2808·5 cm^{-1}. Hence 129·0 cm^{-1} = 1·542 kJ mol^{-1} is evolved during the reaction.

3.3 The intensity of the hot band is about 0·36 that of the fundamental.

3.4 18·8 cm^{-1}.

3.5 (*a*) 1; (*b*) 4; (*c*) 3; (*d*) 30.

3.6 (*a*) about 2550 cm^{-1}; (*b*) about 975 cm^{-1} (taking $\nu_{\mathrm{CO}} \approx 1100$ cm^{-1}).

Chapter 4

4.1 Raman spectroscopy; spacing = 243·2 cm^{-1} ($B = 60{\cdot}8$ cm^{-1}).

4.2 No. The nuclear spin affects only the line intensities and in this case produces a strong, weak, strong, weak, ... alternation of intensities.

4.3 Molecule is linear (*PR* contour of an infra-red band) and has a centre of symmetry, hence is A—B—B—A. 3374 cm^{-1} and 3287 cm^{-1} are close to the ≡CH stretching frequency (given in Table 3.4 as 3300 cm^{-1}) so molecule is acetylene, HC≡CH. Assignments:

3374 cm^{-1}:	symmetric CH stretch
3287 cm^{-1}:	asymmetric CH stretch
1973 cm^{-1};	C≡C stretch
729 and 612 cm^{-1}:	bending vibrations

4.4 Non-linear and no centre of symmetry, hence

3756 cm^{-1} and 3652 cm^{-1} are in the region of OH stretching frequency, so molecule is H_2O. Assignments:

3756 cm^{-1}:	asymmetric stretch
3652 cm^{-1}:	symmetric stretch
1595 cm^{-1}:	bend

4.5 Both molecules, no centre of symmetry. N_2O linear (*PR* bands), hence N—N—O. NO_2 non-linear, hence either

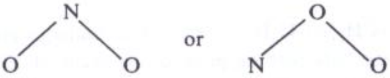

Chapter 5

5.1 5331·55 cm^{-1}, 7799·29 cm^{-1} and 9139·80 cm^{-1}. Ionization energy = 12 186·40 cm^{-1} (≡1·511 eV).

5.2 $L = 2$; $S = \frac{3}{2}$, $J = \frac{5}{2}$. Minimum number of electrons = 3; possible electron configurations include: *spp*, *ppp*, *ppd*, etc. (all non-equivalent electrons).

5.3 (*a*) $^1S_0$, $^3S_1$; (*b*) $^1D_2$, $^1P_1$, $^1S_0$, $^3D_{3,2,1}$, $^3P_{2,1,0}$, $^3S_1$; (*c*) $^1D_2$, $^3D_{3,2,1}$; (*d*) $^1F_3$, $^1D_2$, $^1P_1$, $^3F_{4,3,2}$, $^3D_{3,2,1}$, $^3P_{2,1,0}$.

5.4 (*a*) $^1S_0$; (*b*) $^1D_2$, $^1S_0$, $^3P_{2,1,0}$; (*c*) $^1G_4$, $^1D_2$, $^1S_0$, $^3F_{4,3,2}$, $^3P_{2,1,0}$.

5.5 $^4S_1$: Total spin = $\frac{3}{2}$, hence J must be half-integral; $^2D_{7/2}$: $S = \frac{1}{2}$, $L = 2$, hence J cannot be greater than $\frac{5}{2}$; $^0P_1$: $2S + 1$ cannot be zero.

5.6 $^2P_{3/2} \rightarrow {}^2D_{3/2}$: 10 lines; $^2P_{3/2} \rightarrow {}^2D_{5/2}$: 12 lines; $^2P_{1/2} \rightarrow {}^2D_{3/2}$: 6 lines.

Chapter 6

6.1 By plotting the given data, extrapolating and taking the area under the graph, the dissociation energy is found to be approximately 12 100 cm^{-1} or 144·7 kJ mol^{-1}.

6.2 490·3 kJ mol^{-1} (or 41 000 cm^{-1}).

6.3 Ground state: $v_{max} = 69$; $D''_e = 690{\cdot}0$ kJ mol^{-1}
$D''_0 = 680{\cdot}2$ kJ mol^{-1}
Excited state: $v_{max} = 53$; $D'_e = 581{\cdot}3$ kJ mol^{-1}
$D'_0 = 570{\cdot}7$ kJ mol^{-1}

6.4 Ground state: $D''_0 = 345{\cdot}8$ kJ mol^{-1}
Excited state: $D'_0 = 237{\cdot}4$ kJ mol^{-1}

The answers to question 6.3 are inaccurate (in this case badly so) because Eq. (6.10) relies on the use of terms up to $(v + \frac{1}{2})^2$ only; a better treatment would involve terms in $(v + \frac{1}{2})^3$ and $(v + \frac{1}{2})^4$.

6.5 Band head is in the *P* branch at $p = 14$ (Eq. (6.23)), and the position of the band head is at 19 358 cm^{-1}. The ground state has the larger internuclear distance.

Chapter 7

7.1 For H: $B_z = 0{\cdot}7107$ T (7107 gauss). For ^{13}C: $B_z = 2{\cdot}8266$ T (28 266 gauss).

7.2 Chemical shift positions are 5·75δ and 1·05δ; $J_{AX} = 10$ Hz.

7.3 Eight lines of equal intensity, symmetrically disposed about the midpoint; taking the midpoint at 0·0 Hz, the lines are at: −77·5, −57·5, −27·5, −7·5, +7·5, +27·5, +57·5 and +77·5 Hz. (N.B. the J_{HH} values given are irrelevant to the ^{19}F spectrum if the chemical shifts are large.)

7.4 The BH_4 group will give rise to a 1 : 3 : 3 : 1 quartet because of coupling to the CH_3; conversely the CH_3 group will show a 1 : 4 : 6 : 4 : 1 pentet, with the same separation between the lines as exhibited in the quartet.

7.5 (*a*) 6; (*b*) 12; (*c*) 9; (*d*) 12.

7.6 Each D nucleus, having a spin of 1, splits the neighbouring H (of CHD_2) into three lines of equal intensity. Use the family tree method to show that the resultant overlapped spectrum is a 1:2:3:2:1 pentet.

7.7 Small groups, such as —CH_3 or C_6H_5—, may often undergo internal rotation at temperatures not too far below the bulk melting point of the material. This lengthens the relaxation time of the nuclei and so sharpens the resonance frequency.

Chapter 8

8.1 Recoil velocity = $39{\cdot}7\ \mathrm{m\,s^{-1}}$; Doppler shift = $3{\cdot}97 \times 10^{11}$ Hz.

8.2 (*a*) 5 lines; (*b*) 12 lines; (*c*) 12 lines.

INDEX